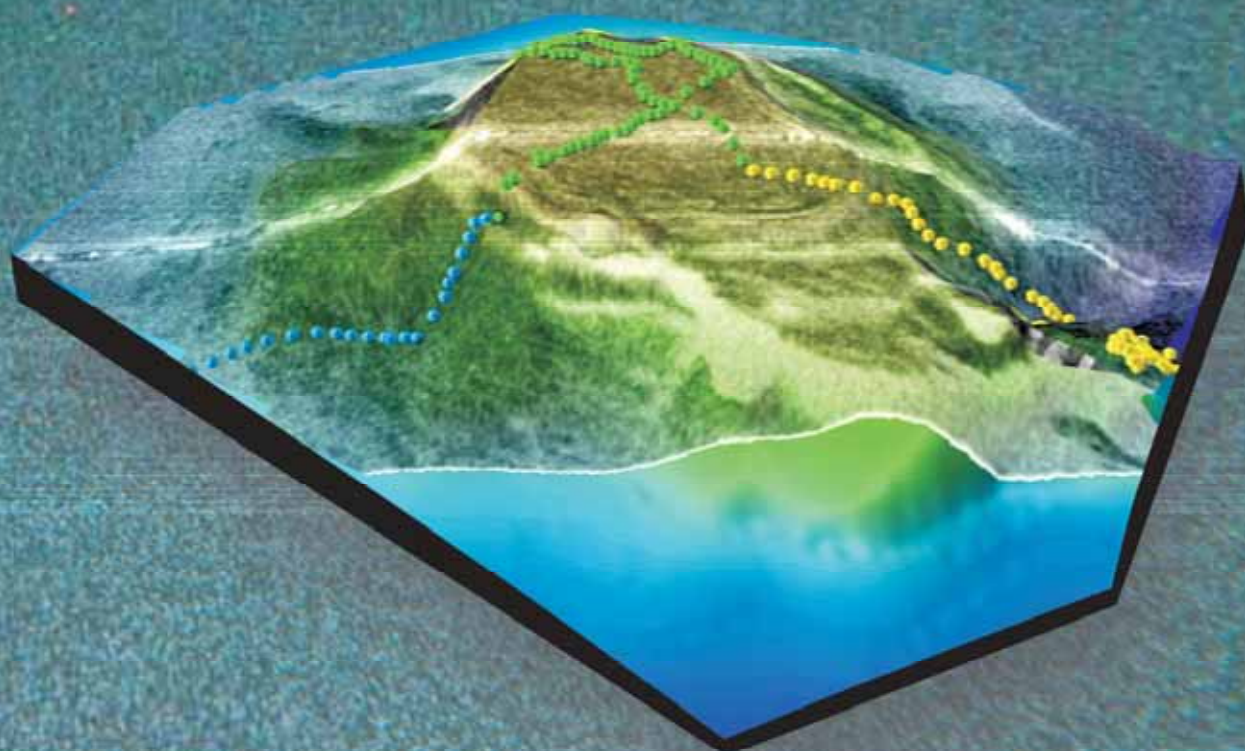




Deep-water cold seeps, sedimentary environments and ecosystems of the Black and Tyrrhenian Seas and the Gulf of Cadiz

Preliminary results of investigations
during the TTR-15 cruise of
RV *Professor Logachev*
June-August, 2005



**Deep-water cold seeps, sedimentary
environments and ecosystems of the Black
and Tyrrhenian Seas and the Gulf of Cadiz**

Preliminary results of investigations during the TTR-15 cruise of
RV *Professor Logachev*
June-August, 2005

Editors: A.M. Akhmetzhanov
 M.K. Ivanov
 N.H. Kenyon
 A. Mazzini

The designations employed and the presentation of the material in this publication do not imply the expression of any opinion whatever on the part of the Secretariats of UNESCO and IOC concerning the legal status of any country or territory, or its authorities, or concerning the delimitation of the frontiers of any country or territory.

For bibliographic purposes, this document should be cited as follows:

Deep-water cold seeps, sedimentary environments and ecosystems of the Black and Tyrrhenian Seas and Gulf of Cadiz. *IOC Technical Series No. 72*, UNESCO, 2007 (*English*)

Cover design: A. Akhmetzhanov

Cover images: Variations of seabed faunal assemblages across Meknes mud volcano, Gulf of Cadiz (front, See Fig. 76 for details); sample photos from TTR-15 (back); Black Sea seafloor (courtesy of University of Bremen) (background)

Printed in 2007

by the United Nations Educational,
Scientific and Cultural Organisation
7, place de Fontenoy, 75352 Paris 07 SP

Printed in UNESCO's Workshops

©UNESCO 2007 *Printed in France*

(SC-2007/WS/13)

TABLE OF CONTENTS

ABSTRACT	iii
ACKNOWLEDGEMENTS	iv
INTRODUCTION	1
LIST OF PARTICIPANTS	3
METHODS	4
I. BLACK SEA (LEGS 1 AND 2)	12
I.1. Introduction	12
I.2. Seismic profiling data	13
I.2.1. Shatsky Ridge/Tuapse Trough Area	13
I.2.2. Batumi/Poti Area	14
I.2.3. Ochamchira area	18
I.2.4. Samsun area	19
I.3. Sidescan sonar data	21
I.3.1. Trakya area	21
I.3.2. Shatsky Ridge/Tuapse Trough area	21
I.3.3. Batumi/Poti area	23
I.3.4. Ochamshira area	26
I.3.5. Samsun area	27
I.4. Gas seepage at Batumi seep off Georgia: results from ROV investigations	29
I.5. Bottom sampling data	30
1.5.1. Trakya area	30
1.5.2. Shatsky Ridge/Tuapse Trough area	34
1.5.3. Georgian margin	38
1.5.4. Samsun area	46
II. TYRRHENIAN SEA	47
II.1. Deep-sea transport and deposition of the Stromboli 30/12/2002 landslide	47
II.2. Sedimentary processes in the Calabrian and Sicilian margin	51
II.2.1. Angitola slope valley	51
II.2.2. Cefalu basin	55
III. GULF OF CADIZ (LEG 4)	56
III.1 Introduction and Objectives of the TTR-15 Leg 4	56

III.2. Geological Setting	57
III.3. Cold seeps of the Gulf of Cadiz	59
III.3.1. Seismic and Acoustic Data	59
<i>III.3.1.1. Seismic data</i>	<i>59</i>
<i>III.3.1.2. MAK deep-towed sidescan sonar data</i>	<i>66</i>
III.3.2. Bottom camera survey	70
III.3.3. Bottom Sampling	73
<i>III.3.3.1. Bottom samples</i>	<i>73</i>
<i>III.3.3.2. Micropaleontological investigation of matrix and clasts from mud volcanoes</i>	<i>80</i>
III.3.4. Biology and Microbiology	82
III.3.5. Gas biogeochemistry	86
III.4. Ship wreck	88
III.5. Seabed processes and ecosystems in the Portuguese Cadiz margin canyons	90
REFERENCES	96
ANNEX I. CORE LOGS	
ANNEX II. LIST OF TTR RELATED REPORTS	

ABSTRACT

Interdisciplinary studies of deep-water cold seeps, sedimentary environments and ecosystems were conducted by RV *Professor Logachev* in the Black and Tyrrhenian Seas and the Gulf of Cadiz during the 15th Training-through-Research Cruise of UNESCO-IOC.

During Legs 1 and 2 TTR-15 investigated active seep sites in the Russian, Georgian and Turkish sectors of the Black Sea. Long-range OKEAN sidescan sonar and deep-towed high-resolution MAK-1M sidescan sonar mapping as well as seismic profiling were used to locate sites of active fluid and gas discharge. Detailed observations by video-guided instruments and ROV investigations were performed prior to seafloor sampling by a gravity corer and a TV-grab. Seeps, where free gas bubbles are escaping from the sea floor, were successfully observed on the Kobuleti Ridge (Georgia), at water depths between 1100 - 850 m, by acoustic anomalies in the water column on raw sonar data and as high backscatter intensity areas. Since free gas should become converted to gas hydrate at depths below 750 m of the Black Sea, the presence of free gas is explained by fast transport from a large gas reservoir below the lower boundary of the gas hydrate stability field in the sediments. Bottom-seismic reflections are well imaged in the area. The seeps on the Kobuleti Ridge (Georgia), as well as on the first anticline of the Tuapse Foldbelt and the Shatsky Ridge, are characterised by carbonate and shallow gas hydrate deposits. At four distinct mound locations, three on the Kobuleti Ridge and one on the Shatsky Ridge, oil and other higher hydrocarbon gases have been detected for the first time, indicating seepage from deeper petroleum reservoirs.

During Leg 3 a survey of the northern slope of the Stromboli volcano in the Tyrrhenian Sea continued the work commenced during TTR-14 cruise aimed at collecting more high resolution data for ongoing study of the volcano flank collapses. Results indicate that the thickest, coarse-grained landslide deposit extends over a NNW elongated area at water depths between 1000 and 2000 m at a distance of 6 to 8 km from the shoreline. The deposit consists of several discrete, mainly chaotic assemblages of fresh cobble-sized scoriae and lava flow clasts within a coarse sand matrix. Down-slope and laterally, the coarse-grained deposit grades to black volcanoclastic sand often arranged in ripple bed forms. A turbidity current generated by the event traveled for at least 24 km and was capable of depositing sand on a 200 m high opposite flank of Stromboli Canyon.

New sidescan sonar data were acquired from the Angitola slope valley area on the Calabrian margin. They were integrated with already available multibeam bathymetry and show that the valley is composed of three tracts with different gradient, planform, cross section and sedimentary processes.

30 kHz sidescan sonar coverage of the Cefalu basin located on the Sicilian margin revealed a widespread sediment instability affecting channel-levee complexes, which dominates the slope settings in the area.

During Leg 4, three main areas were investigated in the Gulf of Cadiz: (1) the Moroccan Mud Volcano Field; (2) the Deep Portuguese Mud Volcano Field; (3) a submarine canyon system in the northwest Portuguese sector.

High resolution sidescan sonar, underwater video and bottom sampling data enabled the detailed characterization of several previously known mud volcanoes and associated cold seeps and ecosystems on the Moroccan Margin.

Four (4) mud volcanoes were discovered in the deepwater part of the Portuguese margin. Their location seems to be controlled by major very deep strike-slip faults.

A sunken 200-meter long cargo vessel that transported anthracite (presumably during the 1st World War) was discovered on the bottom of the Gulf of Cadiz and investigated with a deep towed video camera.

The underwater camera run across the head of the Cadiz submarine valley investigated the changes in the local ecosystems related to the presence of the Mediterranean Outflow Water. The study also highlighted the significant level of pollution in the axial part of the canyon system with various types of man-made objects (e.g. bottles, tins, plastic bags etc.).

ACKNOWLEDGEMENTS

The fifteenth Training-through-Research cruise has received financial support from a variety of sources. Legs 1 and 2 were run in collaboration with the University of Bremen (Germany) through its METRO project funded by the Federal Ministry of Education and Research (BMBF, contract no. 03G0604A). Leg 3 was a collaborative effort with Istituto di Scienze Marine (INMAR) of CNR (Italy). Leg 4 was jointly funded by the HERMES EU Integrated Project (GOCE-CT-2005-511234), University of Aveiro (Portugal) through the MVSEIS Euromargins Project (PDCTM/2003/DIV/40018/99) and University of Gent (Belgium) through a UNESCO/IOC project on "Geosphere-Biosphere Coupling Processes in the Ocean: the Training-through-Research approach towards Third World involvement", funded by the Government of Flanders.

The cruise was also supported by the Russian Ministry of Science and Technological Policy, the Polar Marine Geological Research Expedition (PMGRE) of the Russian Ministry of Natural Resources and Moscow State University (Russia). Logistic support was provided by the Netherlands Institute for Sea Research (NIOZ).

A number of people from different organizations supported the Training-through-Research Programme and were involved into the cruise preparation. The editors would like to express their gratitude for the contributions made by Prof. I. F. Glumov (Ministry of Natural Resources of the Russian Federation) and Dr. P. Bernal (Executive Secretary, IOC).

Credit also should be given to Dr. Maarten van Arkel of the NIOZ, Prof. Dr. D. Y. Puscharovsky (Faculty of Geology, Moscow State University) and Dr. A. Suzyumov (IOC Consultant) for their continuous support.

Thanks are due to the administration and staff of the PMGRE (St. Petersburg) for their co-operation and assistance with the cruise organization and execution. Captain V. Pidenko and the skilful crew of the RV *Professor Logachev* insured the smooth operations at sea.

Staff and students of the UNESCO-MSU Marine Geosciences Centre provided a valuable support in processing the acoustic data and preparation of illustrations.

INTRODUCTION

The TTR-15 cruise was carried out on board the RV *Professor Logachev* from 6 June to 5 August 2005. The cruise focused on geological processes in the Black Sea, Western Mediterranean Sea and North Atlantic and was executed as part of the international scientific programme of UNESCO/IOC "Training-through-Research" ("Floating University"). It also contributed to the HERMES project and a number of national programmes and projects as indicated in the Acknowledgements. The cruise was subdivided into four legs. Legs 1 and 2 took place in the Black Sea, Leg 3 in the Tyrrhenian Sea and Leg 4 in the Gulf of Cadiz (see the cruise map below). The ship had port calls in Istanbul, Turkey (7-8 June, 31-1 July), Trabzon, Turkey (20 June), Palermo, Italy (18-19 July) and Porto, Portugal (5-6 August)

The cruise's co-chief scientists were:

Legs 1-4: Prof. Dr. Mikhail Ivanov (Moscow State University, Russia)

Legs 1, 2: Prof. Dr. Gerhard Bohrmann (University of Bremen, Germany)

Leg 3: Dr. Michael P. Marani (ISMAR, Italy)

Leg 4: Prof. Dr. Luis Pinheiro, (University of Aveiro, Portugal)

Leg 4: Dr. Neil Kenyon (NOCS, UK)

The principal purpose of the cruise was to conduct interdisciplinary studies of deep-

water cold seeps, sedimentary environments and ecosystems in the Black Sea, Mediterranean (Tyrrhenian) Sea and North Atlantic (Gulf of Cadiz), as well as to train students from Europe, Africa, Asia and Russia in marine research. The latter task was entrusted to TTR-15 by the EU/HERMES project, through IOC.

Participants in the cruise were 80 researchers and students from the following 14 countries: Belgium, China, Germany, Georgia, Italy, Morocco, Mozambique, Norway, Portugal, Russia, Spain, Switzerland, Turkey and UK.

Shipboard training of students and younger scientists was provided through their involvement in execution of the scientific programme of the cruise and participation in a series of daily lectures or seminars given onboard by co-chief scientists and other leading researchers.

Legs 1 and 2 (The Black Sea)

Several areas located on the continental margin around the Black Sea, where previous studies, performed by Georgian, German, Russian and Turkish scientists, as well as by international research programmes, revealed numerous hydrocarbon vents exhausting onto the seafloor, were selected for detailed investigations. The aim of this work was to better understand geological, geochemical and microbiological



TTR-15 cruise location map

processes of cold seeps and to increase the knowledge about the role of methane in the worldwide carbon cycle. Manifestations of gas venting were reported to be present both in the water column (gas flares) and in the bottom sediments. The areas of interest were planned to be covered by long-range sidescan sonar and seismic surveys with detailed studies of identified target areas, with high-resolution acoustic mapping of the seafloor, underwater video and ROV surveying. An extensive sampling program with a variety of samplers including TV guided grab, autoclave, pressurised piston corer and gravity corer was designed to obtain samples of bottom sediments, gases, chemosynthetic fauna, authigenic carbonate crusts and gas hydrates.

Leg 3 (The Tyrrhenian Sea)

Typified by Vulcano and Stromboli Islands, arc volcanism in the Tyrrhenian Sea is presently active and responding to the dynamics of the geological environment in the southern Tyrrhenian Sea. Stromboli Island has been affected by repeated collapse events of the Sciara del Fuoco slope and the structure of its submarine flanks is the result of the interaction of the related erosional and depositional processes with the present-day sedimentary dynamics. The Sciara del Fuoco volcanoclastic material progrades into the deep sea portion of the Stromboli canyon which subsequently funnels a large input of sedimentary material into the Marsili abyssal plain. As a result, a deep-sea fan spans almost the whole eastern portion of the Marsili basin. The recent 2003 eruption of the volcano and collapse event of the Sciara del Fuoco, renders the study of the flanks and deeper portions of the Stromboli/Marsili depositional system an important target for understanding the fate of the material and the processes involved in events of catastrophic volcanic island flank collapse. Intended methods were deep-tow sidescan sonar surveys and sampling, including vibrocoreing.

High resolution sidescan sonar surveys in two other areas along the Calabrian and

Sicilian margins aimed to study processes of sediment transport and deposition.

Leg 4 (The Gulf of Cadiz)

The Gulf of Cadiz has been intensively studied during several recent TTR expeditions with the work focused mainly on mud volcanism, fluid venting and related phenomena. Several tens of mud volcanoes have been discovered and confirmed by sampling. Gas hydrates, carbonate crusts and nodules, as well as benthic chemosynthetic communities were sampled from some of these structures. Large carbonate chimneys, possibly related to fluid escape were sampled and recorded by a deep-towed video system. Within the TTR-15 cruise, further detailed interdisciplinary investigations of known mud volcanoes and their ecosystems were conducted, together with a search for new structures of similar origin. The ecosystems associated with canyon systems influenced by different water masses were also studied by an underwater video survey.

LIST OF PARTICIPANTS

TTR-15 Cruise
6 June - 5 August 2005
RV Professor Logachev

BELGIUM

Hans Pirlet
Noemie Wouthers

CHINA

Feng Ding

GEORGIA

Nona Lursmanashvili
Irma Makalatia

GERMANY

Gerhard Bohrmann
Fritz Abegg
Werner Dimmler
Matthias Haeckel
Gregor Halem
Hans-Jurgen Hohnberg
Hanno Keil
Tobias Mohr
Antonie Nolte
Harry Schulz
Michelle Wagner
Kristin Nass
Marlene Bausch
Marlene Reusche
Manfred Schulz
Bettina Domeyer
Katja Heeschen
Verena Heuer
Ingo Klaucke
Heiko Sahling
Tilmann Schwenk

ITALY

Michael Marani
Fabiano Gamberi
Alessio Di Roberto
Elisa Leidi
Rita Lecci

MOROCCO

Bouchta El Fellah
Mohamed Laadraoui
Rabi Kharbaoui
Amine Hazim

MOZAMBIQUE

Esmeralda Muchangos

NORWAY

Adriano Mazzini

PORTUGAL

Luis Pinheiro
Catarina Lemos
Carlos Pinto
Fatima Mirante
Marina Cunha
Clara Rodrigues
Luisa Santos
Joao Duarte
Cristina Roque
Vitor Hugo Magalhaes

RUSSIA

Michael Ivanov
Elena Kozlova
Valentina Blinova
Andrey Ovsyannikov
Igor Kuvaev
Dmitry Korost
Daria Titkova
Anna Zotova
Roman Murzin
Dmitry Nikonov
Ilya Fokin
Dmitry Nadezkin
Alexandra Sharapova
Antonina Saveljeva
Yulia Titova
Anastasia Belova
Yulia Malykh
Vladislav Malin

SPAIN

Xavier Prieto-Mollar
Jorge Iglesias
Javier Gonzalez

SWITZERLAND

Nicole Hurtig

TURKEY

Serhan Copur
Saliha Doundar
Seda Okay
Bade Pekchetinoz

UK

Neil Kenyon
Rebecca Moremon
Emily Morris
Andrey Akhmetzhanov
Zuzia Stroynowski
Julia Sas

METHODS

The RV *Professor Logachev* is a Russian marine geology research and survey vessel equipped with geophysical survey and seabed sampling equipment. She is operated by the State Enterprise "Polar Marine Geosurvey Expedition" St. Petersburg. The vessel has: a draught of 6.66 m, length of 104.5 m, width of 16 m, net tonnage of 1351 ton, displacement of 5700 ton and is powered by two 3500 hp diesel engines.

Navigation

Positioning during the TTR-15 cruise was acquired using an Ashtech GG24 GPS + GLONASS receiver. The use of both GPS and GLONASS satellite configurations allows for greater accuracy than is available from conventional GPS alone, with up to 60% greater satellite availability. Positions are calculated in real-time code differential mode with 5 measurements per second and an accuracy of

+/- 35 cm (75 cm at 95% confidence limits) with optimal satellite configuration. Realistic positioning accuracy under normal satellite configuration for European waters is assumed as ca. 5 m. Positioning when the vessel is moving also utilizes Doppler velocity determinations from the differential code signal to generate a vessel speed accuracy of 0.04 knots (0.1 at 95% confidence limits) with optimum satellite configuration.

The GPS+GLONASS receiver is located centrally with accurate levelling to sampling and equipment deployment positions on the vessel allowing precise back navigation. Seabed sampling positions with the gravity corer are normally 5% of the accuracy of the vessel position due to their rapid deployment. MAK-1M sidescan sonar and deep-towed video system are all fitted with a pinger allowing precise navigation between the vessel and sub-sea surface position. This is necessary as deep-towed equipment is



RV Professor Logachev in the Black Sea

subject to greater spatial differences with respect to the vessel. This underwater navigation is based on the Sigma-1001 hydroacoustic system. Four stationary aeri-als, spaced 14 m apart, are hull mounted and receive acoustic signals from pingers attached to deployed equipment in short-base mode operating between 7-15 kHz. The signal emitted by the sub-surface pinger is tracked on board and accurate x,y positioning of the device relative to the vessel is computed taking into account roll, trim and ship's speed. Error positioning of this method usually does not exceed 1-2% of water depth.

The navigation system is linked with the ship's main and additional thrusters enabling highly accurate dynamic positioning, which is routinely used during deep-towed acoustic and video surveys and sampling operations.

Seismic profiling

RV Professor Logachev single channel seismic system

The seismic source usually consisted of one 3 litre airgun, at a pressure of 120 bar (12 MPa). The airgun was towed at a depth of approximately 2-2.5 m and was fired every 10 seconds (i.e. approximately every 30 m). The streamer consisted of one active section, 30 m long, with 50 hydrophones, towed at a depth of approximately 2.5-3 m. The offset between the seismic source and the centre of the live hydrophone array was 135 m.

The data was acquired digitally using MSU developed software and preliminarily processed with RadExPro software, which was provided to the UNESCO-MSU Centre for Marine Geosciences by GSD Productions, Moscow. The signals were low-pass filtered analogically to 250 Hz in the acquisition stage. The sample interval was 1 ms and the record length 3 seconds.

The basic processing sequence consisted of definition of the acquisition geometry, static shift correction, spiking deconvolution, amplitude recovery by spherical divergence correction and Butterworth bandpass filtering (20-60-180-240 Hz).

Bremen University multichannel seismic system

T. SCHWENK, F. DING, I. FOKIN, C. PINTO,
Y. TITOVA, A. SAVELJEVA AND R. KHARBAOUI

The Bremen multichannel seismic system is specifically designed to acquire high resolution seismic data through optimizing all system components and procedural parameters. Due to usage of the system on two parallel cruises in July/August 2005 the equipment had to be split in two parts and consequently several compromises had to be accepted, which are described below. Additionally, a new recording system was used after installing and improving during TTR-15 Legs 1 and 2. The operation of the system was carried out by a joint team of German and Russian scientists and students. This cooperation worked exceptionally well.

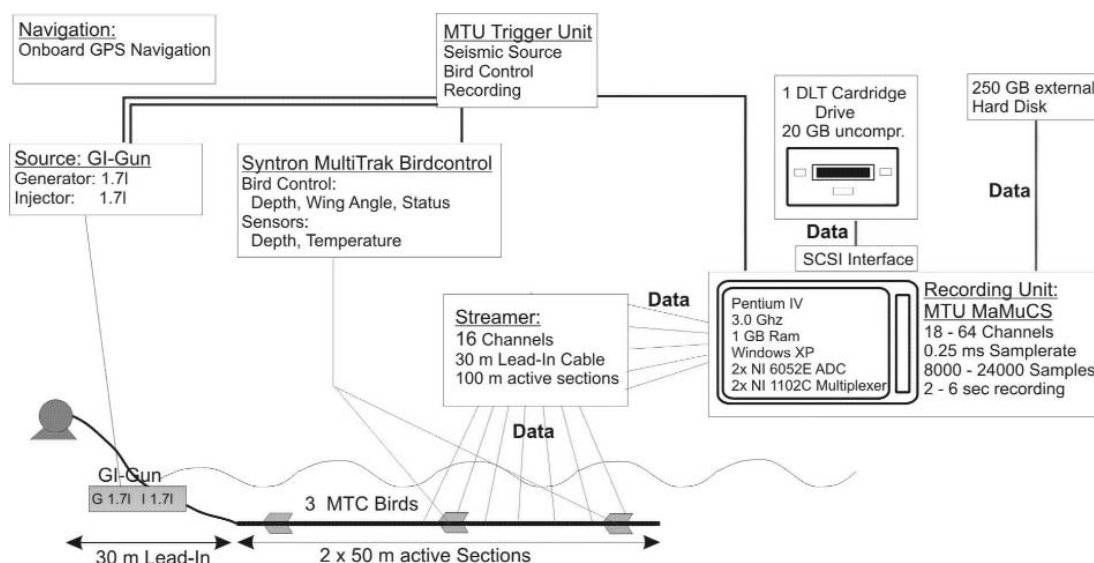
DESCRIPTION OF THE SEISMIC SYSTEM

Seismic Sources and Compressor

As the main seismic source for the surveys, a Sodera GI-Gun was used, in true GI-Mode. The gun was equipped to 2x1.7l chamber volume. The trigger interval for the 1.7l GI-Gun was changed to adapt the shot interval to the available air supply, which depended on the number of shipboard compressors on duty. Namely, the gun was fired at intervals of 12 - 16 seconds. This resulted in an average shotpoint-spacing of 31 to 41 m at 5 kn ship speed (operation parallel to OKEAN) and 12 to 16 m at 2 kn ship speed (operation parallel to MAK). The gun was shot at a mean pressure of 120-150 bar.

Ship velocity during deployment and retrieval was between 1.5 and 2.5 knots, respectively, depending on weather conditions and surface currents. Seismic equipment was always deployed after the accompanying sidescan systems and retrieved before them.

The seismic source was towed by an outrigger at the port side of RV *Logachev* approximately 18 m behind the ship. Two different towing methods were used for different sig-



nal frequencies and penetration. One method was optimized for lower frequencies and deeper penetration, towing the gun by connecting the towing wire to a hanger, to which the gun was attached with 60 cm long chains. From the end of the hanger a rope led to one or two small buoys, which towed the gun in horizontal position when the ship reached profiling speed of 5 knots. This method worked only for speeds around 5 kn. For surveys parallel with the MAK system sailing at only 2 kn, a different towing method was used: the hanger was connected with chains to an elongated buoy, which stabilized the gun in a horizontal position, with a 60 cm long pair of chains giving a total towing depth of approximately 1.8 m. The towing wire then was connected directly to the buoy.

Streamer

The multichannel seismic streamer includes a lead-in and 2 active sections of 50 m length each. A 30 m long deck cable connected the streamer to the recording system. During operations the streamer was secured using two ropes and a tie-off block at the plug of the first section. The tow-lead was laid out ca. 20 m.

The 2 active sections (SYNTRON) are each subdivided into 8 hydrophone groups. Each of the 6.25 m long hydrophone groups

is again subdivided into 5 subgroups of different length. One of the subgroups is a high-resolution hydrophone with pre-amplifier. A programming module distributes the subgroups of 4 hydrophone groups, i.e. a total of 20 groups to 5 channels. To adapt the system to the water depth, deep water programming modules (instead of module 1, which could not be removed) were selected, so that every second 6.25 m hydrophone group was completely used with all 13 hydrophones.

Deployment and retrieval lasted approximately 45 minutes including installation of three Remote Bird Units.

Birds (Cable levelers)

Altogether, up to 3 MultiTrak Remote Units (MTCBirds) were attached to the streamer. Each bird includes a depth sensor as well as adjustable wings. Normally, the birds are controlled by a MultiTrak controller in the seismic lab. Controller and birds communicate via communication coils nested within the streamer. A twisted pair wire within the deck cable connects controller and coils.

Data Acquisition System

During cruise TTR-15 Leg 4, a newly designed custom data acquisition was used

for the first time. The whole system was developed at the group for marine technology/environmental research at the University of Bremen. It was used for the first time on legs 1 and 2, and have been improved by Leg 4, where it ran without problems. It consists of a Pentium IV based PC (3 GHz, 1GB RAM, Windows XP) with two NI6052E 16bit AD-converters. Each ADC is connected to a 32 channel multiplexer (NI-SCXI1102-C) with onboard preamplification and anti-alias filter. The system therefore provides a maximum of 64 channels at maximum sampling rate of 10 kHz per channel. Sample rate can be increased dynamically if the number of channels is reduced.

The acquisition software is also a custom development and provides nearly continuous recording of the 64 channels with data storage in demultiplexed SEG-Y to hard disk. The software, so far, allows online quality control by displaying shot gathers and an online profile plot using brute channel stacks of arbitrary channels. The online profile can additionally be printed immediately to an attached windows printer and / or stored in SEG-Y format. The acquisition system was very reliable.

Data were recorded at 4 kHz over lengths of 4 - 6 seconds depending on water depth with no delay, resulting in 16000 - 24000 samples per trace. Data backup was performed by writing recorded files on DLT4000 cartridge tape and storing additional copies on an external USB-Harddrive with 250 GB.

This type of data management allowed immediate postprocessing of the data, which was very important on the cruise for planning purposes. After each end of line a new file was started for further recording and after the data was moved via the shipboard 1Gbit network, rudimentary post-processing started on an additional PC (see below).

Trigger Unit

The custom trigger unit controlled seismic sources, seismograph and the MTC bird controller. The unit is set up on an IBM compatible PC with a Windows NT 4.0 operating

system and includes a real-time controller interface card (SORCUS) with 16 I/O channels, synchronized by an internal clock. The unit is connected to an amplifier unit and a gun amplifier unit. The PC runs a custom software, which allows definition of arbitrary combinations of trigger signals.

Trigger times can be changed at any time during the survey. Through this feature, the Shot interval could be adjusted to air supply without interruption of data acquisition. The amplifier unit converts the controller output to positive or negative TTL levels. The gun amplifier unit, which generates a 60V/8 Amp. trigger level, controls the magnetic valves of the individual seismic sources.

During the cruise, the trigger of Gun and Acquisition were set to 0 seconds to acquire the data without delay. The trigger period was set accordingly due to the compressors deliver and changed between 12 and 16 seconds.

SEISMIC PROCESSING

To display and print the seismic data for interpretation as soon as possible after the end of the profile, fast but efficient processing was carried out with the Seismic processing software Vista 5.1. The main target of the processing was to enhance the signal to noise ratio. This ratio was insufficient due to the combination of towing a short streamer with only 16 channels near to a noisy ship and using a new acquisition system, with inadequate analogue bandpass filter and pre-amplifier. During the cruise, a ship's-own pre-amplifier and filter were integrated into the Bremen University system, but caused ringing in the data, and all attempts to improve it failed. The signal to noise depends strongly on the profile velocity, towing method and weather conditions.

Therefore, the following processing flow was routinely applied to the data. First, a wide bandpass filter of 5-800 Hz was used to allow trace editing. After removing bad traces, an f-k filter was applied. The filter design consists in the k-domain of two outside end rejection zones, which depends on

the noise character of the data. In the frequency domain a rejection above 200 Hz was chosen. As a next step, spherical divergence was corrected, followed by a common-shot stack. For some profiles with obvious diffraction hyperbolae, an f-k migration was used with estimated shot spacing and a constant velocity model. After processing, the data were printed and exported as seg-y files and loaded into the interpretation software Kingdom Suite 7.4 for a first structural and stratigraphic interpretation.

Hull-mounted acoustic profiler

A hull-mounted 5.1 kHz profiler was routinely used during most of the operations, with a continuous paper output and a selective recording of the digital data.

Sidescan sonar systems

OKEAN

The OKEAN is a long-range sidescan sonar operating at a frequency of 9.5 kHz, which, with its up to 15 km swath range and 6 knots towing speed, is well suited for reconnaissance surveying of large deep-sea areas. The OKEAN vehicle is towed behind the ship at about 40-80 m below the sea surface. Depending on the waterdepth and resolution required the swath could be set to 7 or 15 km.

MAK-1M

The MAK-1M deep-towed hydroacoustic system contains a high-resolution sidescan sonar operated at frequencies of 30 and 100 kHz, with a swath range of up to 2 km (1 km per side) and a subbottom profiler, operated at a frequency of 5 kHz. The sonar has a variable resolution of about 7 to 1 m across track (maximum range to centre) and along track (center to maximum range). During TTR-15, the fish was towed at a nearly constant altitude of about 100-150 m above the seafloor at a speed of 1.5-2 knots for 30 kHz surveys and about 50 m above seafloor for 100 kHz. The positioning of the tow-fish was

archived with a short-based underwater navigation system.

The data from the tow-fish was transmitted on board through a cable, recorded digitally, and stored in Seg-Y format, with a trace length of 4096 2-byte integer samples per side. Time-variant gain was applied to the data while recording, to compensate the recorded amplitudes for the irregularity of the directional pattern of the transducers as well as for the spherical divergence of the sonic pulse.

Onboard processing of the collected data included slant-range-to-ground-range (SLT) correction of the sonographs, geometrical correction of the profiles for recovery of the real seafloor topography, and smoothing average filtering of both types of records. Individual lines were geometrically corrected for the towing speed of the fish, converted into a standard bitmap image format. Some image processing routines, such as histogram equalization and curve adjustment, which are aimed at improving the dynamic range of the imagery, were also applied before printing out. Geographic registration of the acquired images was also done onboard.

Underwater photo and television system

The television system operating onboard cruise TTR-15 is a deep towed system designed for underwater video surveys of the seabed at depths of up to 6000 m. It consists of onboard and underwater units. The onboard part comprises the control units with video amplifier and VCR. The power for the underwater system is supplied through a conductive cable. The underwater equipment comprises the support frame with light unit, the high-pressure housing containing a "Canon M1" digital camera and the power supply unit.

The TV system is controlled from onboard by the winch operator, who visually controls the distance from the camera to the seafloor. This is assisted by a 1.5 m long rope with a weight at the end attached to the frame. It is usually towed along the seafloor enabling the operator to estimate the altitude

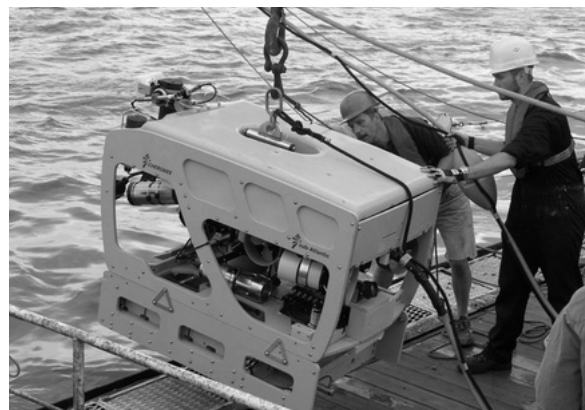
of the instrument above the seafloor. Lights and video camera are switched on/off by the operator from onboard. The non-stop underwater record on the digital camera lasts for 2 hours in the "LP" mode. Onboard VCR keeps a continuous record during the whole survey, which can be up to 6 hours.

Remotely Operated Vehicle (ROV) CHEROKEE

The remotely operated vehicle (ROV) CHEROKEE, is deployed by the DFG Research Center Ocean Margins (Germany) in water depths up to 1000 m. This electronically driven system is primarily distinguished by its relatively small size compared to its significantly large load capacity (60 kg). It can be deployed by almost all of the German research vessels. Its work has included the mapping of volcanic lava flows, observation and sampling of hydrothermal fields, video recording of deep-sea coral reefs, and sampling of hardgrounds at these reefs.

ROV specifications

Vehicle	<i>SubAtlantic CHEROKEE</i>
Depth rated	1000m
Weight	250kg
L x B x H	1.3 x 0.9 x 0.9 m
Payload	60kg
Power	12kW at 440VAC, 50/60Hz
Propulsion	4 electrical thrusters
Telemetry	4 x Video
	4 x RS 232
	4 x RS 285
Sensors / Tools	5 function manipulator "Hydrolek EH5"
	Tritech SeaKing Scanning Sonar (325/675kHz)
	2 x JAI PencilCams
	Tritech "Typhoon" color zoom camera
	SubAtlantic Pan/Tilt unit
	4 x 250W dimmables
Control units	Altimeter
	3 Racks for navigation and video recording (2 x mini-DV)
Winch	<i>MPD custom design spooling winch</i>
Power	1,5 kW
L x B x H	2.3 x 1.3 x 1.4m
SWL	5 kN
Spooling velocity	30m/min
Tether	1000m type JDR 27mm
Fibres	4 x Multimode
Power lines	12 x 220V



ROV CHEROKEE

Sampling Tools

Gravity corer

Coring was performed using a 6 m long c. 1500 kg gravity corer with an internal diameter of 14.7 cm.

One half of the opened core was described on deck, paying particular attention to changes in lithology, colour and sedimentary structures. All colours relate to Munsell Colour Charts. The other half was measured for changes in magnetic susceptibility using a Bartington Instruments Magnetic Susceptibility meter with a MS2E1 probe. Magnetic susceptibility reflects the ease with which a material can be magnetised. This property is most strongly influenced by grain-size, heavy mineral content and is inversely related to carbonate content and diagenetic ferric mineral reduction.

Samples were also taken for coccolith and micropalaeontological assays from smear slides. This was done to generate a preliminary chronostratigraphy for the cores.

Box Corer

Box cores were taken using a Reineck box-corer with a 50 x 50 x 50 cm box capable of retrieving 185 kg of undisturbed seabed surface sample. Lowering and retrieving operations are conducted using a hydraulic A-shaped frame with a lifting capacity of 2 ton.

Kasten-corer

The corer is square in cross-section with a weight of about 600 kg and dimensions of 0.4x0.4x1.8 m. The recovery volume is up to 0.3 m³. The closure of the instrument is performed by two sliding plates and triggered during pull-up. The instrument is particularly useful for obtaining large samples of loosely packed coarse-grained sediment.

Dredge

The dredge comprises a 1 m², rectangular steel gate with chain mesh bag trailing behind and a 0.5 ton weight attached to the wire 3 m in front of the gate. The mesh bag also has a rope bag inside and the mesh size is ~5 cm. The dredge was deployed ~250 m in front of the identified target site and the ship moved at 0.5 kts between 500 and 1500 m ensuring the dredge was pulled up-slope. On some sites, the bottom was monitored with a 3.5 kHz hull-mounted single-beam echosounder. At all times, the ship's velocity and position were monitored using GPS. Tension on the trawl-wire was monitored in the winch cab by both ink-line paper roll and by a tension meter. "Bites" of up to 10 tons on the trawl wire were recorded in this way.

TV-guided grab

SGS-4/1 hydraulically operated grab system was used during the cruise. The 3100 kg system is able to sample dense clayey and sandy sediments as well as deep water basalts and sulphide ores. SGS-4/1 can be used at depths up to 4000 m. The maximum sample volume for soft sediment is 1 m³. The grab is controlled by an operator from onboard and can be opened and closed again at any given time. The grab is positioned with the short base SIGMA 1000 underwater navigation system. The grab is equipped with a built-in digital camcorder with the video signal being both stored locally and transmitted back onboard to enable control for the grab operation as well as back-up recording. The lights are powered by a rechargeable battery, enabling up to 1 hour

of continuous operation. A second battery kept on board was used to perform consecutive dives.

Autoclave tools

HANS-JURGEN HOHNBERG

The Multi Autoclave Corer (MAC) and the Dynamic Autoclave Piston Corer (DAPC) were developed with the aim of recovering, preserving and analyzing sediment cores under in-situ conditions of the deep sea.

Multi Autoclave Corer (MAC)

The MAC, developed by TUB/MAT, can cut four sediment-cores from the upper sea bottom sediment layers (max. 55 cm) simultaneously at any chosen water depth. The cores can be recovered at in-situ-pressure corresponding to water depths of up to 1400 m. The MAC consists of a deployment frame with a damping system including a pull rope releaser system and eight further large structural components, namely the four coring units and the four pressure chambers. In addition, every pressure container is equipped with a pressure preserving system (accumulator) supporting the closure of the pressure chambers during the coring procedure and enabling pressure preservation over several weeks.

Each of the cores is kept in a liner which is pulled into the respective pressure chamber and trapped inside in vertical direction. The MAC is deployed on the deep sea cable. When the system hits the seafloor, it is left to rest there for a certain time before being hoisted back. Function groups are activated that control the processes of coring, pulling the liner into the pressure chamber, sealing the pressure chamber and hauling under in situ pressure. Each of the four pressure chambers is enclosed by a transparent mantle tube which is filled with sea water, providing sufficient cooling of the pressure chamber. Cooling is especially vital for sediment samples that contain gas hydrate. The sediment cores can be used for various physical, chemical or biological examinations. For

example, they can be scanned using non-invasive technology or they can be released from the pressure chamber for description and analysis immediately after recovery. The pressure chambers were checked and approved by the Berlin TUV (Technischer Überwachungsverein, technical inspection authority of Germany). Stored in a safe transport box, they are suitable for transport by sea or road.

Dynamic Autoclave Piston Corer

The DAPC is a sediment core sampling device. Its total length is 7.2 m, its total weight 500 kg. It was designed to cut sediment cores from the seafloor surface to a maximum length of 2.3 m and preserve them at in situ pressure corresponding to water depths of up to 1500 m. Like the MAC, the DAPC is equipped with a pressure control valve allowing deployment to up to 6000 m water depth. The cutting pipe, which is relatively short (2.7 m), hits the seafloor with a very strong impact. Therefore, it is especially suitable for sampling layered, gas-hydrate-bearing sediment. The device allows various analytical approaches. Due to the novel construction of the pressure barrel, this is the first system that allows CT scanning of such cores (80 mm in diameter) in their pressurized state. The pressure barrel consists of glass-fiber reinforced plastic (GRP), aluminium alloys, seawater resistant steel and aluminium bronze. The pressure chamber is 2.6 m long and weighs about 180 kg. All parts of the pressure chamber exposed to sea water are suitable for long-term storage of cores under pressure for several weeks. The DAPC is to be deployed from a research vessel on the deep sea cable. It can be released from variable heights (1-5 m) and enters the seafloor in free fall.

I. Black Sea (Legs 1 and 2)

I.1. Introduction

G BOHRMANN AND M. IVANOV

The Black Sea comprises two extensional basins formed in a back-arc setting above the northward subducting Tethys Ocean, close to the southern margin of Eurasia. The two basins coalesced late in their post-rift phases in the Pliocene, forming the present single depocentre. The Western Black Sea was initiated in the Aptian, when a part of the Moesian Platform (now the Western Pontides of Turkey) began to rift and move away to the south-east. The Eastern Black Sea probably formed by separation of the Mid-Black Sea High from the Shatsky Ridge during the Palaeocene to Eocene. Subsequent to rifting, the basins were the sites of mainly deep water deposition; only during the Late Miocene was there a major sea-level fall, leading to the development of a relatively shallow lake. Most of the margins of the Black Sea have been extensively modified by Late Eocene to recent compression associated with closure of the Tethys. The presence of

the Palaeozoic and the Upper Eocene sources, with the latter being a major regional source known to be generating oil and gas in large amounts, is a significant positive factor for a number of petroleum plays considered for the Black Sea (Roberts et al., 1996).

Leg 1 and 2 study areas (Fig. 1) were identified from several sources. Russian state-owned survey and exploration company Yuzmorgeologia have been working in the Black Sea for a long time and kindly provided a generalized seepage location maps for the Russian margin (L. Meisner, R. Kruglyakova, Pers. Comm.).

Some seismic data from the Turkish margin (Trakya and Samsun areas) were made available for onboard planning by Turkish colleagues from the national petroleum company, TPAO. The seismic data showed several possible mud volcanic structures in the Trakya Area (southwestern Turkish margin).

Shatsky Ridge/ Tuapse Trough is a well-known oil and gas province, which attracted interest from several energy companies in the last ten years. Several oil and gas discharge structures were known in the area from recent Yuzmorgeologia cruises (Kruglyakova et al., 2002).

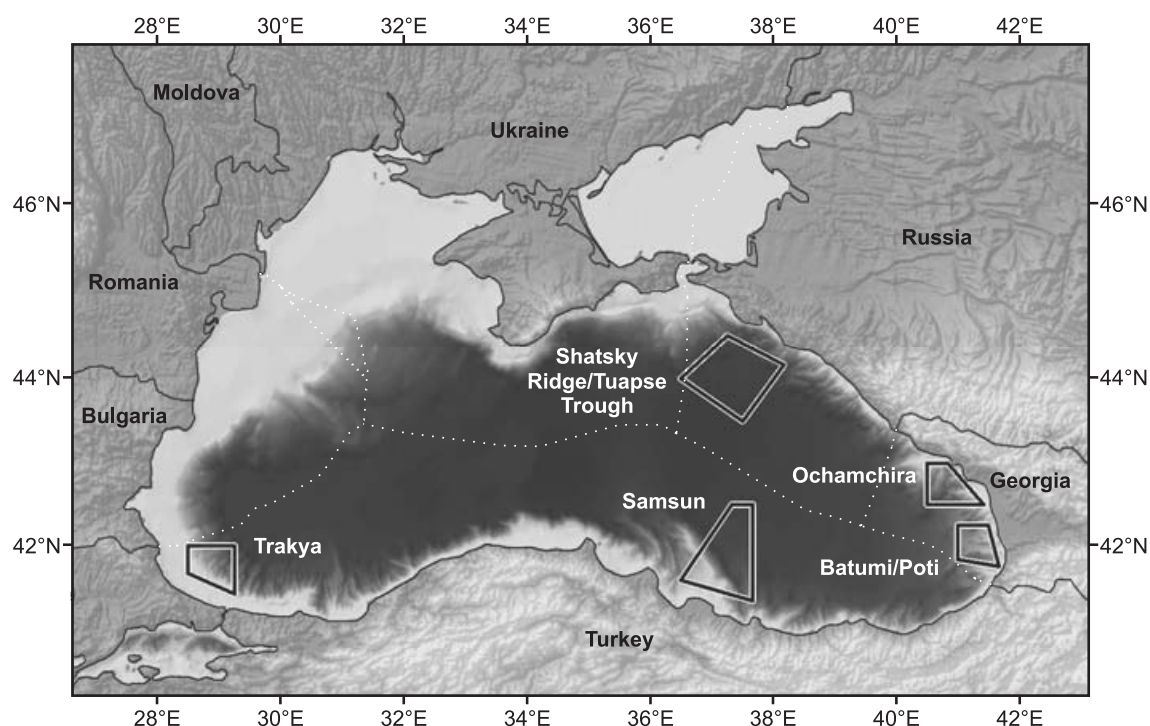


Figure 1. Study areas of the Legs 1 and 2 in the Black Sea.

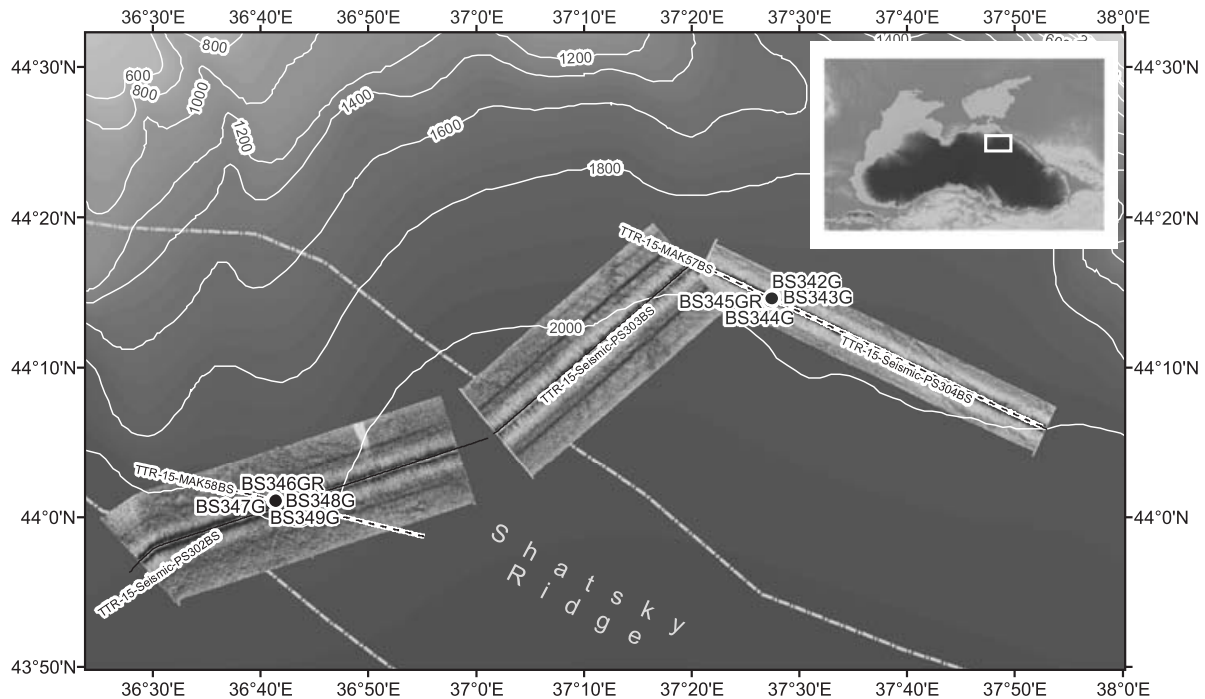


Figure 2. Location map of the Shatsky Ridge/Tuapse Trough Area.

Several gas seeps and near-surface gas hydrate deposits have been identified in 850-900-m water depth on the continental slope offshore Batumi and Poti (Georgia, eastern Black Sea) during an acoustic seabed mapping program conducted by the German FS *Poseidon* in 2004 (Klaucke et al., 2005, 2006)

Acoustical imaging systems were intensively used for reconnaissance tasks in the working areas. A first overview on the sea floor characteristics was obtained using the long-range sidescan sonar OKEAN, parallel towed with a short multichannel seismic system. The seismic data served as the primary tool to analyze the internal structure of sediments to locate gas carrying sediments and possible seepage areas. Near surface structures were additionally investigated using the shipboard 5.1 kHz subbottom profiler. For detailed studies of potential seep areas and mound structures the deep-towed high-resolution sidescan sonar MAK-1M was deployed, operating at 30 or 100 kHz signal frequency. The MAK-1M is also equipped with a 5 kHz subbottom profiler, which yielded detailed insight in the first few tens of meters of sediment.

The extensive groundtruthing campaign with various sampling techniques has been

carried out on the basis of the new seismic and acoustic data.

I.2. Seismic profiling data

I. FOKIN, H. KEIL, I. KLAUCKE, S. DOUNGAR,
I. KUVAEV, N. LURSMANASHVILI, I. MAKALATIA,
V. MALIN, R. MURZIN, D. NIKONOV, S. OKAY,
D. TITKOVA, M. WAGNER-FRIEDRICH AND
A. ZOTOVA

Seismic surveying during Legs 1 and 2 of the TTR-15 cruise was carried out to gain sufficient overview information about subsurface structures such as diapirs, mounds and mud volcanoes as well as indications of gas and gas hydrate bearing sediments and potential gas seepage areas. The acquired seismic data had to be processed producing brute stacks by stacking the channels 26, 49-50 and 52-64 in order to select the most promising sites for detailed studies. In total, 20 seismic profiles with a length of 677 km were shot during the cruise.

I.2.1. Shatsky Ridge/Tuapse Trough Area

Three profiles were shot within this study area offshore Russia (Fig. 2). Two pro-

files, GeoB05-050 (PS302BS) and Geob05-051 (PS303BS), oriented in the SW-NE direction cover the Shatsky Ridge and the Tuapse Trough, showing a well stratified record with no indications of gas seepages. The profile GeoB05-052 (PS304BS) (Fig. 3) was shot in the NW-SE direction and crosses two ridges of the Tuapse Fold Belt.

The Tuapse Fold Belt is characterized by the protrusion of diapirs forming 3 ridges striking in the SW-NE-direction. The northernmost and the middle ridge are crossed by seismic line GeoB05-052 (PS304BS). The folds are imaged as transparent zones and are interpreted as mud diapirs originating from the water saturated low-density clays of the Maikopian Formation. In the subsurface the diapirs are observed up to 100 ms TWT bsf in the North and 400 ms TWT bsf in the South. The protrusion of the southern diapir is expressed by a morphological uplift on the seafloor. The ridge rises up to 200 m above the seabed and blurred chaotic reflections can be traced down to the diapir. On the top and the flanks of the diapirs "bright spots" in a depth of 100-250 ms TWT bsf indicate the

presence of underlying free gas in the sediments. The diapirs are separated by a small basin with well stratified infill, showing a signal penetration down to 800 ms TWT. Above the diapirs one small mound is formed on the seafloor. Beneath the mound the record is characterized by the presence of an acoustically transparent zone with a width similar to the diameter of the mounds. This zone probably acts as a migration pathway for gas and its presence suggests that the mound is a potential gas seepage location.

I.2.2. Batumi/Poti Area

The majority of the seismic profiles were shot offshore Batumi and Poti (Georgia) (Fig. 4). The margin in the area is characterised by the presence of a complex system of canyons and dividing ridges. The first four profiles were shot during Leg 1 and eight more during Leg 2. Four ridges and canyons are crossed by five seismic lines in the strike direction. Several seepage sites such as the Batumi seep located on the Kobuleti Ridge, were known in the area from hydro-acoustic

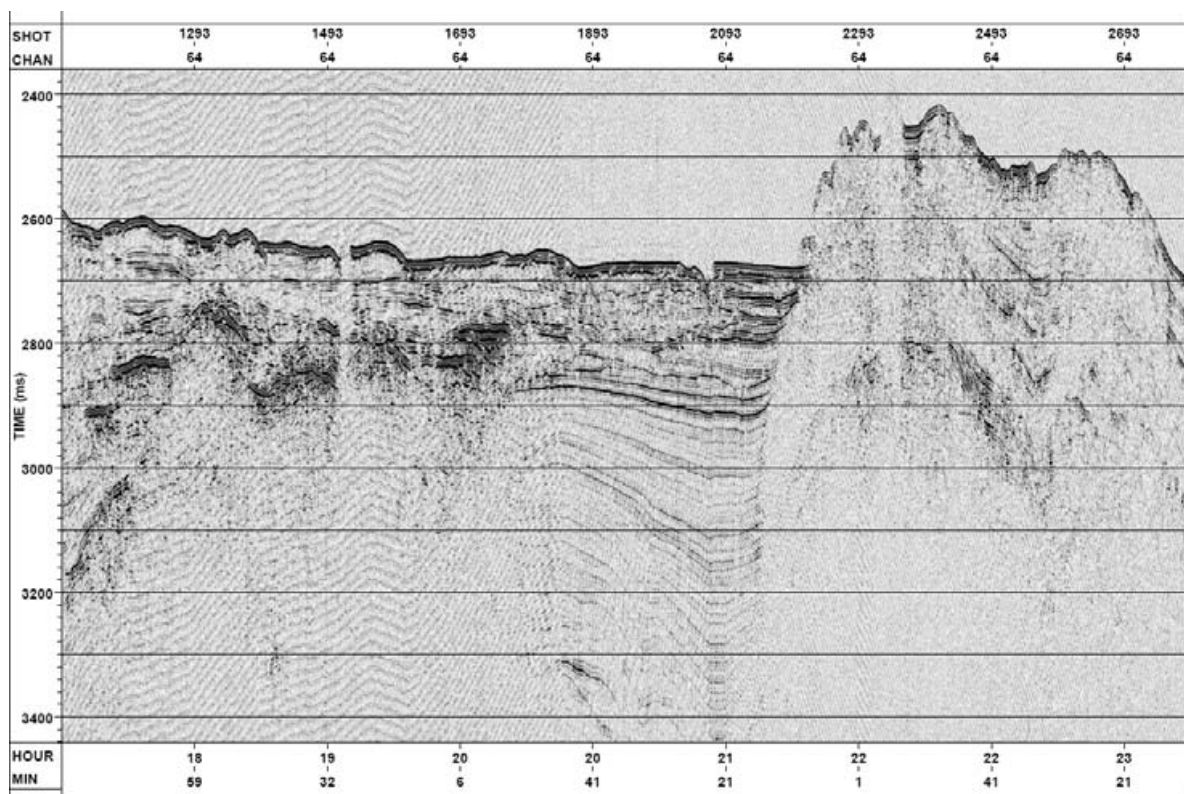
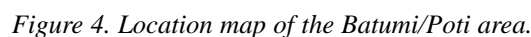


Figure 3. Seismic line PS304BS.



ridge slides are suspected from the character of the record. The Kobuleti Ridge has a height of about 400 m above the surrounding channels.

Along the most westward profile GeoB05-054 (PS306BS) (Fig. 5) two small mounds, the Pechori and the Iberia Mound were crossed on the Kobuleti Ridge. The Pechori Mound is located at the northern edge and the Iberia Mound at the southern edge of the Kobuleti Ridge. They are cone-shaped with a height of about 75 m and a diameter of 2-2.5 km. Beneath vertical acoustic transparent zones indicate gas saturated and homogeneous material migrating towards the seafloor. Due to the signal attenuation it is not possible to detect if faults are

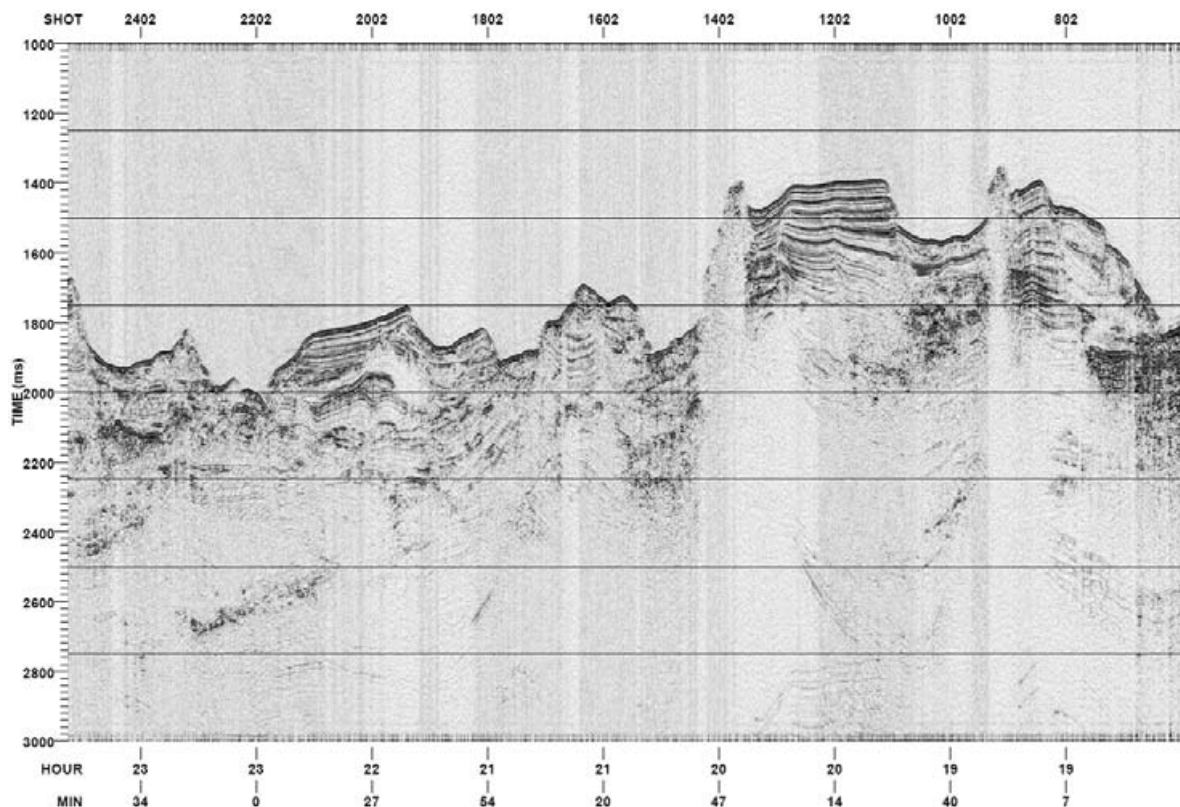


Figure 5. Seismic line PS306BS.

acting as pathways. However, several faults affect the surrounding sediments and upward gas migration is probably related to faults.

Two small diapiric folds occur in the subsurface of the Kobuleti Ridge rising up to 500 ms TWT bsf. Their flanks are onlapped by weak reflections of stratified sediments. Bright spots, observed at 300 ms TWT beneath the Iberia mound on the top of the diapiric structure and to the south of the Pechori mound in 300 ms TWT bsf, indicate the presence of shallow gas. In the north of the Kobuleti Ridge the profile covers several unnamed ridges and canyons showing less topography. The base of the Supsa Canyon to the north of the Kobuleti Ridge is characterized by strong reflectors with a thickness of 350 ms TWT, which might represent different unconformities, and showing recent activity of the channel. Beneath these reflections the signal is attenuated.

The Profile GeoB05-056 (PS308BS) (Fig. 6) crosses the central part of the study area and covers the same ridges and channels as profile GeoB05-054 (PS306BS), but shows

some different morphology and structural features. Additionally the Adjara Ridge and the Natanebi Canyon further southward are covered by this profile. The Adjara Ridge has a height of up to 500 m and shows very steep flanks. On its southern flank two slides occurred. A further slide took place on the southern flank of the Kobuleti Ridge, which was also identified on profile GeoB05-054 (PS306BS). The subsurface of the Adjara Ridge is characterized by signal attenuation while the Kobuleti and a further ridge in the North show well stratified bedding with increased signal penetration. This profile crosses the Batumi seep area located on the Kobuleti Ridge, which was known from the survey of the Poseidon Cruise in 2004. In the seismic data the seep area is represented by a small build-up on the seafloor, but no direct indications of seepage are seen. But a BSR like reflection in ~ 300 ms TWT bsf partly crosscutting the surrounding strata of the Kobuleti Ridge indicates the presence of free gas bearing sediments. The seismic reflection characteristics show that the seep area is located above several near vertical faults,

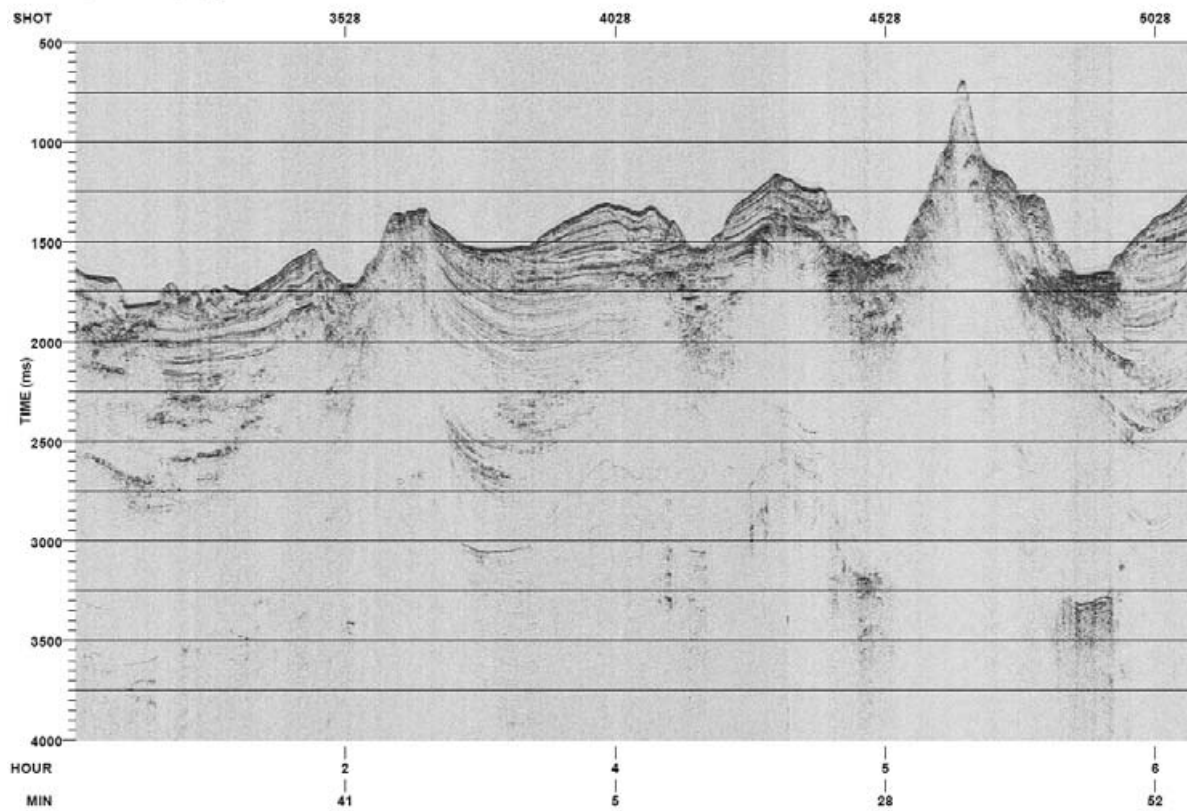


Figure 6. Seismic line PS308BS.

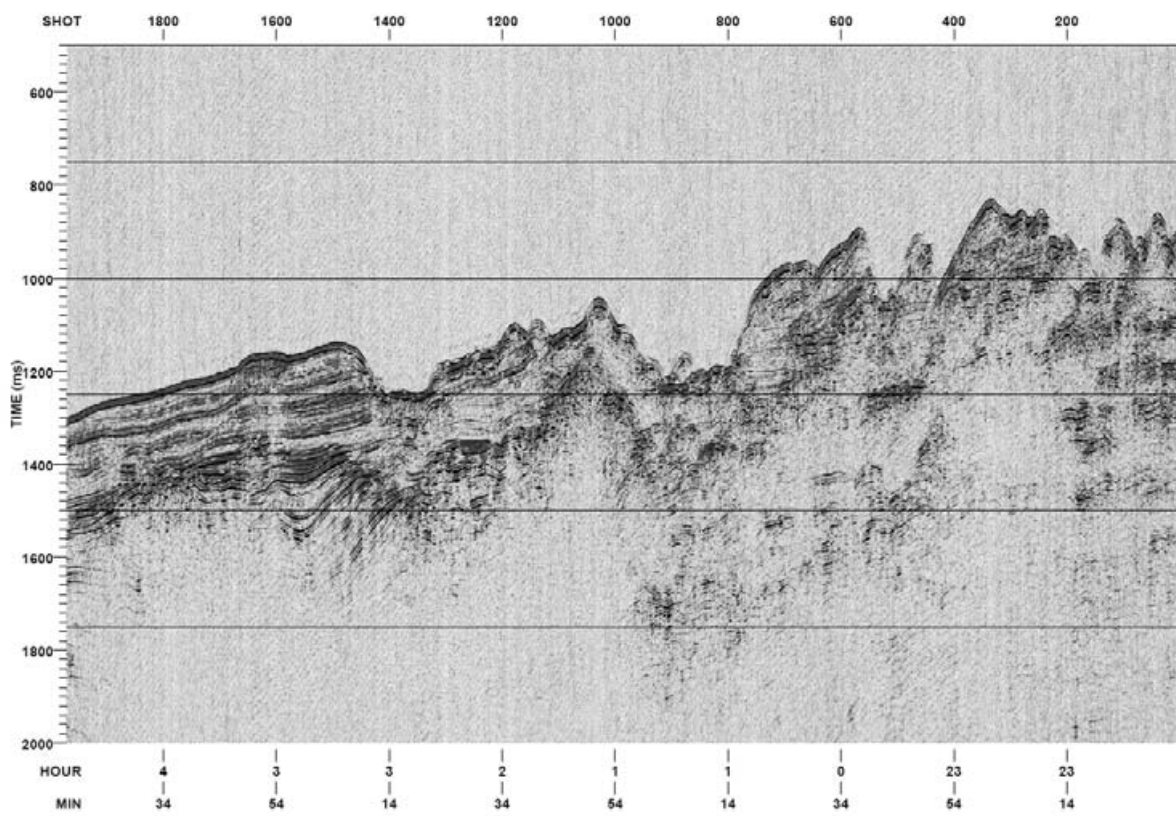


Figure 7. Seismic line PS314BS.

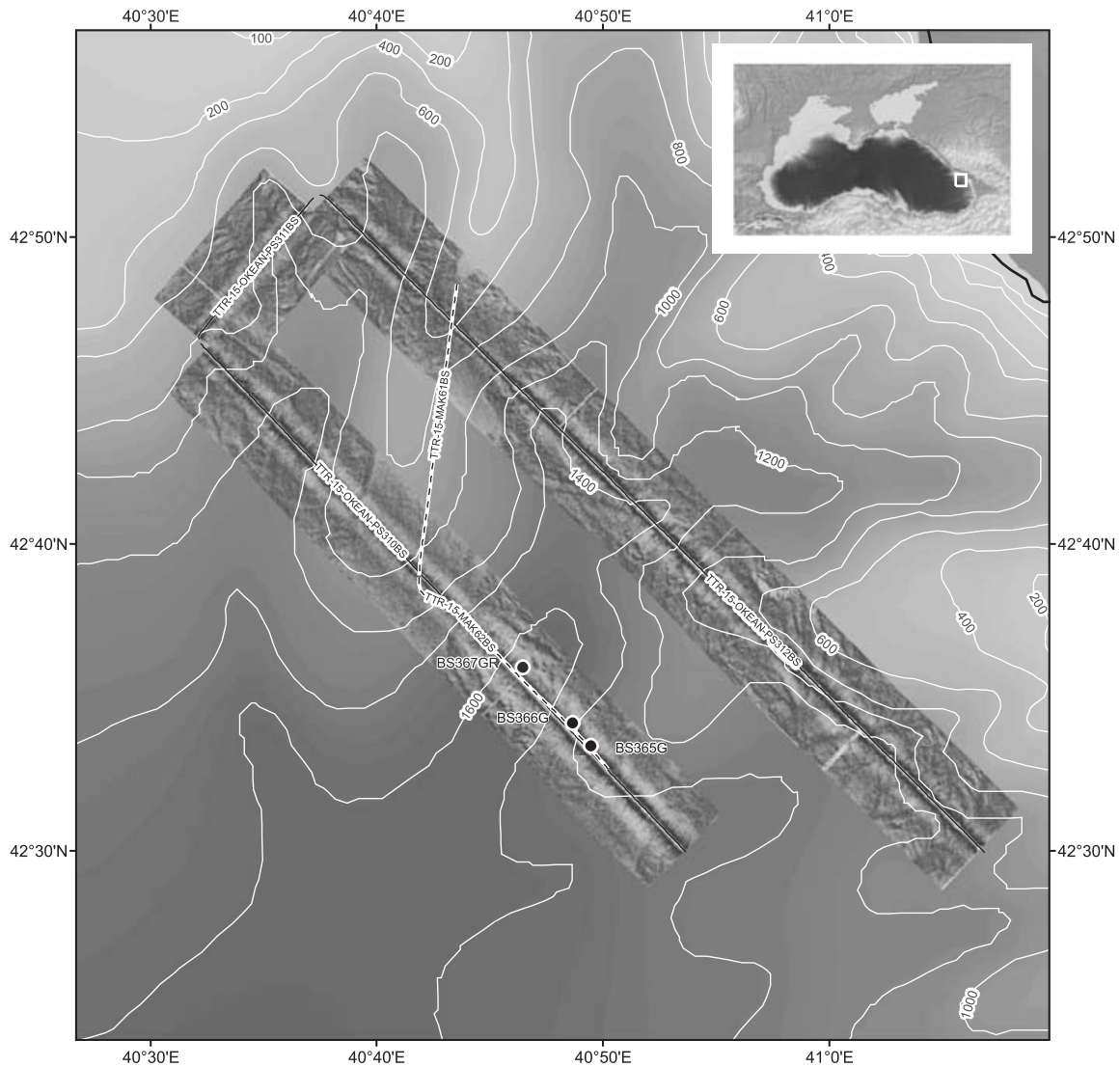


Figure 8. Location map of the Ochamchira area.

which can be traced from the BSR towards the seafloor. One of them, disrupting the seafloor reflection, is recently active. The Batumi seep area was intensively observed by gravity cores, autoclave, multicorer, TV grab and ROV. For further investigations a cross line GeoB05-062 (PS314BS) (Fig. 7) was shot in the W-E direction along the Kobuleti Ridge. On this profile a vertical transparent zone beneath a small build-up on the seafloor with washed out chaotic reflections indicates a seep structure. In the subsurface again a BSR is observed at the same depth. The lateral extension of the Batumi Seep is about 900 m on Profile GeoB05-056 (PS308BS) and about 1200 m on Profile GeoB05-062 (PS314BS).

I.2.3. Ochamchira area

At the beginning of Leg 2 we shot three seismic profiles in the Ochamchira Area offshore Georgia (Fig. 8). This area is located to the north of the Batumi/Poti Area and is also characterized by the presence of canyons and ridges. Two profiles are oriented in the NNW-SSE direction, crossing two canyons and ridges. The general structures of the area are seen in Profile GeoB05-058 (PS310BS) (Fig. 9). A large ridge is observed in the centre of the profile, showing well stratified bedding with strong and continuous reflections, which can be traced down to 700 ms TWT bsf. The ridge rises up to 750 m above the seafloor of the surrounding canyons. The top of the ridge shows only low topography, but

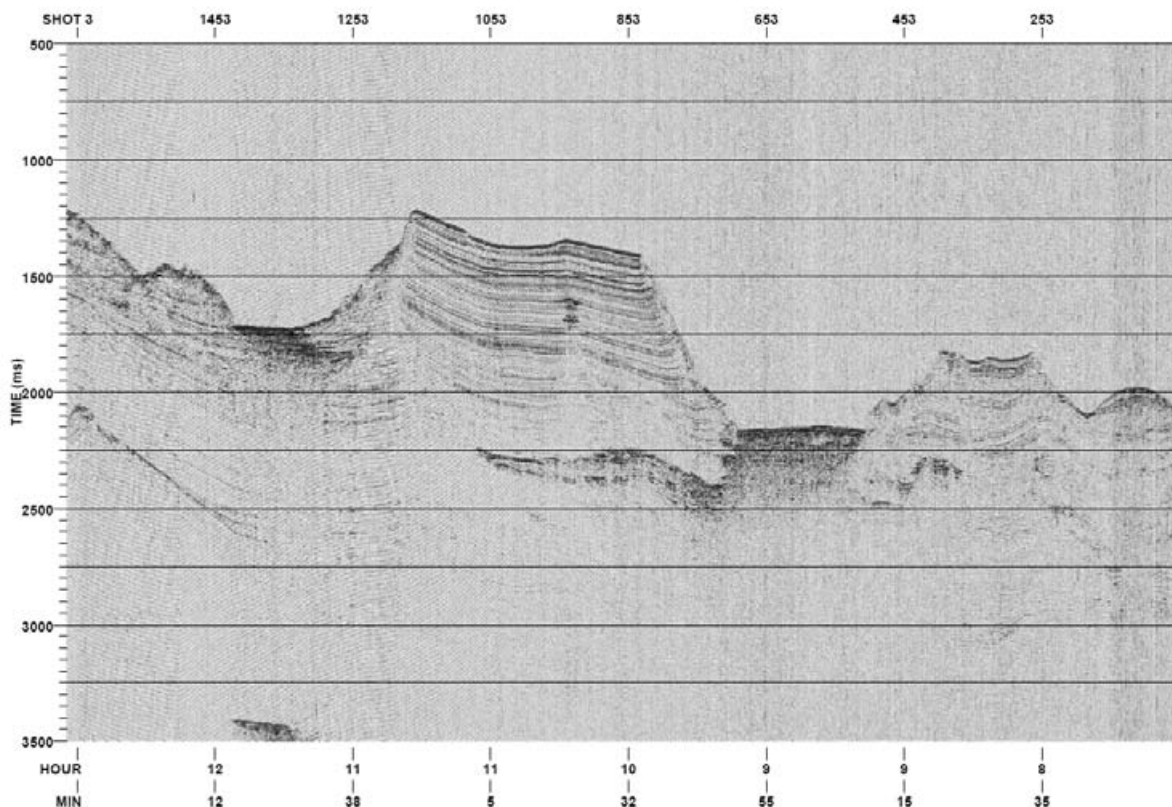


Figure 9. Seismic line PS310BS.

its flanks dip steeply down to the channels. Bright spots are observed in the southern part of the ridge at different depth of 500-500 ms TWT bsf, bent toward faults. But no evidences for gas migration towards the seafloor and gas discharge could be identified. Two strong reflectors at a depth of 1s TWT and 1.1s TWT bsf between the shot points 700 and 160 are still of unknown nature. The reflectors are located in the south of Channel 1 and can be traced northward, wedging out in the middle part of the ridge. The seafloor of the channels has high amplitude and shows strong chaotic reflections beneath. For further investigation a MAK-line was carried out along Channel 1. A further small ridge is imaged to the south of Channel 1, showing well stratified layers. Its northern flank shows two small build-ups characterized by acoustic transparency beneath, maybe indicating shallow gas. In the subsurface beneath these build-ups a BSR-like structure is observed.

I.2.4. Samsun area

Three seismic lines were collected along the Turkish margin (Fig. 10). The lines GeoB05-068 (PS320BS) and GeoB05-070 (PS320BS) were shot parallel to each other in the NW-SE direction in the Samsun Area. The third line GeoB05-071 (PS322BS) is oriented in the NE-SW direction, crossing both lines.

An overview of the general features along the Turkish margin is shown on the profile GeoB05-068 (PS320BS) (Fig. 11). The sediments are mostly well stratified, but showing vertical variations in amplitudes below a depth of 100 ms bsf. In the upper part of the slope the sediments are disturbed by several gas columns, characterized by acoustic transparency. Between the shot points 1040-1400 sediment waves are observed in the near subsurface, probably generated by turbidity currents. At the southern edge of the profile the sediments are affected by recently active faults. Between the shot points 860 and 960 a channel cuts about 150 m into the sediments.

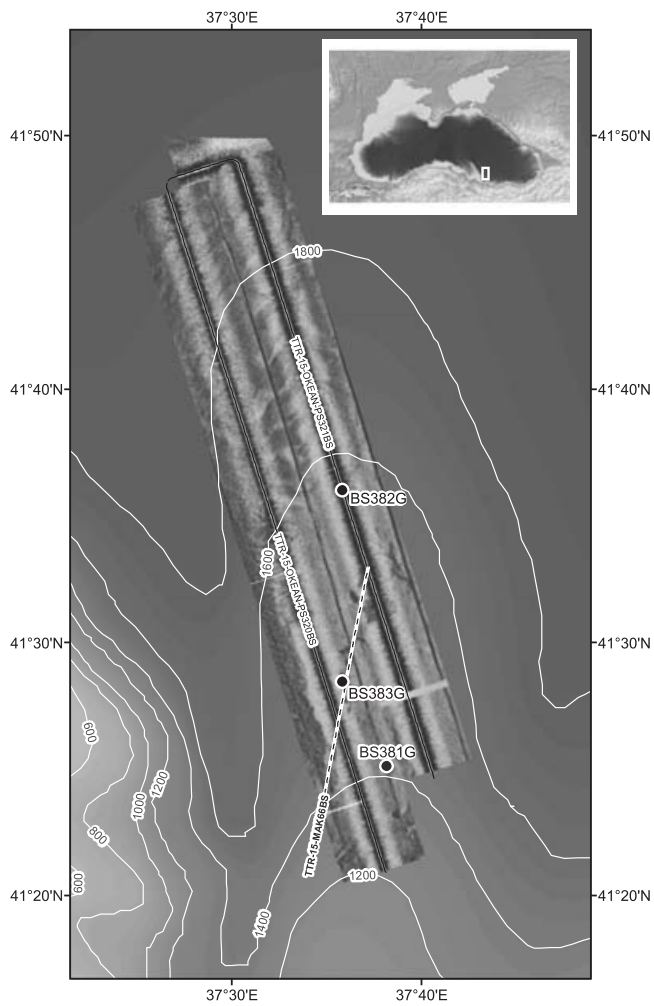


Figure 10. Location map of the Samsun area.

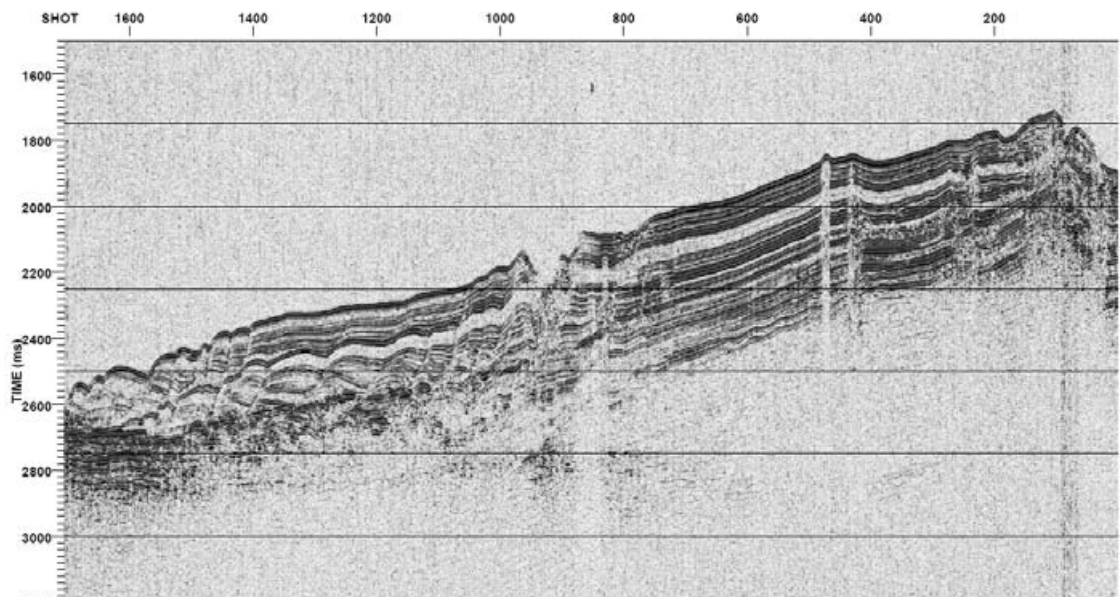


Figure 11. Seismic line PS320BS.

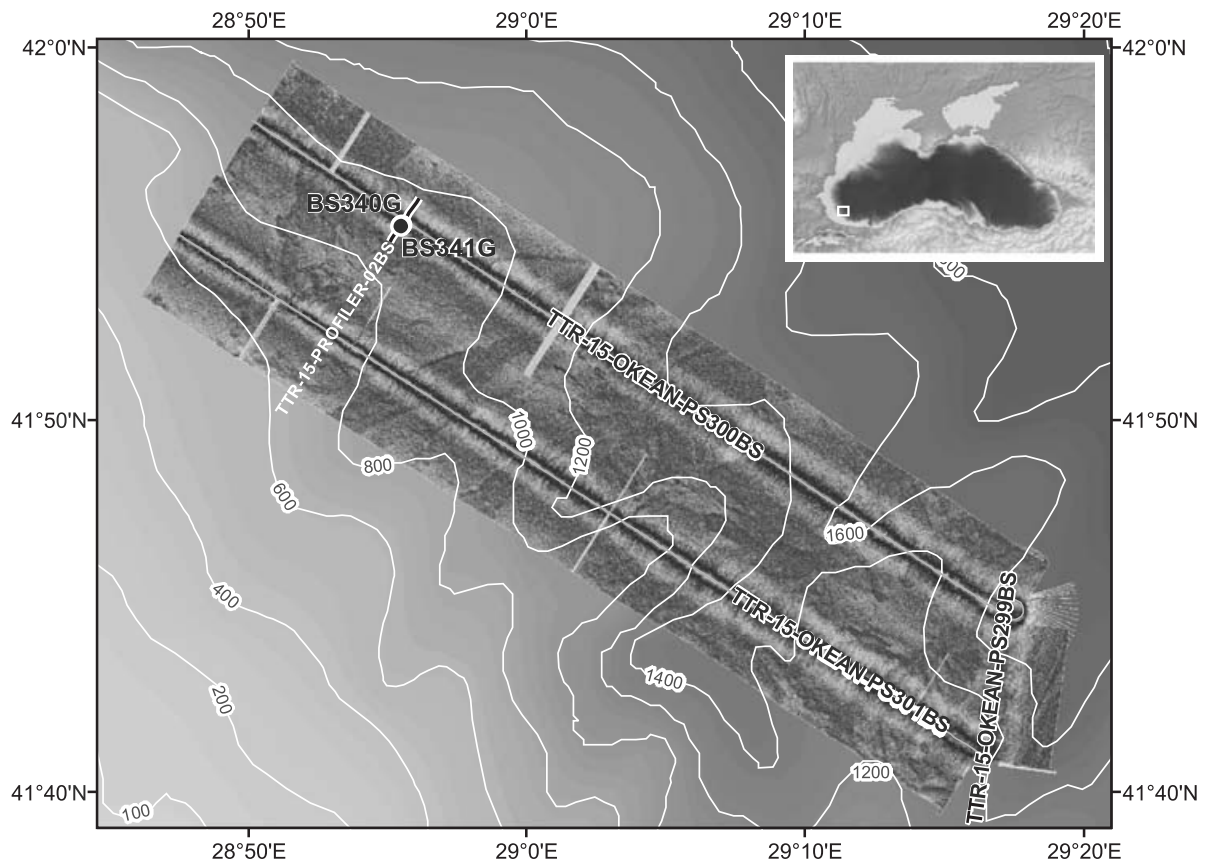


Figure 12. Location map and the OKEAN image of the Trakya area.

A BSR can be seen at the northwestern edge of the line at a depth of 300 ms TWT bsf. Acoustic transparency beneath the BSR indicates that sediments are gassy.

I.3. Sidescan sonar data

I. FOKIN, I. KLAUCKE AND A. AKHMETZHANOV

I.3.1. Trakya area

A short OKEAN and hull mounted profiler survey was conducted on the southwestern Turkish margin in order to map seabed features related to hydrocarbon fluid seepage (Fig. 12).

The survey covers a portion of a canyon dissected slope in the water depths of 800-1600 m to the northwest of the Bosphorus Strait.

The OKEAN imagery shows an area of high backscatter along the canyon axes suggesting seabed erosion by bypassing gravity flows (Fig. 12). Slopes of dividing ridges also

show areas of high acoustic backscatter which are attributed to sediment failures. Several high backscatter targets recognised along the crests of ridges were crossed with a 3.5 kHz profiler. The record along Profile 02BS showed that one of the targets is a positive acoustically transparent feature protruding from under the hemipelagic cover suggesting that it may be a mud volcano (Fig. 13).

I.3.2. Shatsky Ridge/Tuapse Trough area

Acoustic seafloor mapping was carried out on a sector of the Russian margin. The survey comprised three OKEAN and two MAK lines which covered the base of the Pallas Uplift to the southeast and northern Tuapse Trough (Fig. 2). The western part of the study area is located above the Shatsky Ridge and seabed features related to deeper sourced seeps were expected to be found here.

OKEAN records along lines PS302-

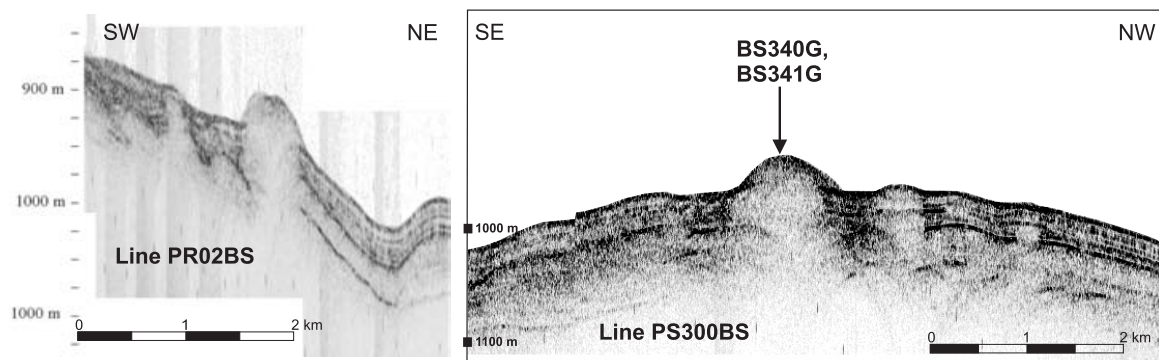


Figure 13. 3.5 kHz profiles from Trakya area with a new mud volcano and sampling stations location.

304BS show that the seafloor lacks large scale features. Several areas of high backscatter can be attributed to slope instability features, thalwegs of large canyons such as Anapa Canyon crossed by Line PS-303BS and diapiric ridges within Tuapse Trough (Line PS-304BS).

A 30 kHz MAK line MAK-57BS was run along the seismic and OKEAN line PS-304BS covering the axial part of the northern Tuapse Trough. At the southeastern end of the line a 250 m high diapiric ridge is crossed. The sonographs shows widespread sediment instability features along the ridge flanks suggesting recent movements (Fig. 14). To the west of the ridge the line crosses a broad valley developing beyond the mouth of a canyon system offshore Novorossiysk. The seafloor is characterised by a complex acoustic pattern related to seafloor erosion and sediment instability. The subbottom profiler record shows a well developed levee

along the western flank of the valley. Reduced acoustic penetration beneath the valley's floor suggests the presence of coarse grained sediments.

A high backscattering circular conical structure about 500 m in diameter and 25 m high is recognised on the sonograph and sub-bottom profiler record on the western flank of the valley (Fig. 15). The structure was found to be a seepage site and called Petroleum Mound. A profiler record across the mound shows a well developed moat surrounding the mound. The presence of the moat suggests frequent activity of gravity flows bypassing the site.

Another 30 kHz MAK line MAK-58BS was run oblique to the seismic line PS-302BS at the base of the Pallas Uplift. The profiler record shows that the sedimentary sequence of the area is dominated by up to 30 m thick acoustically transparent lens-shaped units interbedded with thin, up to 10 m acoustical-

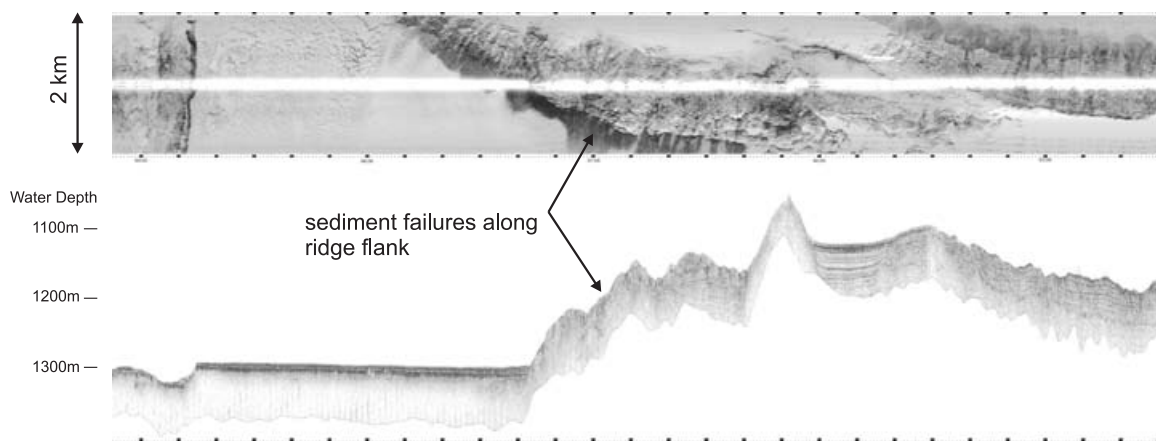


Figure 14. Fragment of MAK Line MAK57BS showing details of a diapiric ridge in the Tuapse Trough.

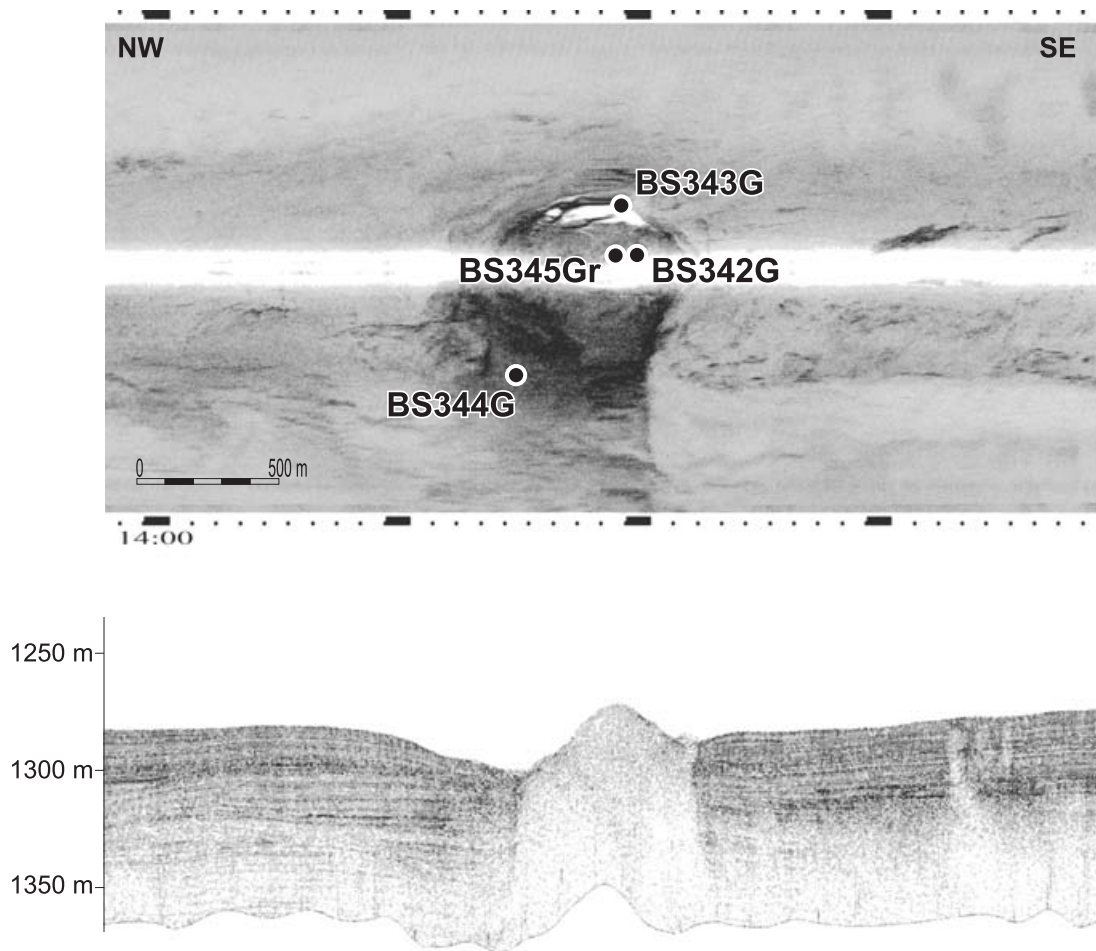


Figure 15. Fragment of MAK Line MAK57BS showing details of the Petroleum Mound. Location of sampling stations is also shown.

ly stratified intervals. The transparent units are interpreted as debris flow deposits which is in agreement with the rough surfaces and presence of rafted blocks observed on the sonographs. Near the western end of the line a structure called Dolgovskoy mound is crossed. The structure represents a conical feature up to 75 m high and almost a kilometre wide characterised by a high backscatter on the sonograph (Fig. 16).

1.3.3. Batumi/Poti area

Survey with the OKEAN long-range sidescan sonar along lines PS-305-308BS and PS-313-319BS covered a total area of nearly 1300 km² on the continental margin offshore Batumi and Poti (Fig. 4). The slope is dissected by several large canyons like Northern,

Supsa, Central and Natanabi and as a result a complex acoustic backscatter pattern is observed on the OKEAN imagery. A brief analysis of the imagery shows that the areas of highbackscatter forming the pattern are produced by gullied canyon slopes, canyon thalwegs and slope instability features developing along slopes of the canyons or adjacent ridges.

5 MAK lines were collected in the area in order to obtain a high resolution imagery of the seep areas and surrounding environments.

Line MAK-59BS runs along the slope of the area at the water depths about 1000-1200 m and crosses Northern, Supsa and Natanebi Canyons and a gently sloping rise which can be considered as an extension of the Kobuleti Ridge and hence will be called, later in the

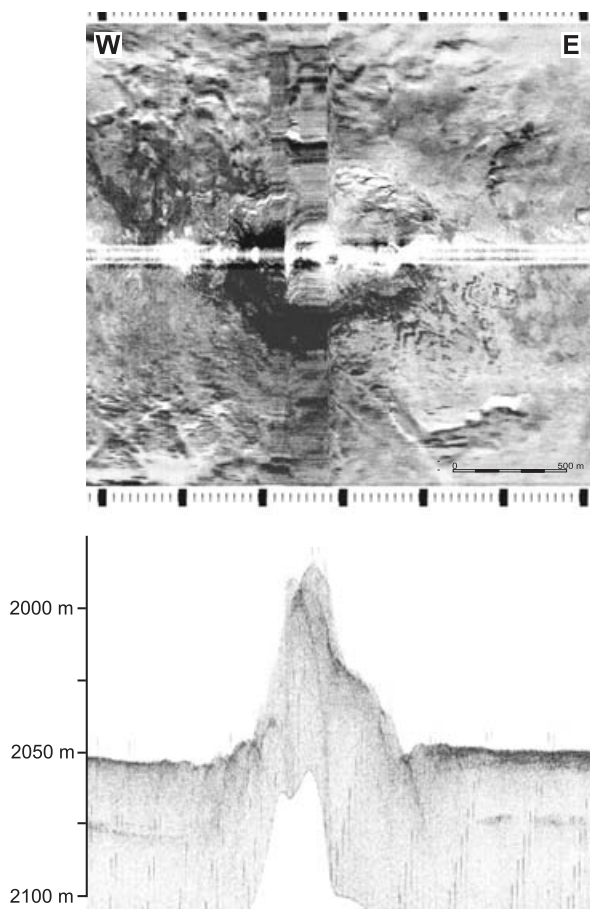


Figure 16. Fragment of MAK Line MAK58BS showing details of the Dolgovskoy mound.

chapter, the Kobuleti Rise (Fig. 17). Two seep structures, Pechori and Iberia Mounds, are also crossed.

The thalweg of the Northern Canyon is imaged at the northern end of the line. The sonograph shows the intensive erosion of the seafloor suggesting the active status of the canyon. The walls of the canyon are steep and fault-bounded which is well seen on the profiler record. The Supsa Canyon is crossed about 4 km to the south and appears less active in the recent times as the sonograph and profiler record show the development of a thin sedimentary drape over the canyon's features. To the south of the Supsa canyon the line runs across the Kobuleti Rise. The profiler record shows a number of faults, which not only bound it along both flanks but also displace its surface at several places, with offsets being up to 50 m. The Rise hosts two seep structures: Pechori and Iberia

Mounds. The Pechory Mound has a 20 m high elevation which is associated with a fault bounding the north side of the Kobuleti Rise. The top of the Mound is characterised by high acoustic backscatter on the sonograph. Unprocessed sidescan sonar records show multiple gas flares in the water column above the top of the Mound (Fig. 17) similar to those found above other seep structures in the area (Klaucke et al., 2005, 2006). The Iberia mound is located near the southern flank of the Kobuleti Rise where it is also associated with a fault. The Mound is a conical feature nearly 30 m high and a kilometre wide. Gas flares were also detected in the column at its top (Fig. 17).

At its southern end the line crossed the Natanebi Canyon which is also characterised by steep, fault-bound walls and intensively scoured thalweg. The sonograph and profiler record suggest that there are active flows in the canyon.

Line MAK60BS was run along the axis of the Natanebi Canyon and crossed a junction between two tributaries, approaching the junction point from the east and the south. Since the line was run almost along the eastern tributary its meandering thalweg was particularly well imaged. The record shows that the canyon has extensively gullied walls but is draped by a thin veneer of hemipelagic sediment. Only a small portion of the southern tributary was crossed by the line but the data show that it serves as one of the major conduits for gravity flows in the Natanebi Canyon. The thalweg of the tributary is located 140 m lower than the thalweg of the eastern one. The sonograph shows a spectacular field of gravel waves characterised by contrasting very high backscatter. The length of the waves is 30-40 m and they are 2-3 m high (Fig. 18).

Line MAK63BS was run from the east to the west in the margin's dip direction, crossing Supsa and Central Canyons, Kobuleti Ridge and the Batumi seep area. The Supsa and Central Canyon show the presence widespread sedimentary failures along their flanks. Most of the failures have arcuate shapes common for many canyons worldwide.

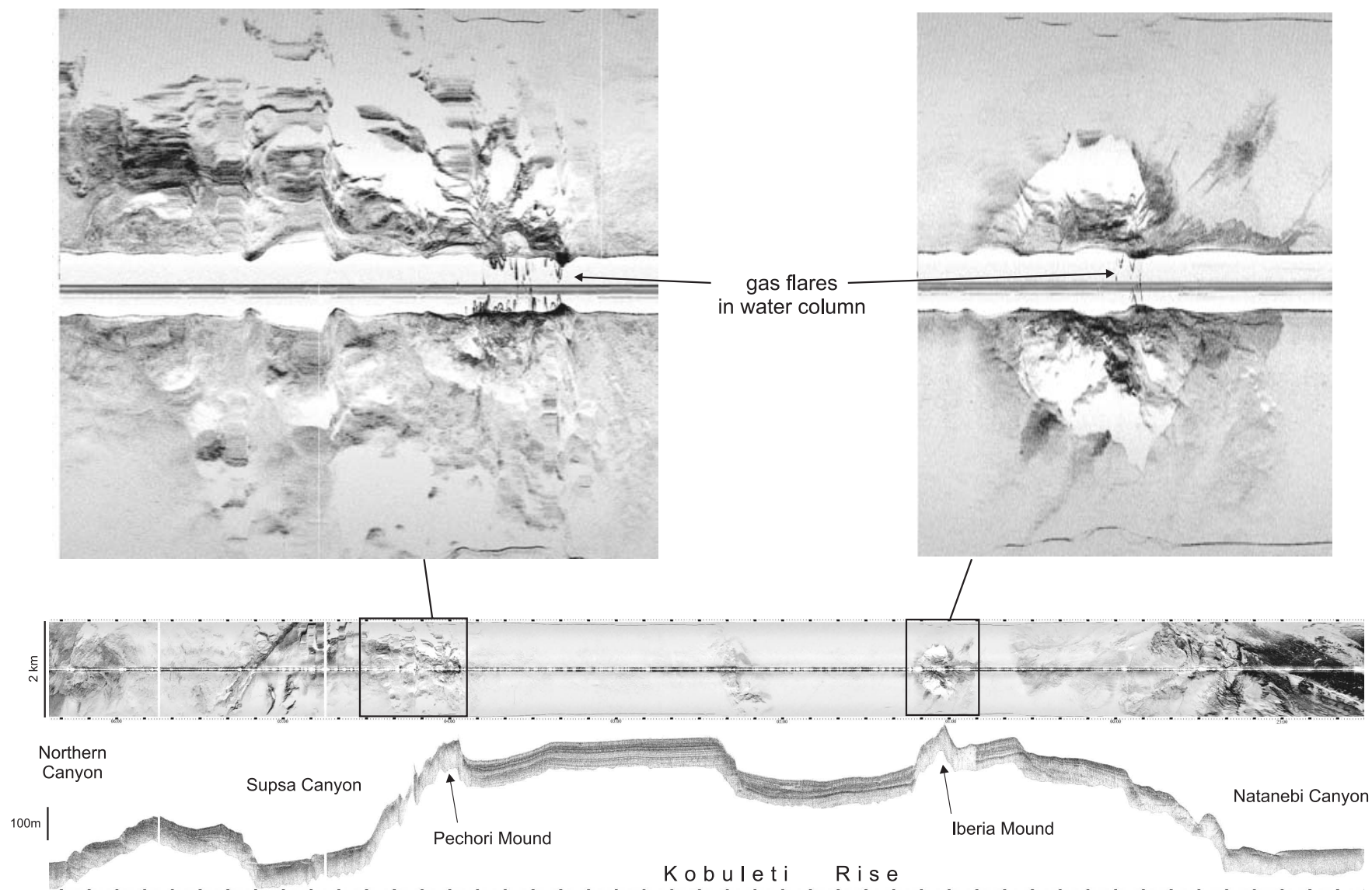


Figure 17. Fragments of MAK Line MAK59BS. Close ups of the unprocessed record across Pechori and Iberia mounds show gas flares in the water column.

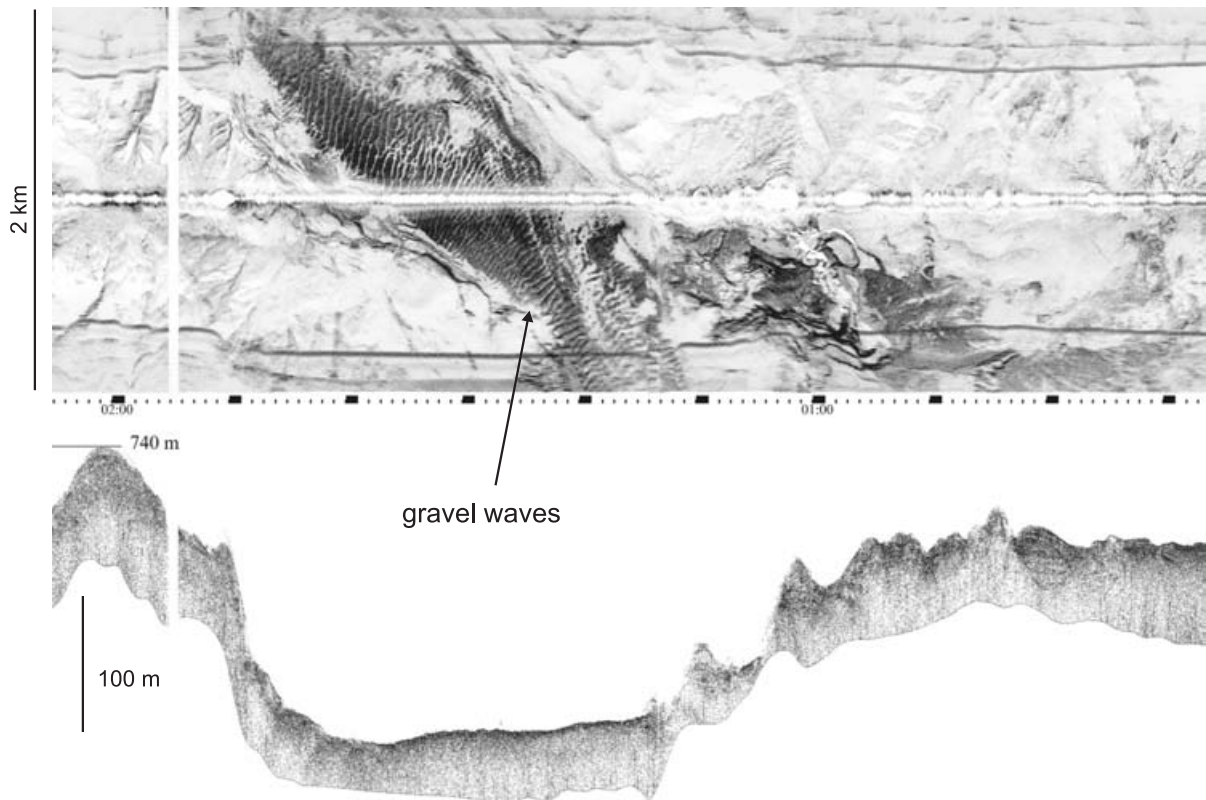


Figure 18. Fragments of MAK Line MAK60BS showing gravel waves at the bottom of the Natanebi Canyon at the depth of about 800 m.

The Batumi seep (Klaucke et al., 2006) is seen on the sonograph and profiler record near the western end of the line. The system of criss-crossing and en-echelon fractures within which the seep develops is imaged particularly well. Comparison with the multibeam bathymetry of the area collected during FS *Poseidon* cruise (Klaucke et al., 2006) indicates that these fractures could be part of a much larger fault system bounding a large depression on the top of the Kabuleti Rise, which was also crossed by the Line MAK59BS (Fig. 17).

Line MAK64BS was run along the lower reaches of the Poti Ridge. The sonograph and profiler record show a thick hemipelagic cover developing over the area affected to a small degree by sediment instability processes. As a result small debris flows and creep structures are observed in a few places.

Line MAK65BS crossed the lower reaches of the Supsa Canyon and then went across Colkheti seep structure. The sonograph showed a field of giant arcuate scours up to 500 m across and 10 m deep within the

canyon thalweg. The scours are draped by a few meters thick hemipelagic veneer indicating the absence of recent activity. At the southern end of the line the Colkheti seep structure is crossed. It represents a plateau-shaped elevation developing on the flank of fault-bound Kobuleti Rise. The top of the structure has a patchy contrasting backscatter pattern. The sonograph also shows a possible mud flow emanating from the seep and running down the Rise flank.

I.3.4. Ochamshira area

Three OKEAN lines (PS310-312BS) provided a regional coverage of a portion of eastern Black Sea margin offshore Suchumi in the water depths between 1100 and 1600 m. The lines were run parallel to the slope crossing several submarine canyons and dividing ridges. The canyon walls and thalwegs are characterised by a patchy backscatter due to widespread gullies and slope instability features. The dividers have more uniform backscatter suggesting the presence

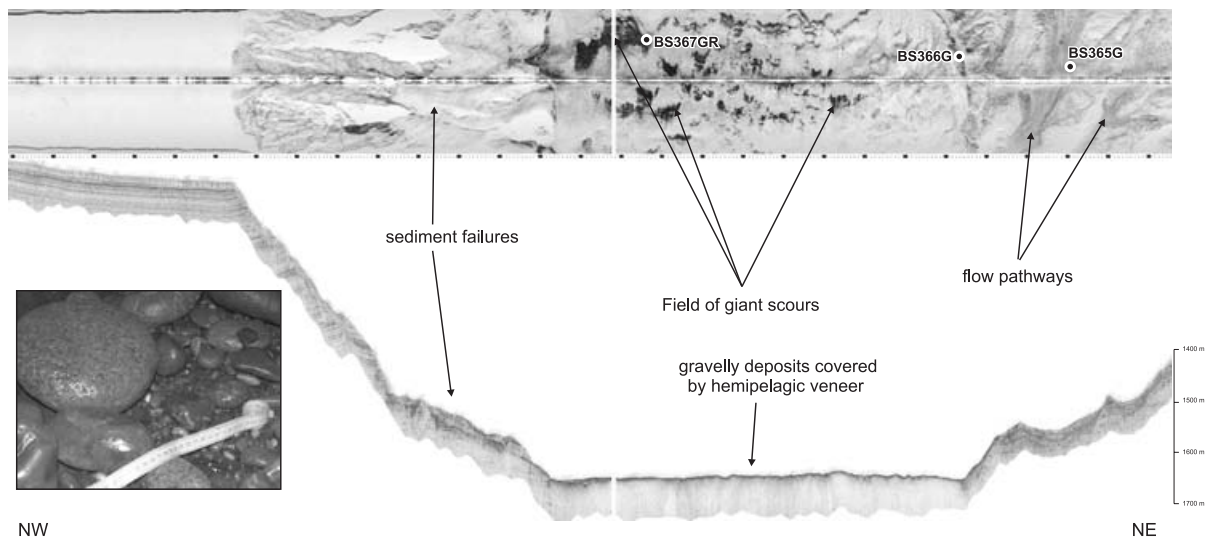


Figure 19. Line MAK62BS showing details of the Suchumi canyon. Sampling station locations are shown. Inset shows boulders and pebbles recovered at the station BS367Gr.

of a relatively undisturbed hemipelagic cover.

Two MAK lines were run in the area. Line MAK61BS was run along the ridge to the west from the Sukhumi Canyon and Line MAK61BS went across the Canyon.

Line MAK61BS running along the dividing ridge recorded mostly undisturbed seabed covered by an acoustically well stratified sediment with visible thickness of more than 50 m. In the upper part of the slope the line crossed a cauliflower-shaped, in plan-form, head of a tributary canyon about 125 m deep, which developed as a series of retrogressive failures. Further down the slope the subbottom profiler record indicated the presence of a buried slide and associated debris flow which could be traced along the line for almost 8.5 km

The sonograph and profiler along Line MAK62BS showed the details of the canyon walls and thalweg. According to the new data the canyon is 13.5 km wide and 570 m deep. It has a U-shaped profile with the thalweg being about 6 km wide (Fig. 19). The profiler record indicated that the flanks of the canyons are covered with a thick hemipelagic drape. The western wall is steep and subjected to multiple failures, with large blocks displaced along normal faults and talus deposits accumulating at the base of the wall. The record across the thalweg shows

flat seafloor with very limited penetration, suggesting the presence of coarse-grained deposits. The contrasting backscatter pattern observed on the sonograph is thought to be produced by the exposures of these deposits from under thin hemipelagic veneer. The eastern wall of the canyon is less steep and is formed by several displaced large blocks which are covered by a hemipelagic drape. The sonograph shows several flow pathways developing along the depressions between the blocks. These flows are likely to be produced by local sediment failures which appear to be frequent along this wall.

I.3.5. Samsun area

Acoustic mapping was carried out along a submarine ridge to the east of Samsun. The OKEAN survey covers about 550km² along the ridge crest running in the water depths between 1200 and 1800 m. The slope above 1600 m is characterised by a uniform low backscatter suggesting the presence of a thick hemipelagic drape. Several high backscattering patches, a few hundreds meters across and aligned in SSW-NNE direction, were observed on the image. Below 1600 m the backscatter distribution becomes more variable due to the presence of low backscattering bands on a generally medium backscatter background. Hull-mounted profiler records

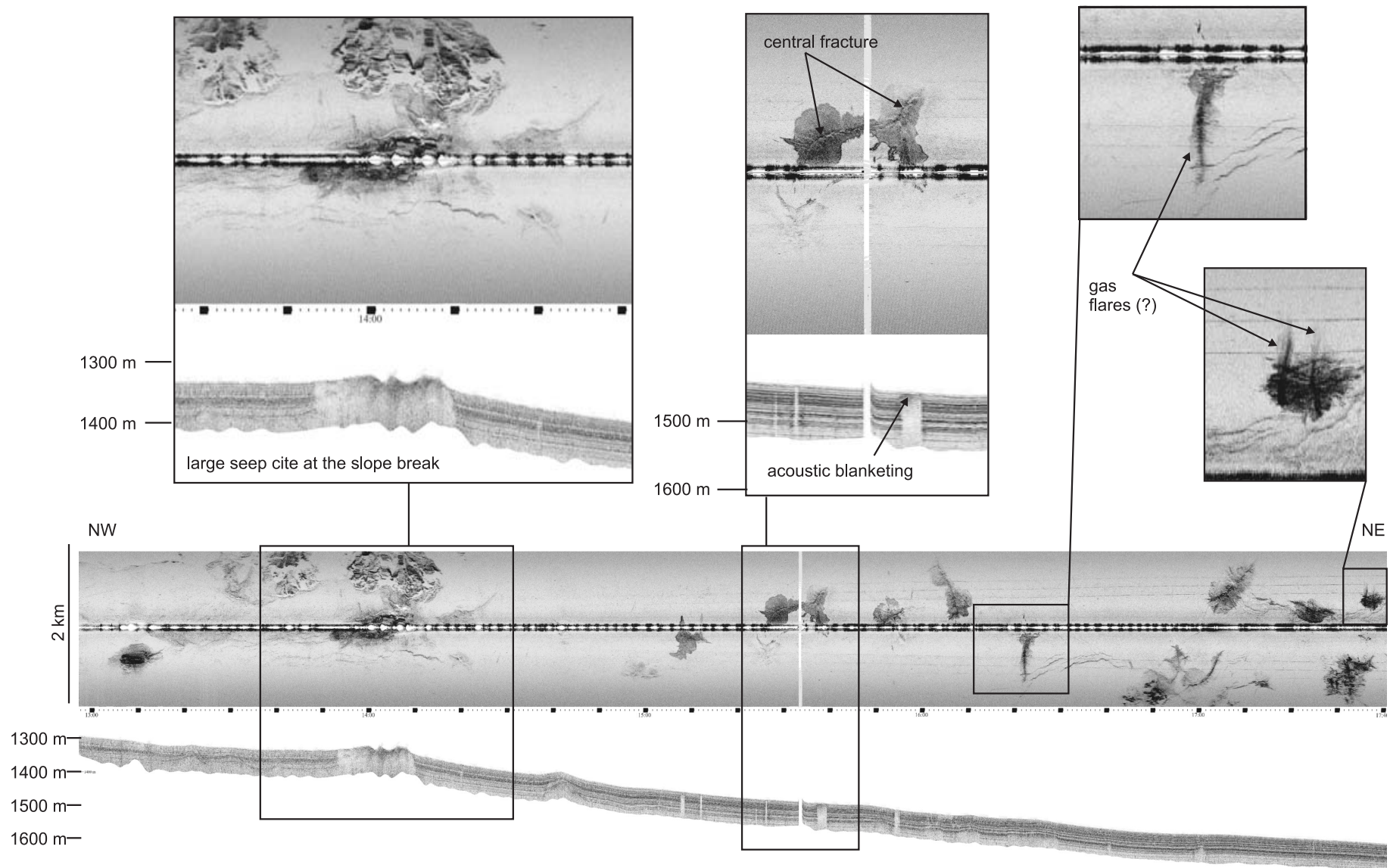


Figure 20. Fragment of Line MAK66BS showing details of seeps on the top of the submarine ridge offshore Samsun area.

along the lines show that such a pattern is due to the presence of large rotated blocks displaced downslope along a series of lystric faults.

Line MAK66BS was run in order to obtain a high resolution image of the high backscattering targets identified on the top of the submarine ridge from the OKEAN data. The sonograph shows a generally low backscattering seafloor with a sequence of well stratified hemipelagic sediments on the profiler record. There are 14 high backscattering patches scattered along the line (Fig. 20). A few large structures up to 1 km across associated with elevated outcrops of acoustically chaotic material are found at the upper part of the slope. They seem to develop along a fault as suggested by a noticeable slope break observed on the profile. High backscattering features down the slope are smaller, up to 500 m across, and have very sharp and irregular edges. Most of them develop around a central fracture or a system of fractures. Acoustically transparent conduits are observed on the profiler record where it crosses the fractures. Several causes of high backscatter are suspected for these features: gasified sediments, methane-derived carbonate crusts and near-surface gas hydrates. Some of the structures have linear feather-edged features associated with them which could be gas flares. According to their lengths on the sonograph they can be 55-120 m high (Fig. 20).

I.4. Gas seepage at Batumi seep off Georgia: results from ROV investigations

H. SAHLING, A. NOLTE, F. ABEGG, G. BOHRMANN,
I. KLAUCKE AND M. IVANOV

Three dives with the ROV Cherokee were conducted at Batumi Seep and an additional high-backscatter feature in the direct vicinity, named Kobuleti Seep. The dives gave a new insight into the process of methane seepage. Most remarkably, we found several individual sites of gas escape. The intensity varies between a few released bubbles every second to a very vigorous stream of bubbles of about 20 cm in diameter (named "Bubble Hole") (Fig. 21). The smaller streams escape from the seafloor which is perforated by holes of a few centimetres in diameter. We interpret these holes as evidence for recent to sub-recent seepage activity. Only a few of these holes showed active bubble escape during our observations. The vigorous escape site "Bubble Hole" was located in a disturbed seafloor area. This is probably the surface expression of a fault system imaged by sidescan sonar.

The ROV-mounted horizontally looking sonar system (frequency 325 kHz) was a powerful tool for detecting gas. The sonar is normally used to image the seafloor morphology. For detecting gas bubbles the ROV was moved above the seafloor until the

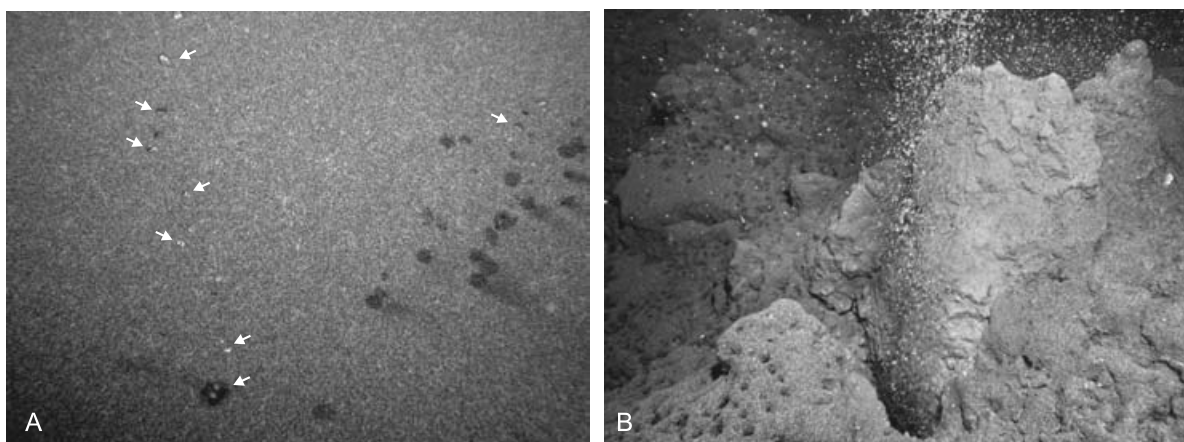


Figure 21. Gas bubbles observed during ROV Cherokee dives. A: low intensity bubbling (white arrows); B: Vigorous stream of bubbles from the "Bubble Hole".

seafloor morphology was not visible anymore. The gas bubbles, however, showed up as very strong reflections in the water column. It was very easy to move with the ROV to these sites and follow the stream of bubbles down to the seafloor. We used the sonar to map large areas of the Batumi Seep and found that many individual gas streams occur in this area.

I.5. Bottom sampling data

A. MAZZINI, E. KOZLOVA, V. BLINOVA,
A. OVS'ANNIKOV, D. KOROST, D. NADEZKIN,
A. SHARAPOVA, A. BELOVA AND Y. MALYKH

Recent sedimentation in the Black Sea

Most of the sampling stations collected during the TTR15 Leg 1 retrieved the top three modern sedimentary units that characterise most of the deep water areas of the Black Sea. A brief description of these units follows. The shallowest Unit 1 (Djemetinian layers) consists of thin alternating coccolithic ooze (mostly *Emiliana huxleyi*), and clayey sediment laminae; Unit 2 (Kalamitian layers) consists almost entirely of thin laminations of sapropel with occasional coccolithic ooze laminae; Unit 3 (Novoeuxinian layers), interpreted to be a lacustrine facies, consists of laminations of terrigenous clayey material, sometimes with abundant silty admixture, sometimes very fine and well sorted, commonly containing hydrotroilite layers. These units reach their maximum thickness in the central part of the Black Sea; Unit 1 and 2 are on average 30 cm thick, while Unit 3 can reach several metres in thickness (Ross and Degens, 1974).

Authigenic carbonates

The same types of authigenic carbonates described by Mazzini et al. (2004) were retrieved in several areas sampled during this leg. The authigenic carbonate types used in this report includes: Type U1 (consisting of layered slabs of carbonate cemented clayey and, mainly, coccolith ooze layers from Unit 1); Type U2 (consisting of layered

slabs of carbonate cemented sapropelic Unit 2), Type U3 (layered carbonate cemented Unit 3), Type MB (carbonate cemented mud breccia), Type MSa (structureless micrite-cemented clayey fraction) usually forming laterally extensive pavements at sea floor where hydrocarbon-rich fluid seepage occurs.

Core locations are summarized in Table 1, core logs follow in Annex I.

1.5.1. Trakya area

Newly discovered mud volcano

Two sampling stations were selected from an area where the subbottom profiler revealed diapiric-like structures and where the presence of gas was inferred (Fig. 13). The two gravity cores showed the presence of Unit 1 and 2 overlying mousse-like breccia sediment.

Station BS-340G

318 cm of sediment were retrieved at this station. The uppermost interval is a 0.5 cm thick dark grey silty water-saturated layer. The unit below (Unit 1) consists of alternate light (coccolith-rich) and dark grey (clay-rich) layers in planar lamination. The upper 10 cm of the unit is more water-saturated. At 10 cm and between 40-44 cm two carbonate cemented coccolith-rich layers are visible (Fig. 22). The unit below (62-150 cm) is dark grey finely laminated sapropel (Unit 2). Randomly distributed carbonate cemented layers (up to 1 cm in thickness) were observed throughout the unit. Below 85 cm the sediment is extremely disturbed, presumably due to the dissociation of gas hydrates and due to the large amount of carbonate-cemented crusts broken during splitting operations. A strong smell of H_2S is present throughout the unit. The lowermost interval (150-168 cm) consists of grey structureless gas saturated clayey mousse-like breccia with gas hydrates in the upper part of the interval where a small clast was also found. Between 249-270 cm some patches of stiffer clay are visible.

Table 1. General information on the cores sampled in the Black Sea (Legs 1 and 2).

LEG 1

Core N	Date	Time, GMT	Latitude	Longitude	Depth, m	Recovery, cm
BS340G	10.06.05	17:23	41°55.242	28°55.495	883	318
BS341G	10.06.05	18:25	41°55.203	28°55.479	880	138
BS342G	13.06.05	20:04	44°14.621	37°27.445	1920	CC
BS343G	13.06.05	21:21	44°14.709	37°27.521	1952	CC
BS344G	13.06.05	22:37	44°14.455	37°27.281	1980	366
BS345GR	14.06.05	00:35	44°14.811	37°27.608	1952	0.5 t
		01:45	44°14.636	37°27.409	1944	
BS346GR	15.06.05	01:00	44°00.957	36°41.349	1985	0.5 t
		03:23	44°01.134	36°41.366	2004	
BS347G	15.06.05	05:57	44°01.182	36°41.300	2007	58
BS348G	15.06.05	07:11	44°01.154	36°41.355	1946	CC
BS349G	15.06.05	08:23	44°01.141	36°41.408	1955	68
BS350G	16.06.05	09:50	41°57.521	41°17.581	856	400
BS351DAPC	16.06.05	11:22	41°57.525	41°17.579	855	1.5
BS352G	16.06.05	13:54	41°57.523	41°17.576	855	185
BS353G	16.06.05	14:57	41°57.525	41°17.574	855	310
BS354ROV	17.06.05	11:23	41°57.526	41°17.608	855	-
		17:47	41°57.532	41°17.342	852	
BS355G	18.06.05	09:59	41°58.772	41°07.588	1045	110
BS356G	18.06.05	10:51	41°59.004	41°07.405	1033	154
BS357G	18.06.05	11:41	41°58.929	41°07.482	1040	20
BS358GR	18.06.05	13:13	41°59.006	41°07.438	1033	0.5 t
		15:22	41°58.872	41°07.457	1032	
BS359DAPC	18.06.05	16:55	41°58.998	41°07.406	1031	1.5
BS360G	18.06.05	18:29	41°59.000	41°07.410	1030	255
BS361G	19.06.05	07:27	41°52.754	41°10.056	988	99
BS362G	19.06.05	08:27	41°52.738	41°10.028	990	155
BS363G	19.06.05	11:37	41°57.256	41°16.734	888	435
BS364G	19.06.05	16:30	41°52.858	41°18.832	641	100

LEG 2

Core N	Date	Time, GMT	Latitude	Longitude	Depth, m	Recovery, cm
BS365G	22.06.05	12:49	42°33.428	40°49.459	1488	552
BS366G	22.06.05	14:02	42°34.176	40°48.666	1590	CC
BS367GR	22.06.05	16:19	42°35.972	40°46.409	1590	0.5 t
		19:01	42°35.986	40°46.446	1589	
BS368G	23.06.05	11:33	41°57.245	41°16.696	894	
BS369MUC	23.06.05	13:34	41°57.527	41°17.571	850	-
BS370MUC	23.06.05	15:58	41°57.543	41°17.258	850	-
BS371DAPC	23.06.05	17:37	41°57.624	41°17.519	859	-
BS372G	23.06.05	18:49	41°57.554	41°17.231	852	226
BS373ROV	24.06.05	10:54	41°57.538	41°17.140	853	-
		22:17	41°57.564	41°17.244	850	
BS374G	25.06.05	11:26	41°58.379	41°06.158	1141	322
BS375G	25.06.05	12:40	41°58.159	41°06.207	1132	510
BS376GR	25.06.05	16:12	41°57.817	41°06.336	1103	-
		19:35	41°58.072	41°06.192	1140	
BS377GR	26.06.05	09:28	41°57.563	41°17.238	850	0.5 t
		11:06	41°57.556	41°17.239	853	
BS378DAPC	26.06.05	12:17	41°57.556	41°17.199	851	18
BS379ROV	26.06.05	15:32	41°57.375	41°17.881	860	-
		20:29	41°57.242	41°17.778		
BS380GR	26.06.05	13:34	41°58.383	41°06.141	1142	0.5 t
	27.06.05	01:18	41°58.079	41°06.169		
BS381G	28.06.05	10:31	41°25.124	37°38.155	1423	450
BS382G	28.06.05	20:33	41°36.035	37°35.808	1583	576
BS383G	28.06.05	22:31	41°28.455	37°35.826	1431	475

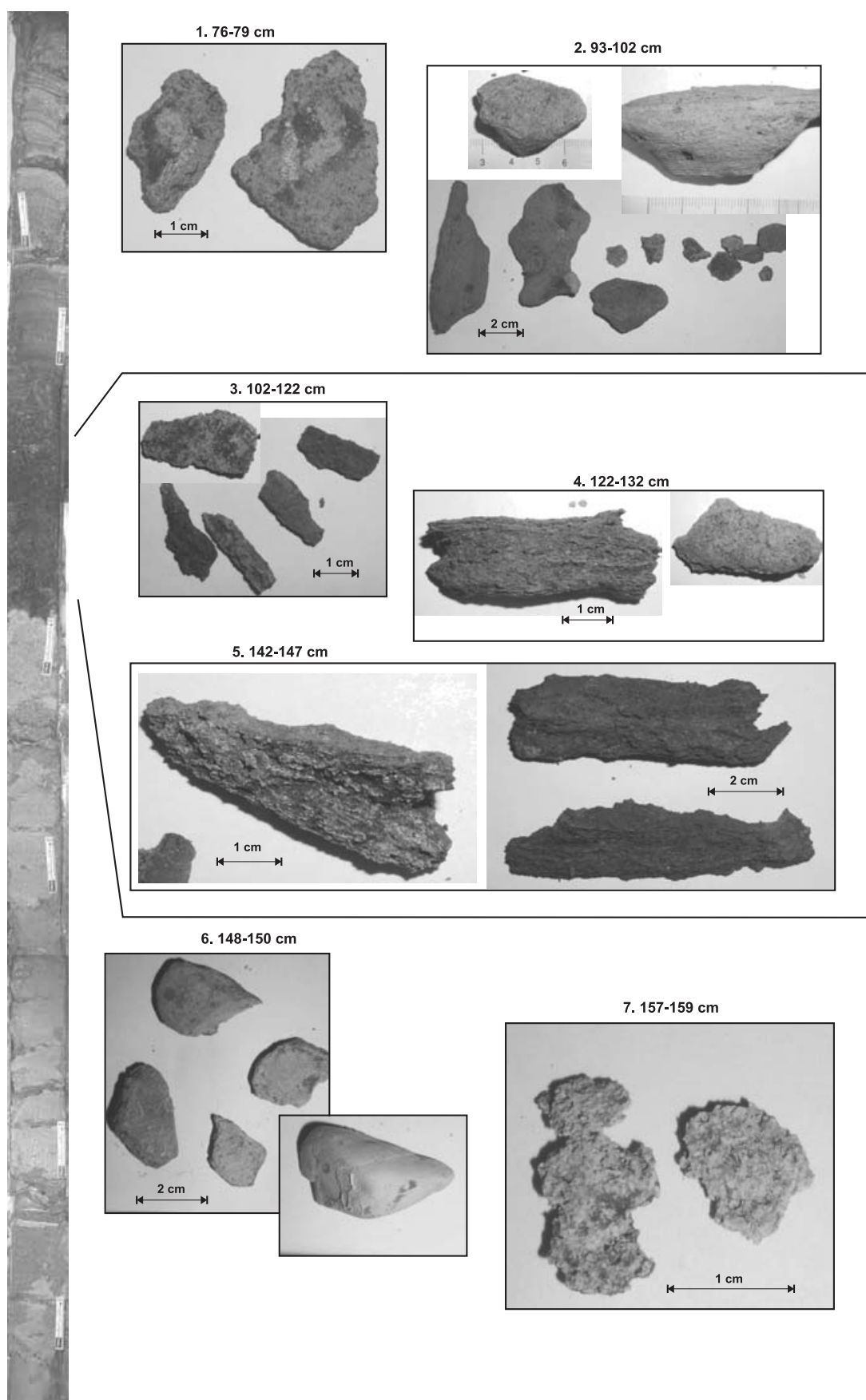


Figure 22. Carbonate crusts recovered at the site AT340G.

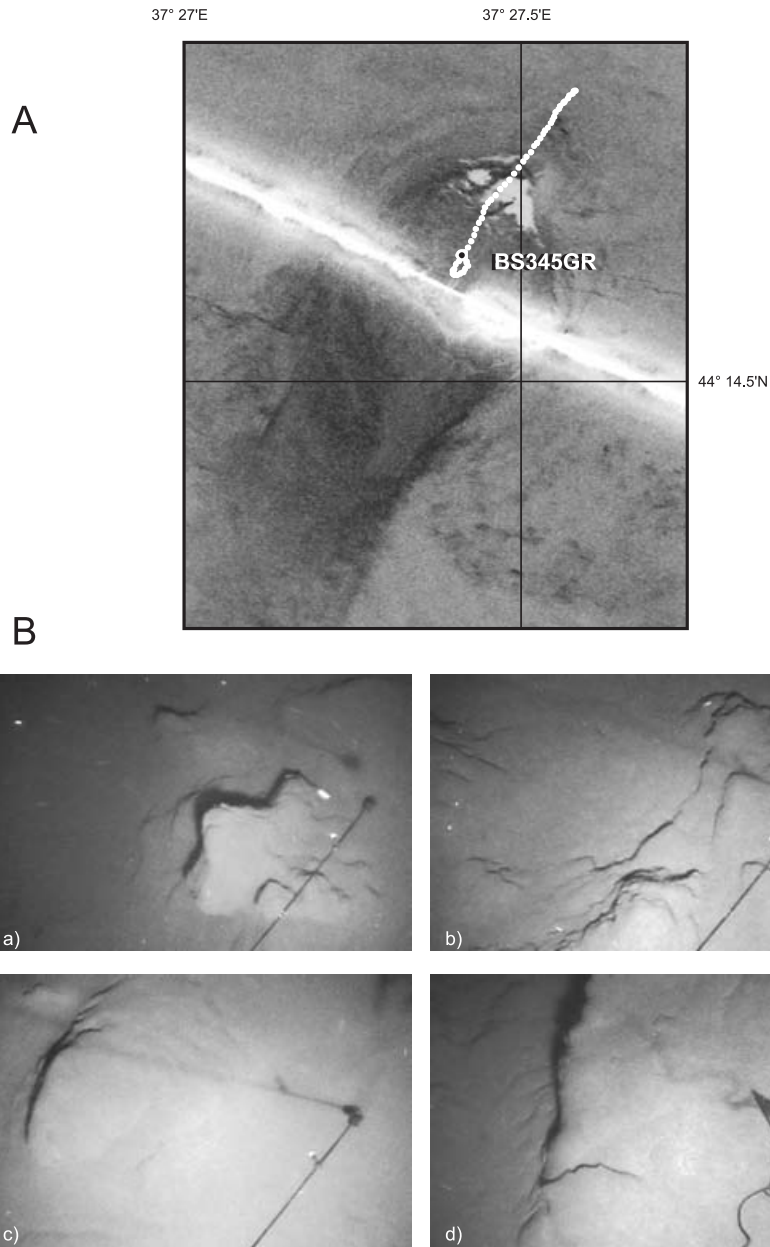


Figure 23. Track of the TV survey of the Petroleum Mound and stills from the record showing seabed irregularities due to the presence of carbonate crusts.

BS-341G

The core consisted of 138 cm of sediment. The uppermost interval is a very thin layer of water-saturated silt, covering the 36 cm thick Unit 1, represented by planar lamination of grey water-saturated clay with a small amount of silty admixture and carbonate cemented coccolithic ooze. Between 25-36 cm evidence of gas saturation was observed. Strong smell of H₂S was detected throughout the unit. The Unit 2 below (36-96 cm) consists of dark grey, finely laminated sapropel. Between 36-67 and 77-92 cm the sediment

contains a large amount of carbonate cemented layers. The lowermost interval (96-138 cm) is a grey homogeneous mousse-like breccia. The last 18 cm of the unit contains some light coloured clasts (up to 0.8 cm in size).

Conclusions

A new mud volcano structure has been discovered in the south western part of the Black Sea as indicated by the presence of gas saturated mousse-like breccia. For the first time gas hydrates were observed in this

region. At both stations Units 1 and 2 were recovered overlying the mousse-like breccia. In both units carbonate cementation of the sedimentary layers is observed. The presence of thin dark microbial mats on the interface between the laminae is also observed suggesting that the anaerobic oxidation of methane is ongoing and is inducing the precipitation of carbonate cement. The two cores also showed clearly that the carbonate precipitation preferentially occurs in the more porous coccolith-rich layers characterizing in particular Unit 1.

1.5.2. Shatsky Ridge/Tuapse Trough area

Eight attempts were made to sample two diapir-like structures observed on the MAK-1M profiler. Two main structures were sampled: Petroleum Mound and Dolgovskoy Mound.

Petroleum (Neftyanoy) Mound

Four attempts were made to sample this structure using TV-controlled grab and gravity core (Fig. 15). Clear evidence of oil seepage was observed.

Station BS342G-BS343G

Two attempts were made to sample the top of this structure. Only a small amount of sediment was retrieved in the core catcher at station BS342G. The recovery consists of structureless very stiff clay with a small amount of silty admixture. Traces of oil covering the liner and mixed within the sediment were observed. Also clasts of indurated dark clay (up to 3 cm in size) were found within the dark grey silty clayey fraction. Also at station BS343G a small portion of sediment was recovered. The top of the sediment (1-2 cm) contains black coloured clayey matrix, hydrotroilite-rich. The same clayey matrix was observed in the lower part with a small portion of silty admixture. Clasts of indurated clay (< 0.5 cm in size) were also observed randomly distributed in the clayey matrix. The bottom part of the recovery has showed a silvery grey colour, probably due to presence of oil.

Station BS344G

Coring from the foot of Petroleum Mound retrieved 366 cm of sediments. Unit 1, with some oil traces, was described in the upper part of the unit (0-17 cm). A 5 cm thick layer of grey water-saturated clay with small clasts separates Unit 1 and Unit 2. Unit 2 (22-97 cm) is a fine laminated grayish brown sapropel, containing grey layers of structureless homogeneous clay between 30-40, 59-64 and 89-93 cm and a dark grey clayey layer with poorly lithified clasts of mudstones in the top part. Oil traces were observed at 37 and 59 cm. Unit 3 (111-357 cm) consists of grey silty clay, sometimes darker in colour, with vaguely laminated hydrotroilite-rich patches throughout. Distinct layers of water-saturated clayey and silty matrix with poorly lithified and subrounded (Maikopian?) clasts occur throughout Unit 3. Occasional oil traces were observed in these layers.

Station BS345Gr

The top of the Petroleum Mound was sampled again using the TV-controlled grab. The TV survey started from the base and continued towards the top of the structure (Fig. 23A). The bottom part showed homogeneous flat sea bottom covered by a thick sedimentary unit. The mound has a complicated structure. Several cone shaped structures capped by small depressions were found at the top of the mound. Within these depressions irregular shaped angular features, cracks and small elevations covered by hemipelagic sediments are observed (Fig. 23B). Also several dark patches (possibly oil) are seen. The grab finally sampled the edge of an inferred carbonate deposit having a small elevation on the sea floor.

Once the device was retrieved onboard an oily film was observed on the water trapped inside the grab. Evidence of gas bubbling was also observed for more than 10 minutes during sampling operations. A very strong smell of H₂S was also detected. Once a liner was pushed inside the sediment a significant amount of oil was observed appearing on the surface. The recovery of the grab consisted of mud breccia with dark grey clayey silty sediment mixed with a large

amount of clasts (Maikopian claystone) of different sizes. Also a small amount of brownish claystone was observed. Oil was noticed throughout the recovery and in oil saturated pockets. On the surface large (up to 25-30 cm) carbonate slabs were observed. Authigenic carbonate Type M_{Sa} was observed on the top part of these slabs, while the bottom part consisted of carbonate cemented clasts (of different size) and fine clayey silty sediment (Type M_B). Evidence of whitish and bluish microbial filaments was

observed in the fine sediment forming a sticky network. Microbial mats were also observed within the slabs coating the carbonate cemented clasts and filling microfractures and voids. This observation suggests the presence of microbes living in anoxic conditions where oil and gas seepage occur. Microbial mats were also observed on the surface of the sediment suggesting that the carbonate slabs are currently forming by carbonate precipitation triggered by microbial activity.

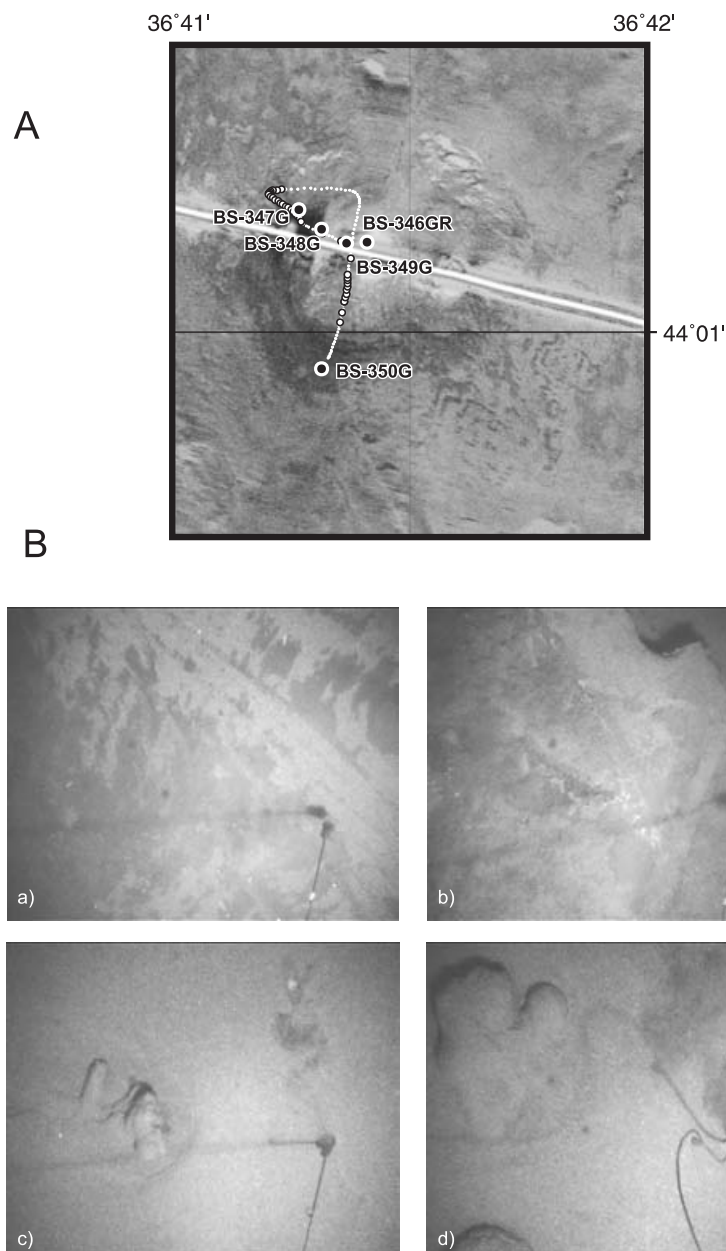


Figure 24. A: Fragment of sonograph along the line MAK58BS showing the Dolgovskoy Mound with sampling stations and video survey track. White circles indicate areas where carbonate crusts were observed on the seafloor. B: Stills from the video record showing carbonate crusts.

Conclusions

The acoustic data combined with the ground truthing results confirm the presence of a mud volcano, as clearly shown at station BS346Gr. The origin of the clast-rich layers in core BS344G is considered as possible debris from the structure rather than as mud breccia flows. This is inferred from the partial sorting of sediment and from the subrounded clasts, suggesting that the strong currents flushing the area washed these deposits. The origin of the oil cannot be defined. It seems likely that a deep sited reservoir releases fluids through the feeder channel of the mud volcano. Further investigations should be conducted on the homogeneous grey clayey layers that cross cut the sapropelic unit. Their origin remains unclear.

Dolgovskoy Mound

Four attempts were made to sample Dolgovskoy Mound using TV-controlled grab and gravity corer (Fig. 24A). Thick

microbial mats and authigenic carbonates were collected.

Station BS346Gr

The top of the structure was explored with TV grab that showed large areas covered by hemipelagic sediments. At the beginning and at the end of the TV-line dark (brownish to black in colour) patches and stripes were observed (Fig. 24B, a). Irregularities on the seafloor are marked with white dots in Figure 24A. Escarpments up to 1-2 m high were observed in the central part of the mound (Fig. 24B, b). Large blocks of rocks and small pebble-like features buried by sediments were also detected at this location (Fig. 24B, c). A lot of wood remains were seen littering the seafloor. On the western part of the mound small escarpments, crusts and tubular shaped features were observed. The grab sampled the central part of the structure where some irregular shaped features occur (Fig. 24B, d).

The grab retrieved onboard a full recovery of mixed soupy Unit 1 and authigenic

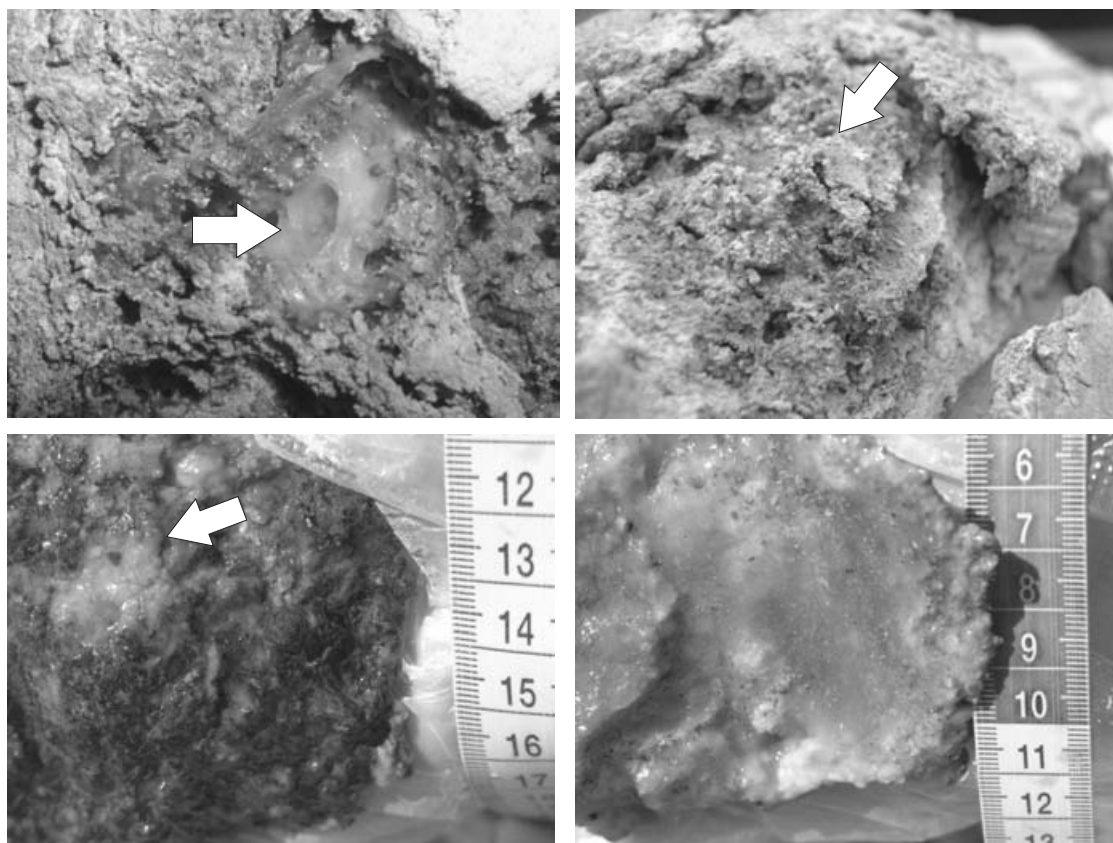


Figure 25. Bacterial mats recovered at the station BS346GR.

carbonates. A large amount of microbial mats were observed on the surface (Fig. 25). Large slabs (up to 60 cm in size) form laterally extensive carbonate cemented sections of Unit 1 (Type U1) (Fig. 25). These slabs were covered on both sides with microbial colonies of differing colours (i.e. whitish, yellowish, pinkish). Carbonate-coated cavernous structures were observed within the sediment, where also pipe-like features (up to 5 cm in diameter) form a network in the subsurface. The thickness of the carbonate crusts appears to be highest at places where presumably more focussed seepage occurs. At these sites the slabs show positive relief and the highest concentration of microbial mat, carbonate minerals and black (Fe-rich) minerals (pyrite). Fe oxidation on the external surfaces of the samples was observed the next day. The slabs retrieved in the bottom part of the dredge consist uniquely of Type U1 while the one observed on the surface display two types of carbonates: the top part appears lighter in colour and shows no internal evidence of sedimentary structure (Type MSa), while the bottom part consists of Type U1.

Station BS347G

The flank of the structure was sampled in a high backscatter area of the sidescan sonar record. The corer retrieved 58 cm of sediment. The top 5 cm consisted of thick extremely water-saturated and disturbed

Unit 1 covering a 1 cm thick layer of stiff authigenic carbonate, Type U1, covered with pink and yellow microbial mat. The remaining part of the core was mostly very stiff grey clay (5-54 cm) with patches of fine sandy sediment between 6-25 cm, as well as fine sandy layers with oblique orientation (20-43 cm). A continuous grey sandy layer containing a dark grey layer rich in silty admixture was observed between 44-46 cm. Fine grained sand and carbonate crust, covered by microbial mat, represented the four lowermost cm of the core. This sand consists mostly of quartz with fragments of carbonate rocks, old glauconite, rare grains of plagioclase, tourmaline, zircon and dolomite. Among the authigenic minerals pyrite was observed.

Station BS348G

A new attempt to sample the top retrieved only a small portion of carbonate cemented crusts covered by microbial mat. As observed at station BS346Gr, even in this core the crusts show two types of layering: the top part consists of structureless light grey micrite (Type MSa) while the bottom part consists of carbonate cemented unit 1 (Type U1). Presumably, the penetration was prevented by the presence of these hard crusts on the sea floor.

Station BS349G

An area of medium backscatter close to the summit of the mound was observed on

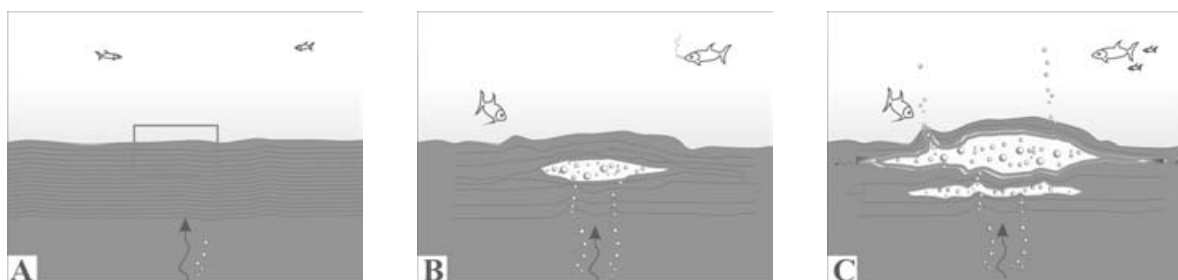


Figure 26. Conceptual evolutionary cartoon of fluid seepage and carbonate precipitation in the subsurface. (A) Fluids rising from greater depth reach the near subsurface moving by diffusive flow through layered sediment deposits; (B) detail from area framed in image A. When more sustained fluid seepage occurs and when the seeping fluids reach thicker clayey layers, their rise is impeded and deform the soft sediment creating chambers where gas is accumulated; (C) microbial colonies grow in the internal part of these chambers (pink framing line) and precipitation of authigenic carbonate occurs. The overpressured fluids continue to move laterally, forming a network of pipes and tubular features that extends horizontally through the soft sediment. Note: the fish has a purely decorative purpose for the cartoon, as we are considering anoxic conditions (i.e. water depth ~1700 m).

the sidescan sonar record and sampled. Sediments of Unit 1 represent the top 10 cm, consisting of thin alternations of light grey clay and coccolithic ooze, covered by 1 cm of light grey highly water-saturated clay. A 2 cm thick layer of grey homogeneous, water-saturated clay separated Unit 1 and Unit 3. Unit 3 (12-68 cm) was represented by grey homogeneous, less water saturated clay with silty admixture. Fine grained well sorted sand is observed at 20 cm. Thin layers and patches of hydrotroilite were observed between 18-68 cm of the unit. Towards the bottom the colour becomes darker and silty admixture increases. The bottom part of the interval is a lamination of dark grey silt with clayey and sandy admixture.

Conclusions

Station BS346Gr revealed important information about one of the mechanisms of gas escape at seeps. We suggest (Fig. 26) that a focussed seepage of a large amount of free gas was ongoing at this site. The laterally extensive and finely laminated sediment of Unit 1 was impeding the immediate release of the gas. Thus the gas was trapped in the subsurface, deforming the soft layers and forming cavities and void areas where microbial colonies are growing and inducing the

precipitation of carbonate minerals via AOM. The tubular features observed in the subsurface indicate that a large amount of gas was seeping preferentially along defined networks in the subsurface. The samples retrieved highlight that carbonate Type MSa seems to be broadly diffused on the sea floor where gas seepage occurs. No mud breccia was collected, although previous interpretations of this structure indicated it as a mud volcanic structure. The sandy layers described at station BS347G presumably represent debris of sand deposited in the upper part of the mound as observed at station BS349G.

1.5.3. Georgian margin

Batumi seep area

Several sampling stations were completed in an area previously investigated during the POS317 cruise (RV *Poseidon*, 2004), where gas flares were observed on the sidescan sonar record (Fig. 27). All the stations show the presence of a significant amount of gas hydrates as also initially indicated by the large bubbles appearing in the water surface while the corer was being recovered onboard.

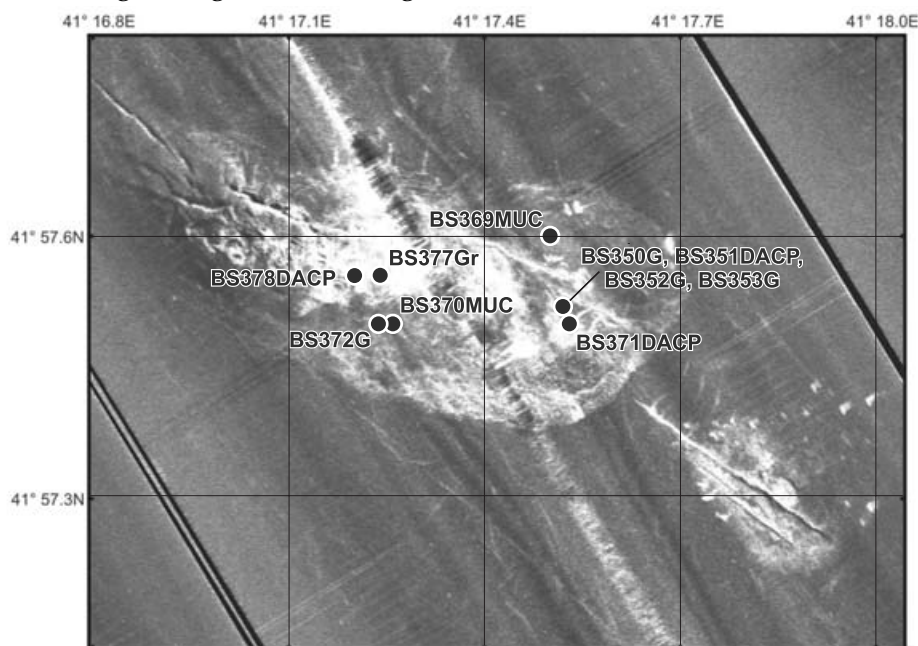


Figure 27. Fragment of mosaic of sidescan sonar DTS-1 (cruise P317/4 R/V *Poseidon*, Klaucke et al., 2006) with location of TTR-15 Leg 1 and 2 sampling stations.

Station BS350G

The uppermost interval (Unit 1; 0-42 cm) was represented by alternations of clay and coccolith ooze strongly disturbed with gas hydrates seen along the sedimentary layers (Fig. 28). The interval between 36-42 cm is extremely water saturated and darker in colour; it could represent Unit 2 but the total absence of structures does not allow any definitive interpretation. The unit below (42-400 cm) consists of grey clay, structureless, water-saturated with gas hydrates. The sediment below 120 cm is soupy and extremely water- and gas hydrates saturated. This interval could represent Unit 3 as suggested by the presence of tabular shaped gas hydrates.

Station BS352G-BS353G

The same location was sampled again at these stations in order to collect extra material for geochemical analyses. The recovery of both cores was very disturbed due to the presence of gas and the gas hydrates dissociation. The samples for geochemical analyses were collected immediately after extruding the core without splitting it, therefore the sediment was heavily disturbed during this procedure. Nevertheless we were able to distinguish the different sedimentary units. Station BS352G retrieved 94 cm of Unit 1 and Unit 2 extended to the bottom of the core (185 cm). Gas hydrates were observed mostly in the bottom part of Unit 1 and throughout Unit 2. Similarly, at station BS353G were retrieved Unit 1 (0-120 cm), Unit 2 (120-160 cm) and also Unit 3 (160-310 cm). The majority of the gas hydrates were observed in the soupy Unit 3 and had a laminar shape and were mostly oriented along the interface between sedimentary layers.

Station BS368G

554 cm of sediment were retrieved. The liner was cut in 1 meter long sections for further studies in base laboratories.

Station BS372G

The top 80 cm of sediment consists of Unit 1 that appears laminated (0-50 cm) and extremely disturbed with carbonate cement-

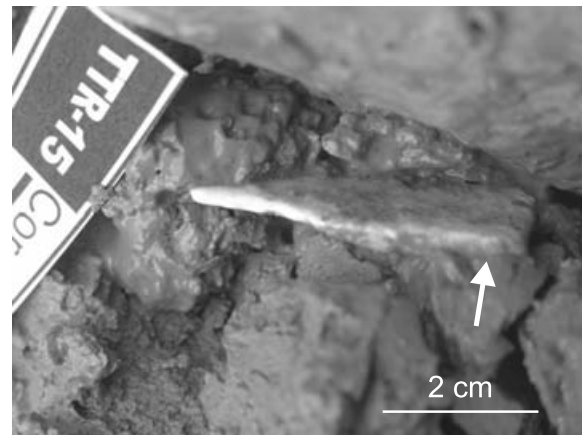


Figure 28. Tabular gas hydrates observed along the sedimentary layers within core BS350G.

ed layers (50-80 cm). Unit 2 (87-116 cm) appears very disturbed with occasional carbonate cemented layers. The remaining part of the core consists of very disturbed sections of light grey (possible Unit 3) and brownish grey (possible Unit 2) patches containing layered authigenic carbonates. Presumably the different lithologies were involved in several slumping events in the faulted area of active seepage. It is also possible that the strong seepage observed on the sea floor contributes to mix the sediments. Microscopy observations on the coarser fraction reveal the presence of calcite, fragments of quartzite, quartz shell fragments, amphibolite and pyrite, suggesting that a possible origin from a deeper sited diapir cannot be ruled out.

Station BS377Gr

The TV-grab was deployed in an area where the ROV survey showed gas bubbling and carbonate chimney-like structures. Three TV lines were run around this site. Several small areas (up to 10-15 m in diameter) of active seepage were found. Dark oil patches were detected at the beginning of the line (Fig. 29a). The TV-grab sampled the southern depression where cracks, breaks and irregularly shaped uplifts were observed (Fig. 29c-d). Also dense fields of degassing holes were found in this area (Fig. 29e-f). A large amount of soupy sediment was retrieved on board together with greenish grey carbonate cemented layered blocks. Brownish orange microbial mats with botryoidal shape were

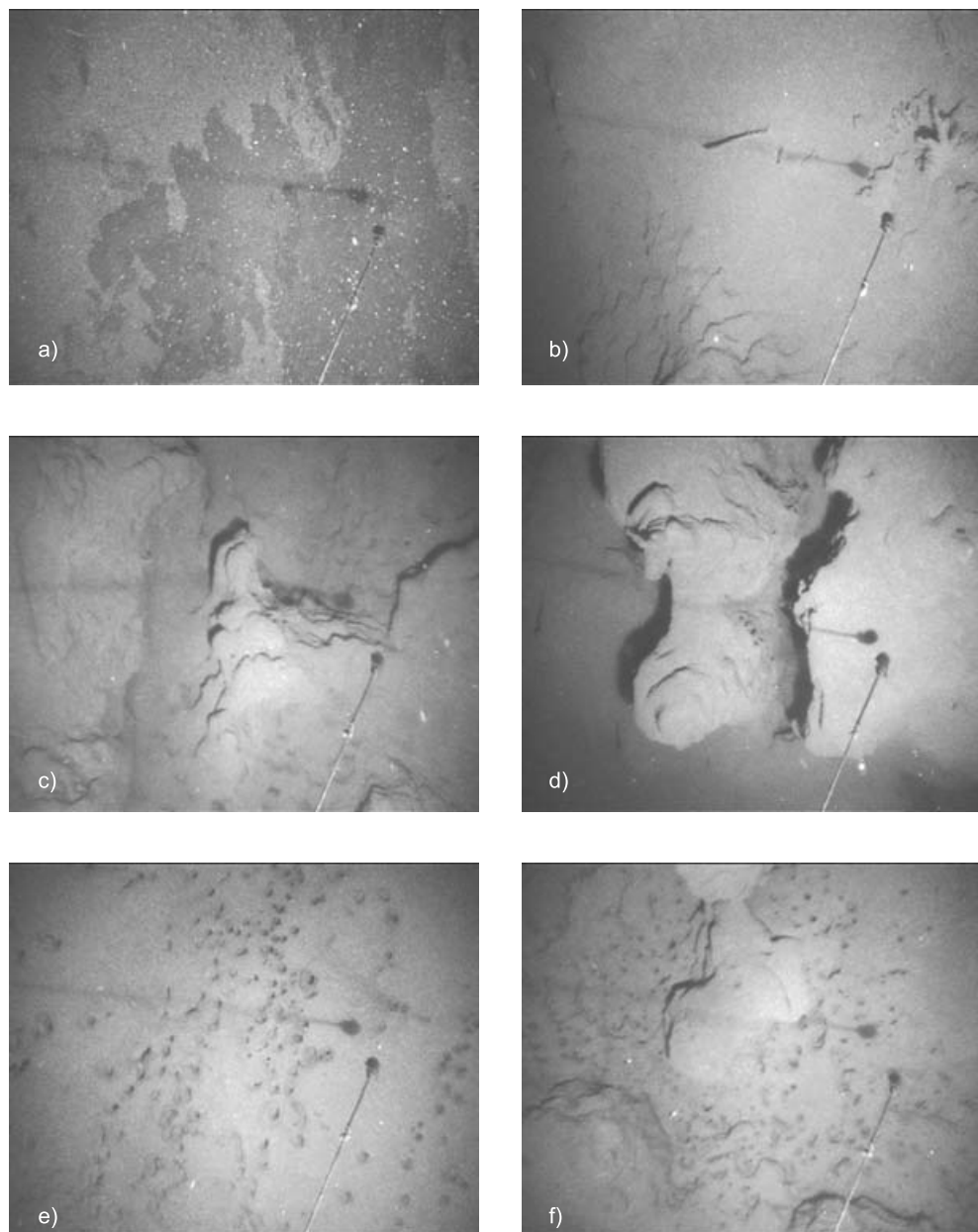


Figure 29. Stills from video survey along the track BS377Gr.

observed covering the carbonate blocks. These blocks are not well lithified and highly fractured. Their irregular shape is quite different from the classic tabular shape observed for carbonates at other stations. Microbial mats are visible along the layer interfaces but are mostly concentrated in the fractures. Also Fe-rich sediments are mostly visible around fractures where, presumably, stronger seepage occurred. Similar observations were described at BS346Gr station. This suggests that an initial phase of less sustained seepage allowed partial cementation

of the layers. A second vigorous seepage was probably fracturing the semi-lithified sediment. The fractures then acted as main pathways for fluid seepage allowing the development of thick microbial colonies.

Conclusions

All the cores, taken at this area, highlight the presence of gas hydrates. Sedimentary structures appear to control the shape of the clathrates (i.e. tabular shape). This suggests that the vertical rise of the fluids is impeded

when they encounter more impermeable clayey layers hence migrating preferentially horizontally. The presence of gas hydrates and the gas saturation gave the sediment a soupy or moussy texture that was often overprinting the original sedimentary structures. Based on the shape of hydrates we can speculate that the deeper units observed at stations BS353G consisted of sedimentary Unit 3. The faults that were observed cross cutting the area are presumably used as preferential pathways for the fluids to rise. In the faulted area it is likely that the sediment got disturbed by the rising fluids.

Pechori Mound

This structure was observed on the deep-towed sidescan sonar record (MAK-1M) and was sampled using gravity corer, DAPS and TV-controlled grab devices (Fig. 30). All the stations showed the presence of oil-saturated sediments and gas hydrates, usually below 50 cm.

Station 355G

The top 50 cm of sediment consisted of soupy and extremely water saturated clay with silty and sandy admixture. In the lower part of this interval clasts of mudstone and poorly lithified clay with sandy admixture are observed together with oil traces and gas hydrates. The lower unit (50-110 cm) consists of dark grey moussy oil-rich mud breccia. Clasts (up to 10 cm in size) were observed in the clayey silty sandy matix. Clasts vary in lithology including mudstone, carbonate cemented layered fragments, carbonate tectonic breccia. Gas hydrates with irregular shapes were observed throughout the unit.

Station 356G

A large oily film was observed on the sea surface while retrieving the corer onboard. 164 cm of sediment were obtained. The top 35 cm consisted of laminated Unit 1 that is soupy and water saturated in the top 13 cm with some oily traces. Clear evidence of planar lamination was observed in the rest of the section. Between 35-67 cm a water-oil saturated soupy unit highlights the presence of

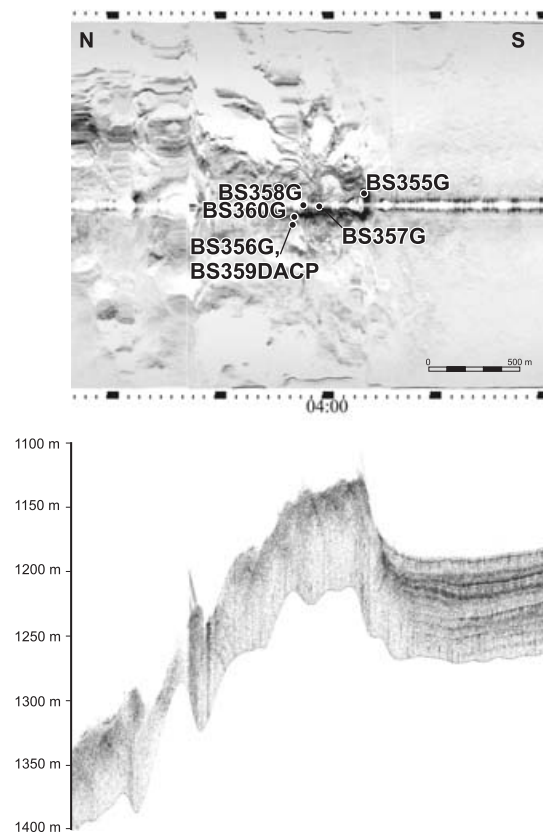


Figure 30. Fragment of sonograph and subbottom profiler records along the line MAK59BS showing the Pechori Mound with locations of sampling stations.

dispersed gas hydrates. It is difficult to detect if this section represents Unit 2, but the colour appears very similar to the following unit (69-154 cm) that shows clear sapropelic lamination between 69-94 and is more disturbed between 110-154 cm. The other intervals appear oil- and gas hydrate-rich (tabular shaped) in the moussy texture. Oil was observed bleeding out the sediment for several tens of minutes.

Station 357G

Soupy sediment was observed shooting out of the corer once the device was taken onboard. 20 cm were finally recovered. The top 15 cm, consisted of clayey soupy sediment, water and oil saturated with dispersed porefilling hydrates. Degassing through the sediment was observed for approximately 30 minutes. The bottom 5 cm consist of moussy grey sediment with faint lamination (Unit 1).

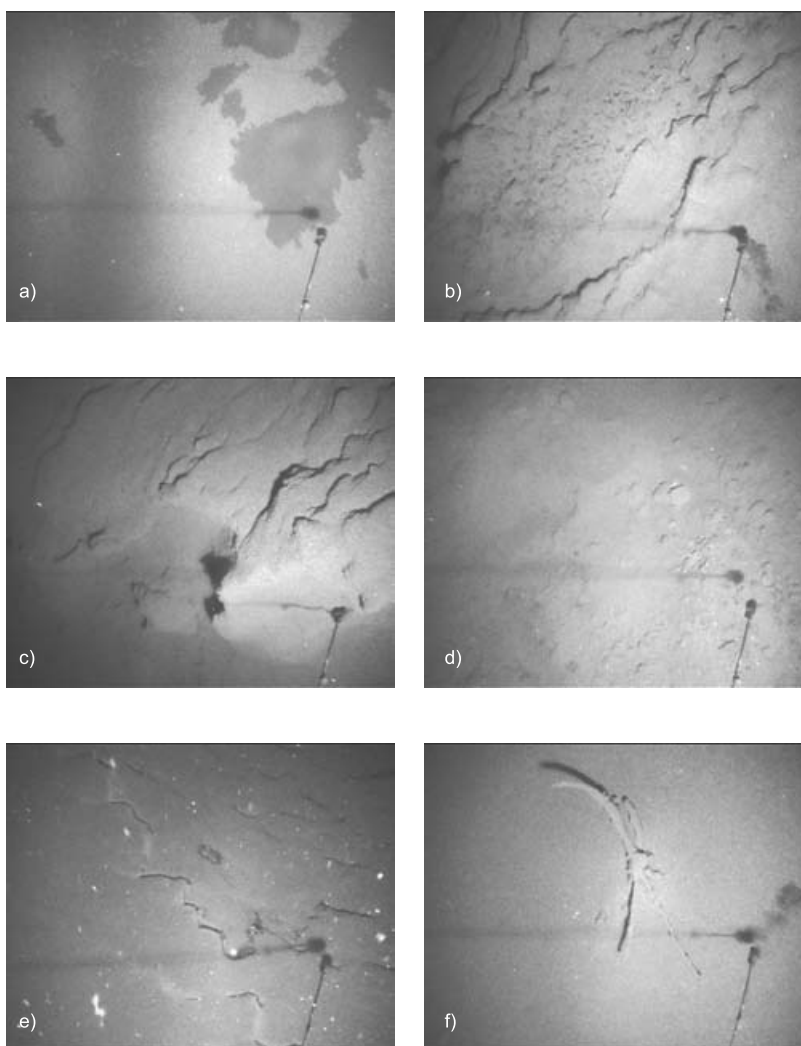


Figure 31. Stills from video survey along the track BS358Gr.

Station 358Gr

The beginning of the TV line was characterized by the presence of a lot of dark oily patches (Fig. 31a). Also irregular relief with small knobs, cracks and benches covered by sediments were recorded (Fig. 31c-e). Two sites characterized by a high concentration of small holes were found along the line (Fig. 31b). These holes are interpreted as evidence of gas (oil) emission from the deeper sources as also suggested by the cloudy water and particles in the water column. Numerous wood trunks and branches were observed (Fig. 31f).

A small amount of sediment, mostly represented by grey, structureless, homogeneous, water- and gas saturated clay, was retrieved by the TV-controlled grab. Lots of

oil patches and small concretions (up to 10 cm) of cemented coccolithic ooze (Type U1) were also observed.

Station 360G

It was very difficult to distinguish the lithological variations due to the immediate sampling of the core without splitting it. About 225 cm of sediment were retrieved onboard. The top part (0-40 cm) consists of by grey structureless clay with traces of oil. The rest of the core consists of structureless oil-rich moussy clay with gas hydrates (40-70 cm), and a similar moussy clay extremely oil-saturated with larger amount of irregularly and tabular shaped gas hydrates randomly distributed throughout the section. (70-225 cm).

Conclusions

Sampling stations revealed that at Pechori Mound a significant amount of oil is rising towards the surface and gas hydrates are present within the sedimentary units. In the central part of the structure the sediment appeared more soupy with smaller sized pieces of gas hydrate.

Iberia Mound

Stations BS361G and BS362G sampled an inferred seepage feature observed in the profile MAK59BS. Authigenic carbonates and mud breccia were retrieved.

Station BS361G

The 99 cm of recovery consisted of laminated Unit 1 with carbonate-cemented intervals (mostly coccolith ooze-rich) between 36-99 cm (authigenic carbonate Type U1).

Station BS362G

The recovery at this location was very similar to the previous core. The first 85 cm consisted of laminated Unit 1. The interval between 85-148 cm showed gradually stiffer Unit 1 with carbonate cemented sedimentary layers (Type U1). Oil traces are observed in the bottom of this unit. Between 148-155 cm oily mud breccia was observed containing oil semi-saturated clasts in a clayey sandy matrix.

Conclusions

The two stations revealed the presence of authigenic carbonates Type U1 indicating that AOM is presumably ongoing triggering the precipitation of carbonates. The presence of mud breccia suggests that terrigenous material and small clasts are brought to the surface during the rise of mud.

Station BS363G

A reference core was taken on the Georgian margin close to the Batumi seep area. 435 cm of sediment included the full succession of the three main sedimentary units. Laminated Unit 1 (0-107 cm) and Unit

2 (107-163 cm) were followed by Unit 3. This interval consisted of grey clay with a small amount of silty admixture, planar laminated in the upper 102 cm of the interval. The sediment showed layers and patches enriched in hydrotroilite throughout the unit, and a thick interval extremely rich in hydrotroilite between 265-377 cm.

Station BS364G

This station sampled the flank of an inferred seepage structure. The core consisted of 100 cm of grey stiff silty clay with some slumped features between 42-57 cm. Hydrotroilite patches and irregular layers were observed throughout. At 80x7x6 cm clast of semi lithified siltstone indicates slumping activity.

Suchumi Canyon area

Three sampling stations were taken from an area of high backscattering observed on the MAK-1M sidescan sonar record (Fig. 19).

Station BS365G

The 552 cm recovered consisted of laminated Unit 1 (top 88 cm), slumped Unit 3 in the bottom part. Evidence of slumping is clearly visible between 88-125 cm where disrupted fragments of Unit 1 are surrounded by disturbed Unit 3. Between 159-185 cm a hydrotroilite-rich interval of Unit 3 shows evidence of planar lamination. This unit could represent a large block whose internal structure remained partly undisturbed within the slumped body. Between 185-369 cm more obvious slumped structures are observed in brownish clay with silty admixture and traces of Unit 3. The bottom part of the core (369-552 cm) consisted of undisturbed homogeneous grey clay with silty admixture (Unit 3) with hydrotroilite-rich patches, layers and sections. Organic remains were observed at 293, 312, 329 and 365 cm.

Station BS366G

A small amount of black clay was retrieved together with some poorly sorted

black sand (volcanic?). Microscopy observations identified a significant amount of quartz and amphiboles; minor amounts of pyroxenes, chlorite, feldspar and mica were also observed. Also a small portion of grey (Unit 3?) clay was distinguished. The sandy sediment presumably prevented the penetration of the corer.

Station BS367Gr

The TV controlled grab was deployed on an area characterized by strong backscatter on the sidescan sonar record. At the beginning of the line small rounded pebbles were observed. Also several small depressions and dark patches were found. The grab collected pebbles from the same site where the TV survey started. The total recovery consisted of pebbles of different lithology and roundness (~70%) mixed with grey clayey sediment (~30%). Also the same sandy fraction described at station BS366G was observed. Pebbles consist of granite, gneiss, volcanic and metasedimentary rocks. Their size varies from a few cm up to 25 cm.

Conclusions

Bottom sampling completed at station BS365G highlighted the presence of one (or two) slumping events from the eastern flank of the canyon. The channel cored at station BS366G has coarse material (poorly sorted coarse sand) suggesting that the channel is probably active. The high backscatter area observed on the sidescan sonar record is caused by the presence of fields of poorly sorted sand and large pebbles on the seabed.

Colkheti seep

Colkheti seepage area (Fig. 32) was found to be another location where a significant amount of oil is present.

Station BS374G

The top ~150 cm of sediment were lost during the retrieval operations. It is difficult to define the type of sediment, but the presence of authigenic carbonate Type U1 suggests that at least part of the sediment lost

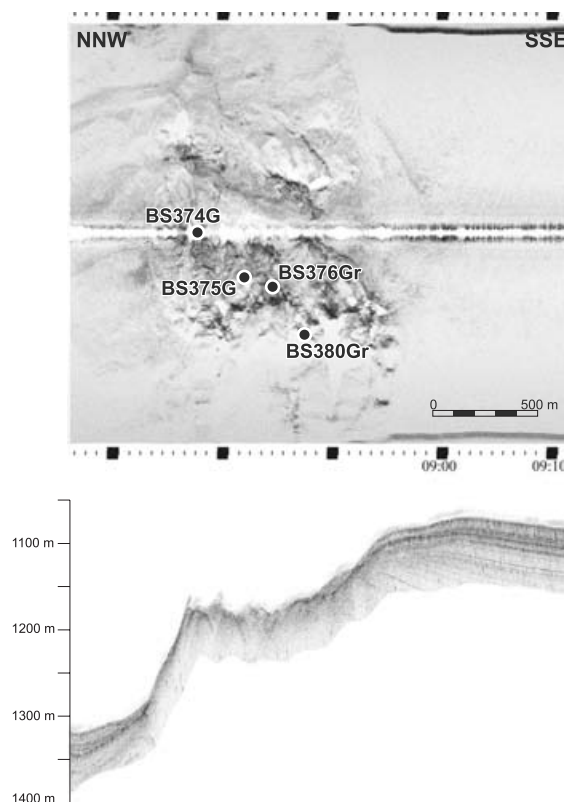


Figure 32. Fragment of sonograph and subbottom profiler records along the line MAK65BS showing the Colkheti seep and the sampling stations locations.

consisted of Unit 1 containing a significant amount of oil. Fragmented Unit 2 was observed at 157 cm, while the remaining part of the core consists of mousse-like breccia. A significant amount of oil was observed bleeding from the fractures in the sediment throughout the core. Gas hydrates were observed between 280-368 cm occasionally concentrated in preferential layers. In the bottom 10 cm the terrigenous admixture increases.

Station BS375G

Large bubbles were observed appearing on the sea surface during retrieval. Eight and a half sections of soupy and extremely water saturated sediment were recovered. The entire core was water-gas-oil-gas hydrates saturated. Continuous bubbling was observed for several tens of minutes through the sediment. The top 180 cm contained porefilling gas hydrates while in the remaining part of the core larger gas hydrates were observed. Below 240 cm the sediment is

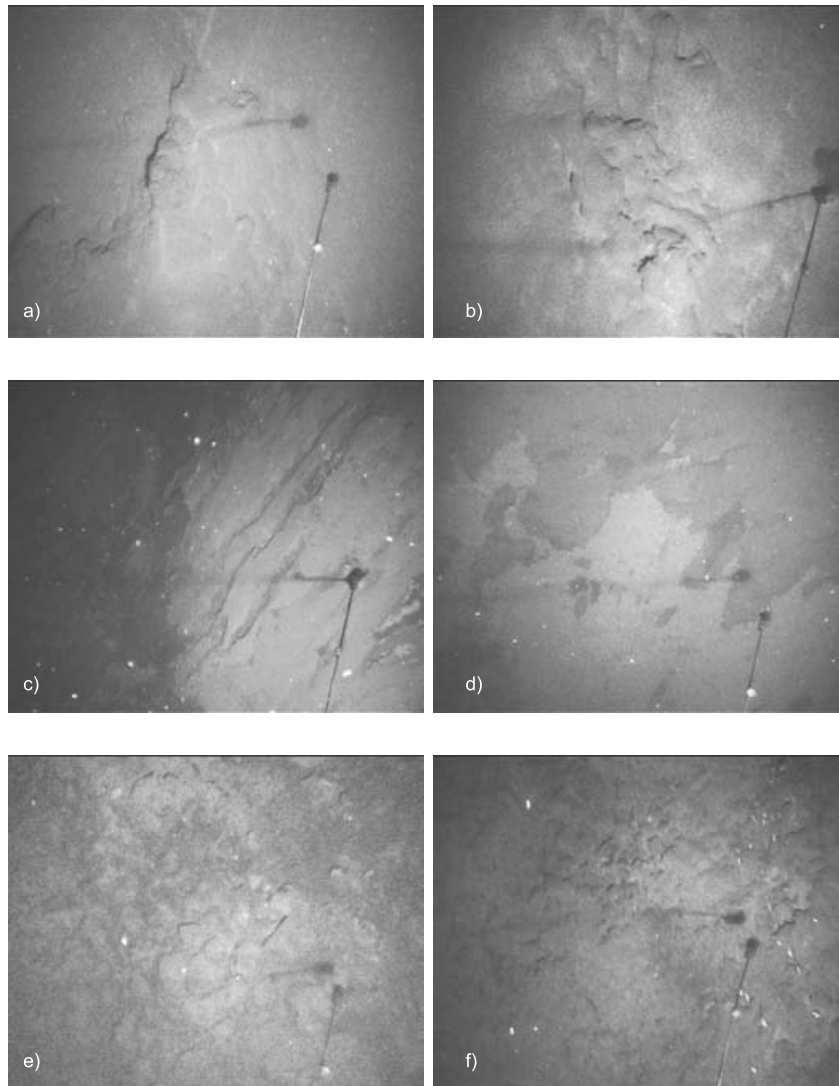


Figure 33. Stills from video survey along track BS376Gr.

slightly less water saturated and at 400 cm fragments of authigenic carbonates Type U1 were observed.

Station BS376Gr

Large dark spots of oil were observed at the beginning of the line (Fig. 33, c-d) across the Colkhetti mud mound. Also several areas of irregular sea bed morphology were seen (Fig. 33, a-b). Suddenly, gas bubbles were observed (Fig. 33, f) rising from the sea floor. Three sample attempts were unsuccessful due to technical problems. During the first sampling attempt oil came into the hydraulic cylinder and locked the system.

Station BS380Gr

The TV-grab was a repeat of the unsuccessful TV-grab BS376GR at the Colkhetti

mound. The TV-line started from the north heading towards the south of the structure. Homogeneous seabed covered by sediments was observed at the beginning of the line. At the end of the TV-survey (position of the BS376GR) an irregular sea bottom with a lot of holes was observed. The grab sampled an area on the seafloor with "breccia-like" texture. A full recovery of extremely gas-oil-gas hydrates saturated sediment was obtained at this station (Fig. 34). Within the clayey sediment (presumably Unit 1) large blocks of gas hydrate were observed. The blocks of hydrates mixed with greenish grey brown sediment reached 20 cm in diameter. Gas hydrates seems to have a mostly sub horizontal shape and appear to incorporate centimeter sized fragments of sedimentary unit. The fragments appear tilted indicating that

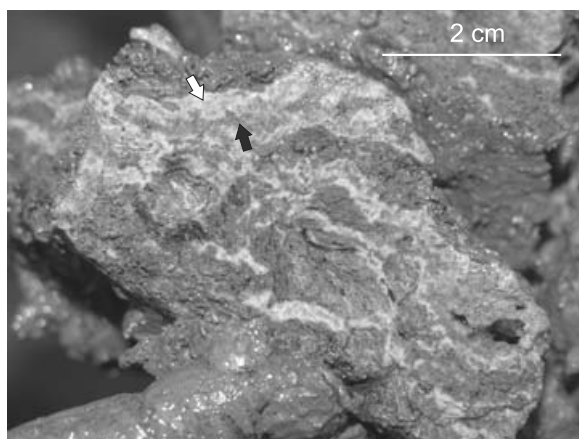


Figure 34. Oil (black arrow) impregnated gas hydrates (white arrow) from the site BS380G.

during the growth of hydrates the sediment was disturbed or that probably the seeping fluids were breaking apart parts of soft sediment. The thickest hydrates reached approximately 10 cm. Porous structure within the hydrates was observed. Oil was also observed included within the hydrates. A large amount of oil was observed flowing on the deck once most of the hydrates had dissociated. Authigenic carbonates observed consist of thin layered carbonate cemented Unit 1 (Type U1). Also alternations of thin (~3 mm) carbonate cemented laminae and thicker (up to several centimeters) gas hydrate layers were observed in several blocks. This suggests that the shape of gas hydrates is controlled by sedimentary structures and that authigenic carbonates are closely spaced with gas hydrates. The carbonates presumably precipitated during periods of partial dissociation of the hydrates or, alternatively, formed before the formation of the hydrates.

Conclusions

Colkheti seep was one of the most successful locations. A large amount of oil and gas hydrates were observed at this site. It is difficult to explain the origin of the mousse-like breccia observed. It is possible that hydrocarbon-rich fluids are rising along the faults cross cutting the structure bringing to the surface oil, gas and a terrigenous admixture from depth.

1.5.4. Samsun area

The Samsun area was sampled three times in order to investigate the origin of some diapir like structures showing high backscatter on the sidescan sonar profile (Fig. 35).

Station BS381G-BS383G

The two stations retrieved a very similar sedimentary succession that is typical of the Black Sea. In both cases the top part of the core consisted of laminated Unit 1 overlying laminated sapropel Unit 2. Within Unit 2 there was a few cm thick layer consisting of semilithified aragonite with some coccoliths. The bottom part of Unit 2 is disturbed and indicated slumping activity that continues in the top part of Unit 3. The remaining part of the core is in both cases characterized by the presence of uniform Unit 3 with gas hydrates retrieved in the core catcher in a hydrotroilite rich interval.

Station BS382G

The recovery consisted of 576 cm of sediment. The uppermost interval (Unit 1) is finely laminated planar lamination of grey clay with white coccolithic rich layers. Between 30-174 cm grey layers of homogeneous clay interrupt the unit. The thickness of the layers varies from a few mm up to 5 cm. A similar pattern was observed in the Unit 2 (174-309 cm) where sapropelic layers intercalate structureless clayey layers. The lowermost interval (309-576 cm) consists of grey clay with some silty admixture with some dark patches of hydrotroilite. Between 379-431 and 490-518 cm the sediment is extremely enriched in hydrotroilite. The colour of the clay is darker towards the bottom of the unit.

Conclusions

The three structures investigated reveal very similar sedimentary features. In two cases (BS381G-BS383G) the presence of gas hydrates in the bottom part suggests that methane-rich fluids are present near the seabed. Station BS382G revealed the presence of unusual layers of homogeneous and

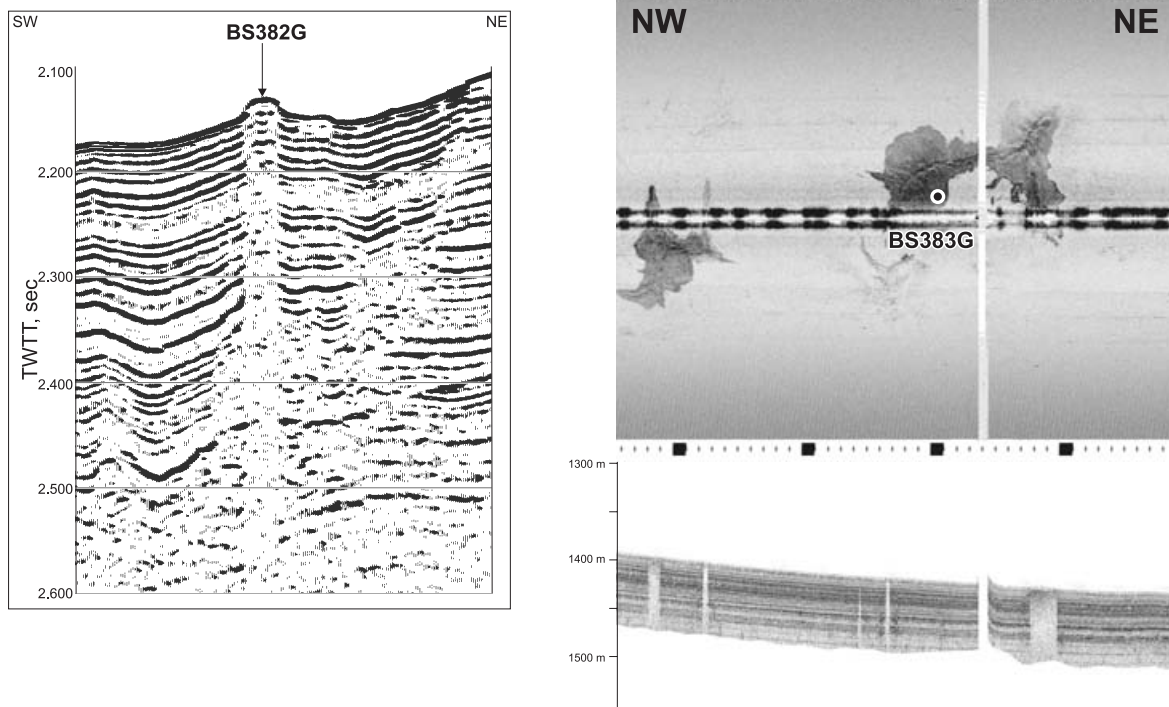


Figure 35. Location of sampling sites BS382G and BS383G along seismic line PS321BS and MAK line MAK66BS in the Samsun area.

structureless clay that require further investigation for a proper interpretation. A preliminary interpretation suggests that they represent the deposit of the sediment in suspension from a distal part of a turbidite event. No mud breccia was observed in any of these sites.

II. Tyrrhenian Sea

Arc volcanism in the Tyrrhenian Sea, typified by Vulcano and Stromboli Islands, is presently active and responding to the dynamics of the geological environment. Stromboli Island has been affected by repeated flank collapse events of Sciara del Fuoco and the structure of its submarine flanks is the result of the interaction of the related erosional and depositional processes with the present-day sedimentary dynamics. The Sciara del Fuoco volcanoclastic material progrades into the deep sea portion of the Stromboli canyon which subsequently funnels a large input of sedimentary material into the Marsili abyssal plain. As a result, a deep-sea fan spans almost the whole eastern portion of the Marsili basin. The recent 2003 eruption of the volcano and collapse event of

the Sciara del Fuoco, renders the study of the flanks and deeper portions of the Stromboli/Marsili depositional system an important target for understanding the fate of the material and the processes involved in events of catastrophic volcanic island flank collapse. Survey of the northern slope of the Stromboli volcano continued the work commenced during TTR-14 cruise, aimed at collecting more high resolution data for an ongoing study of the volcano flank collapses (Fig. 36).

Surveys in two other areas investigated during the Leg, Angitola slope valley and Cefalu basin, had the aim of studying the sedimentary processes acting along the Calabrian and Sicilian margins (Fig. 36).

II.1. Deep-sea transport and deposition of the Stromboli 30/12/2002 landslide

M. MARANI, F. GAMBERI, A. DI ROBERTO,
H. PIRLET, M. IVANOV., A. AKHMETZHANOV
AND TTR15 SCIENTIFIC PARTY

On 28 December 2002, lava emission and slope movements of the Sciara del Fuoco (SdF) preceded the tsunamigenic landslide

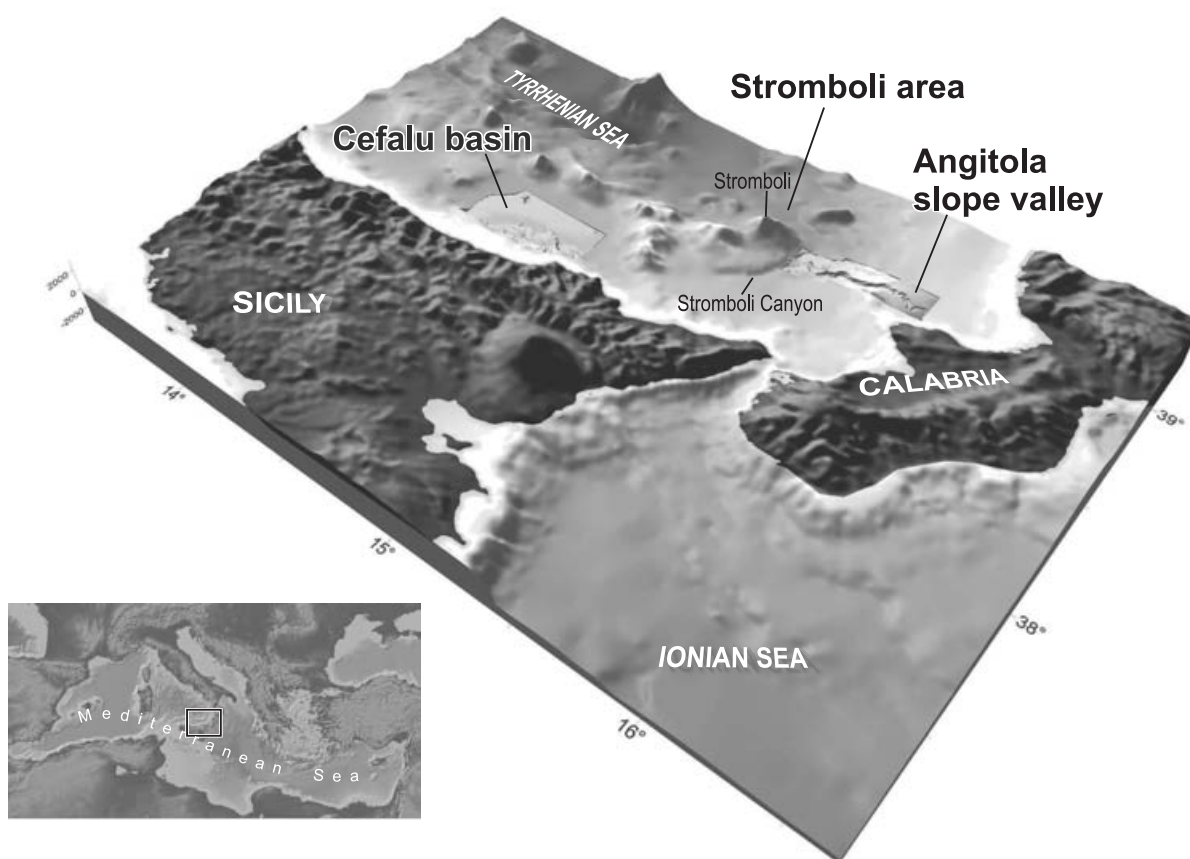


Figure 36. Overview of working areas of the Leg 3 in the Tyrrhenian Sea.

that took place three days later, on 30 December 2002, involving 25-30 x 106 m³ of volcanic material. Deposits of the landslide in both its distal and proximal facies were investigated during two high resolution marine surveys conducted offshore of the SdF (TTR-14 and TTR-15) on board the RV *Professor Logachev*.

During TTR-15 three additional MAK lines with 100kHz resolution were collected in the area extending the coverage of the landslide affected submarine slope of the Stromboli volcano. 7 TV-guided grab samplers and 4 bottom camera deployments along with 17 bottom sampling stations were conducted in order to groundtruth the acoustic data (Fig. 37, Table 2, Annex I).

Results indicate that the thickest, coarse-grained landslide deposit extends over a NNW elongated area at water depths between 1000 and 2000 m at a distance of 6 to 8 km from the shoreline. The deposit consists of several discrete, mainly chaotic assemblages of fresh cobble-sized scoriae and lava

flow clasts within a coarse sand matrix (Fig. 38). Down-slope and laterally, the coarse-grained deposit grades to black volcanoclastic sand, often arranged in ripple bed forms. The landslide material contrasts with the surrounding seafloor in being completely devoid of a hemipelagic sediment cap. Extensive sampling of landslide derived material was performed in its proximal and distal facies utilising TV-guided grabs, gravity and box cores. Initial interpretation of depositional textures indicate that the proximal, coarser deposits derive from low-coherence, granular debris flow processes.

Distally, box coring performed about 24 km north from the NW shoreline of Sciara del Fuoco, in a site located on the right (far) side of the Stromboli canyon, sampled a sediment sequence capped by a 2-3 cm-thick sandy layer (Fig. 39). Sedimentological and compositional features of the layer are consistent with an origin from a volcanogenic turbidity current cogenetic to the debris flow generated by the 2002 landslide.

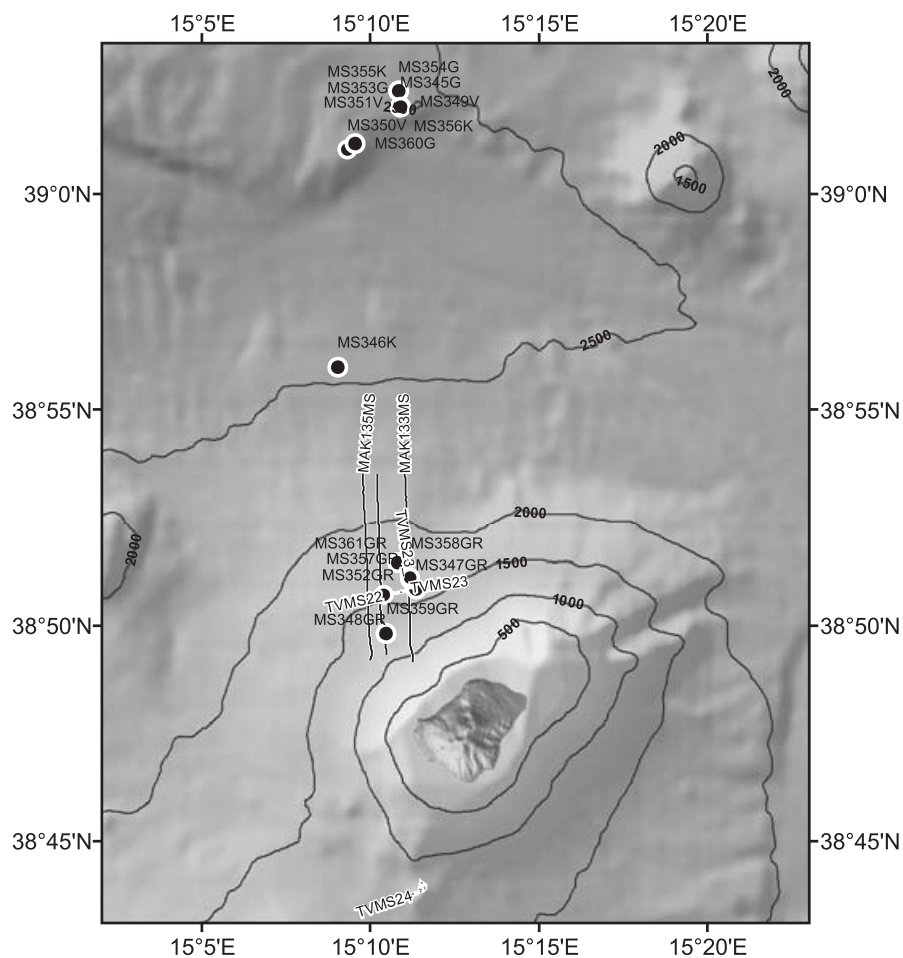


Figure 37. Location map of the Stromboli area.

Table 2. General information on the cores sampled in the Tyrrhenian Sea during Leg 3.

Core N	Date	Time, GMT	Latitude	Longitude	Depth, m	Recovery, cm
MS345G	05.07.05	13:37	39°02.003	15°10.864	2510	CC
MS346K	05.07.05	20:02	38°55.983	15°09.024	2536	15 cm
MS347GR	06.07.05	18:41	38°50.853	15°11.343	1609	0.5 t
		19:35	38°50.841	15°11.342	1602	
MS348GR	06.07.05	21:57	38°50.705	15°10.385	1515	0.5 t
		22:27	38°50.707	15°10.386	1512	
MS349V	07.07.05	03:42	39°02.008	15°10.880	2508	162 cm
MS350V	08.07.05	00:04	39°01.021	15°09.306	2505	10 cm
MS351V	08.07.05	12:23	39°02.009	15°10.881	2508	111 cm
MS352GR	08.07.05	15:02	38°51.069	15°11.129	1660	Few pieces
		16:22	38°51.073	15°11.169	1659	
MS353G	09.07.05	13:42	39°02.009	15°10.880	2510	CC
MS354G	09.07.05	15:33	39°02.370	15°10.826	2510	CC
MS355K	09.07.05	17:04	39°02.374	15°10.831	2512	20 cm
MS356K	09.07.05	18:37	39°02.010	15°10.879	2500	CC
MS357GR	09.07.05	22:40	38°51.104	15°11.152	1655	0.5 t
		22:52	38°51.112	15°11.176	1655	
MS358GR	10.07.05	01:18	38°51.462	15°10.757	1755	0.5 t
		01:24	38°51.467	15°10.788	1755	
MS359GR	10.07.05	03:55	38°49.823	15°10.432	1193	0.5 t
		04:00	38°49.819	15°10.458	1193	
MS360G	10.07.05	09:20	39°01.165	15°09.536	2489	CC
MS361GR	10.07.05	22:23	38°51.451	15°10.796	1741	0.5 t
		22:33	38°51.463	15°10.785	1747	

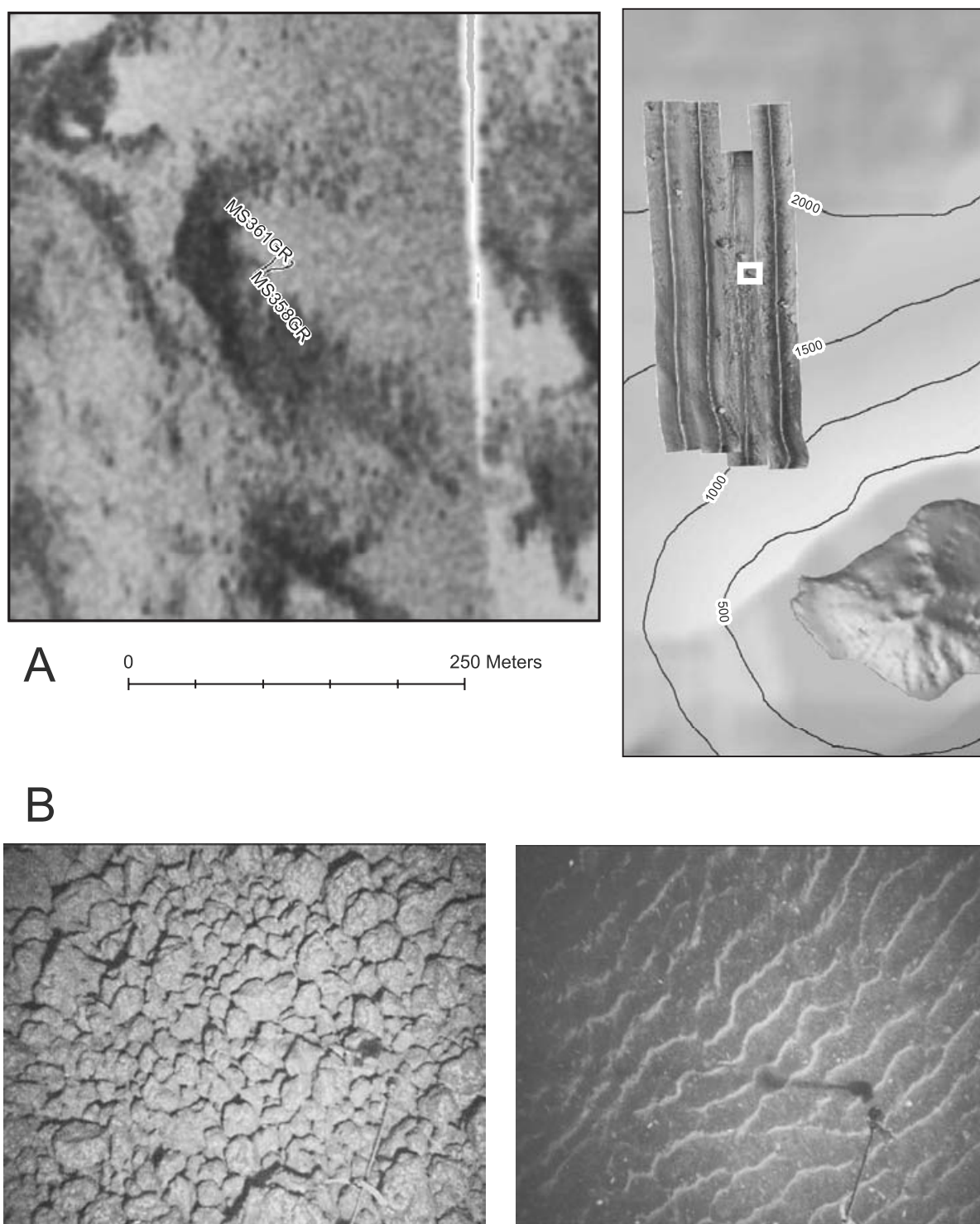


Figure 38. TV guided grab sampling sites MS358GR and MS361GR (A). Large piles of rounded lava clasts and fields of rippled sand are observed on the video footage (B).

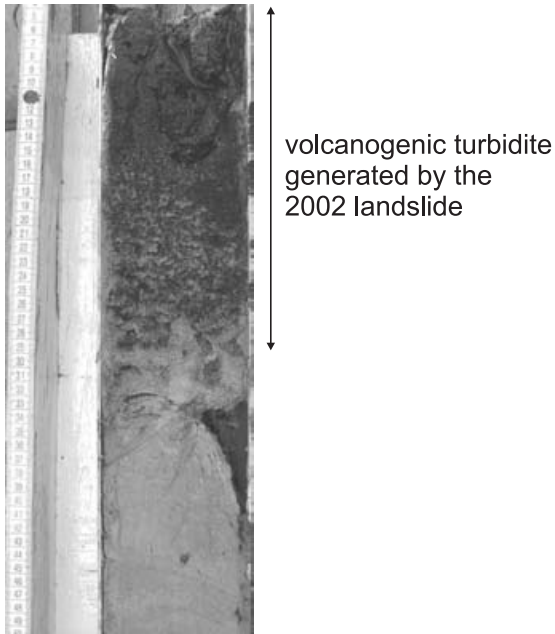


Figure 39. Upper part of the Core MS351V containing volcanogenic turbidite cogenetic to the debris flow generated by the 2002 landslide.

II.2. Sedimentary processes in the Calabrian and Sicilian margin

F. GAMBERI, M. MARANI, M. IVANOV., A. AKHMETZHANOV, A. DI ROBERTO, N. HURTING, R. LECCI, E. LEIDI, R. MOREMON, E. MORRIS, H. PIRLET AND TTR-15 SCIENTIFIC PARTY

II.2.1. Angitola slope valley

On the Calabrian margin, a sidescan sonar mosaic covering an area of about 480 km² was acquired over the Angitola slope valley from a depth of around 700 m down to its junction with the Stromboli valley at around 2500 m (Fig. 40). A single seismic line, crossing the Angitola valley and the surrounding slope, was also shot. The sidescan sonar data, integrated with already available multibeam bathymetry show that the Angitola slope valley is composed of three tracts with different gradient, planform, cross section and sedimentary processes.

The upper tract of the Angitola valley (Fig. 41) has a low gradient, a meandering planform and a flat bottom. The sidescan sonar data show a series of terraces hanging

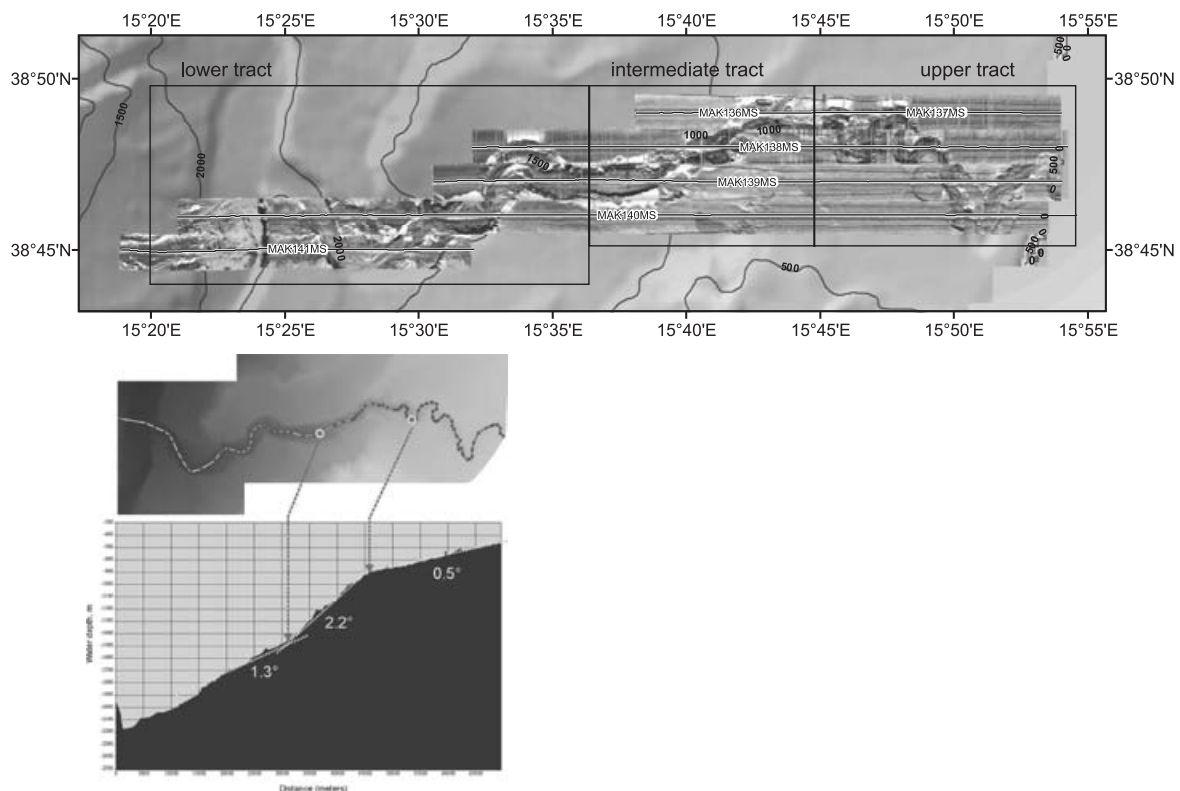


Figure 40. Location map of the Angitola area.

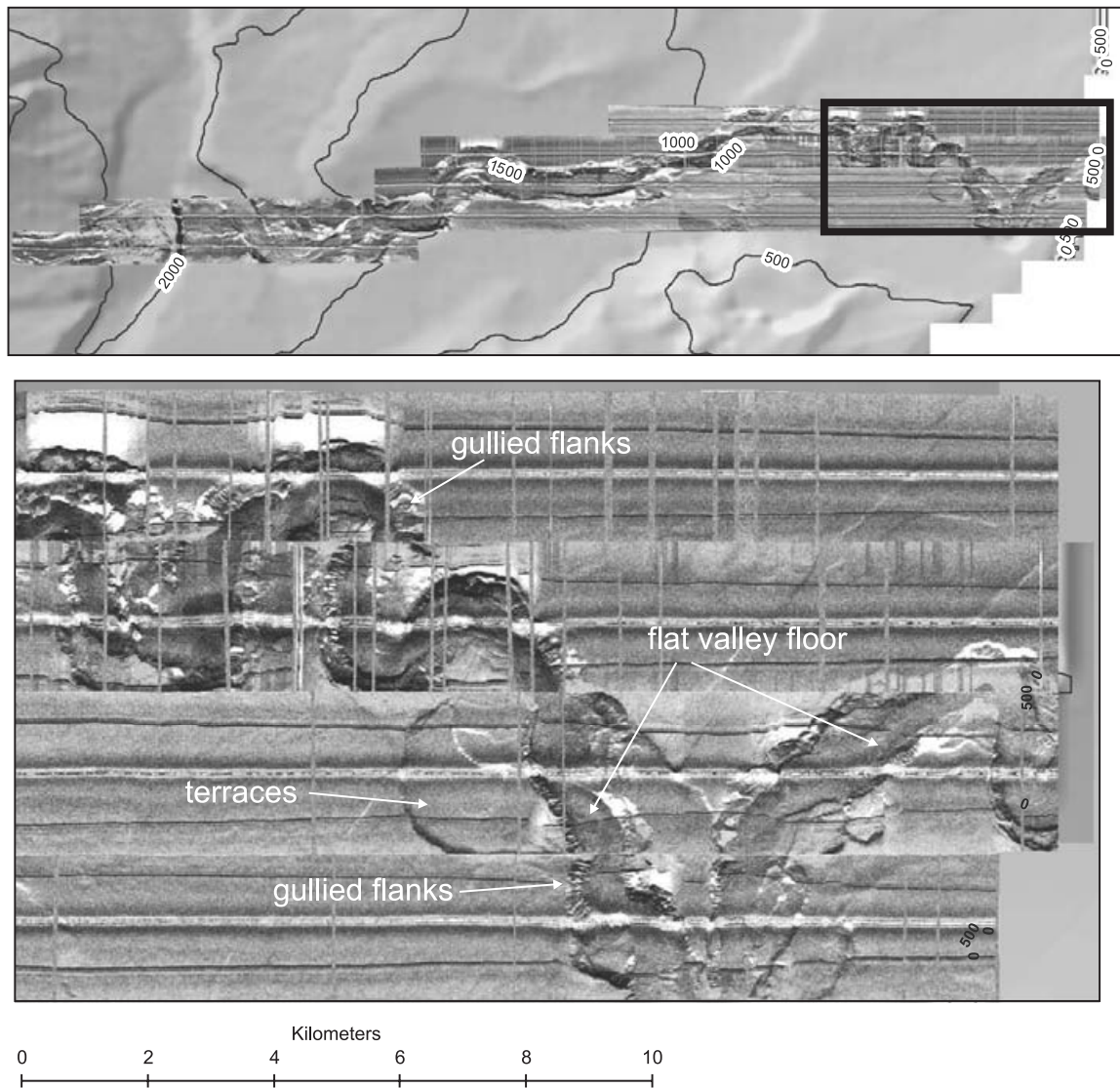


Figure 41. Details of the upper Angitola valley tract.

at different heights above the present day channel floor that represent abandoned meander loops, evidence of an ongoing deepening of the valley floor. The valley floor entrenchment is also accompanied by gullying along most of the flanks. The valley is in general devoid of levees; small levees are present exclusively in the outer sides of two meander bends.

The intermediate tract of the Angitola valley (Fig. 42) coincides with the crossing of an extensional fault, at a depth of around 1000 m, where a sudden increase in the valley floor gradient occurs. It has a V-shaped cross section, a straight planform and has a relief of around 200 m. Mass wasting processes are widespread on the flanks of the

slope valley, as evidenced by frequent circular slump scars. A dendritic pattern of erosion is also present along some portions of the slope valley. Slump deposits accumulate on the floor of the valley that has often a blocky pattern. Along the flanks of the valley, terracing corresponds in general with the areas of sediment removal but the entrenchment of an inner thalweg is responsible for the lowermost terrace along much of the length of the intermediate tract of the Angitola slope valley.

The lower tract of the Angitola valley (Fig. 43) departs from the intermediate one only in having meandering planforms. The sidescan sonar data and the seismic line furnishes also a coverage of the slope surround-

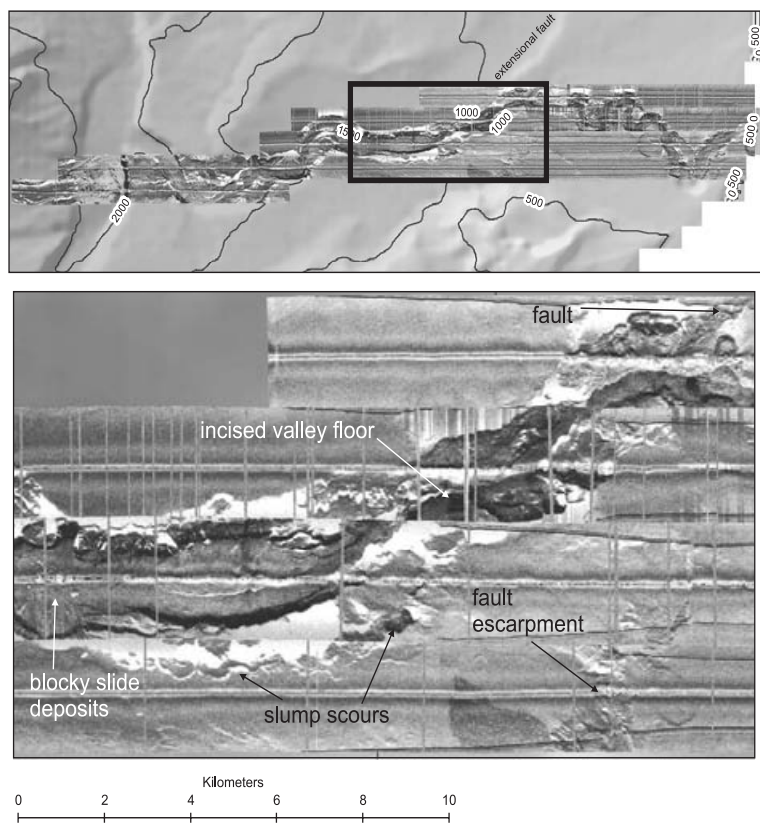


Figure 42. Details of the intermediate Angitola valley tract.

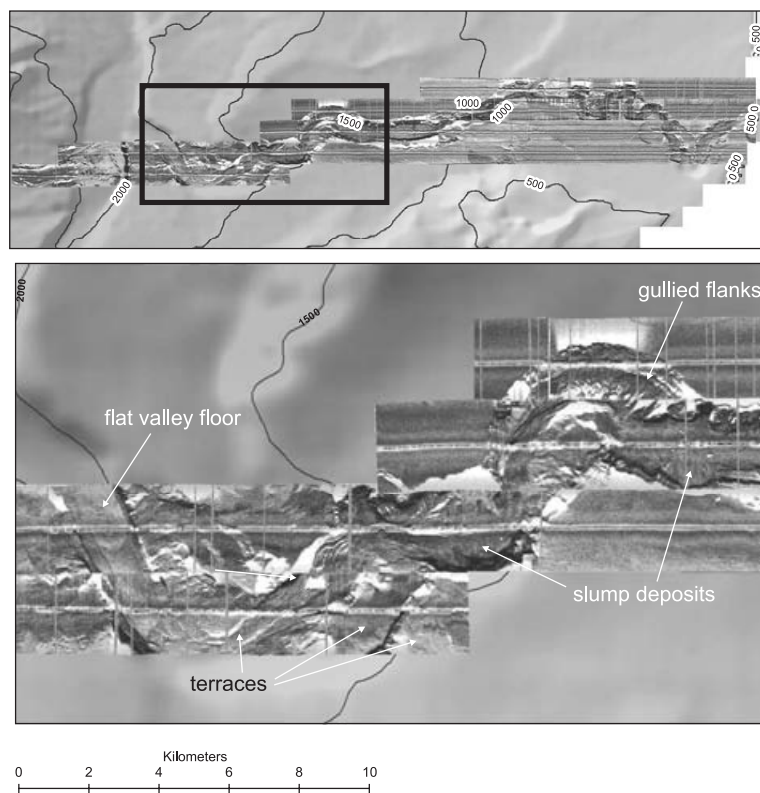


Figure 43. Details of the lower Angitola valley tract.

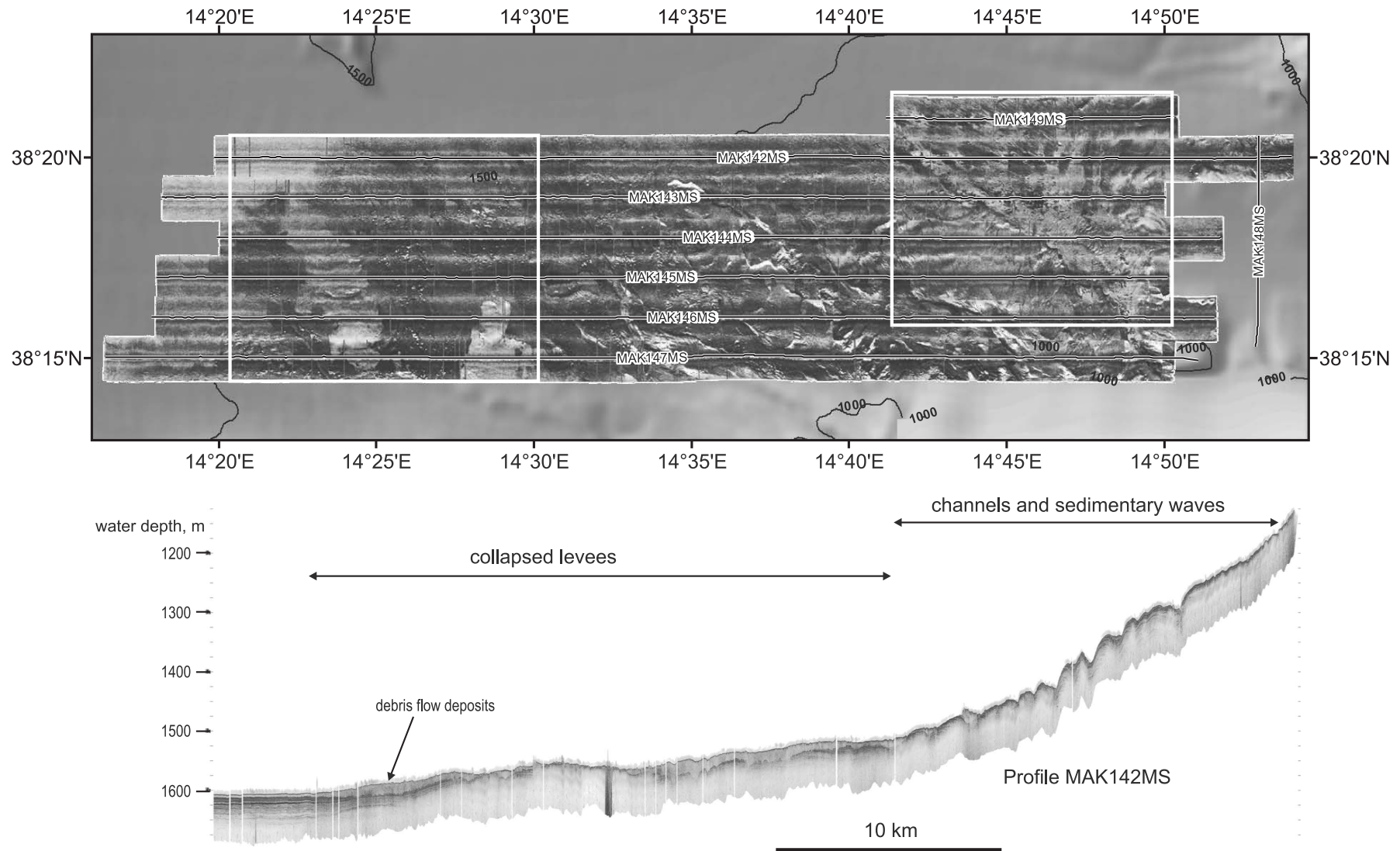


Figure 44. Location map of the Cefalu basin area.

ing the Angitola slope valley. In particular, at the base of the Capo Vaticano high, a subtle escarpment bounds an area with hummocky seafloor overlying a 100 m thick package of sediments that show evidence of internal deformation. It has been interpreted as an area characterized by incipient slope instability where the recent sediments are undergoing a slow downslope movement. Smaller scale slump deposits are also found as blocky seafloor portion at the base of the major faults that surround the Angitola slope valley.

II.2.2. Cefalu basin

On the Sicilian margin, the focus of the investigations, with the acquisition of nearly 930 km² of 30 kHz sidescan sonar coverage was the Cefalu basin (Fig. 44), where multi-

beam data shows that a slope apron consisting of coalescing channel levee deposits is present. In the eastern part of the basin only the distal portion of the slope apron, characterized by the convergence at the base of slope of channels and canyons from the Aeolian and Sicilian slope, was imaged. Here, flows spread over a 10 km wide area causing fields of sediment waves and scours (Fig. 45). In the western portion of the basin, sediment waves and scours are also present in high backscatter floor of the channels. However, the salient feature of the Cefalu basin slope apron is the high degree of instability that affects the levees. Ubiquitous small scale landslide scars are present in the inner sides of the levees. Larger scale mass wasting processes are on the contrary taking place in the outer sides of some of the levees, affected for their whole length by downslope elongat-

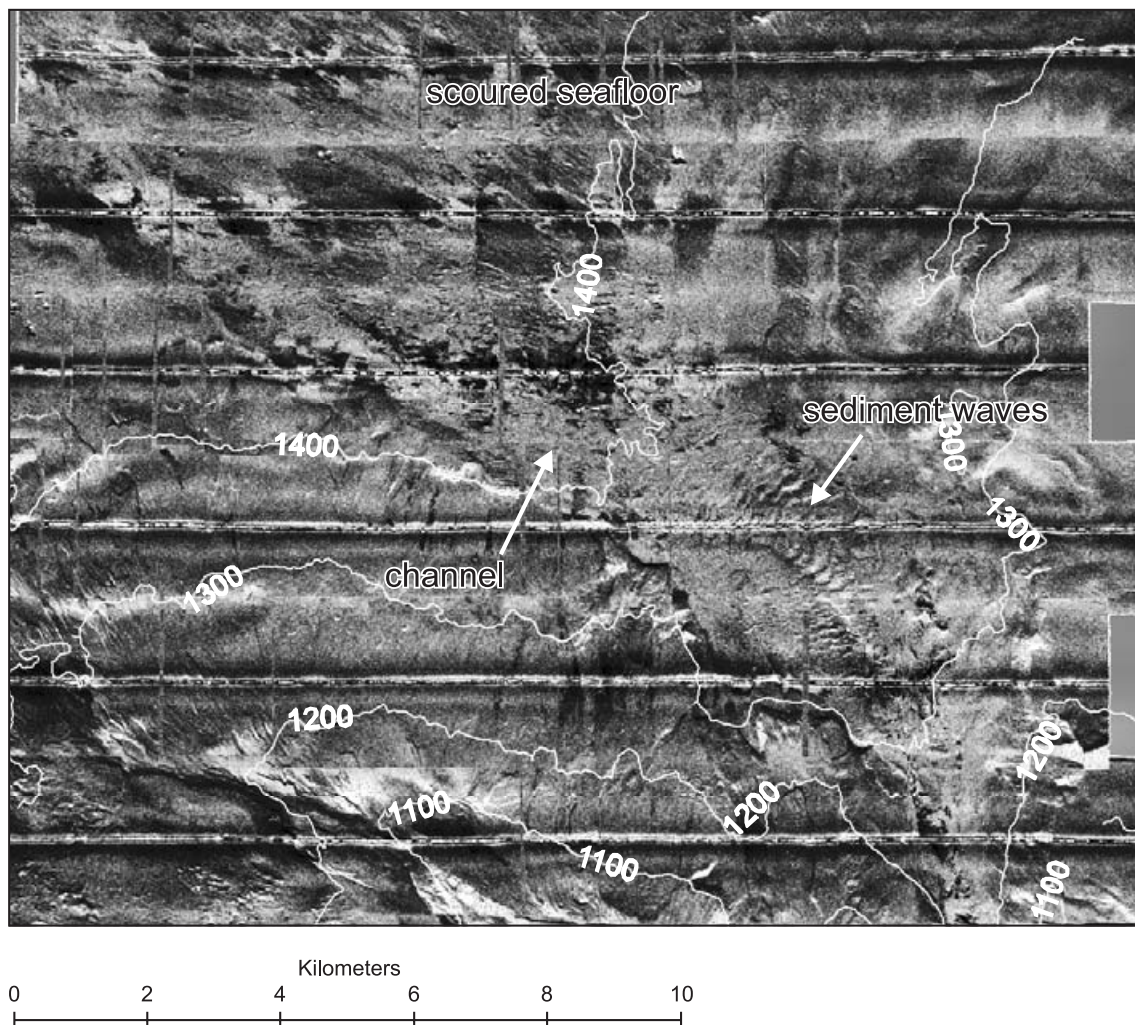


Figure 45. Details of the eastern part of the Cefalu basin dominated by channel-levee complexes.

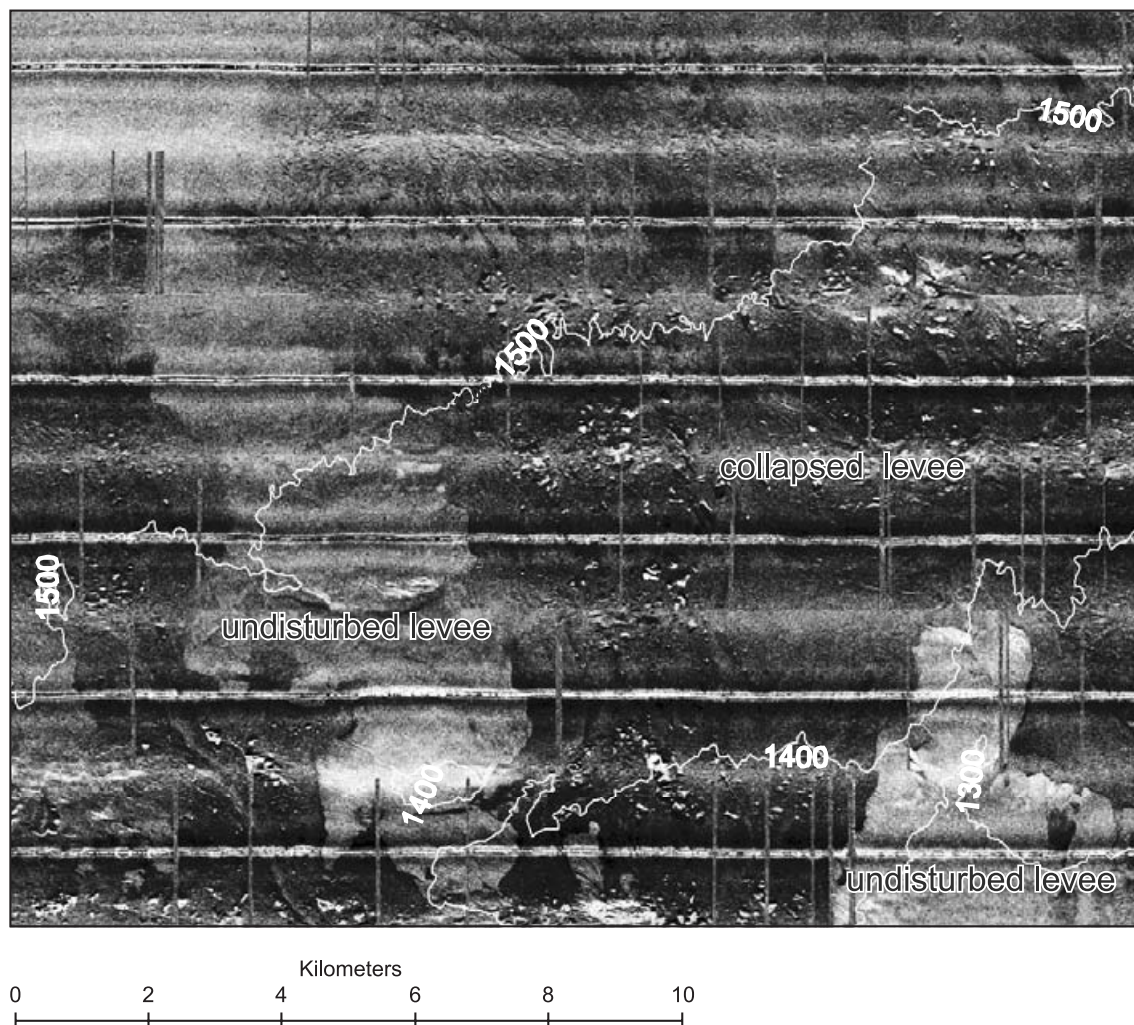


Figure 46. Details of the western part of the Cefalu basin dominated by collapsed levees and widespread occurrence of slide and debris flow deposits.

ed areas of sediment removal. In some cases, landslide scars connect contiguous channels and probably represent incipient avulsion points. Large blocks of displaced undeformed levee sediments are sometimes found in close associations with the removal area. More often, however, the instability processes give rise to debris flow deposits with a variety of surface texture on sonographs (Fig. 46). Subbottom profiler records show them as transparent, up to 10 m thick, layers that pinch out in the distal part of the basin plain (Fig. 46).

III. Gulf of Cadiz (Leg 4)

III.1 Introduction and Objectives of the TTR-15 Leg 4

L. PINHEIRO, M. IVANOV AND N. KENYON

During TTR-9 (1999) a large mud volcano field was discovered in the Spanish and Moroccan sectors of the Gulf of Cadiz (Gardner, 1999; Kenyon et al., 2000; Gardner, 2001), based on the interpretation of a side-scan mosaic collected in the area in 1992 (courtesy by Joan Gardner, Naval Research Laboratory (NRL), Washington D.C.). Five mud volcanoes were then identified in this area: TTR, Kidd and Adamastor, in the Eastern Moroccan Field, and Yuma and Ginsburg, in the Middle Moroccan Field. Gas

hydrates were recovered from the Ginsburg Mud Volcano. The following year, a deep mud volcano field was discovered in the South Portuguese Margin (Pinheiro et al., 2003). In the subsequent years the Gulf of Cadiz has been extensively investigated during 8 research cruises: TTR-10, Anastasya (Somoza et al., 2001), TTR-11, TTR-11A, Tasyo, Cadipor, TTR-12, GAP and TTR-14. A large number of mud volcanoes (30 confirmed by coring), as well as several mud diapirs (e.g. Lolita, Iberico) and elongated diapiric ridges (e.g. Guadalquivir, Cadiz, Formosa, Vernadsky and Renard) have been identified up to the present. Extensive areas of carbonate crusts and chimneys were found in the northern part of the Gulf of Cadiz, near the main channel of the Mediterranean Outflow (MOW), in several diapiric ridges, characterized by a strong-backscatter signature on side-scan sonar images (Diaz-del-Rio et al., 2003). Gas hydrates have been recovered from three mud volcanoes in this area (Bonjardim, Captain Arutjunov and Ginsburg) and there are indications that gas hydrates may also occur in the Carlos Ribeiro mud volcano.

The main objectives of TTR-15 Leg 4 (Fig. 47) were:

- (1) To investigate several mud volcanoes (Mercator, Gemini, Kidd, Tangier, Adamastor, Olenin and Meknes) and ridges (Vernadsky Ridge, Pen Duick Escarpment) in the Moroccan sector of the Gulf of Cadiz with high resolution side-scan sonar, multi-channel reflection seismics (16 channels), coring and underwater TV lines.
- (2) To investigate the possible continuation to the east and west of the southernmost known mud volcano field in the NW Moroccan margin.
- (3) To investigate, with geophysical methods and coring, several high backscatter features observed on the available sidescan sonar imagery from the deep Portuguese sector of the Gulf of Cadiz. Some of these features have a corresponding bathymetric expression and need testing to ascertain if they are mud volcanoes.
- (4) To investigate the structural control of the fluid escape structures in the Gulf of Cadiz.
- (5) To investigate the fauna associated with fluid seepage in new areas of the Gulf of Cadiz, to revisit several known structures for more detailed work and to obtain quantitative samples on active structures.
- (6) To collect specimens for chemosynthetic endosymbiont identification and for genetic and stable isotope studies.
- (7) To investigate the faunal distribution in transects across the head of the Cadiz submarine valley in the SE Portuguese Margin.

III.2. Geological Setting

L. PINHEIRO

The Gulf of Cadiz is located at the westward front of the Betic-Rifian Arc, in the easternmost sector of the Azores-Gibraltar segment of the Africa/Eurasia collisional plate boundary. It has had a very complex geological history and has undergone several episodes of rifting, compression and strike-slip motion since the Triassic (Wilson et al., 1989; Dewey et al., 1989; Maldonado et al., 1999). The westward migration of the Alboran domain during the Miocene caused the Gulf of Cadiz to form as a forearc basin associated with the formation of the Betic-Rifian Arc (Bonnin et al., 1975, Auzende et al., 1981; Maldonado and Comas, 1992; Lonergan and White, 1997; Maldonado et al., 1999). This phenomenon was related to the post-Oligocene extensional regime in the western Mediterranean and the formation of the Neogen backarc basins (Royden, 1993; Lonergan and White, 1997; Rosenbaum et al., 2002). In Tortonian times, a large tectonic body was emplaced in the Gulf of Cadiz.

During the final stages of the accretion of the Betic-Rifian Arc and the emplacement of the thrusting units, gravitational sliding of mobile shale and salt stocks formed a giant complex of mass-wasting deposits, generally known as the Gibraltar Olistostrome that reached as far west as the Horseshoe and Seine abyssal plains. This feature appears as a chaotic, highly diffractive body, with high-amplitude reflections on the seismic sections (Riaza and Martinez del Olmo, 1996) and it consists of a mixture of Triassic, Cretaceous, Paleogene and Neogene sedimentary units,

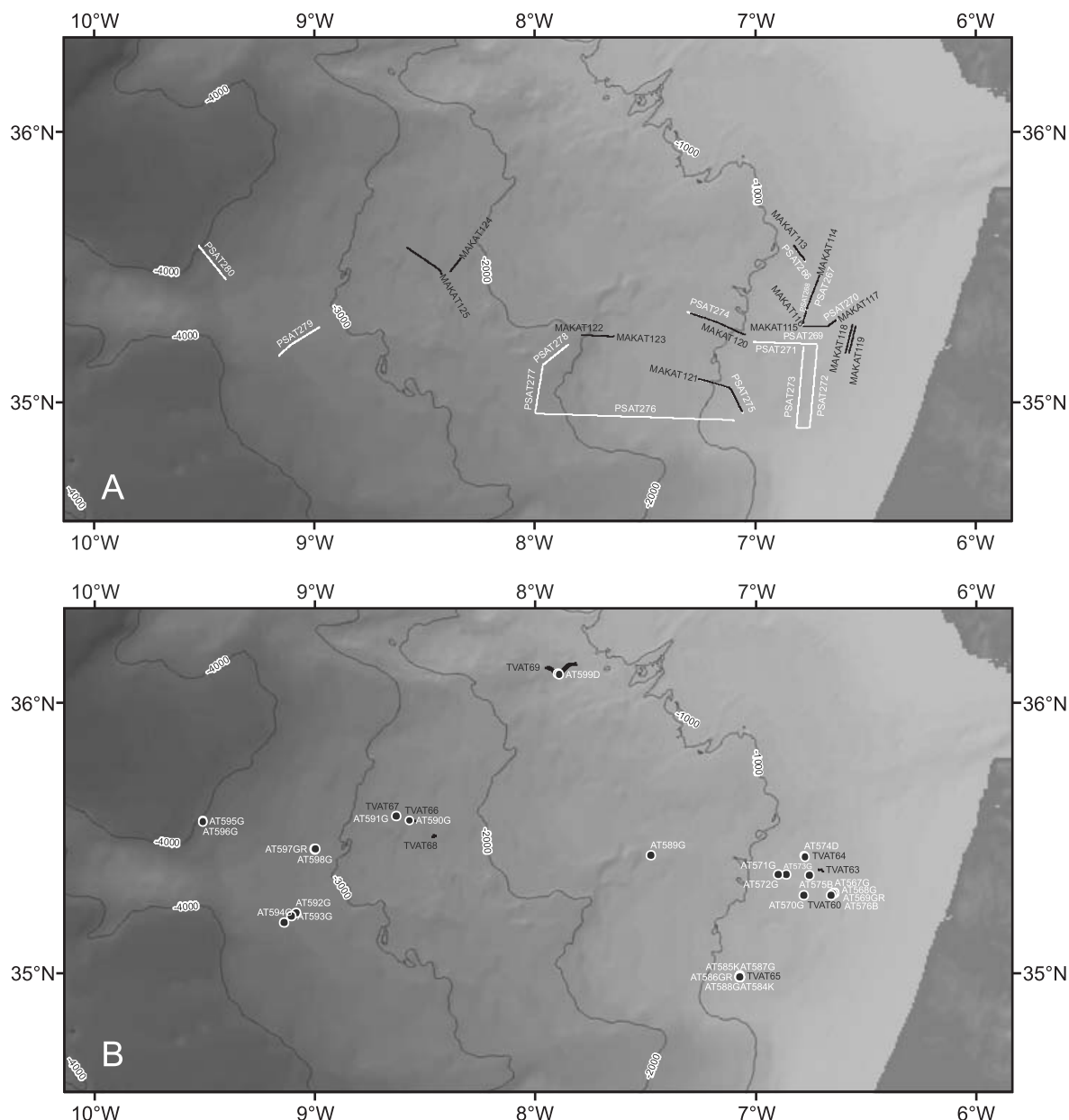


Figure 47. Summary of the research work carried out during the TTR-15 Leg 4. A: OKEAN, seismic and MAK lines; B: camera surveys and sampling stations.

overlying a Palaeozoic basement (Maldonado et al., 1999). It involves a huge volume of mud and salt diapirism of Triassic salt units and undercompacted Early-Middle Miocene plastic marls (Maldonado et al., 1999). The origin of this chaotic body is highly controversial. It has been interpreted as a complex of olistostromes and debris flows, originated by gravitational sliding, and tectonic thrust units - tectonic melanges (Torelli et al., 1997; Maldonado et al., 1999; Medialdea et al., 2004). Alternatively, it was

also interpreted as an accretionary complex related to the migration of the Alboran terrain as a consequence of a once active subduction zone (Royden, 1993; Lonergan and White, 1997; Rosenbaum et al., 2002). Recently, Gutscher et al. (2002) proposed that this subduction is still active beneath Gibraltar.

Throughout this area, extensive hydrocarbon-rich fluid venting and mud diapirism are observed, which includes numerous mud volcanoes, methane-related authigenic car-

bonates (crusts, chimneys and carbonate mounds) and pockmarks (Baraza and Ercilla, 1996; Gardner, 2001; Kenyon et al., 2000; Diaz del Rio et al., 2001; Pinheiro et al., 2003; Somoza et al., 2003). These are related to both the high sedimentation rates during the Pliocene, associated with high subsidence (Maldonado et al., 1999), and to the lateral compression due to the Africa-Eurasia convergence, both of which promoted the fluid migration to the surface. Several NE-SW oriented mud diapiric ridges have been found in the NE sector of the Gulf of Cadiz, which are characterized by high backscatter on the available side-scan sonar imagery. There is a strong suggestion that these features are strongly structurally controlled. Sampling has shown that the high backscatter is related to a high abundance of carbonate chimneys and crusts on these ridges (Diaz del Rio et al., 2001; Somoza et al., 2003).

Focal mechanism solutions show that the stress regime along the Africa-Eurasian plate boundary in this area is a combination of dextral strike-slip and a NW-directed compression near Gorringe Bank and the Gulf of Cadiz (Fukao, 1973; Borges et al. 2001). Presently, the direction of maximum horizontal compressive stress along this segment of the plate boundary is estimated to be approximately WNW-ESE in the Gulf of Cadiz, leading to a general transpressive regime in this area (Cavazza et al., 2004).

III.3. Cold seeps of the Gulf of Cadiz

III.3.1. Seismic and Acoustic Data

III.3.1.1. Seismic data

L.M. PINHEIRO, C. ROQUE, T. SCHWENK, F. DING,
J. CRESPO, J. SANZ, A. BELOVA, C. LEMOS,
J. DUARTE AND B. EL FELLAH

During the TTR-15 Leg 4 cruise, 15 seismic lines (Fig. 47a), covering a total of 161.2 nautical miles, were recorded in two distinct areas of the Gulf of Cadiz: the Moroccan Mud Volcano Field and the Deep Portuguese Mud Volcano Field.

Moroccan Margin

This is the area where the largest mud volcanoes in the Gulf of Cadiz can be found. During the TTR-15 cruise, the lines shot in this area aimed at investigating new structures and also at revisiting several mud volcanoes and tectonic structures for more detailed work.

Line PSAT-266

This is a short NNW-SSE seismic line, approximately 9 km long (Fig. 48). It crosses the Tangier mud volcano, which is clearly visible on the NRL side-scan sonar mosaic, and which was first investigated in 1999, during the TTR 9 cruise (seismic Line PSAT 121).

The NW end of this line shows a nice image of the Tangier mud volcano, with a typical Christmas-tree structure, indicating multiple pulses of past activity. Below 1400 ms (TWT) the mud volcano structure appears to be bounded by steeply-dipping strong reflections, which could represent faults or, more likely, the limit a wide mud intrusion zone above a probably much narrower conduit (the northernmost reflection is very continuous and dips to the south, whereas the southernmost reflection dips to the north and is more discontinuous).

The sedimentary section is slightly deformed, with some evidence of faulting, in particular near the mud volcano and also in the SE portion of the line. Several seismic-stratigraphic units have been identified. The uppermost sedimentary Unit 1 is fairly transparent and it is essentially undeformed, with some evidence of minor faulting (close to the seismic resolution). Some of this faulting appears to be rooted in better defined faults that affect the underlying units, some of which appear to be fairly deep, such as the fault near SP-280, and may have acted in places as fluid conduits (possible gas chimneys, given some observed acoustic blanking).

In the southern part of the line a fairly deep basin is observed (down to at least 1900 ms) which is affected by an apparent SE-dipping reverse faulting. This faulting appears

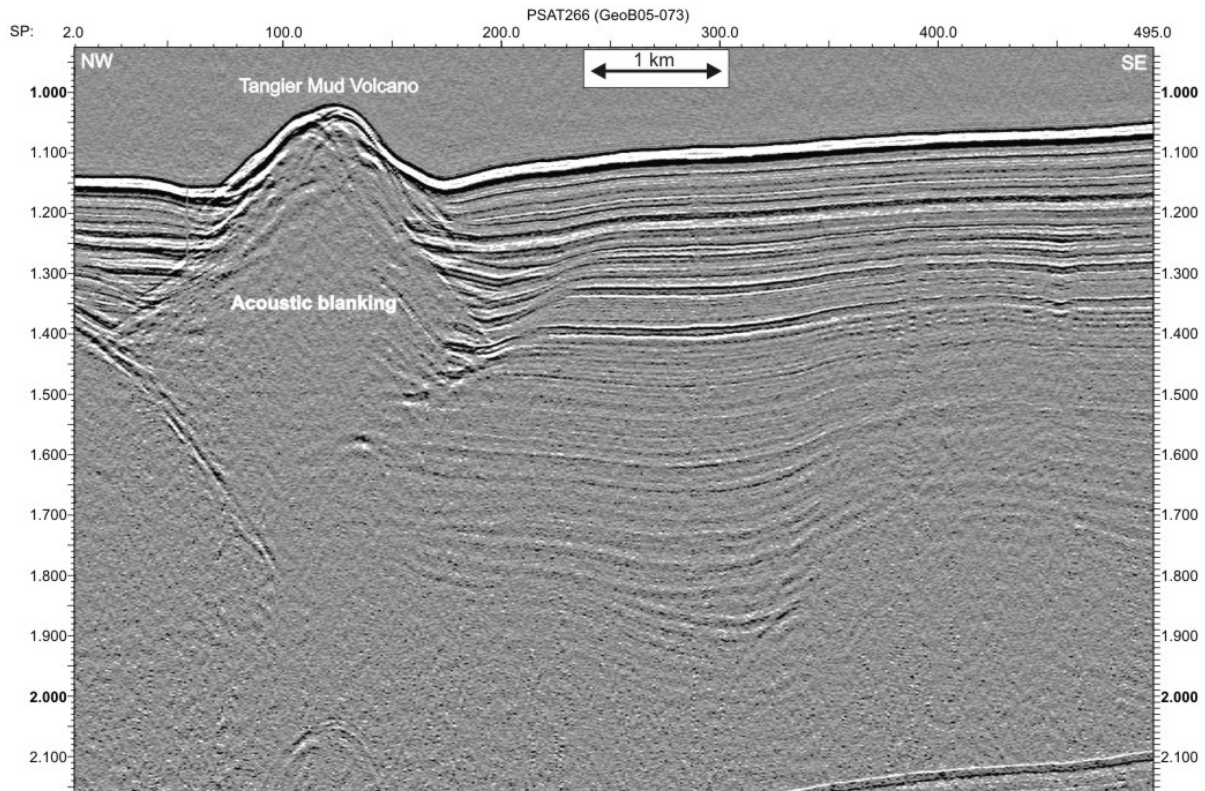


Figure 48. Seismic profile PSAT266. See Figure 47 for location.

to have been particularly active until the top of Unit 4.

Line PSAT-267 and 268

This is a NNW-SSE seismic line, approximately 21 km long. It was shot in two consecutive parts. PSAT-267 is approximately 15 km long and PSAT-268 is approximately 6 km long. It crosses the Kidd and the Adamastor mud volcanoes. On this line, the Adamastor mud volcano profile is fairly symmetric, with a moat around it. It is situated over a fairly deep asymmetric sedimentary basin (approximately 800 to 1500 ms TWT), bounded to the south by a north-dipping thrust (Fig. 49). This fault appears to be active, since it deforms the uppermost layers and the seafloor.

The Kidd mud volcano, in contrast, is strongly asymmetric on this line and it appears to be fault-controlled by active north-dipping ENE-WSW thrusts (two such faults are clearly visible on Line PSAT-267 near SPs 620 and 760. These faults appear to be active, since they deform the upper sedimentary layers and seafloor. At the NNE end

of the line, over a seafloor depression, several approximately E-W small patches with low relief, that could be carbonates mounds, are recognized. At the southern end of line PSAT-268 there is another thrust and another possible carbonate mound is found at the end of the line.

Line PSAT-269

This is an E-W seismic line, approximately 9 km long (Fig. 50). This line crosses the Gemini mud volcano and also a very high backscattering NW-SE ridge. The Gemini mud volcano appears to be faulted by three major faults, two NNW-SSE and another NW-SE.

The high backscatter NW-SE feature that is interpreted as a possible diapiric ridge, is bound by what appears to be erosional moats, and it is also strongly faulted. The sedimentary basins on either side of the ridge show evidence of syn-sedimentary deformation related to movement in the diapiric ridge.

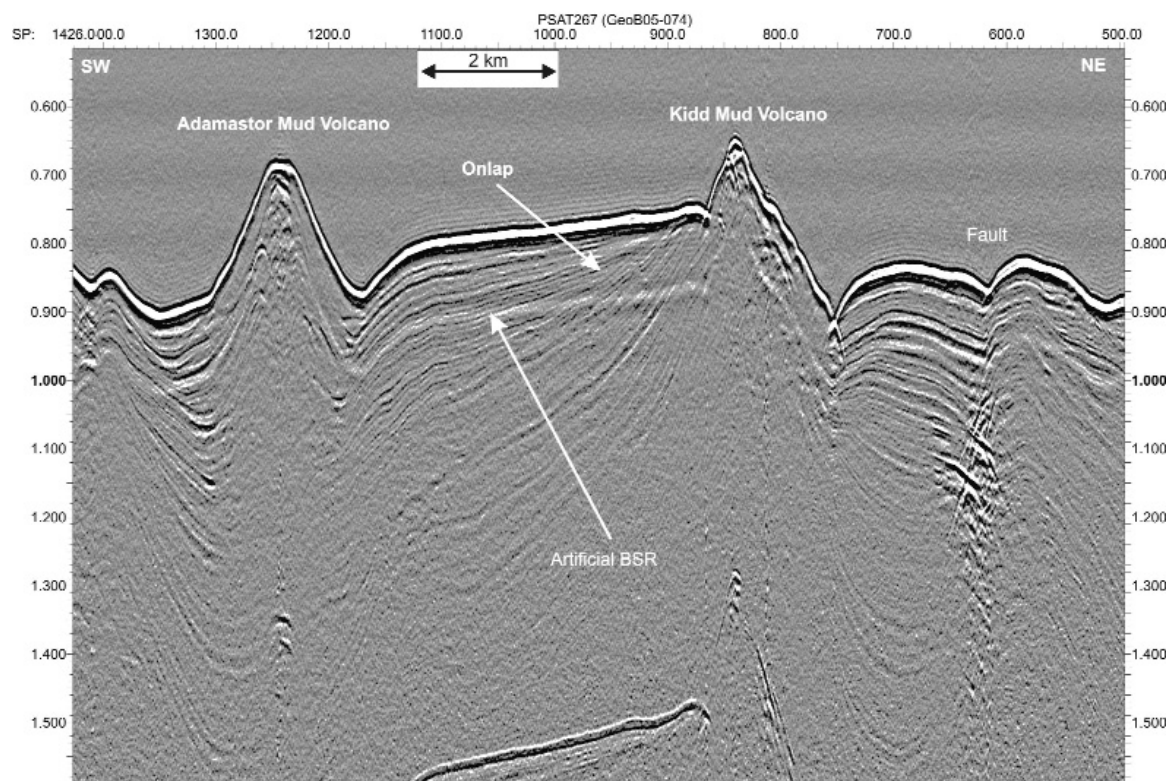


Figure 49. Seismic profile PSAT267.

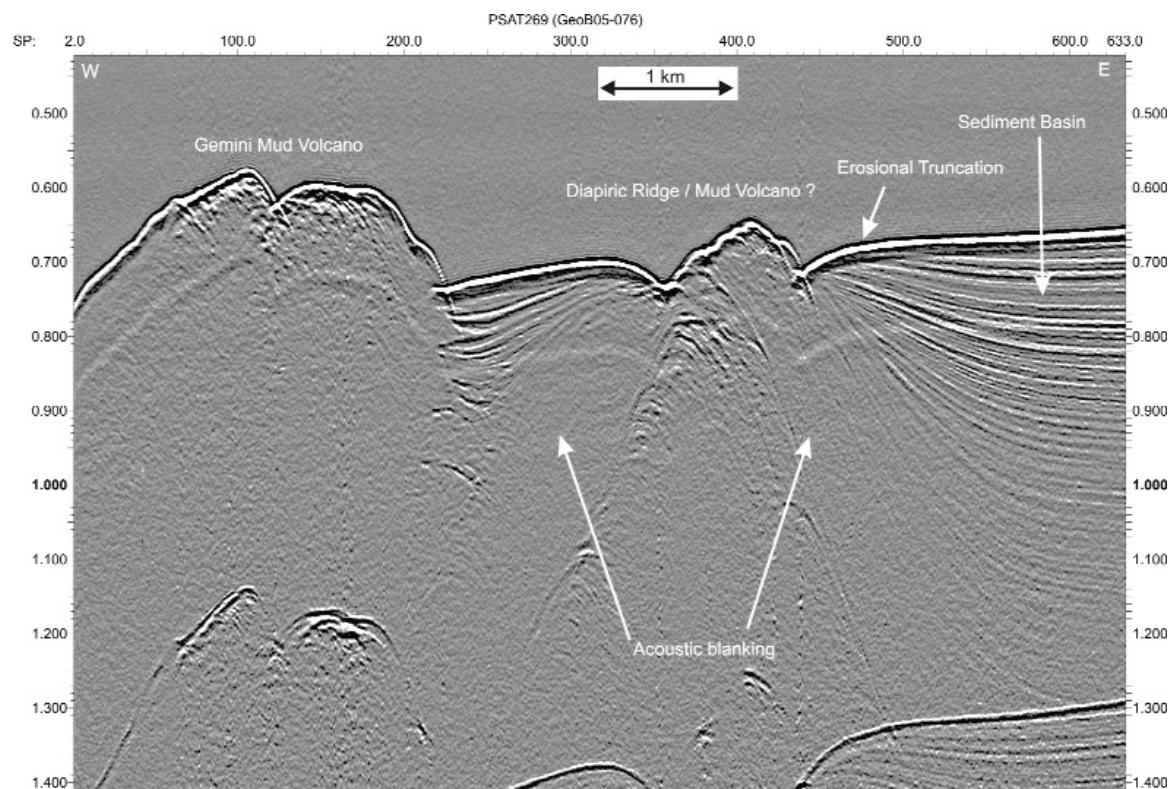


Figure 50. Seismic profile PSAT269.

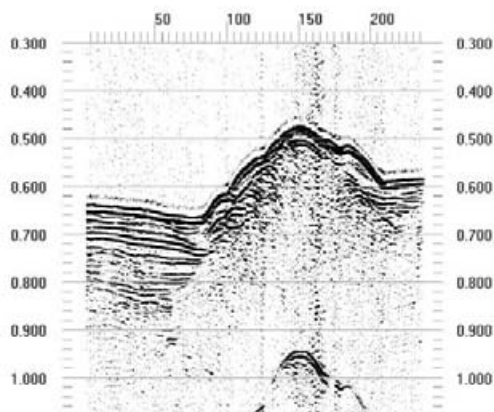


Figure 51. Seismic profile PSAT270.

Line PSAT-270

This NE-SW short seismic line, approximately 3 km long, crosses the Mercator mud volcano (Fig. 51). On this line, the mud volcano exhibits the typical "christmas tree" structure.

Line PSAT-271

This is a W-E seismic line, approximately 22 km long (Fig. 52). The sedimentary section, which includes a fairly thick basin in the

east, has been deformed by thrust faulting during deposition. Combined interpretation of the seismic profile and the OKEAN-271 line, which was acquired simultaneously, shows that the seismic section appears to be crossed by a complex fault system. This includes a NW-SE trending thrust dipping to the NE, which appears to be crossed (offset?) by a major WNW-ESE strike-slip fault, possibly dextral. This fault is the southeastward prolongation of a major fault clearly visible on the sidescan sonar mosaic collected during the TTR-12 cruise. The upper sedimentary units are also offset by several antithetic normal faults, two of which offset the seafloor (at approximately SPs 270 and 380).

Line PSAT-272

This line is a N-S seismic line, approximately 33 km long, shot in an area with no previous information. The purpose of this line was to extend the sidescan sonar mosaic obtained during the TTR-14 cruise to the east, near the Moroccan margin. This line shows a morphology dominated by sedimentary and erosional processes, well-repre-

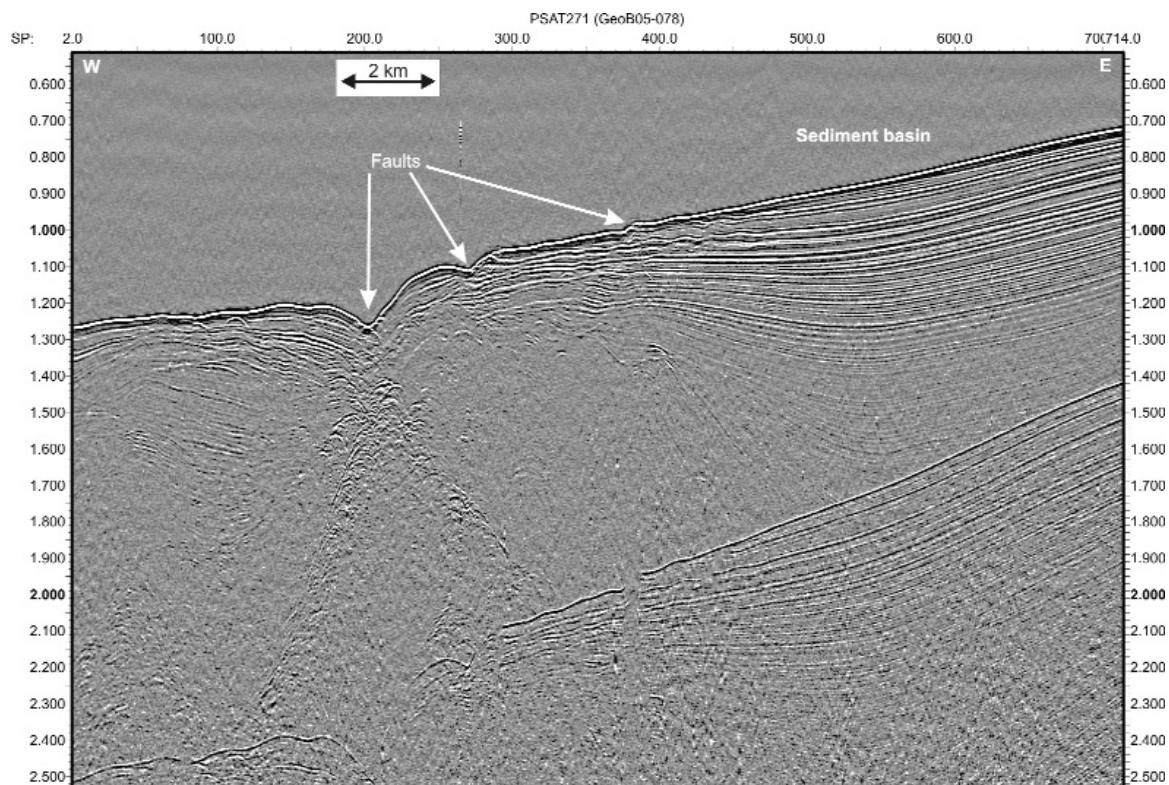


Figure 52. Seismic profile PSAT271.

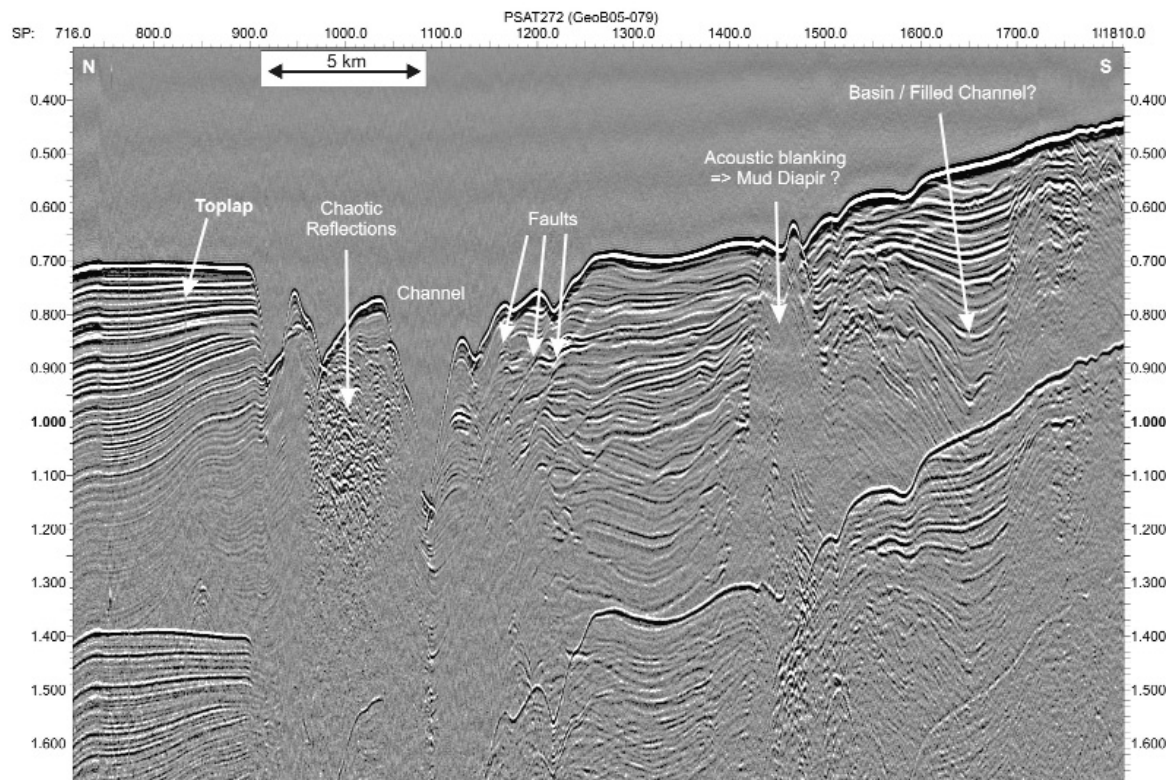


Figure 53. Seismic profile PSAT272.

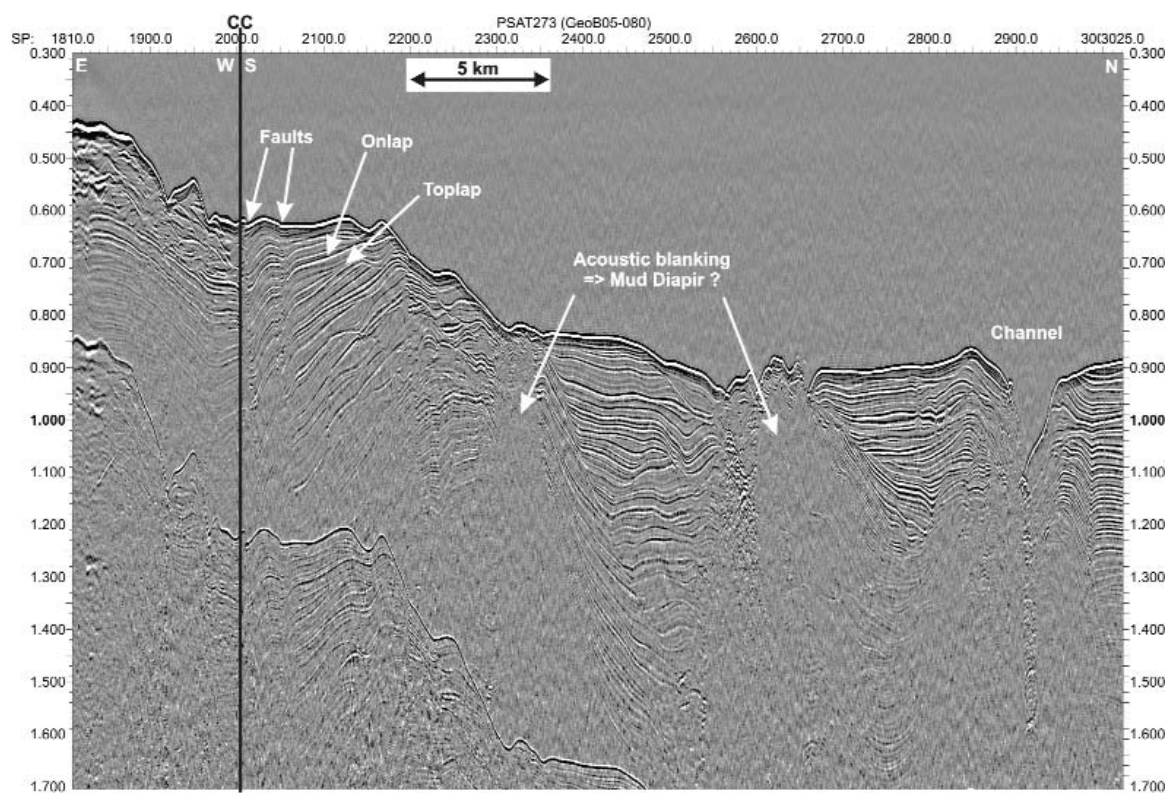


Figure 54. Seismic profile PSAT273.

sented in the northern part of the line by a very thick and undeformed stratigraphic sequence cut by a NE-SW trending submarine canyon system, visible on the GEBCO bathymetry (Fig. 53). In the central part of the line a thick channel-levee sequence (about 0.4 sec TWT) is observed, showing migration towards the north of the submarine canyon. At present the active canyon is deeply incised and reaches a maximum depth of about 330 m below the average seafloor depth in this area. The southern part of the line shows an asymmetric sedimentary basin overlying older sedimentary sequences which are strongly deformed under compression. One possible mud diapir or mud volcano is situated at approximately SP 1480. In the southern end of the line, the asymmetric sedimentary basin appears to be bounded by a major fault, to the south of which acoustic blanking is observed below the upper sedimentary units suggesting possible gas/mud diapirism.

Line PSAT-273

This seismic line consists of two segments with different orientations: W-E between the start of the line and the SP 2010,

and then WNW-ESE (Fig. 54) The line shows a complex wrench fault system, with major high-dip strike-slip faults with a typical flower-structure, and northward-dipping thrust faults. The faults, in general, affect the uppermost units of the thick sedimentary sequence and disrupt the sea-floor. Asymmetrical sedimentary basins were developed, with several unconformities, possibly related to the main tectonic events that affected this area and also to a strong bottom-current activity. In the northern part of the seismic line, gas chimneys are observed. An asymmetrical submarine canyon is incised in the sedimentary deposits near the north end of this line. There are two areas of localized acoustic blanking that may represent mud diapirs.

Line PSAT-274

This seismic line runs almost parallel to a major wrench(?) fault system. Combined interpretation of the seismic profile and the 30 kHz MAKAT120 sidescan sonar image (Fig. 55), collected simultaneously, shows that a major fault, F2, very likely a strike-slip fault, crosses the seismic line in two places, near SPs 640 and 1240. This fault appears to

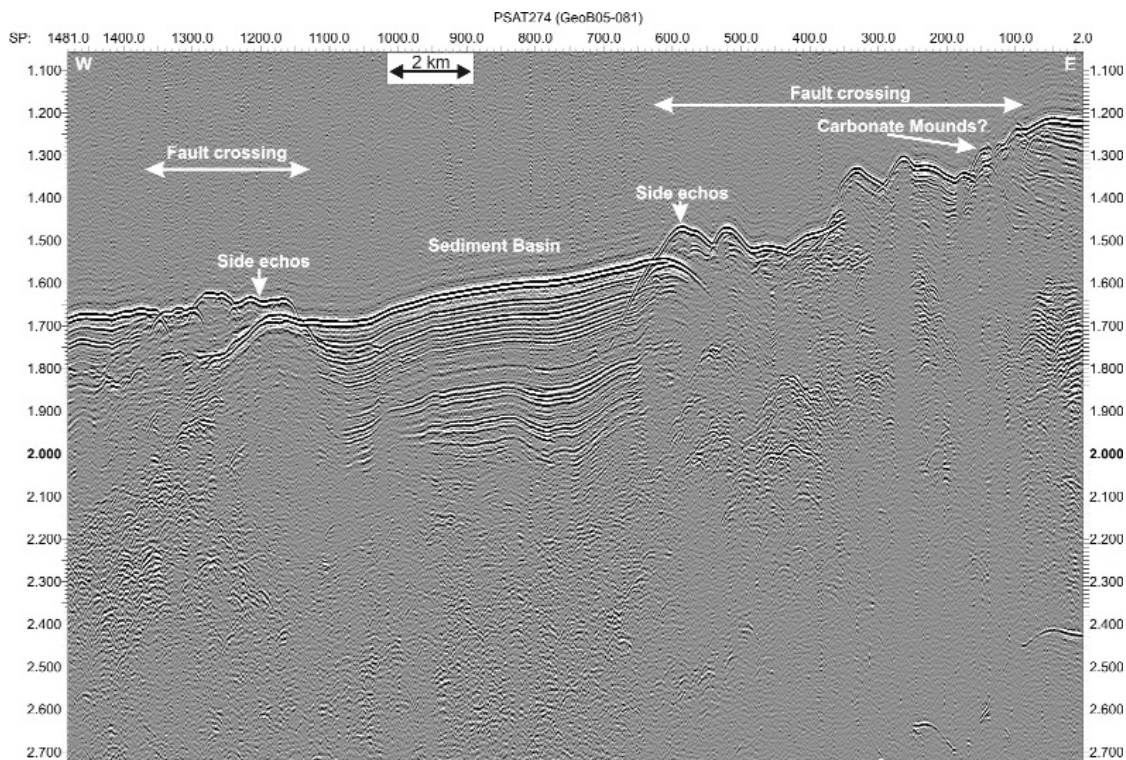


Figure 55. Seismic profile PSAT274.

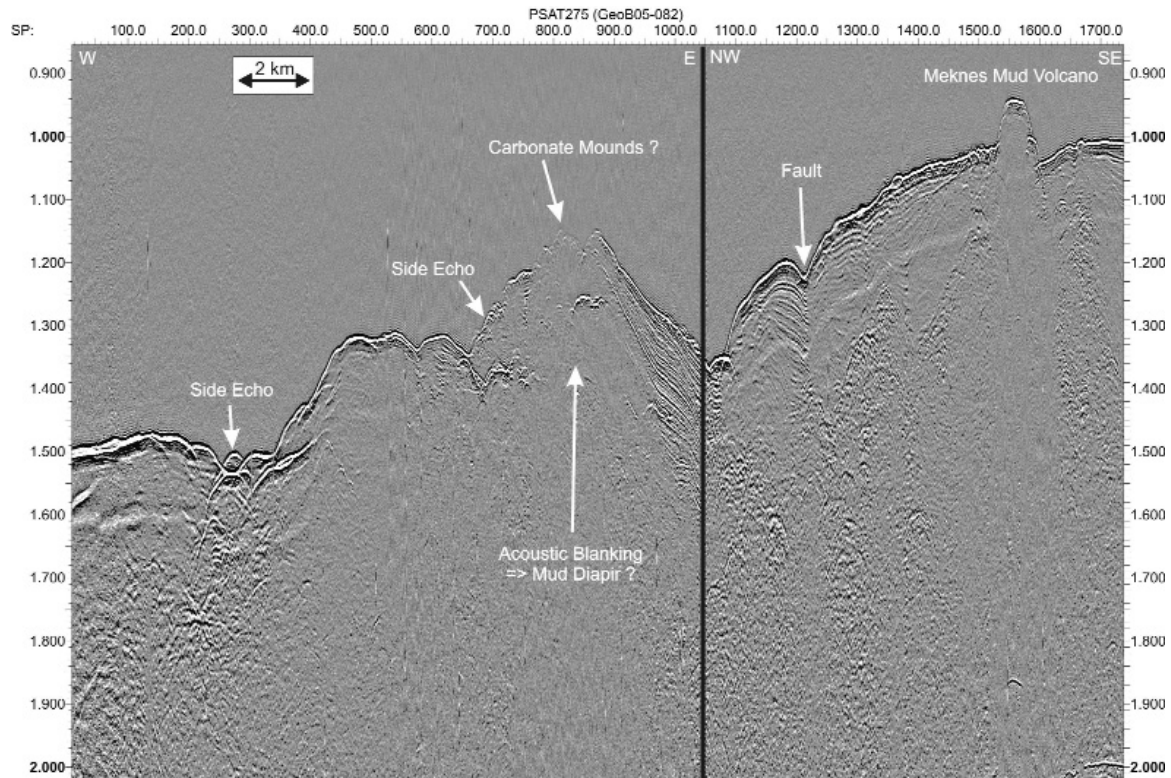


Figure 56. Seismic profile PSAT275.

be undulating, ranging from WNW-ESE to ENE-WSW; nevertheless, the possibility that we are imaging two faults instead of one cannot be completely ruled out. Between the two crossings of the fault, a sedimentary basin, bounded by small highs, is observed. It could be a small pull-apart basin, consistent with a dextral movement along the fault. Several small highs, some of them aligned, are observed on the SE segment of the line. They are interpreted here as possibly carbonate mounds. They also appear to be associated with an other fault system (F1), that looks conjugate to F2. Below these structures there is some evidence of acoustic blanking, which may indicate the presence of fluid escape structures.

Line PSAT-275

This line has two distinct segments: the westernmost was shot in a WNW-ESE direction, while the easternmost segment was shot NW-SE (Fig. 56). These two segments join near SP 1100. The total length of the seismic line is approximately 26 km, and it crosses the Meknes mud volcano at the end of the line. The interpretation was done by combining

the seismic data and the side-scan line MAK121. In the seismic line between the SPs 0 and 850, the presence of possible thrust-faults dipping ESE is suggested by sea-floor disruption, imaged as scarps in MAK121 line. Between SPs 650 and 1100 continuous aligned features imaged in the MAK record appear to be good evidence for the presence of carbonate mounds. These are possible NW-SE carbonate ridges between SPs 1050 and 1100. These ridges are bounded to the southeast by a NE-SW trending fault. Towards the southeast, well-developed syn-tectonic basins form the back of the main thrust-faults. Finally, a chaotic body is observed below these basins.

Lines PSAT-276, PSAT-277 and PSAT-278

These 3 contiguous seismic lines are described here together. Line PSAT-276 is an E-W line approximately 62 km long, line PSAT-277 (20 km long) is approximately S-N and Line PSAT-278 (13 km long) is SW-NE.

Line PSAT-276, to the west of the area near the Meknes mud volcano, was shot to investigate a region with no previous data except for a few lines shot during the TTR-14

cruise. This seismic section shows evidence of intense faulting and erosional processes. Three major faults, probably strike-slip, cross this section. The central part of the line shows several "suspended" basins, highly faulted, with sedimentary sections that can reach a total thickness of about 270 m (350 ms TWT).

The presence of carbonate mounds in this area could be inferred by small diffractions observed at SPs 150 and 300.

Line PSAT-279

This is NW-SE trending line, that crosses three new mud volcanoes discovered during this Leg. These structures follow a general NW-SE direction and are located approximately between 3200 and 3375 m water depth.

III.3.1.2. MAK deep-towed sidescan sonar data

N.H. KENYON AND A. AKHMETZHANOV

Line MAKAT-113

The 30 kHz line runs SE across the Tangier mud volcano. At the north end of the line is an alignment of small pinnacles oriented ENE. They may be on a ridge that was not crossed by the profile. At what is believed to be the foot of the ridge there is a line of higher backscattering that may mark its foot. The pinnacles have a "ribbed" appearance. They resemble the pinnacles seen later on line MAKAT-121 that were shown by TV and sampling to be related to cold water corals.

Tangier mud volcano was crossed very near to its summit and is about 100 m high. It is a fairly conical shaped mud volcano as the flows radiate out in all directions. Those on the SE half of the volcano are higher backscattering and thus presumed to be youngest, those on the northwest have the lowest backscatter levels and are presumed to be the oldest of the surface flows.

The profiler shows parallel bedded sediments with a high penetration of up to 55 m. There is ponding at the foot of the north side of the Tangier mud volcano. Its origin, usually attributed to turbidites, is not known.

There are refraction patterns at the far range due to stratification in the water column.

Lines MAKAT-114, 115, 116 and 117

These four lines cross the Kidd, Adamastor, Gemini, Don Quichot and Mercator mud volcanoes. Line MAKAT-114 was run at 30 kHz and runs southwards. It has drop outs along most of its length. An E-W trending line of high backscattering patches, up to 100 by 400 m, with low relief, corresponds to an area without bedded sediments. Its origin is unclear. The seismic profile, PSAT- 267, indicates a possible fault but no buried diapiric structure. It may be a line of carbonate crust. Several fields of small high backscatter patches, up to 40 m across, occur nearby. There is a faint line of these patches along a fault seen on PSAT- 267. Kidd mud volcano is conical, surrounded by a moat and has a seabed that is 50 m deeper to the north than to the south. There are concentric faults marking the crater, which is up to 500 m in diameter. There are no obvious radial flows and a generally medium level of backscatter, indicating that any flows are buried by hemipelagic sediments. Adamastor mud volcano is also conical in shape, with a 400 m diameter summit crater. There are radial patterns due to downslope flows but the level of backscatter is uniformly medium. There is a fine speckled pattern in the moat on the north side.

MAKAT-115 is a 30 kHz line that continues to the south across a newly mapped mud volcano as far as the Renard Ridge. The new mud volcano is small, only 1 km in diameter. There is a possible circular crater with low backscatter, just to the east of the line. This mud volcano has no obvious down slope flows. The WNW trending Renard Ridge has a series of mainly NE-SW trending ridges on top of it and on the steep southern Pen Duick Escarpment. These mounds have previously been shown to be probable carbonate mounds (Van Rensbergen et al., 2003).

MAKAT-116 is a 30 kHz line that runs E across the Gemini mud volcano and the Don Quichot structure (Fig. 57). Gemini has two similar, large circular summit craters with

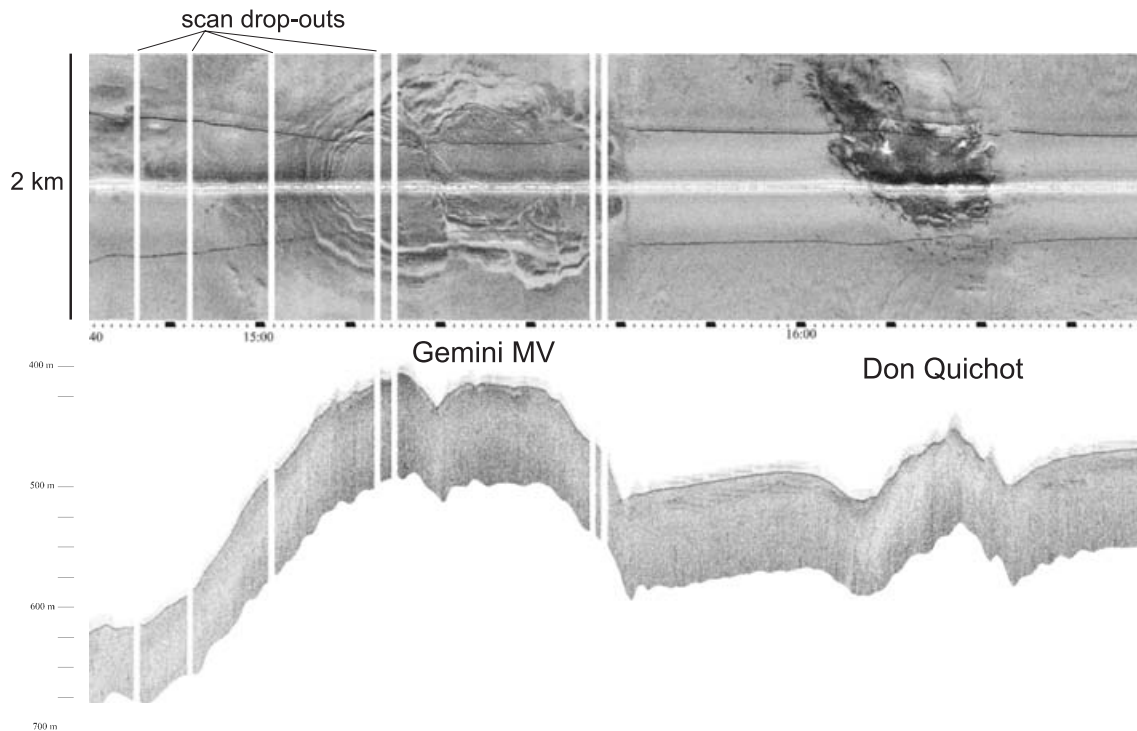


Figure 57. Fragment of the MAK line 116 showing Gemini MV and Don Quichot structure

marked concentric patterns that have fused together. Several faults cut the craters, which are thus presumed to be relatively inactive. The overall backscatter level is medium. The Don Quichot structure is a NW trending ridge that has high backscatter levels. As with all upstanding features in this area, there are moats around them.

MAKAT-117 is a 100 kHz line running NE across the Mercator mud volcano. It is a flat topped volcano with a central crater that is about 700 m in diameter. There are no obvious signs of recent activity such as fresh flows or very high backscattering areas. Faint NNW-SSE trending linear patterns north of the volcano may be longitudinal current formed bedforms.

Lines MAKAT-118 and 119

These two lines extend the coverage of 30 Hz MAK lines to the east of those obtained during TTR-12 over Al Adrissi mud volcano. Around the foot of the mud volcano, seen at the far range of the sidescan record, there is a faint pattern of long, narrow lineations that resemble longitudinal furrows formed by current.

NE of Al Idrissi there is an extensive area of high backscattering mounds, separat-

ed by narrow strips of low backscatter to produce a regular "giraffe" mottling. The mounds vary in height and are up to 10 m high (though there is some doubt about the vertical scale), and rounded in profile. They are presumed to be carbonate mounds.

Line MAKAT-120

The 30 kHz line runs along a WNW trending fault that was identified on the SEAMAP mosaic. The fault was followed for over 30 km and an extension of the fault zone to the east was followed on OKEAN line PSAT- 271. For the most part the fault trace is very sharp, narrow and single and is in the centre of a shallow groove. There is no asymmetry in surface profile across the fault. In detail there are small changes of direction, short splays and places where the fault wall is higher than in others. The effect is of a gently undulating topography displaced by a strike slip fault. Some of the ridges crossed be the fault trend N-S, others are ENE, including a prominent asymmetrical ridge that has mounds scattered irregularly along its crest and southern slope.

Line MAKAT-121

This 100 kHz line runs along a WNW

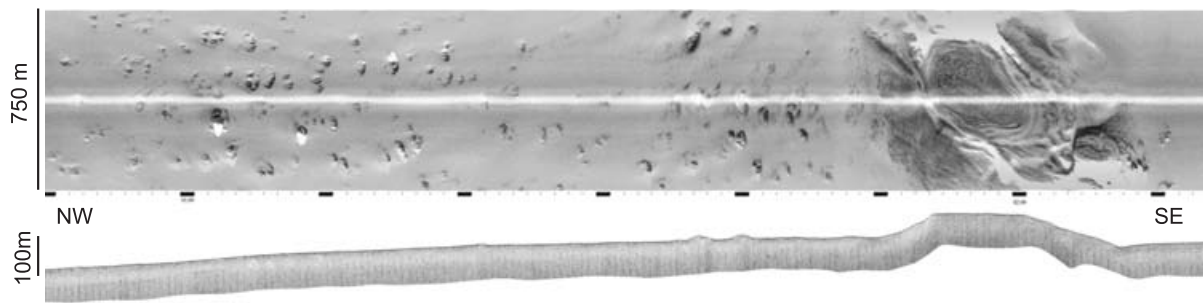


Figure 58. Fragment of the MAK line 121 showing Meknes MV and field of small carbonate mounds developing to the north of the mud volcano.

trending fault, identified in the OKEAN data from TTR-9 (Kenyon et al., 2000), and also crosses the Meknes mud volcano. The fault has a narrow trace with splays and possible pull apart structures (dextral?). At the eastern end of our coverage of the fault the trace follows a channel-like feature, about 60 m wide, with walls on either side.

The fault crosses two areas of higher backscatter, both are probably ridges but only crude bathymetry is available from this region. The westernmost feature trends NW-SE and has outcrops of what look like resistant bedded rocks. There is no penetration seen on the profiler. The linear features are side echoes from the nearby fault trace. At one place the fault cuts through the higher ground and casts a long shadow. The eastern feature is different in that there is good penetration on the profiles. The fault seems to lie to the south of it. A long and continuous shadow implies that there is a sharp ridge crest with a possible scarp to the south of it. Along the crest of the western end of the ridge there are sub circular mounds that, where crossed, are up to 14 m high and 60 m in diameter. Thus they have very steep sides and are presumed to be carbonate mounds at depths of 775 to 825 m. At the eastern end of the feature there is an extensive area of high backscatter due to outcropping bedded rocks. Two adjacent beds are especially resistant and show up as two parallel lines. Many small faults, with a throw of up to about 5 m, displace the outcropping beds and result in a zig-zag outcrop pattern.

At the eastern end of the line there are a group of parallel, NW-SE trending ridges that have pointed ends and a regular pattern

of small scale rugosity. They sit on top of underlying bedded sediments and have clearly built up on them to a height of up to 12 m, where crossed. It is likely from their appearance that these are cold water carbonate mounds in water depths of about 850 m.

After an alteration of course, SW towards Meknes mud volcano, the line crosses another WNW trending fault. North of the mud volcano is an extensive field of small, high backscattering mounds without any obvious elongation direction (Fig. 58). They are equally spaced out, about 100 m apart. They vary in height, as some cast larger shadows than others, but do not vary much in area. They are up to at least 12 m high. They are associated with corals, mainly dead, on TVAT 62-64 (Fig. 61).

Meknes mud volcano has a flat top, at a depth of 550 m, with a central, pear shaped crater of 450 m width along the long axis. There is a marked N-S trend to the crater and to flanking scarps. There is little penetration on the profile even in the sediments surrounding the mud volcano.

There are several lines of evidence for there being current activity in this area:

1. There is extensive erosion even on low slopes where mass wasting due to gravity could not take place.

2. There are areas where no penetration on the profiler occurs that may be due to sands in the surface sediments. Sands were found in core AT-578G near Meknes mud volcano. There is no contrast in backscatter but this has been noted from other places where the 100 kHz sidescan has crossed known sand and mud areas, such as the

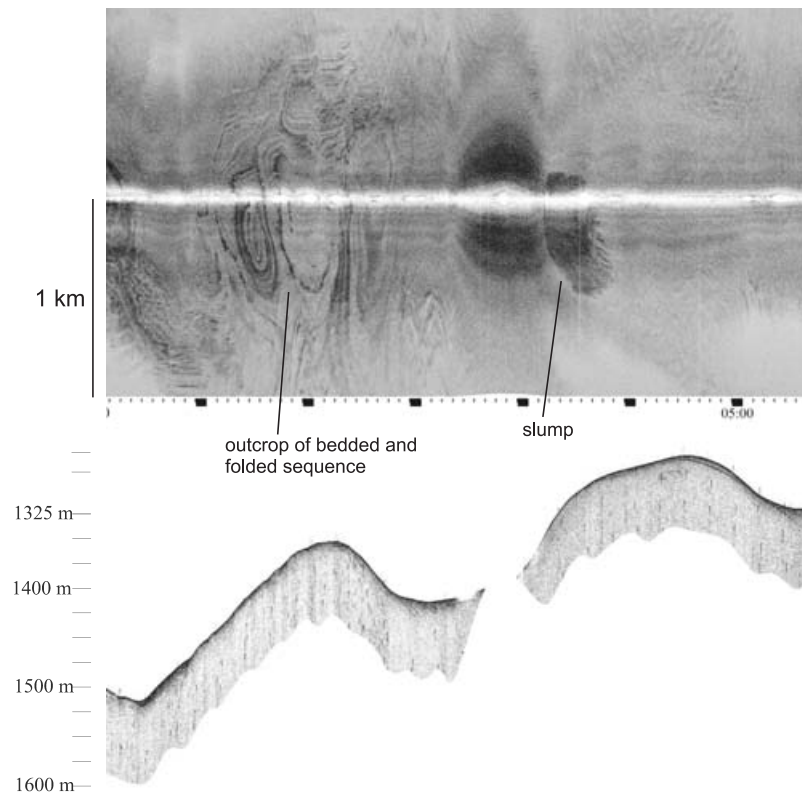


Figure 59. Fragment of MAK line 123 showing slumping and outcrops of bedded sedimentary sequence affected by folding which are found on the slopes of several seabed ridges within a deformation front, SW of the Yuma and Ginsburg mud volcanoes.

Speculobe area (Kenyon et al., 2003).

3. There are possible regular current induced bedforms in a few places. There appear to be obstacle marks indicating SW sediment transport in the area of the westernmost high backscattering feature. Faint E-W lineations, resembling erosional furrows, are seen in two places.

4. The suspected carbonate mounds would only flourish in areas of vigorous currents.

Line MAKAT-122 and 123

These 30 kHz lines run WSW across complex high backscattering features seen on the SEAMAP mosaic. For the eastern, shallowest part of the line there are refraction patterns at far range, indicating that the fish is above a thermocline, perhaps the base of Mediterranean water at about 1400 m. On the side of a hill there is a high backscattering patch that is presumed to be due to a slumped body exposing underlying strata. Any slump must be thin as no head scarp is

seen on the profile. The hills at the eastern end of the line are patchily covered by thin sediments as there are several areas of higher backscatter that show through the uniform low backscattering facies (presumed hemipelagic material). These include a complex outcrop pattern of bedded sediments which shows that there is some folding within the underlying sequence (Fig. 59).

Lines MAKAT-124 and 125

These lines test out possible mud volcanoes in the deeper part of the area. MAKAT-124 is a 30 kHz line running SW across a sub-circular high backscattering patch seen on the SEAMAP backscatter map. The feature is on an asymmetrical high and corresponds to steeper slopes where a superficial layer of the draping beds is missing. Thus this feature is presumably due to a slump that has exposed high backscattering sediments.

MAKAT-125 is a 30 kHz line that runs NW across a potential line of NW-SE trending mud volcanoes that includes Olenin mud

volcano. A steep sided, 100 m high structure was tested out by TV line TVAT-68 which failed to show signs of activity at the structure. It has a very low backscattering area on top that could be a shadow but could be a brine pool, which are known to be able to totally reflect sound.

III.3.2. Bottom camera survey

V. BLINOVA, M. IVANOV, D. NIKONOV AND
A. AKHMETZHANOV

TVAT-60

TV was run across the Mercator mud volcano. It started at the central part of the crater and continued to the edge and slope of the mud volcano. Patches (up to 2 m in diameter) of gray mud breccia with small clasts and shell fragments around were observed in the crater (Fig. 60). At the northeastern part of the crater two gas bubbling sites were

found. At these places the TV-grab was deployed (AT569GR) and showed highly gas saturated mud breccia. A small chimney-like structure situated on the crust was recorded at the southwest flank of the mud volcano (Fig. 60d). Presence of carbonate crusts, fresh mud breccia with shells around and gas bubbling point to the high activity of the Mercator mud volcano.

TVAT-61

TV observation was done on the top of the Adamastor mud volcano. Monotonous hemipelagic sediments, highly bioturbated, were observed most of the time. A few patches of irregular sea bottom and probable mud breccia were found.

TVAT-62, TVAT-63, TVAT-64

These TV-runs were done on different parts of the Vernadskii ridge in order to find live corals communities. A lot of dead corals

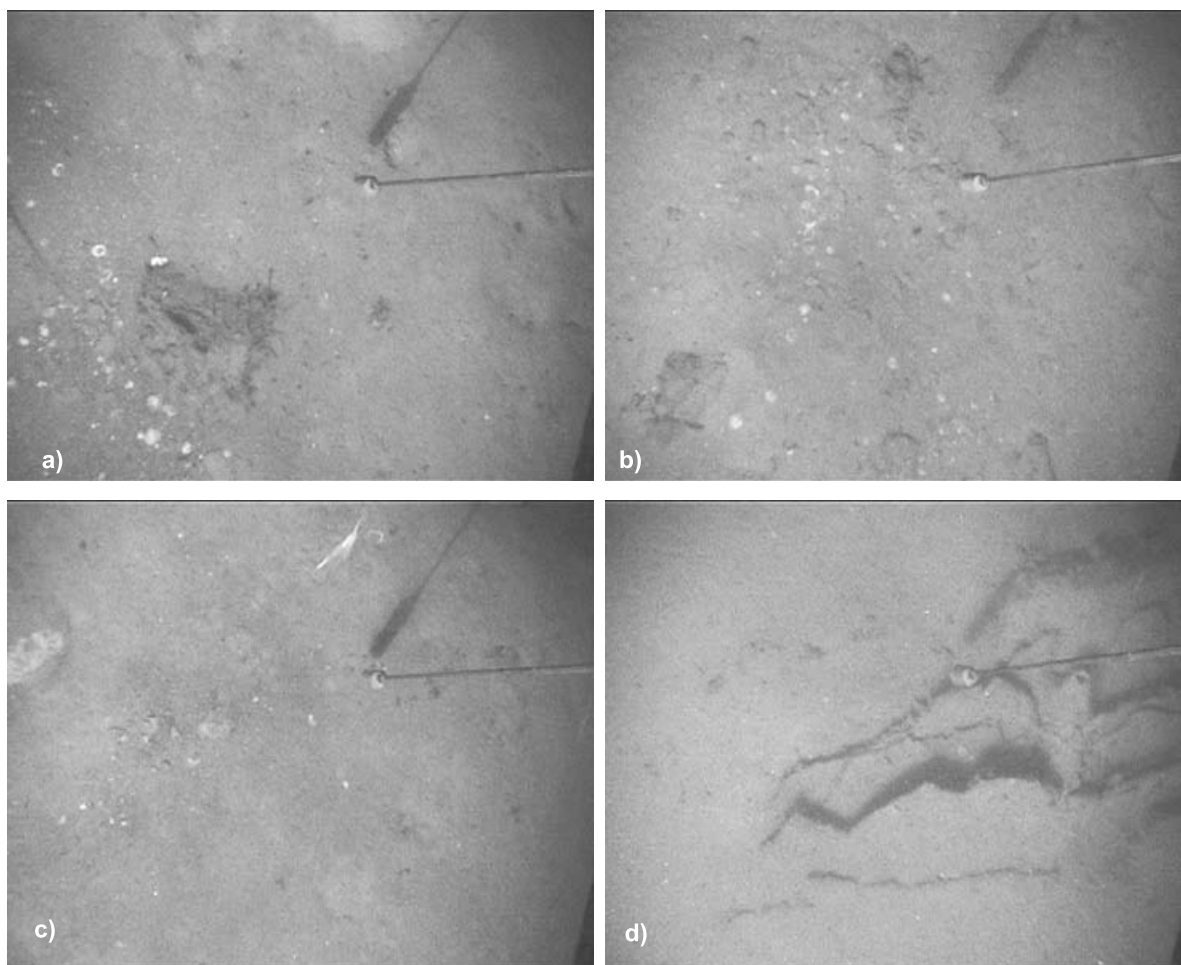


Figure 60. Stills from TVAT60 showing fields of mud breccia and carbonate crusts in the crater of the Mercator MV.

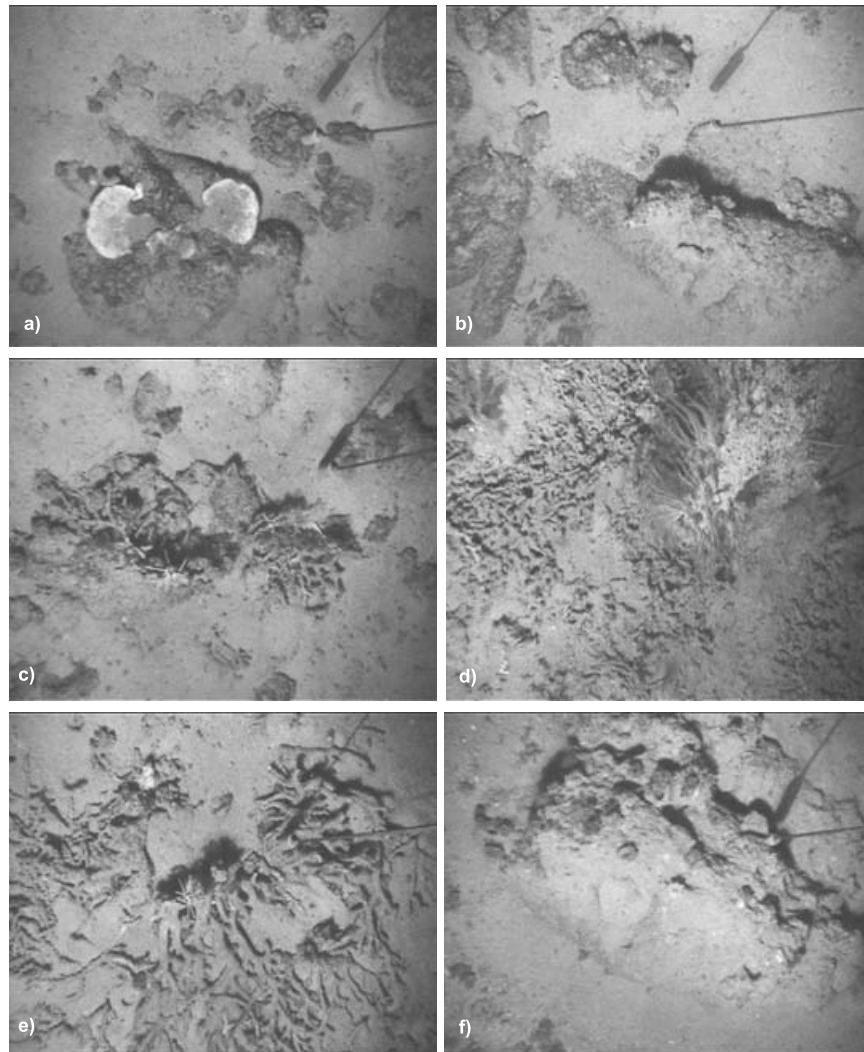


Figure 61. Stills from TVAT62-64.

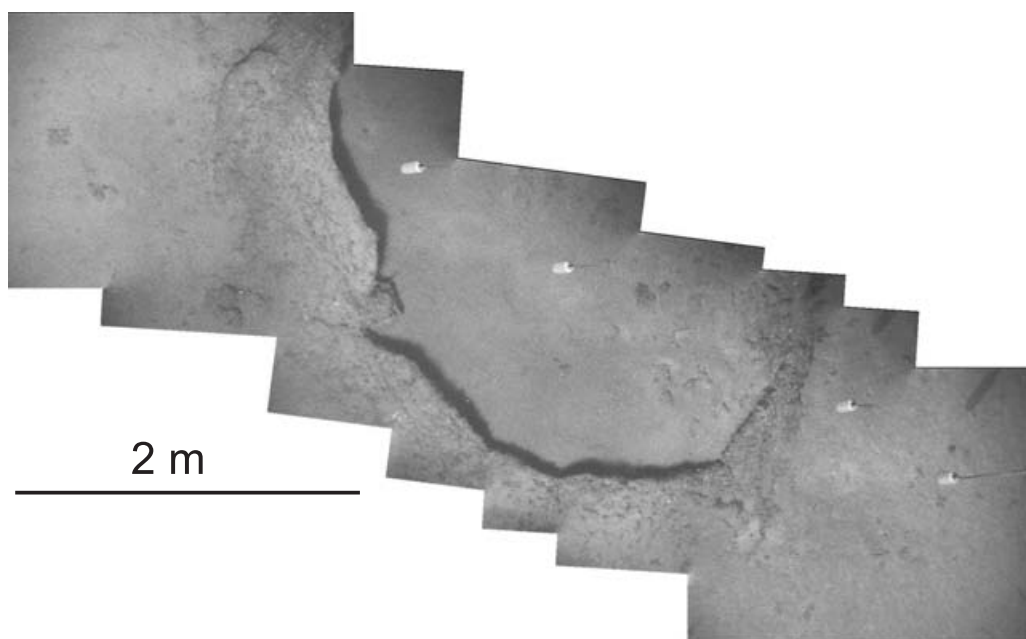


Figure 62. Giant carbonate chimney.

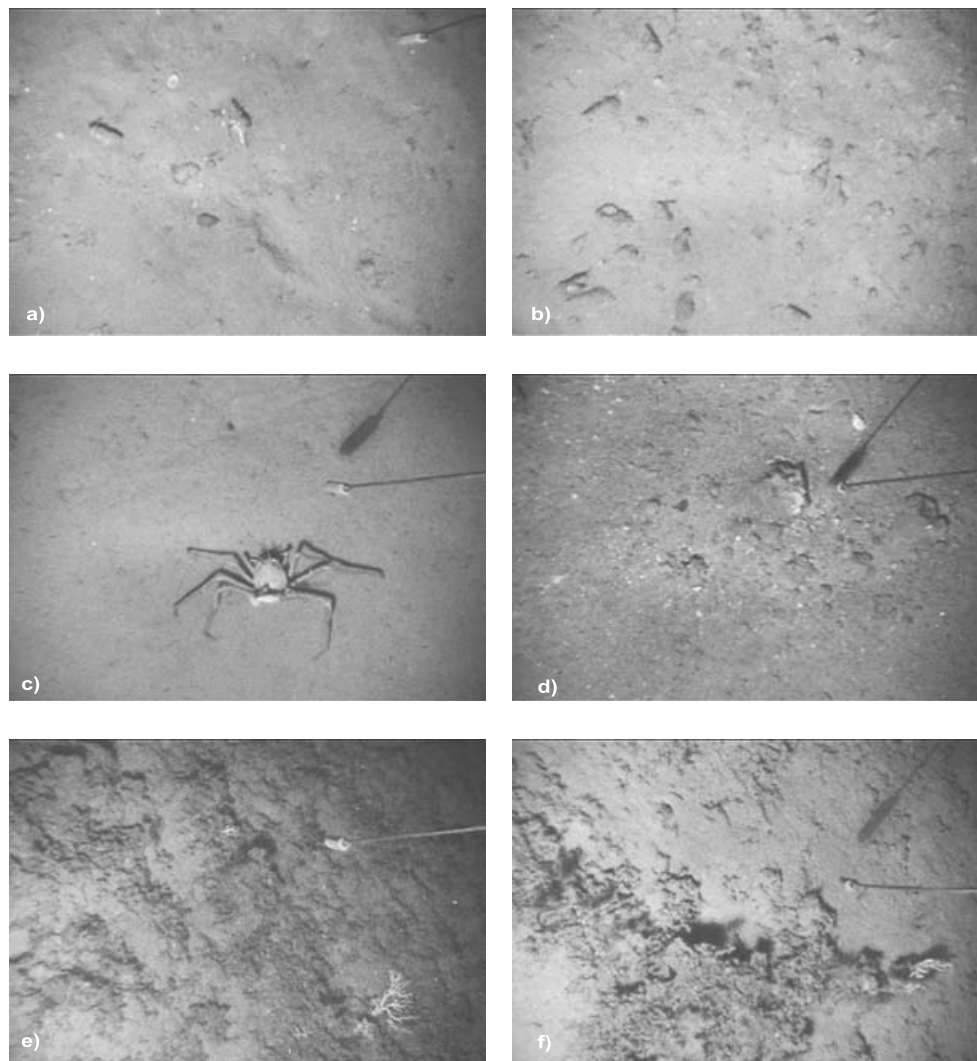


Figure 63. Stills from TVAT65.

were recorded. No live species were detected. Also big blocks and extensive crusts were found along the TVAT-62 line and beginning of the TVAT-63 line (Fig. 61). Big brown carbonate tubes were observed. Some of the chimneys may reached 5 m in diameter of the hole (Fig. 62).

TVAT-65

TV was run across the Meknes mud volcano. The observed seabed was hard, covered by a thin layer of hemipelagic sediments. At the flat surface sponges and tracks of different animals were observed. Small patches of gray mud breccia were found (Fig. 63). Usually a lot of live and dead shells of *Neptunia contraria* were recorded around places with fresh mud breccia. An extensive area of dead corals was found at the north-

west flank of the mud volcano. Several live branches of corals, white in color, were also detected.

TVAT-67

TVAT-67 line was done across Olenin mud volcano. No evidence of activity were observed. Bioturbated hemipelagic sediments cover the sea bottom.

TVAT-68

Cone-like structure to the east of the Olenin mud volcano was investigated. The sea bed was covered by hard hemipelagic material. Holothurians and sea stars were found along the line.

III.3.3. Bottom Sampling

III.3.3.1. Bottom samples

A. OVSYANNIKOV, D. KOROST, A. AKHMETZHANOV,
E. KOZLOVA V. BLINOVA, J. GONZALEZ,
D. NADEZKIN, A. SHARAPOVA, Y. MALYKH,
E. MUCHANGOS, M. LAADRAOUI, R. KHARBAOUI
AND A. HAZIM.

Core locations are summarised in Table 3, core logs follow in the Annex I.

Moroccan margin, Mercator mud volcano
(Fig. 64)

Station AT567G

The top of Mercator mud volcano was sampled at the station. Recovery consisted of 144 cm of sediment, represented by brown hemipelagic silty clay at the top. Between 2-18 cm sediment consists of brown oxidized matrix-supported mud breccia, water-saturated at the top, with shell fragments in the lower part of the interval. The unit below is represented by 7 cm thick grey clast-supported mud breccia with fragments of shells at the bottom. The lowermost interval (25-144 cm) shows the presence of grey matrix-supported mud breccia, containing brownish grey carbonate clasts (up to 5 cm) at 155 and 140 cm.

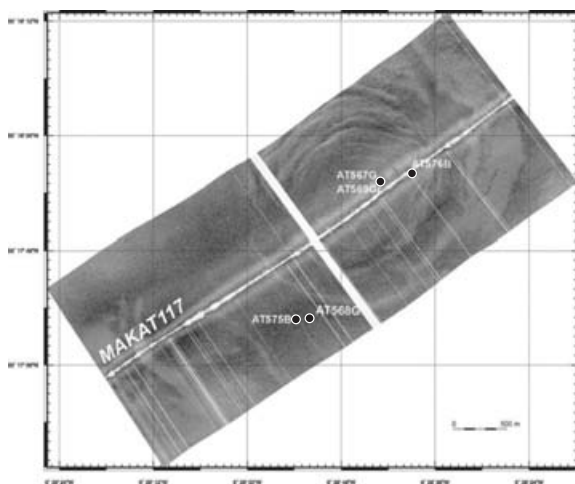


Figure 64. Sampling stations on Mercator MV.

Table 3. General information on the cores sampled in the Gulf of Cadiz during Leg 4.

Core N	Date	Time, GMT	Latitude	Longitude	Depth, m	Recovery, cm
AT567G	24.07.05	20:08	35°17.920N	06°38.716W	358	144
AT568G	25.07.05	01:11	35°17.684N	06°39.131W	418	134
AT569GR	25.07.05	02:31	35°17.919N	06°38.718W	355	0.5 t
		02:46	35°17.917N	06°38.717W	358	
AT570G	25.07.05	04:48	35°17.406N	06°46.996W	580	
AT571G	25.07.05	06:25	35°21.968N	06°51.920W	612	581
AT572G	25.07.05	07:39	35°22.040N	06°53.985W	712	333
AT573G	25.07.05	23:14	35°21.768N	06°45.543W	499	30
AT574D	26.07.05	05:01	35°26.150N	06°46.915W	512	1 t
		05:41	35°25.982N	06°46.661W	508	
AT575B	26.07.05	20:50	35°17.903N	06°38.715W	355	40
AT576B	26.07.05	21:29	35°17.657N	06°39.129W	428	40
AT577B	26.07.05	22:32	35°17.305N	06°39.672W	485	40
AT578G	28.07.05	11:07	34°59.492N	07°04.546W	762	316
AT579G	28.07.05	11:53	34°59.301N	07°04.464W	747	132
AT580G	28.07.05	12:43	34°59.203N	07°04.352W	705	72
AT581GR	28.07.05	13:30	34°59.182N	07°04.344W	700	0.2 t
		13:31	34°59.178N	07°04.353W	700	
AT582G	28.07.05	14:30	34°59.141N	07°04.352W	704	36
AT583G	28.07.05	15:30	34°59.139N	07°04.400W	701	60
AT584K	28.07.05	16:15	34°59.139N	07°04.403W	701	80
AT585K	28.07.05	17:31	34°59.137N	07°04.343W	701	50
AT586GR	28.07.05	18:18	34°59.138N	07°04.316W	702	0.5 t
		18:38	34°59.146N	07°04.380W	701	
AT587G	28.07.05	20:11	34°59.140N	07°04.423W	702	24
AT588G	28.07.05	20:56	34°59.120N	07°04.407W	701	103
AT589G	30.07.05	00:58	35°26.352N	07°28.663W	1270	222
AT590G	31.07.05	08:46	35°34.021N	08°34.333W	2586	231
AT591G	31.07.05	18:42	35°35.027N	08°37.916W	2610	199
AT592G	01.08.05	15:10	35°13.425N	09°05.239W	3242	175
AT593G	01.08.05	19:37	35°12.764N	09°06.498W	3308	177
AT594G	01.08.05	22:24	35°11.356N	09°08.443W	3500	290
AT595G	02.08.05	08:16	35°33.857N	09°30.567W	3890	182
AT596G	02.08.05	10:29	35°33.811N	09°30.532W	3878	213
AT597GR	02.08.05	17:06	35°27.735N	09°00.299W	3070	0.5 t
		21:17	35°27.563N	09°00.030W	3061	
AT598G	02.08.05	23:08	35°27.657N	08°59.994W	3064	245
AT599D	03.08.05	20:29	36°06.538N	07°53.942W	1418	0.1 t
		21:40	36°06.379N	07°53.564W	1275	

Station AT568G

The station sampled the SW slope of Mercator mud volcano and 134 cm of sediment were retrieved. The uppermost interval consists of a 6 cm thick brown water-saturated unit of hemipelagic clay, containing mm fragments of rocks and shells. The interval below (6-22 cm) is represented by brown clast-supported mud breccia, containing fragments of corals. The lower boundary is irregular. The lowermost interval was grey matrix-supported mud breccia. Between 22-34 cm signs of bioturbation were observed. Clasts of limestone were found at 96 and 123 cm.

Station AT569Gr

The top of Mercator mud volcano was sampled once more. Sediment on the top consisted of brown pelagic silty clay covering grey matrix-supported breccia with clasts

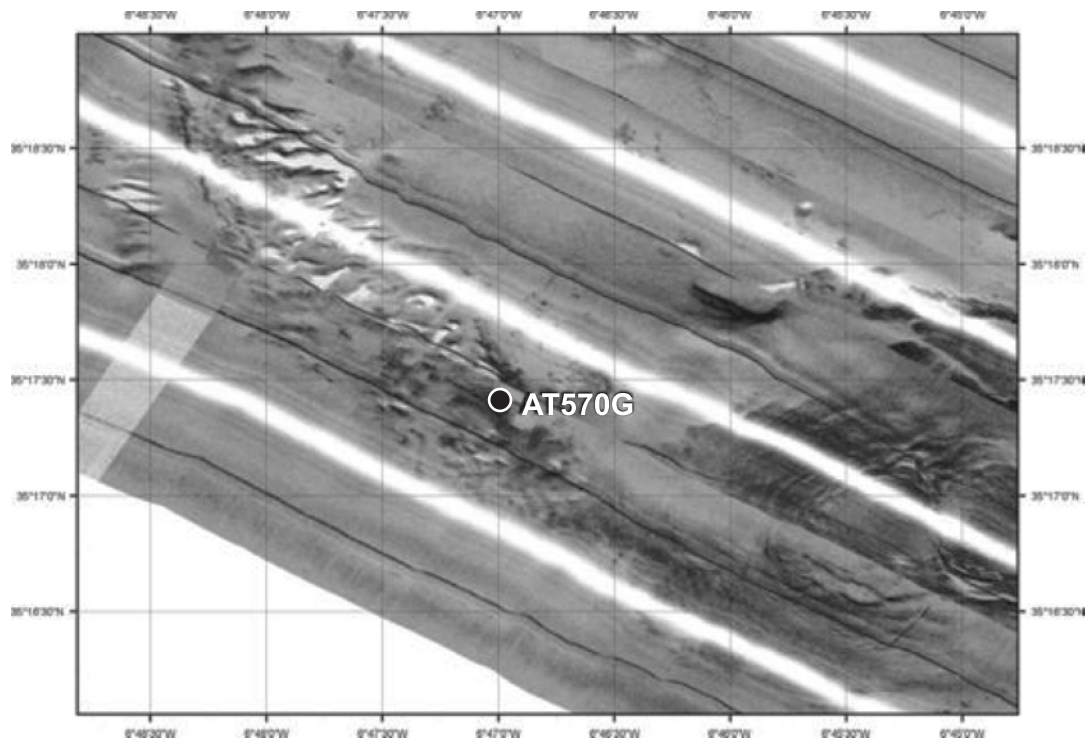


Figure 65. Sampling stations on the Pen Duick escarpment.

of different lithology and size with disseminated sulphides (pyrite-marcasite) and filled fractures. The sulphides form framboidal aggregates, generally less than 2 mm. Several carbonate cemented blocks were observed together with common clasts within the clay matrix.

Stations AT575B-AT577B

Three stations to retrieve samples for further biological investigations were undertaken. The stations AT575B- AT576B showed the presence of grey marix-supported mud breccia covered by 10 cm thick brown pelagic silty clay. At the station AT577B a reference core was take very close to Mercator mud volcano, which showed a hemipelagic succession. Some angular rocks with disseminated sulphides, sulphides disseminated in the mud breccia and two small sections of pyrite burrow were collected.

Pen Duick escarpment (Fig. 65)

Station AT570G

The uppermost interval (0-93 cm) consists of brownish clay, soupy at the top, with coral debris. A large bivalve was found at 63

cm. Below 93 cm a 34 cm thick coral rubble unit was observed, grey in color with silty admixture. Between 127-147 cm a grey clayey unit with silty admixture and foraminifera was observed, containing corals and shell fragments throughout the interval. Grey coral rubble unit, involving soft corals, was found between 147-174 cm, underlying 211 cm thick interval of grey matrix-support-

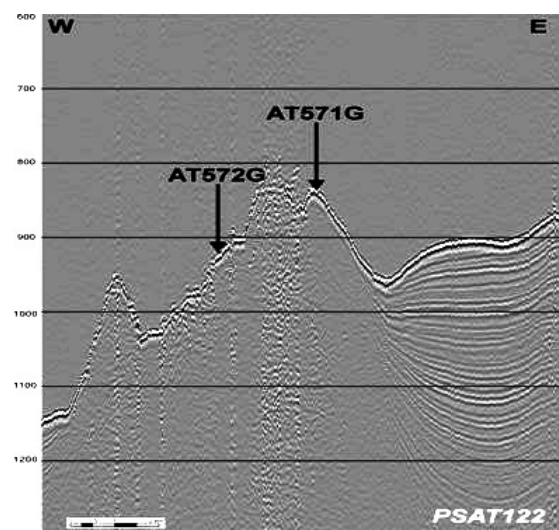


Figure 66. Sampling stations on the Renard ridge.

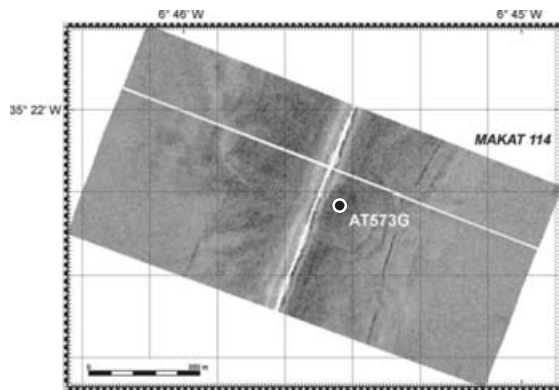


Figure 67. Sampling of the Adamastor MV.

ed mud breccia. Between 174-290 cm fragments of corals were detected. Also shell fragments are present between 174-231 cm. At the top of the interval several dark patches (clasts?) appeared.

Renard ridge (Fig. 66)

Station AT571G

About 581 cm of sediments were retrieved on the station. The top of the core consists of a brownish grey soupy coral rubble unit (0-37 cm) underlain by an interval of olive grey silty clay (37-72 cm) with coral debris. The main part of the succession showed the lamination of grey clayey layers, containing coral debris, with coral rubble units.

Station AT572G

Recovery consisted of 333 cm of sediment, represented by brown pelagic silty clay at the top, containing coral debris. The interval below is greyish-brown on top becoming greyey towards the bottom. Between 7-19 cm shell fragments and coral debris are observed. Intervals 24-30, 26-28, 41-45, 52-59, 62-69 cm are rich in corals. Interval 69-239 cm showed alternation of brownish-grey silty clayey units, containing carbonate grains, with brownish grey coral rubble layers. The lowermost interval (239-267 cm) consists of brownish grey clay with a small amount of shell fragments. Interval 267-277, 280-283, 291-300, 305-320 and 323-333 cm are rich in corals.

Adamastor mud volcano (Fig. 67)

Station AT573G

The top of Adamastor mud volcano was sampled at this station. Only a small amount of grey matrix-supported mud breccia, covered by brown pelagic silty clay, was retrieved at the station. Several fragments of brownish massive sandstones were seen within the sediment.

Vernadsky Ridge (Fig. 68)

Station AT574D

The retrieved dredge was full of rock clasts (from 2 to 50 cm in size). Most of them are dark brow to black. A few are light grey in colour. Dark ones were likely to be fragments of carbonate chimneys (dolomite). Some of them still preserve the tube morphology but the majority don't. The light fragments were also carbonates and possibly were crusts.

Meknes mud volcano (Fig. 69)

Station AT578G

This was a reference core from very close to Meknes mud volcano. About 316 cm of sediment were retrieved, represented at the top by bioturbated brownish grey silty clay rich in foraminifera. The main part of the core is olive brown bioturbated silty clay with foraminifera almost everywhere. Ten sandy units, interrupting normal sedimentation, are seen within the core. Sand is mostly coarse on the top, becoming finer towards

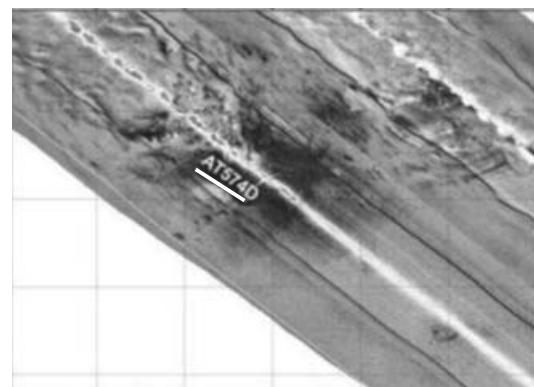


Figure 68. Location of the dredge site AT574D on the Renard ridge.

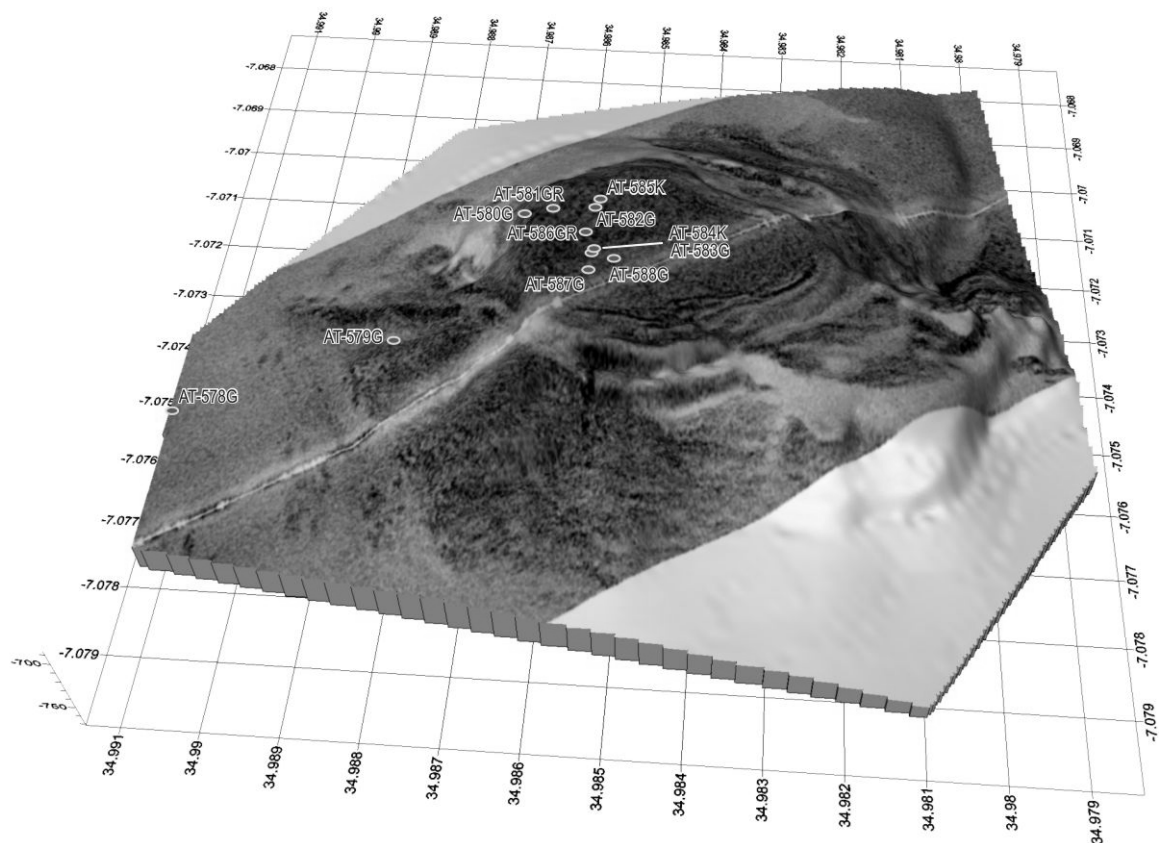


Figure 69. Sampling sites on the Meknes MV.

the bottom of every interval. Foraminifera and traces of bioturbation are also visible within sandy layers. Throughout the succession shell fragments are detected.

Station AT579G

The slope of Meknes mud volcano was sampled. The uppermost interval consists of brown water-saturated clay with corals covering a 13 cm thick unit of brownish-grey water-saturated clay. Between 33-45 cm brownish grey clayey interval with coral fragments. The interval below is grayish brown sandy silty clay with lots of shell fragments and spicules of urchins. Some foraminifera are observed in the lower part of the interval. A green patch filled with the same sediment is found at 53 cm. The lower boundary of the interval is oblique. The lowermost interval is dark grey matrix-supported mud breccia, bioturbated in the upper part of the unit.

Station AT580G

About 72 cm of sediment were retrieved mostly represented by matrix-supported mud breccia (22-35 cm), light grey on the top and becoming coarser towards the bottom. At 25 and 39 cm big clayey clasts are observed. Between 3-22 cm there is a unit of dark grey clast-supported mud breccia, covered by a 3 cm thick interval of brown hemipelagic water-saturated silty clay with foraminifera. In the first 25 cm of the core 0.5-1 mm aggregates of pyrite were seen.

Stations AT581Gr and AT586Gr

The top of Meknes mud volcano was sampled at these stations. The topmost sediment is pelagic brown silty sandy clay covering grey, matrix-supported mud breccia with rock clasts of carbonate cemented breccia. Gastropods, live crustacea, large amount of pogonophora were also observed on the surface of the sediment at station AT386Gr. Mud breccia contains rock clasts with disseminated sulphides (pyrite-marcasite) and filling

fractures. The large amount of chemosynthetic fauna and strong smell of H_2S in the mud breccia show the activity of methane fluxes in this volcano.

Station AT582G

About 36 cm of sediment were retrieved on the station, represented on the top by brown water-saturated sandy silty clay, covering a 10 cm thick (6-16 cm) silty clayey unit grayish brown in colour. Rock clasts are observed between 6-16 cm. Lots of foraminifera are present in the upper part of the core. The lowermost interval consists of dark grey matrix-supported mud breccia, bioturbated in the upper part.

Station AT583G

The uppermost interval consists of brown water-saturated silty clay with foraminifera and pogonophora. The lower boundary is irregular. The unit below is dark grey matrix-supported mud breccia with clasts up to 2 cm in size. The lowermost interval (42-60 cm) is light grey clast-supported mud breccia with carbonate cementation in the middle part of the interval and pyrite nodules between 47-48 cm.

Station AT584K

The lowermost interval is brownish-grey soupy silty clay with lots of foraminifera. Below 5 cm three units of matrix supported mud breccia, different in colour (dark grey - 5-10 cm; light grey - 10-20 cm; grey - 20-80 cm) are observed. Clasts of light coloured marlstones are visible between 20-44 cm. Below 44 cm sediment is highly porous due to degassing. Also some crystalline aggregates of pyrite (0-1 cm) were collected from mud breccia.

Station AT585K

This is a very similar recovery to the previous station was observed. Only samples of water and rock clasts from mud breccia were taken.

Station AT587G

Only 24 cm of sediment were retrieved, represented by grey matrix-supported mud

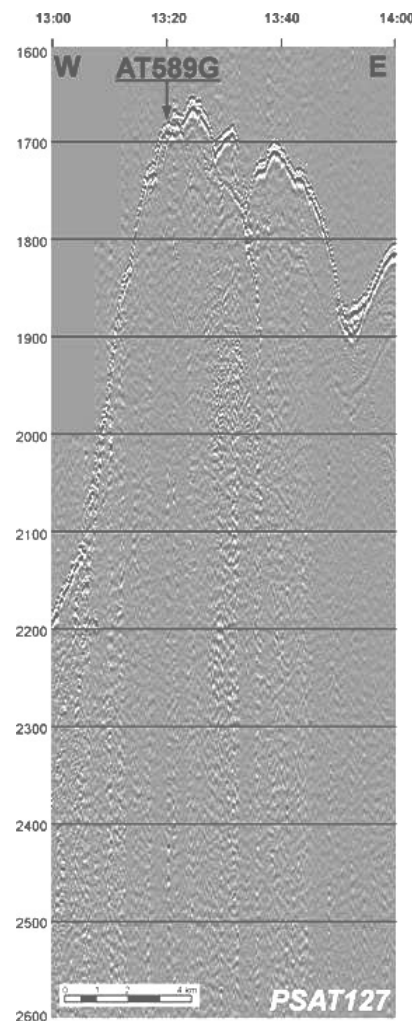


Figure 70. Location of the sampling site AT589 along seismic line PSAT127 (TTR-9) showing a prominent seabed hill - a possible mud volcano.

breccia, covered by a 6 cm thick layer of brownish grey silty sand with an irregular lower boundary.

Station AT588G

The top consists of a 6 cm thick (3-9 cm) brownish grey silty clay unit with foraminifera, covered by a hemipelagic interval of water-saturated brown sandy-silty clay (0-3 cm). The main part of the core is grey matrix-supported mud breccia, containing a sandy admixture increasing towards the bottom. The upper 4 cm of the unit are darker in colour. At 77 cm a big clast of clay is found.

Seabed hill - suspected mud volcano (Fig. 70)

Station AT589G

About 222 cm of sediment were retrieved, mostly represented by light brown marl (0-196 cm) with lots of foraminifera. Intervals 5-9, 60-93, 105-109, 117-180 cm are strongly bioturbated. Between 39-70 a layer very rich in foraminifera is observed. Several burrows, filled with foraminiferan ooze are found in the lower part of the interval. The lowermost interval of the core (196-222 cm) consists of brownish grey strongly bioturbated foraminifera ooze. Sediment becomes lighter towards the bottom.

Olenin mud volcano (Fig. 71)

Station AT591G

About 199 cm were retrieved, consisting of three flows interrupted by hemipelagic sediments. These flows (52-98, 117-125, 193-199 cm) consist of grey matrix-supported mud breccia. Pelagic sediments are represented by grayish clay (98-117, 125-193 cm) with some patches and stripes of organic matter. The upper 52 cm is a layer of brown

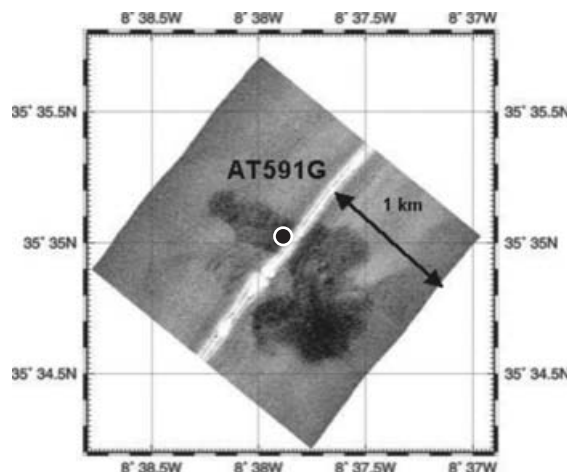


Figure 71. Sampling of the Olenin MV.

marl, water-saturated on the top, with foraminifera.

Portuguese deep water mud volcanoes (Fig. 72)

Three attempts were made to sample three different structures observed on the seismic record.

Station AT592G (Semenovich MV)

About 175 cm were retrieved on the sta-

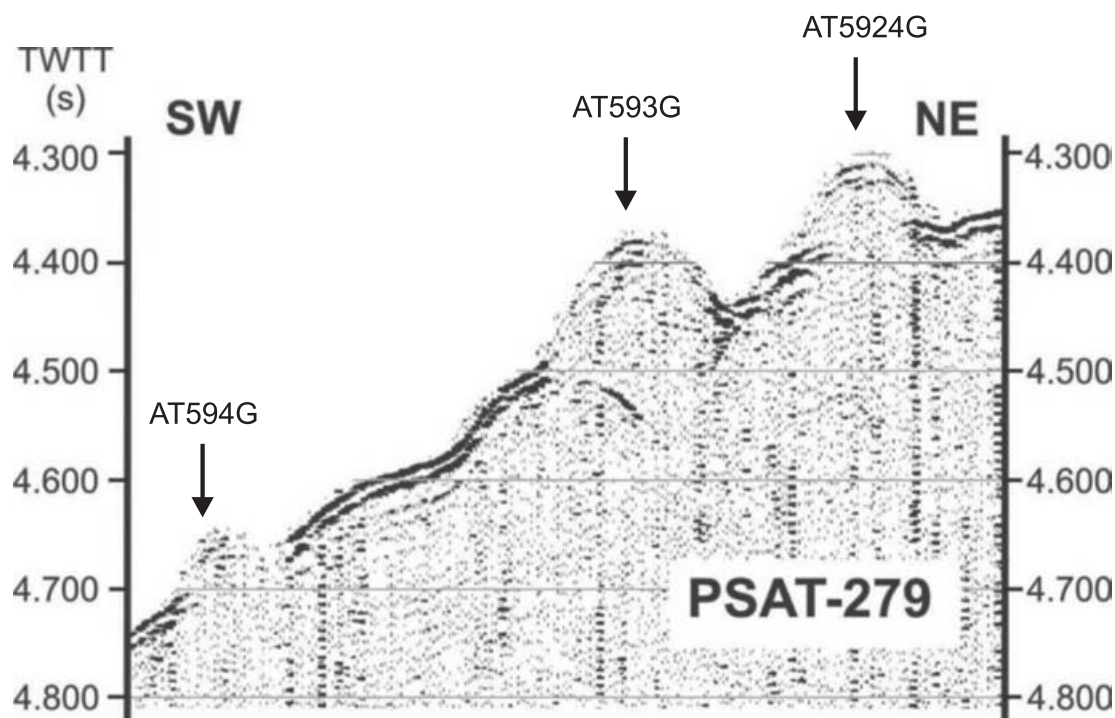


Figure 72. Sampling sites along Line PSAT279 crossing Portuguese deep-water mud volcanoes Carlos Teixeira, Soloviev and Semenovich.

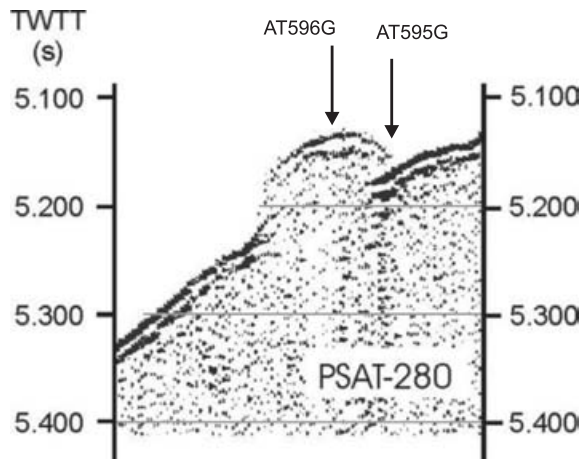


Figure 73. Sampling of the Porto MV.

tion, mostly represented by grey clay with silty admixture and a small amount of foraminifera, covered by a 12 cm thick (0-12 cm) interval of light brown clay with a small amount of silty admixture and foraminifera. Dark stripes and spots are seen below 12 cm. The smell of H_2S was detected in the core.

Station AT593G (Soloviev MV)

177 cm of sediment were retrieved, mostly bioturbated clay with foraminifera and dark stripes of organic matter. The colour changes from brown (at the top) to the grey in the lower part of the core. The uppermost interval is brown water-saturated clay.

There are strongly oxidized layers at 23 and 68 cm.

Station AT594G (Carlos Texeira MV)

Recovery consisted of 290 cm of sediment represented at the top by brown water-saturated clay with foraminifera, strongly oxidized between 46-58 cm. Below 58 cm is a very thick interval of homogeneous bioturbated clay with foraminifera, grayish brown in the upper and lower part of the unit, brownish grey in the middle part.

Porto mud volcano (Fig. 73)

Two samples were taken on the slope and the top of a high seen on the seismic profile.

Station AT595G

The uppermost part of the core (0-25 cm)

is brownish stiff clay with lots of foraminifera, water-saturated in the upper part. The main part of the core is grey bioturbated clay with dark stripes and spots of organic matter throughout the succession. Between 44-48 and 92-104 cm there are large burrows, filled with light clayey material with shell fragments.

Station AT596G

Four units of matrix-supported mud breccia represent the main part of the recovery. Below 143 cm sediment is porous, probably due to degassing. The top of the core is brownish-grey clay, water-saturated at the top, bioturbated, with foraminifera.

Bonjardim mud volcano (Fig. 74)

Two attempts were made to sample possible gas hydrates from the crater of Bonjardim mud volcano.

Station AT597Gr

Recovery consisted of grey matrix-supported mud breccia, covered by a 3 cm unit of brown pelagic water-saturated clay with a small amount of foraminifera. The very cold temperature of sediment indicates the presence of gas hydrates, which had disassociated before recovery.

Station AT598G

The main part of the recovery is grey

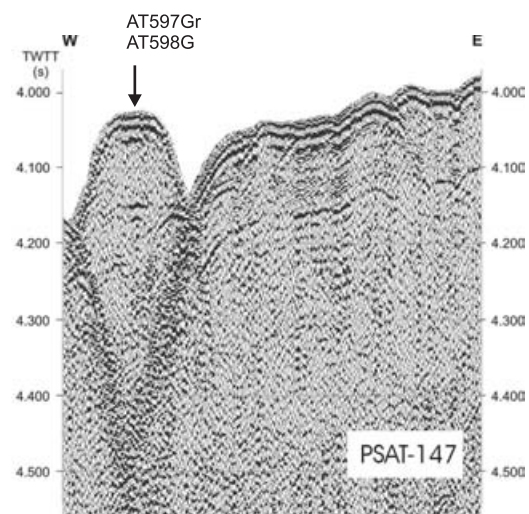


Figure 74. Sampling of the Bonjardim MV.

matrix-supported mud breccia, very dark grey in the lower part of the core. Large clasts of mudstones (up to 5 cm in size) are seen at 167, 197 and 235 cm.

III.3.3.2. Micropaleontological investigation of matrix and clasts from mud volcanoes

ZUZIA STROYNOWSKI

The majority of gravity cores taken during Leg 4 were sampled, either at specific depths from each section, or regularly, at 5 cm intervals, depending on core length, for further micropaleontological analysis. A total of 13 gravity cores from the Mercator, Adamastor, Meknes, Olenin, Bonjardim and four new structures in the South Portuguese margin, were collected. Here we describe preliminary nannolith results from gravity cores AT568G and 570G, from the Mercator crater and its slope, respectively.

Nannofossil dating of selected samples of the mud matrix was done using a light microscope at magnification 1000x. Identification was done according to the methods of Perch-Nielsen (1985). In general, small forms were hard to identify to species level, due to poor preservation, and certain very small species can only be determined by electron microscope. Other species, such as *Nannotetrina* spp. appeared to show overcalcification, which again made identification difficult.

A 134 cm gravity core (AT568G) was recovered from the Mercator crater at a water depth of 418 m. Four smearsides were made from the following depths: 14-15; 44-45; 94-95; 129-130 cm, and the results were combined into one chart (Fig. 75a). The matrix assemblages of nannofossils express a wide range of geological ages, from the Early Paleocene through to the late Pleistocene. As a whole, species were found to be abundant, moderately preserved with high species diversity. Dominant species include: *Emiliana huxleyi*, *Gephyrocapsa oceanica*, *G. caribbeanica*, *Umbellicosphaera sibogae*, *Calcidiscus leptoporus*, *Discoaster* spp., *Neochiastozygus* spp., and *Sphenolithus* spp.

The second gravity core, AT570G, was

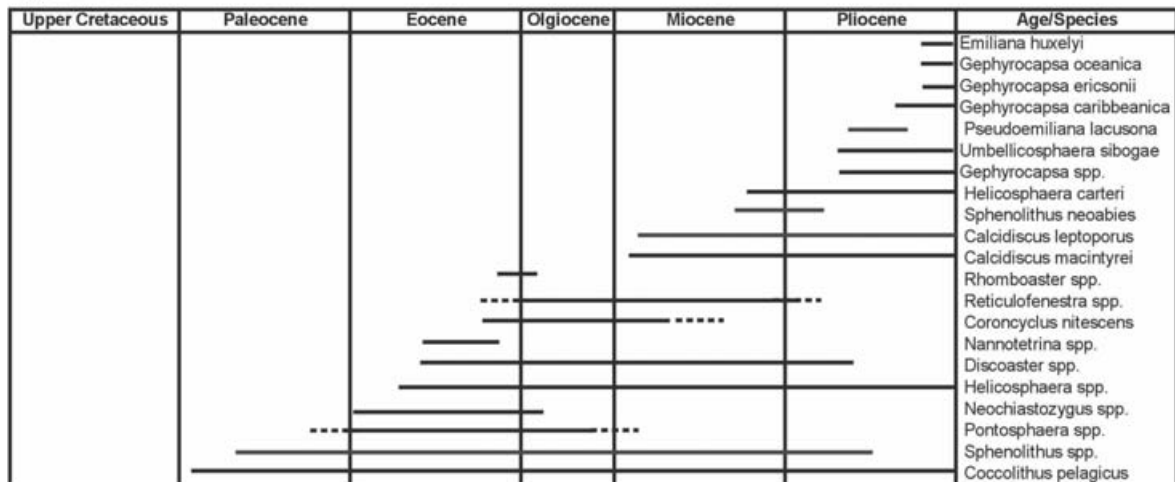
collected from a water depth of 580 m on the slopes of the Mercator mud volcano (known as the Pen Duick Escarpment). Smearsides taken from matrix material were analysed at the following depths: 7-8; 75-76; 114-115; 124-125 cm, and collated into one chart (Fig. 75b). Smearsides made up from clast material are shown separately.

The matrix assemblages, again, show a wide range of geological ages. In general, species were found to be moderately preserved, very abundant and a high species diversity. Dominant species include: *Neochiastozygus* spp., *Micula decessata*, *Gephyrocapsa* spp., *Prolatipatella* spp., *Nannotetrina* spp., *Umbellicosphaera sibogae* and *Calcidiscus leptoporus*. Pelagic material from 7-8 cm depth showed predominantly Pleistocene species, but some species from the Late Cretaceous and Paleocene were found (*Prolatipatella* spp., *Neochiastozygus* spp.), which indicate that some reworking has occurred. In general, the Late Cretaceous was well-represented with *Micula decessata* and *Rhomboaster bitrifida*. It is therefore possible that Late Cretaceous sediments are located near the roots of the Mercator mud volcano.

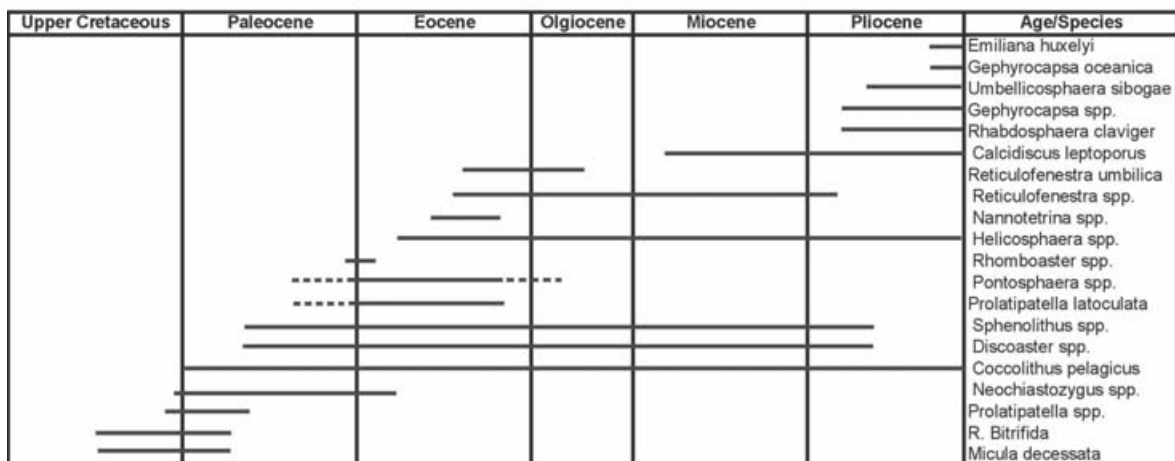
The clast samples were taken from the following depths: 75-76; 114-115 and 124-125 cm. The clast assemblage also showed a wide range of geological scales from the Upper Cretaceous through to the Pleistocene. Species diversity was seen to be significantly lower than its matrix counterpart. The dominant species include: *Reticulofenestra umbilica*, *Nannotetrina* spp., *Rhomboaster* spp., *Pontosphaera* spp., and *Cruciplacolithus* spp. Other, more recent species, such as *Gephyrocapsa* spp. and *Umbellicosphaera sibogae* were present, but relatively few, and showed dissolution. The Upper Cretaceous species were present but preservation was also low. Therefore, it is safe to say that the dominant assemblage group span the Eocene Period through to the Oligocene. This suggests that during mud flows, matrix material from deeper depths may have dislodged clastic material further up the volcano, which is represented by the Eocene-Oligocene clastics.

Figure 75c shows species presence only

(a). AT 568G



(b). AT 570G (Matrix)



(c). AT 570G (Clasts)

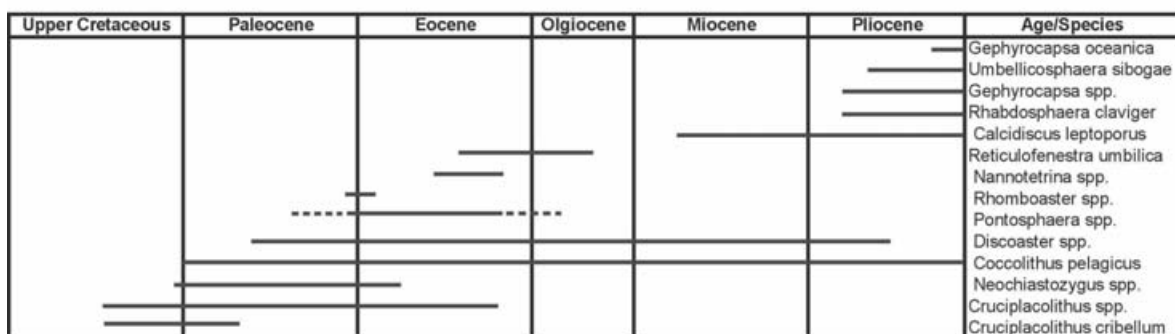


Figure 75. Schematic charts showing nannolith species presence in gravity cores from the Mercator Mud Volcano. Core AT568G: (a) matrix; Core AT570G: (b) matrix; (c) clasts.

and therefore caution must be taken when relating to species abundance, i.e. a greater diversity of species during, lets say, the Miocene, does not mean that the majority of the assemblage is from that period. All it

indicates is that there are more species from the Miocene that can be identified with a light microscope.

III.3.4. Biology and Microbiology

M. R. CUNHA, J. SAS, C. F. RODRIGUES, L. SANTOS
AND N. WOUTERS

Introduction

The Leg 4 of TTR-15 cruise was devoted to geological, geophysics, geochemical and biological subjects concerning the study of mud volcanoes and carbonate chimney cemeteries in the Gulf of Cadiz. The geological samples contained a number of organisms that were collected and preserved for further studies namely isotopic analyses of ^{13}C , ^{15}N and ^{34}S . Moreover, deep-towed TV runs also provided information on faunal zonation. These studies will contribute to the knowledge of biodiversity, distributional ecology and functioning of the ecosystems associated with the bathyal environments mentioned above and complements the material collected during previous TTR cruises. The specimens will be deposited in the Biological Research Collection of the University of Aveiro (Department of Biology) and will be used for ecologic, taxonomic, morphologic and genetic studies.

Mud volcano sediments, with their elevated methane content, are likely to be AOM 'hotspots' though relatively little microbial analysis at these particular seep sites has been undertaken. Another objective of Leg 4 was therefore to collect microbiological samples that could be used to investigate the AOM process in mud volcano sediments from the Gulf of Cadiz.

Methods

A) Bottom sampling - Macrofauna

Grab samples: Conspicuous animals were picked from the surface of the sediments and rocks. When chimneys and crusts were present, specimens were also recovered from their washings. A variable volume of surficial sediments was also collected when available

Dredge samples: The fauna was picked from the surface of the rocks and/or recovered from rock washings and sieved sedi-

ments (the finer sieve used was 0.5 mm).

Core samples: Conspicuous animals were picked from the sediment. Whenever possible at least one quarter of the 25-30 cm of the uppermost part of each core was subsampled.

Box-core samples: The top layer (up to 30-40 cm) was washed and preserved for further analysis.

Except for the box cores, the samples obtained could only be treated in a qualitative way. The specimens picked from sediments and rocks were preserved in 95% ethanol (or deep-frozen) to enable future genetic analysis. Some specimens of selected species were prepared for stable isotope analyses.

The sediments were washed through a sieve column (2, 1 and 0.5 mm). The fauna in the two coarser fractions was sorted and kept in 95% ethanol. The finer fraction (0.5 to 1 mm) of the sieved sediments was preserved in 10% neutralised formalin stained with Rose Bengal to be sorted later under a stereoscopic microscope.

B) Deep towed TV observations

Preliminary lists of the fauna, multivariate analysis and mapping were made from data obtained during real time observations of video footage.

C) Microbiology

The section below provides a brief explanation of the various sampling techniques employed for microbiological work, details of sample collection and shipboard processing methods for the various microbiological samples (Table 4) and an indication of the intended analyses to be conducted in the home laboratories.

Aseptic syringe sub-sampling: Aseptic sub-sampling was used for many of the microbiological sample collections. Appropriately-sized, sterile syringes with their luer end removed were used to extract sediment sub-samples from the gravity/box cores. In these cases, care was taken to avoid

sampling sediment that had been in contact with the core liner to minimise the chance of contamination.

"Clean-dirty hands" sample procedure: This method was also used for some microbiological sample collection. In this case a sterile (ethanol-wiped) spatula was used to collect the samples aseptically. Again care was taken to sample only pristine sediment from the core.

Minicore sampling: This method was used for taking samples for activity measurements and biomass production. These samples were taken across 20cm intervals at the locations described in Table 4. Sterile minicores were inserted into the core lengthways with the aid of a hand held vacuum pump.

Acridine Orange Direct Counts (AODC): A known volume of sediment was fixed in 2% formaldehyde solution, awaiting

Acridine Orange staining and total cell counts.

Fluorescent in situ hybridization (FISH): A known volume of sediment was fixed in 2% formaldehyde solution awaiting further processing and hybridization with specific oligonucleotide-targeted probes in the home laboratories. FISH analysis will allow identification and enumeration of specific phylogenetic/functional groups e.g. those implicated in AOM.

Molecular analysis (including DGGE community profiling): These samples were frozen at -20°C awaiting DNA extraction. Extracted total community sediment DNA will be used for Polymerase Chain Reaction (PCR) gene amplification and phylogenetic analysis of the bacterial groups present. This information will be used as a means of identifying the dominant bacterial groups within the sediment and allow some inferences

Table 4. Details of microbiological sample locations.

Area	Station number	Depths sampled	Sample type
Moroccan Margin	AT568 G	Every 20cm	Enrichment/isolations
		At 1m	DGGE Community Profiling
	AT569 GR	N/a	Molecular analyses of chemosynthetic endosymbionts (Bivalves)
	AT570 G	Every 20cm	Enrichment/isolations
		At 1m	DGGE Community Profiling
	AT571 G	Every 20cm through 1 st 2.5m, every 5cm thereafter	Enrichment/isolations
		At 1m	DGGE Community Profiling
	AT572 G	Every 20cm	Enrichment/isolations
	AT575 B	Every 5cm (up to 25cm)	ATP, EAA, AODC and FISH
	AT576 B	Every 5cm (up to 25cm)	ATP, EAA, AODC and FISH
		At 50cm	DGGE Community Profiling
	AT577 B	Every 5cm (up to 25cm)	ATP, EAA, AODC and FISH
	AT578 G	1 st 20cm of section 1	AODC, Molecular analysis, Enrichments/isolations, Activity measurements
		last 20cm of section 1	
		last 20cm of section 2	
		last 20cm of last section	
		every 20 cm (up to 100 cm)	ATP, EAA, AODC and FISH
	AT579 G	1 st 20cm of section 1	AODC, Molecular analysis, Enrichments/isolations, Activity measurements
		last 20cm of section 1	
		last 20cm of section 2	
		last 20cm of last section	
		every 20 cm (up to 100 cm)	ATP, EAA, AODC and FISH
	AT580 G	1 st 20cm of section 1	AODC, Molecular analysis, Enrichments/isolations, Activity measurements
		last 20cm of section 1	
		last 20cm of section 2	
		last 20cm of last section	
		every 20 cm (up to 100 cm)	ATP, EAA, AODC and FISH
	AT583 G	Surface, 20cm and 50cm	AODC and FISH
	AT577 B	Every 5cm (up to 25cm)	ATP, EAA, AODC and FISH
	AT589 G	At 1m	DGGE Community Profiling
	AT591 G	At 1m	DGGE Community Profiling
Deep Portuguese Margin	AT596 G	1 st 20cm of section 1	AODC, Molecular analysis, Enrichments/isolations, Activity measurements
		last 20cm of section 1	
		last 20cm of section 2	
		last 20cm of last section	
	AT598 G	At 1m	DGGE Community Profiling

regarding the community's function.

Enrichments and culturing: Samples were stored at 4°C in anaerobic bags in order to maintain sample integrity before processing. These samples will be used to make inoculation slurries, which will form the basis of bacterial enrichment and isolation attempts.

Activity measurements (14C uptake): Samples were stored anaerobically at 4°C onboard ship. Radio-labelled substrates will be injected into the sediment sub-samples in order to determine bacterial activity.

Biomass production measurements: Sediment sub-samples were stored anaerobically at 4°C. These samples will be analysed for the determination of bacterial biomass production by 3H-Leucine/Thymidine incorporation.

ATP measurements: Sediment sub-samples were added to boiling tris buffer onboard the ship. Samples were then transferred to ice and stored at -20°C until analysis in the home laboratories. The ATP concentration will be determined by the luciferine-luciferase reaction as a means of quantifying bacterial biomass.

EEA: Sediment sub-sample suspensions were added to model substrates for -glucosidase and for Leucine-aminopeptidase and incubated for 24 h at 4°C. The ectoenzymatic activity will be determined fluorometrically from the hydrolysis rates of substrates.

Virus enumeration: Sediment sub-samples were added to pre-filtered, sterilized sea water containing 2% glutaraldehyde and stored at 4°C. Viruses will be enumerated by TEM.

Results

Macrofaunal results consist of lists of macroinvertebrate organisms obtained from bottom sampling, observations of invertebrate megafauna, fish and life traces during TV-lines. These are compiled in Tables 5 and 6, respectively. A preliminary description of the samples based on the material partially processed on board is given below.

A) Bottom sampling

Moroccan margin

Mercator mud volcano: The grab sample (AT-569GR) collected in this mud volcano yielded numerous Solemyidae and Thyasiridae bivalves, euphausiid shrimps and ophiuroids that were prepared for stable isotope analysis. Pogonophoran worms (*Siboglinum* sp.) were present but their number was insufficient for isotope analyses. Other motile (Polychaeta, Amphipoda, Isopoda) and sessile organisms (Porifera) were recovered from the sieved sediments. Scyphozoan polyps and one ophiurid were collected from the gravity cores (AT-567-568G). Three box cores (AT-575-577B) were also collected in different areas: crater, mud flow and hemipelagic sediments at the outskirts of the mud volcano. These samples were washed and fixed on board but were not sorted.

Pen Duick Escarpment and Renard Ridge: The samples recovered in these areas (AT-570-572G) included abundant biological debris, mainly dead corals, but no conspicuous living organisms.

Adamastor mud volcano: The only sample (AT-573G) taken at this location showed no conspicuous living organisms.

Vernadsky Ridge - Chimneys' area: The chimneys retrieved in a dredge sample (AT-574D) were not heavily colonized by sessile fauna. A few colonies of different cnidarian species and crinoids were removed from the surface of the chimneys. Serpulidae (Polychaeta) tubes and Bryozoan colonies were also observed but difficult to remove. Xanthidae crabs, and Eunicidae polychaetes were also recovered and prepared for stable isotope analyses.

Meknes mud volcano: The core samples (AT-578-580G, AT-582-583G, AT-587-588G) collected in this mud volcano showed no conspicuous living organisms. The grab (AT-581GR, AT-586GR) and kasten core samples (AT-584-585K) yielded numerous specimens of pogonophoran worms (*Siboglinum* sp.) a few Solemyidae bivalves (*Acharax* sp.) and a diversity of other mobile (several species of

Table 5. Listing of the macrofauna collected from bottom samples.

Phylum	POR	CNIDARIA			SIP	MOLLUSCA			NEM	ANN		ARTHROPODA				ECHINODERMATA				BRY
Class		Hyd	Scy	Ant		Polp	Gas	Biv		Poly	Pog	Cir	Malacostraca			Ast	Cri	Oph	Echi	
Order													Dec	Amp	Iso	Tan				
AT567G			+																	
AT568G																			+	
AT569Gr	+							+		+	+		+	+				+		
AT570G																				
AT571G																				
AT572G																				
AT573G																				
AT574D		+	+		+		+	+		+	+		+				+	+		+
AT575Bx																				
AT576Bx																				
AT577Bx													+							
AT579G																				
AT580G																				
AT581Gr	+	+	+					+		+	+		+	+	+		+		+	
AT582G																				
AT583G																				
AT584K				+						+	+		+							
AT585K		+	+					+		+	+		+	+				+	+	
AT586Gr	+	+	+	+				+		+	+	+	+	+					+	
AT587G																				
AT588G																				
AT589G																				
AT590G																				
AT591G																				
AT592G																				
AT593G																				
AT594G																				
AT595G				+																
AT596G																				
AT597Gr		+								+	+									
AT598G																				
AT599D		+	+	+						+										

POR: Porifera; SIP: Sipuncula; NEM: Nemertea; ANN: Annelida; BRY: Bryozoa; Hyd: Hydrozoa; Scy: Scyphozoa; Ant: Anthozoa; Polyp: Polyplacophora; Gas: Gastropoda; Biv: Bivalvia; Poly: Polychaeta; Pog: Pogonophora; Cir: Cirripedia; Ast: Asteroidea; Cri: Crinoidea; Oph: Ophiuroidea; Echi: Echinoidea; Dec: Decapoda; Amp: Amphipoda; Iso: Isopoda; Tan: Tanaidacea

Crustacea, Polychaeta and Echinodermata) and sessile organisms (Porifera, Cnidaria and Cirripedia). Some bivalve, pogonophoran and decapod specimens were prepared for stable isotope analyses.

Seabed hill: The gravity core (AT-589G) collected at this structure showed no conspicuous living organisms.

Deep Portuguese margin

Olenin mud volcano: The gravity core (AT-591G) collected at this structure yielded only biological debris.

New mud volcanoes: A pogonophoran tube was recovered from the gravity core from Semenovich MV (AT-592G) but no other conspicuous living organisms were collected from Soloviev and Carlos Texeira MVs (AT-593G and AT-594G).

Porto mud volcano: A small anemone

(Hexacorallia) attached to an anthipatharian dead branch was recovered from core AT-595G. No conspicuous living organisms were collected from the other core collected at this structure (AT-596G).

Bonjardim mud volcano: Pogonophoran worms of the genus *Polybrachia* sp. were abundant both in the grab and core samples (AT-597GR, AT-598G). The grab samples also contained a few specimens of *Oligobrachia* sp. (a different genus of pogonophoran worm), some polychaete worms and hydrozoan colonies.

Cadiz valley - Chimney area: The chimneys retrieved in the dredge sample (AT-599D), were not heavily colonised by sessile fauna. A few colonies of Hydrozoa, scyphozoan polyps and a polychaete worm were removed from the surface of the chimneys. Serpulidae (Polychaeta) tubes and Bryozoan colonies were also observed but not

Table 6. Listing of the megafauna recorded during real time observation of video footages.

Phylum	Class	Order	TVAT-60	TVAT-61	TVAT-62	TVAT-63	TVAT-64	TVAT-65	TVAT-66	TVAT-67	TVAT-68	TVAT-69
Porifera			+		+	+	+	+	+	+	+	+
Cnidaria	Hydrozoa		+		+	+	+	+				+
	Anthozoa		+	+	+	+	+	+	+	+	+	+
Mollusca	Gastropoda					+		+	+			+
	Cephalopoda								+			
Annelida	Polychaeta		+									
Arthropoda	Malacostraca	Decapoda	+	+	+	+	+	+	+		+	+
		Euphausiacea			+							
Echinodermata	Crinoidea					+	+		+	+		
	Asteroidea							+	+		+	+
	Ophiuroidea									+	+	+
	Echinoidea		+	+	+	+	+		+	+	+	+
	Holothuroidea		+			+	+		+	+	+	+
Chordata	Chondrichthyes					+	+					
	Osteichthyes		+	+	+	+	+	+	+	+	+	+

removed. The sample further yielded several fragments of different species of madreporarian corals.

B) Video observations

A brief description of the selected video observations follows. It was not possible to process all the lines onboard but all observations are summarized in Table 6.

TVAT-60: This TV-line crossed the crater and mud flow of Mercator mud volcano. These two areas showed different assemblages.

TVAT-61: This TV line crossed Adamastor mud volcano. Cnidarian colonies of several different species accounted for 90% of the observations; branched colonies, probably Isididae, were the dominant species. Different fish species and a few shrimps were also observed, mostly in the crater.

TVAT-65: This TV line surveyed the Meknes mud volcano and surrounding area, including two small high-backscattering areas that are revealed to be small coral patches. The observations allowed discrimination of four different sections where changes in the geological setting are clearly accompanied by changes in the benthic assemblage (Fig. 76). The first section is characterized by the occurrence of coral build-ups and coral rubble colonised by small epifaunal organisms; different species of sponges dominate the assemblage and the sediment is highly bioturbated by different kinds of burrows and tracks. The second section, spanning the crater, shows a heavily disturbed mud breccia with scattered clasts

as well as a strikingly large number of empty shells of the gastropod *Neptunea contraria* and a low density of living megafauna, including the gastropod *N. contraria*, the decapod *Paramola cuvieri* (cf.) and some fish. In the third section, the benthic assemblage shows an intermediate abundance mostly of sessile fauna covering the patches of coral rubble and carbonate crusts. Finally, the fourth section crossed an area of rather homogeneous soft sediment characterised by the occurrence of a large number of hexactinellid pedunculated sponges.

III.3.5. Gas biogeochemistry

Past geochemical analyses of gas from the Gulf of Cadiz mud volcanoes have revealed significantly high concentrations of C₂+ hydrocarbons. These hydrocarbons were found to differ between individual mud volcanoes, some of which exhibited a much higher proportion of methane (Mazurenko et al., 2002; Blinova and Bileva, 2003). Methane stable isotope measurements may give a better understanding of the origin of the gas-bearing fluids. Methane stable carbon and hydrogen isotopes have been used for the purpose of constraining the proportion of gas derived from deep-sourced hydrocarbon reservoirs, versus those produced by shallower bacterial activity (e.g. Whiticar et al., 1986). However, stable isotope interpretation is not straightforward and a comparison with a maximum number of biogeochemical parameters is, therefore, necessary. It has been shown that the gases escaping from the Gulf of Cadiz mud volcanoes originate from deep-seated fluids

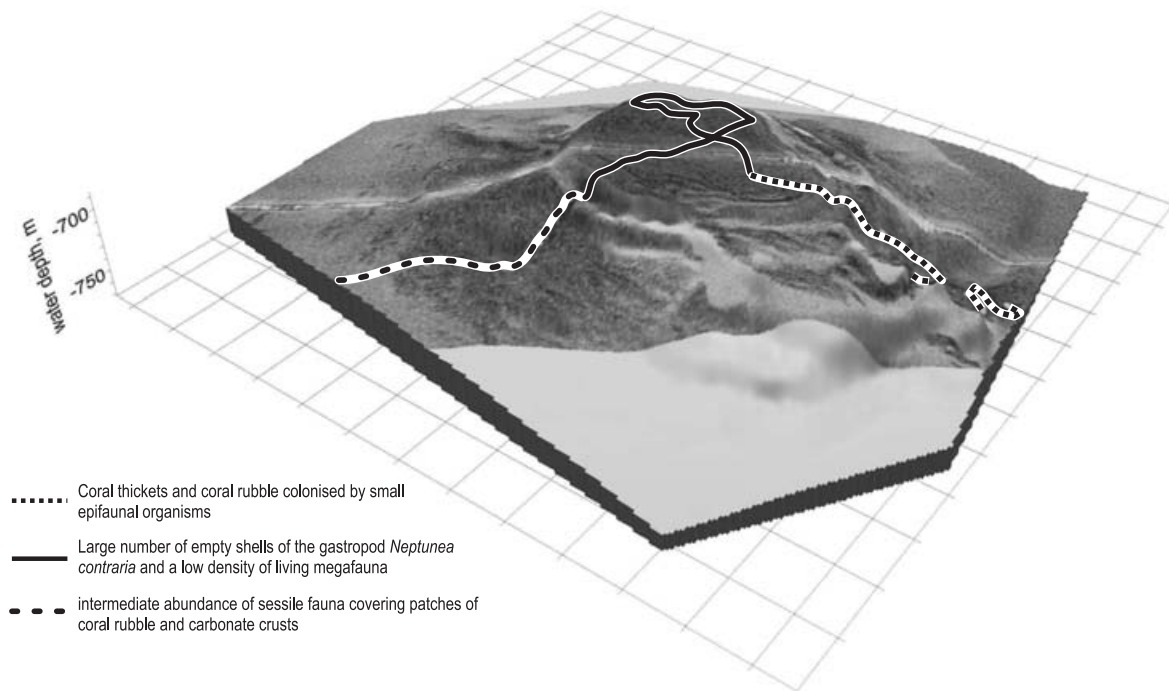


Figure 76. Differentiation of local benthic assemblages in accordance with geological settings on the Meknes mud volcano.

(Blinova and Stadnitskaya, 2001), but the microbial processes affecting these fluids as they rise through the sedimentary column remain largely unknown.

During Leg 4, a large number of samples for gas geochemistry were collected from gravity cores in known active or fairly active mud volcanoes all across the Gulf of Cadiz, and also in new mud volcanoes discovered during this cruise. These include the Meknes mud volcano, where a transect of three cores was made: one background core (AT578G), one core on the slope (AT579G) and one core in the crater (AT580G). Another background site was also sampled in an area close to a shipwreck (AT590G). This was considered an interesting site to study contamination, as anthracite coal, spilled from the ship, was present in the core.

Samples were also taken from three cores (AT592G, AT596G and AT598G) on a new structure that seems to be active due to the presence of degassing dark grey, mud breccia.

Gas sampling

A sediment plug was collected at the fol-

lowing intervals for each section of the core: 20 cm, 30 cm, 40 cm and 50 cm. Duplicates were collected at these intervals and also analysed, to improve accuracy of the results. The samples were collected with a tip-sliced syringe and put in a 30 ml glass vial filled with 10 ml of 10 % KCl solution. The samples were shaken in order to break up the sediment plug and to stop all bacterial activity. The samples were stored upside down to avoid exchanges with room air, and allowed to equilibrate with the vial headspace for two days. The gas was then extracted in a syringe by injecting an equivalent amount of 10% KCl solution.

The total gas was divided into two serum vials filled (bubble-free) with a pH 1 10% KCl solution by displacement of an equivalent amount of solution. The vials were stored upside down in order to avoid exchanges with air through the septum. One of the vials will be used for gas analyses and the other for isotope composition.

Pore water sampling

Sediment samples were also collected between 10-20 cm and 30-40 cm in each sec-

tion for pore water sampling. They were stored in a plastic bag, previously washed with hydrochloric acid and frozen for preservation until analysis in the laboratory.

III.4. Ship wreck

A. AKHMETZHANOV, N.H. KENYON, M. IVANOV,
V. BLINOVA, D. NIKONOV, A. MAZZINI AND TTR-15
SCIENTIFIC PARTY.

A strange, very high backscattering feature observed on the MAK Line MAKAT-125 was investigated (Fig. 77). It had triangular points that radiate out asymmetrically from the widest part of the feature (resembling the outline of a Christmas tree). Where crossed by the profiler there was, unusually, no interruption to the very regularly draping parallel beds. The overall noise level of the profile was lower where it crossed the high

backscatter area. There was a small upstanding bump (less than 2 m) that was sitting on the seafloor and seemed on close inspection to be causing a hyperbolic reflection and hence was probably steep. A shadow about 210 m long was located near the wide end of the patch. Few explanations could be preferred for these observations.

Core AT-590G was collected from the high backscatter patch to groundtruth its cause (Fig. 77). The uppermost interval of the core (0-7 cm) consists of olive-brown water-saturated homogeneous clay with a sharp lower contact. Several clasts of anthracite coal were found within the sediment. The unit below is brown clay with foraminifera.

A towed camera survey (TVAT-66) was run across the high backscatter patch in order to investigate its nature (Fig. 78). As soon as the camera entered the high backscattering area, fragments of coal began

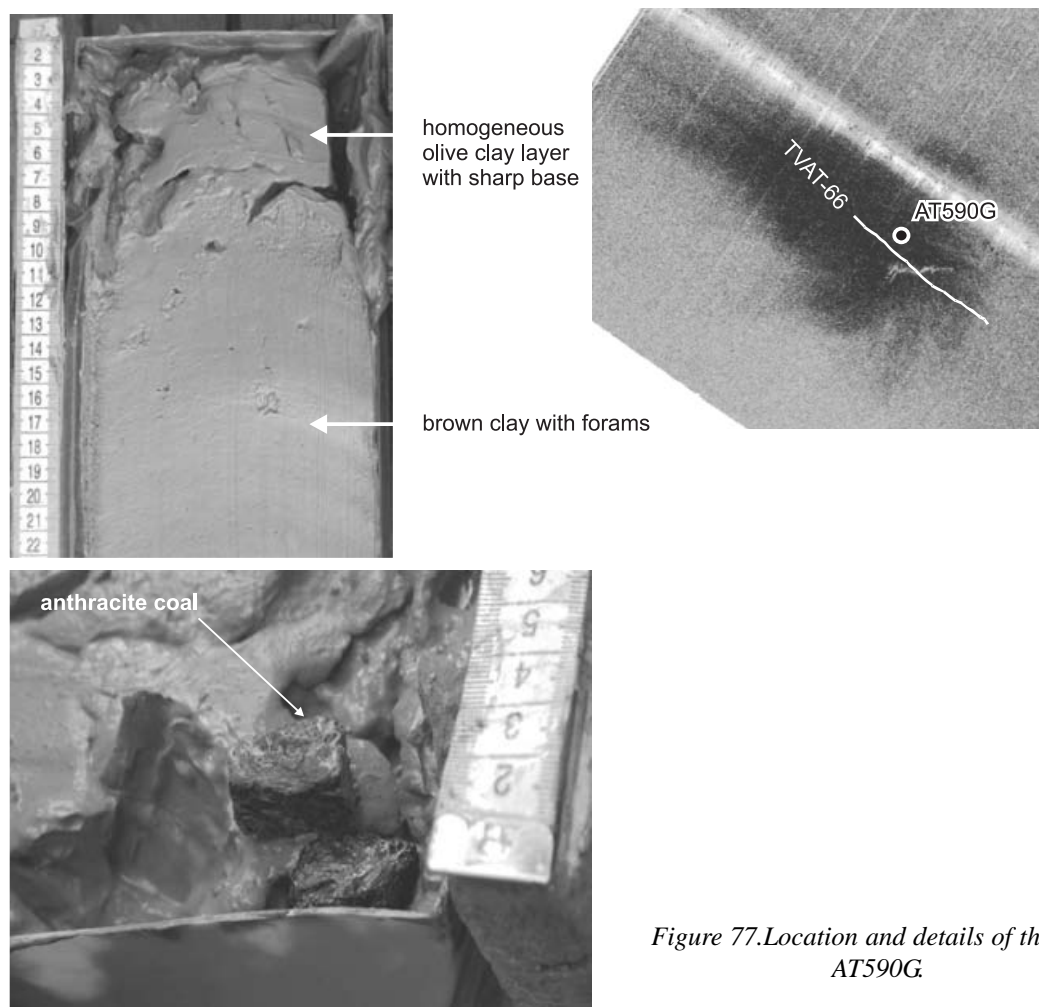


Figure 77. Location and details of the core AT590G.

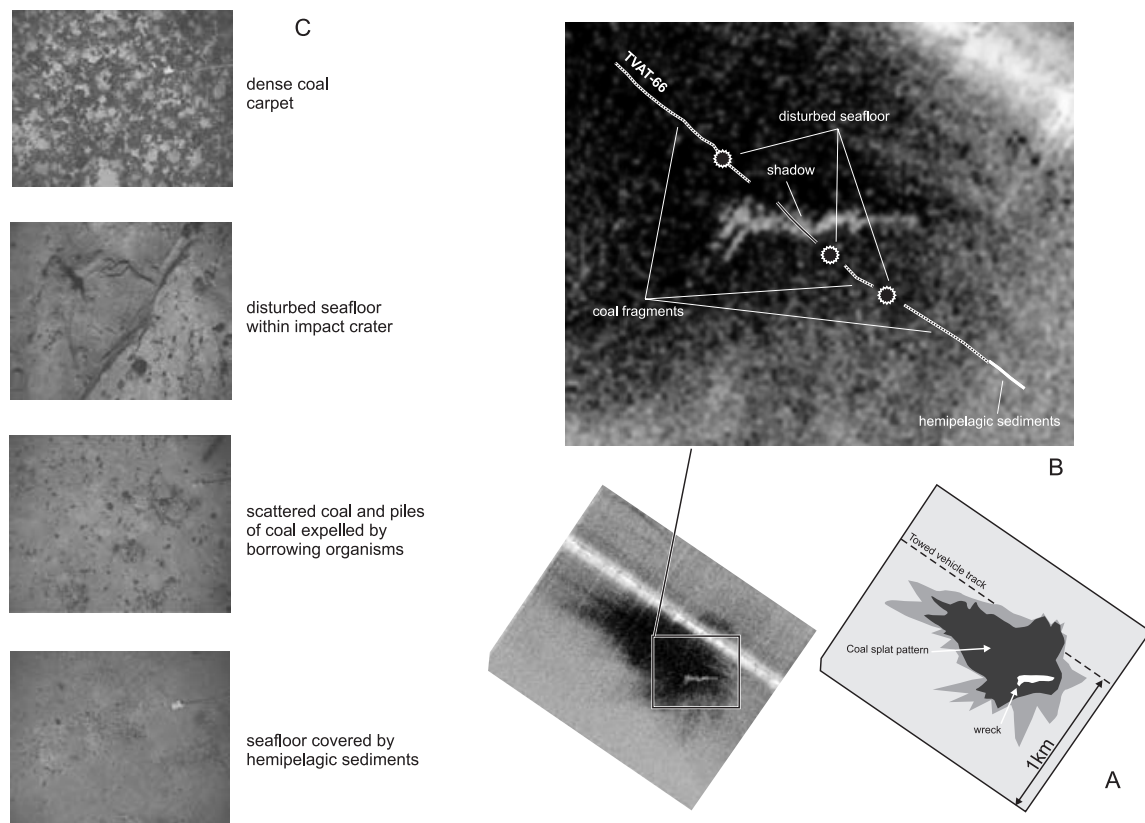


Figure 78. A: Sidescan sonograph from line MAKAT125 showing a splat pattern produced by coal and shadow cast by the wreck; B: Interpretation of the video run (TVAT66); C: Video stills showing typical environments from the wreck site.

to be seen on the seafloor. They were often arranged into small mounds produced by burrowing organisms expelling the coal from under a thin muddy drape. In the vicinity of the elongate target casting the shadow the seabed was severely disturbed with up to a few meters high, fresh looking escarpments seen on the footage. The target itself was crossed and the wreck of a large ship was observed on the footage. The camera traversed a metal deck, side railings, open hatch and upper superstructure of the vessel (Fig. 79), before it was pulled up for safety reasons. The instrument was lowered again beyond the wreck showing that the concentration of coal fragments significantly increased and a dense coal carpet is now covering the seabed.

The results of this short survey show that the high backscattering pattern is a splat pattern which followed a high velocity contact with the seafloor. The shadow is cast by the main part of the ship and the bump on

the profile perhaps being another piece of wreckage. The impact produced a several meter deep crater surrounding the wreck as well as a cloud of suspended sediments which later settled as a distinct layer of homogeneous olive clay.

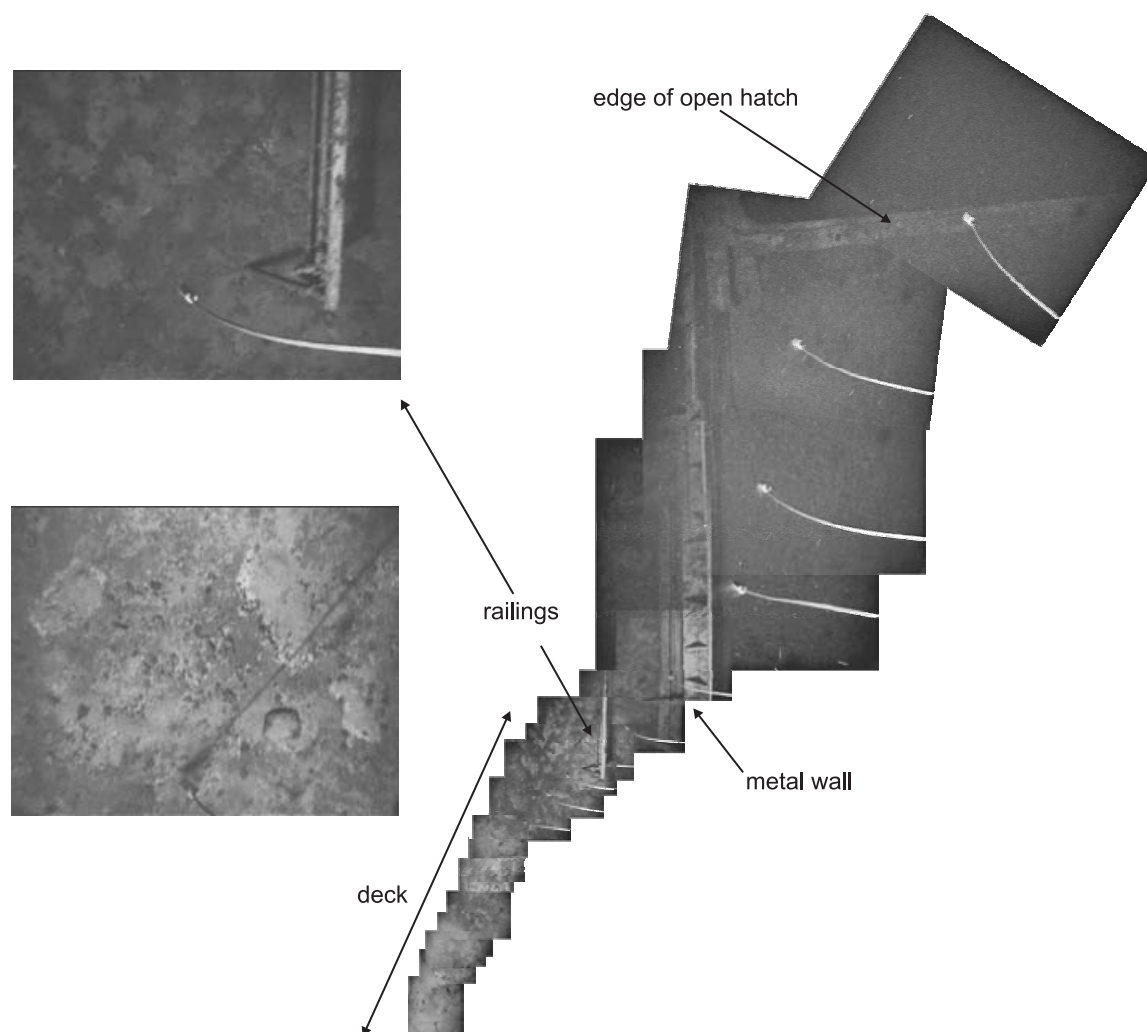


Figure 79. Photomosaic and video stills showing details of the wreck.

III.5. Seabed processes and ecosystems in the Portuguese Cadiz margin canyons.

A. AKHMETZHANOV, N.H. KENYON, M. IVANOV,
M. CUNHA, V. BLINOVA, D. NIKONOV AND TTR-15,
LEG 4 SCIENTIFIC PARTY

Introduction

A short study consisting of a long under-water camera run TVAT-69 was conducted across the head of the Cadiz submarine valley (named in Mulder et al., 2006) on the SE Portuguese Margin in order to investigate seabed processes and faunal distribution in the area (Fig. 47). The valley is known to cut back into the Cadiz channel which is worked by the Mediterranean Undercurrent and

serves as one of its major pathways along the margin. As a result of this the bottom current is partially redirected along the canyon into deeper water. Previous studies found the lower core of the Undercurrent to be present in the area in water depths of between 1000 and 1300 m (Kenyon et al., 2002; Mulder et al., 2004). The TV run was intended to cross the area affected by the Undercurrent down to approximately 1300 m and then to continue into a deeper portion of the slope not affected by the Undercurrent (Fig. 80).

The total length of the track is about 15 km. Due to the limited battery life the seabed video survey was performed only along selected sections of the track. The first section is a transect across the Cadiz Channel within depth range 1080 - 1270 m, which covers an area affected by the Undercurrent. The sec-

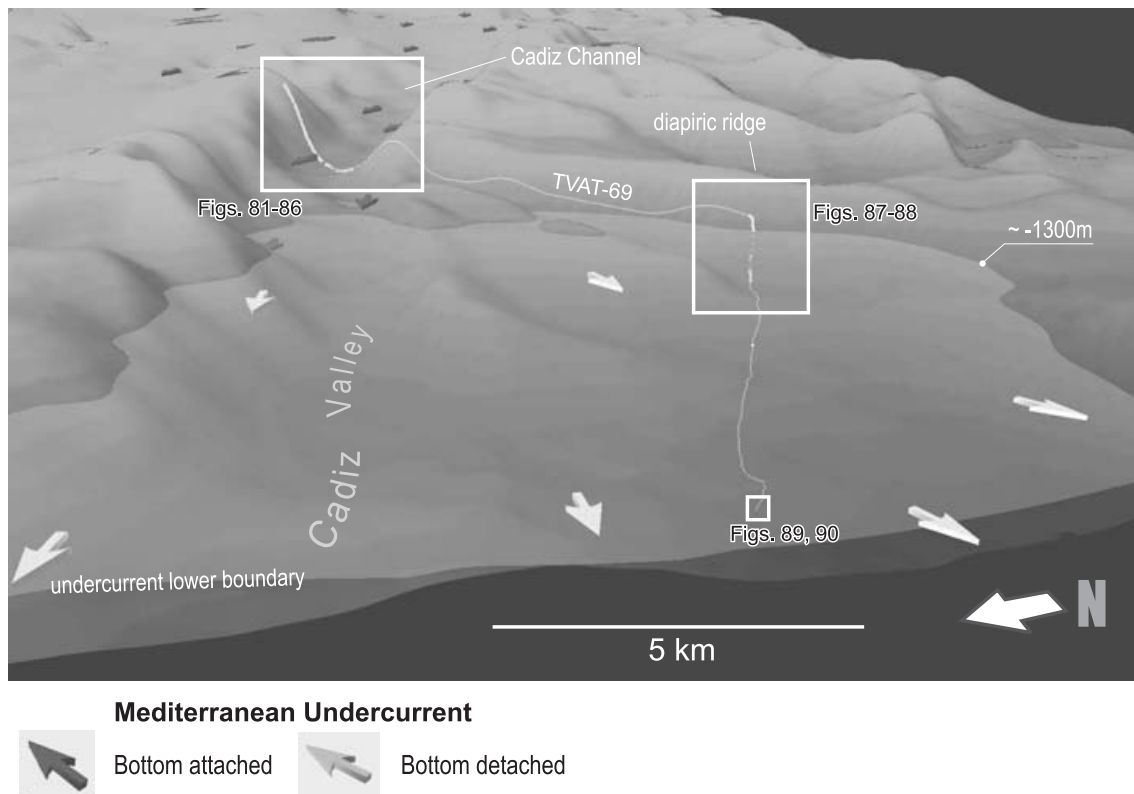


Figure 80. Overview of the environment crossed by the seabed video survey. Bathymetry from SWIM compilation (Diez et al., 2005).

ond section was run below the Undercurrent heading down the slope of the Cadiz valley and covering the depth range from 1290 m to 1430 m. At the end of the track a short portion of the seafloor was checked in the central part of the Cadiz Valley where a sinuous gravity flow channel was observed on existing bathymetry and sidescan sonar data in the depth range 1545 - 1560 m.

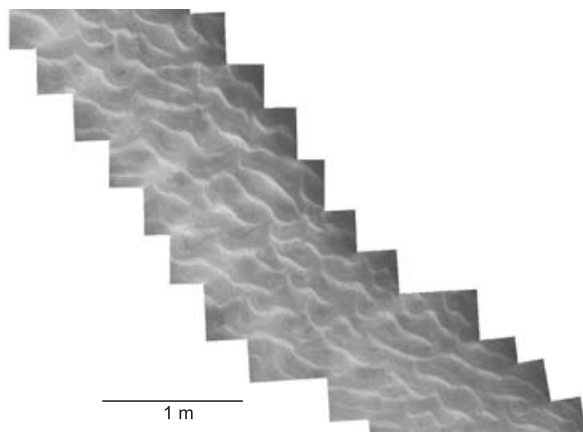


Figure 81. Field of sand ripples - the dominant bed-forms in the Cadiz Channel.

Section across Cadiz Channel

The video transect across the Cadiz Channel is divided into seabed facies types along most of its northern flank, thalweg and half of the southern flank. Available sidescan sonar data for the area showed the erosion of the seabed along the channel thalweg and development of escarpments along the flanks. The dominant seabed facies is rippled sandy seafloor (Fig. 81). Morphology of the ripples varies from long-crested and parallel to linguoid. Numerous steep escarpments up to a few meters high were encountered on the channel flanks (Fig. 82). They are thought to result from slope failures along the flanks of the channel which are undercut by the bottom currents. Submarine talus is often present at the base of the escarpments. Some of the escarpments appear to be fresh with sharp edges suggesting recent instability of the channel flanks. Other escarpments are older and have more rounded edges, often colonised by sponges (Fig. 83).

Within the thalweg the seabed facies distribution changes. Although rippled sand is

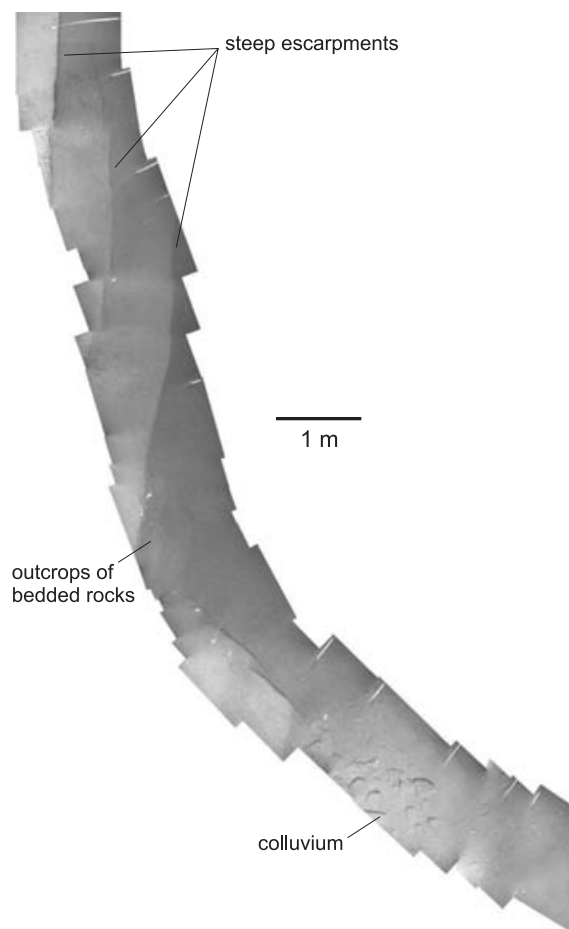


Figure 82. Photomosaic of a series of steep escarpments developing along walls of the Cadiz Channel. Outcrops of bedded rocks and submarine colluvium, seen as talus blocks, are often associated with such escarpments.

still very common, outcrops of lithified clays become more frequent suggesting widespread erosion of the seabed. In some places they appear as erosional remnants surrounded by rippled sand in others the sand is completely removed exposing clayey substratum often with furrows and grooves (Fig. 84). This correlates well with the sidescan sonar data which shows a zone of active erosion along the thalweg of the channel.

At the base of the southern flank of the channel several large clayey outcrops were encountered. Often they are colonised by sponges which appear to prefer settling along lighter coloured grounds, which probably are more consolidated carbonated varieties within the clayey section (Fig. 85). From the above observations it is concluded that sponge settlement benefits from the presence of active hydrodynamic conditions providing a high nutrient flux, the availability of the suitable hardground, e.g. clayey outcrops, and the absence of mobile sand. Some outcrops are extensively burrowed around the edges which could be also attributed to sponges (Fig. 86).

Observations along this section indicated that the Undercurrent is active at present in this part of the Cadiz channel, with the seabed dominated by mobile sand. Flank collapses are common and erosion is

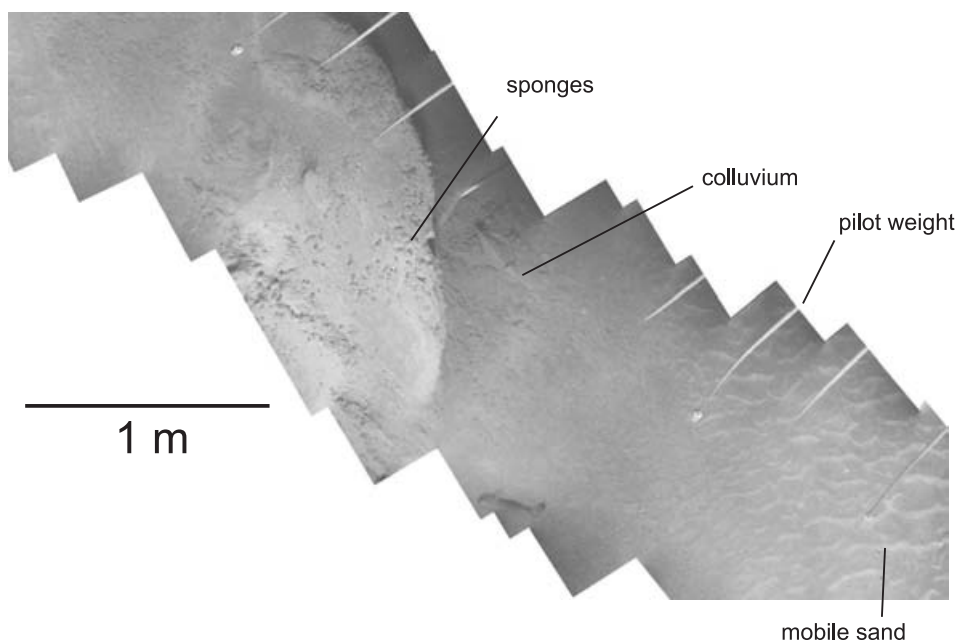


Figure 83. Colony of sponges growing from clayey substratum outcropping along the escarpment edge.

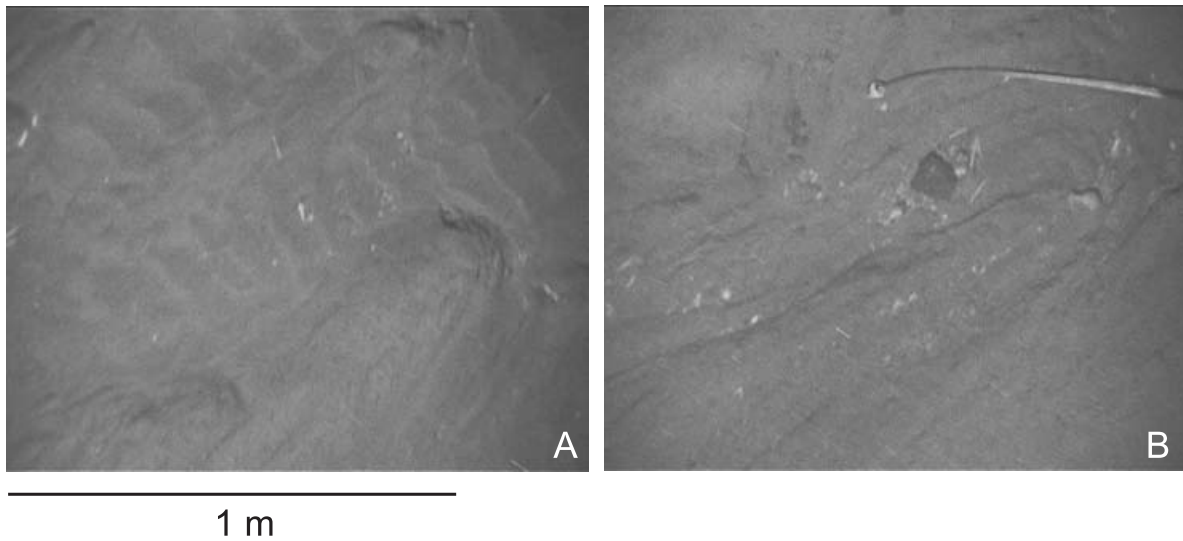


Figure 84. Outcrops of older, diapir-forming, clays in the central part of the channel. A - clayey erosional remnants surrounded by rippled sand; B - erosional furrows developing on clayey substratum.

widespread in the axial part of the channel. Escarpments formed by flank collapses create outcrops of clayey semi-lithified sediments with elevated edges which provide good settlement grounds for numerous colonies of sponges.

Section down the flank of the Cadiz Valley

Observations along the second section of the video survey confirmed the absence of the Undercurrent in this depth range. The seafloor is usually smooth and bioturbated and from observations of bottom contacts of

the pilot weight is covered by fine-grained sediments. According to the available multi-beam bathymetry (Diez et al., 2005) slope gradient along the section is relatively steep, being about 12°. Sediment failures appear to be common and escarpments and outcrops of lithified clayey sediments are frequent. The survey revealed that the clayey outcrops often contain fields of carbonate chimneys (Fig. 87), similar to those found to the north of the area on the slopes of Guadalquivir Ridge and other outcropping diapirs (Diaz del Rio et al., 2003; Kenyon et al., 2002). Chimneys are mostly found to have fallen on

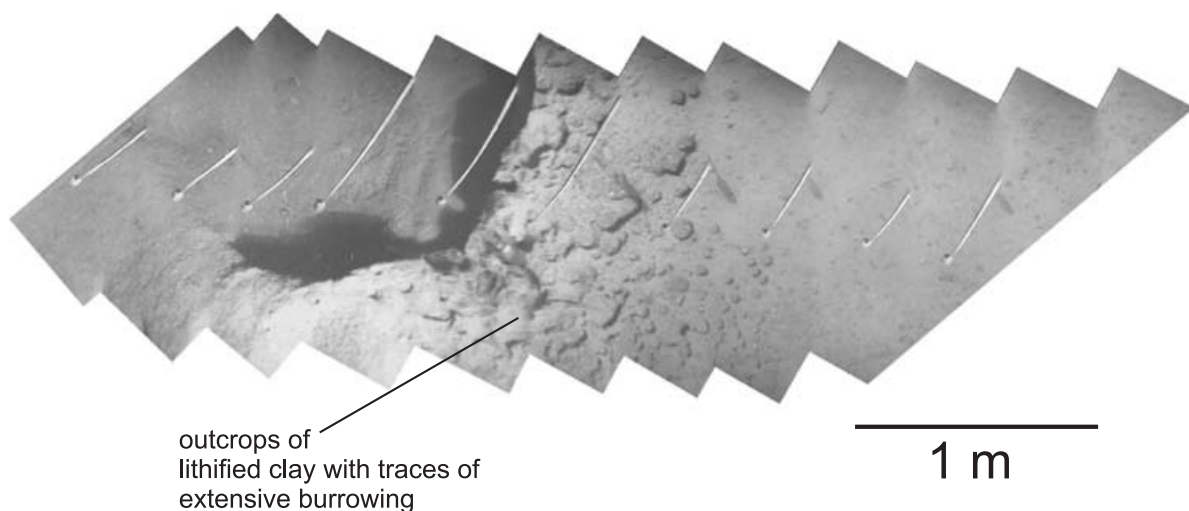


Figure 85. Colonies of sponges growing from harder, possibly semi-lithified, clayey outcrops in the zone of enhanced bottom current.

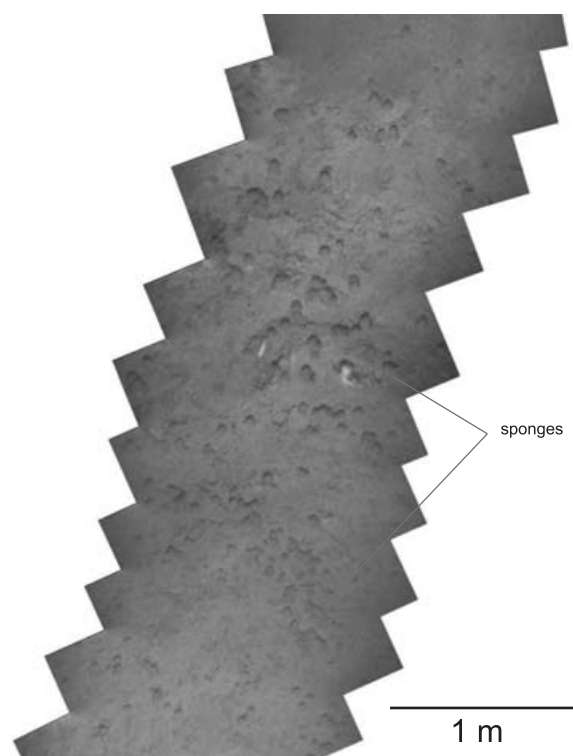


Figure 86. Outcrops of lithified clays extensively burrowed by sponges.

the seabed although several were seen to be upstanding (Fig. 88). Several fragments of chimneys were recovered by dredge at the site AT-599G which were light grey in colour and were made of relatively soft material. These could be examples of chimneys *in situ*, which were growing within the sedimentary section then were extracted onto the surface during dredging.

Biodiversity is higher in this section compared to the Cadiz Channel. Fish, Holothurians and Decapods are common along the track.

Section across the axial part of the Cadiz Valley

A short survey within the axial part of the Cadiz Valley also confirmed the absence of the Undercurrent. The seabed has a smooth character produced by a fine-grained hemipelagic cover. The gravity flow channel found in this area on previous studies (Kenyon et al., 2002; Habgood et al., 2003)

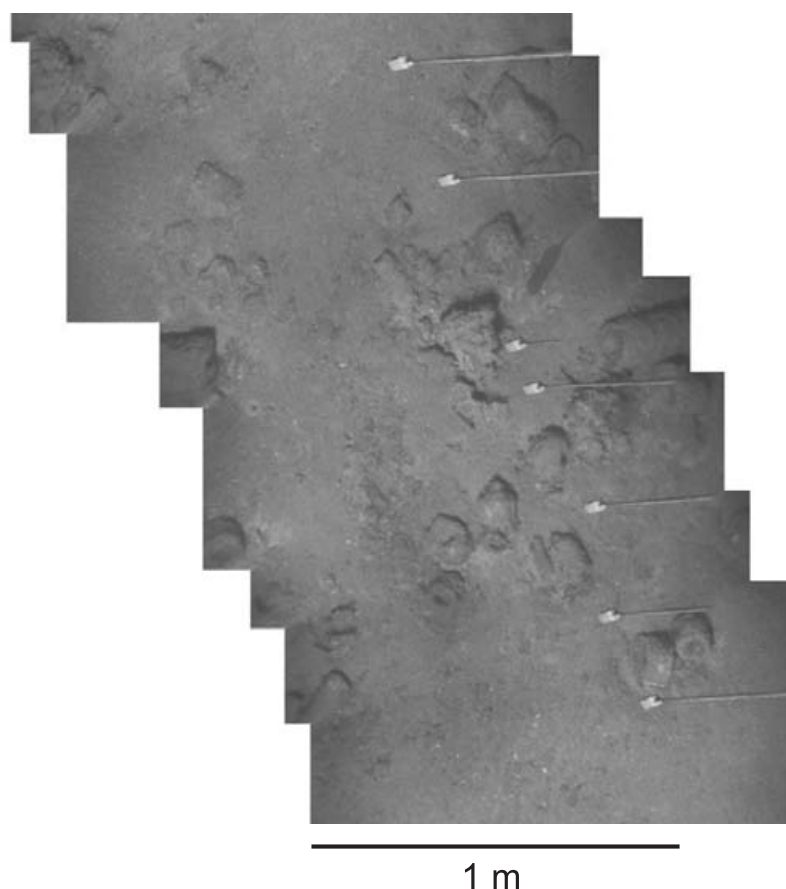


Figure 87. Fragment of photomosaic showing numerous methane derived carbonate chimneys scattered over the seabed.

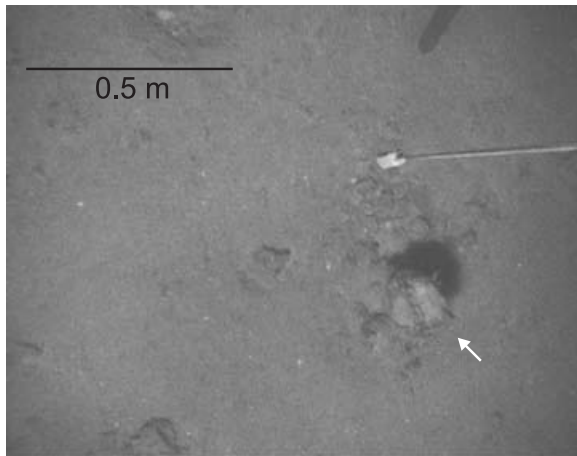


Figure 88. Upstanding carbonate chimney (arrow).

has also been crossed. The video record shows that it has steep flanks along which a bedded section is outcropping (Fig. 89) and a flat thalweg covered by a hemipelagic drape. The presence of the drape suggests the absence of recent activity, however the small scale roughness of the seabed may indicate the presence of debris flow deposits under the thin hemipelagic drape (Fig. 90).

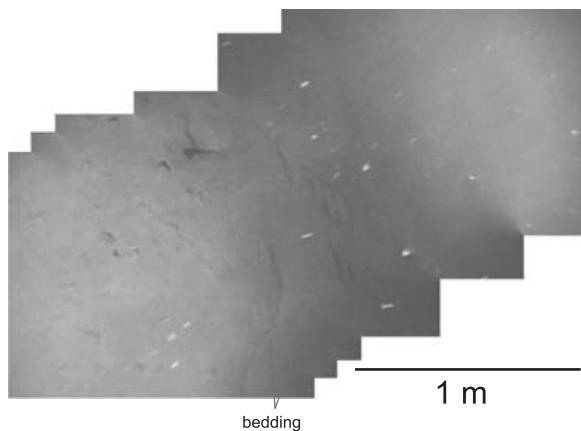


Figure 89. Fragment of a photomosaic showing details of a flank of the gravity flow channel in the axial part of the Cadiz submarine valley..

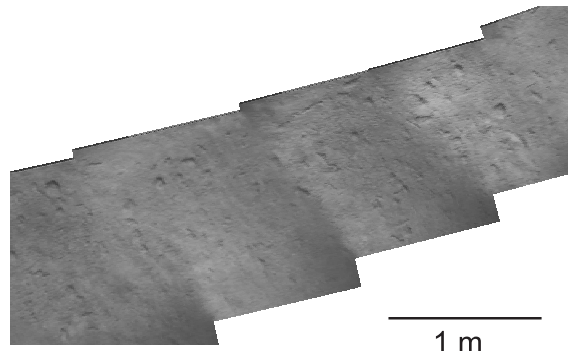


Figure 90. Seabed roughness in the thalweg of the gravity flow channel may be due the presence of debris flow deposits under thin hemipelagic drape.

REFERENCES

- Auzende, J.M., Olivet, J.L. and Pastouret, L. 1981. Implication structurales et paleogeographiques de la presence de Messinien a l'ouest de Gibraltar. *Marine Geology*, 43, 9-18.
- Baraza, J. and Ercilla, G. 1996. Gas-charged sediments and large pockmark like features on the Gulf of Cadiz slope (SW Spain). *Marine and Petroleum Geology*, 13, 253-261.
- Blinova, V. and Bileva, E. 2003. Some geochemical characteristics of relatively active and passive mud volcanoes (Gulf of Cadiz and Alboran Sea). *IOC Workshop Report*, 187, 17-18, UNESCO.
- Blinova, V. and Stadnitskaya, A. 2001. Composition and origin of the hydrocarbon gases from the Gulf of Cadiz mud volcanic area. *IOC Workshop Report*, 175, 45-46, UNESCO.
- Bonnin, J., Olivet, J.L. and Auzende, J.M. 1975. Structure en nappe a l'ouest de Gibraltar. *C.R. Academy of Science*, 280 (5), 559-562.
- Borges, J.F., Fitas A.J.S., Bezzeghoud M. and Teves-Costa, P. 2001. Seismotectonics of Portugal and its adjacent Atlantic area. *Tectonophysics*, 337, 373-387.
- Cavazza, W., Roure, M. R., Spakman, W., Stampfli, G. M. and Zigler, P. A. 2004. The trasmed Atlas: the Mediterranean region from crust to mantle. Springer-Verlag Berlin Heidelberg, Germany, 141 pp.
- Cragg, B. A., Parkes, R. J., Fry, J. C., Weightman, A. J., Rochelle, P. A., Maxwell, J. R., Kastner, M., Hovland, M., Whiticar, M. J. and Sample, J. C. 1995. The impact of fluid and gas venting on bacterial populations and processes in sediments from the Cascadia Margin accretionary system (sites 888-892) and the geochemical consequences. *Proceedings of the Ocean Drilling Program, Scientific Results*, 146, 399-410.
- Dewey, J.F., Helman, M.L., Turco, E., Hutton, D.H.W. and Knott, 1989. Kinematics of the western Mediterranean. *Tectonics*, 7, 1123-1139.
- Diaz-del-Rio, V. , Somoza, L., Martinez-Frias, J., Mata, M.P., Delgado, A., Hernandez-Molina, F.J., Lunar, R., Martin-Rubi, J.A., Maestro, A., Fernandez-Puga, M.C., Leon, R., Llave, E., Medialdea, T. and Vezquez, J.T. 2003. Vast fields of hydrocarbon-derived carbonate chimneys related to the accretionary wedge/olistostrome of the Gulf of Cadiz. *Marine Geology*, 195, 177-200.
- Diez, S., Gracia, E., Gutscher, M.A., Matias, L., Mulder, T., Terrinha, P., Somoza, L., Zitellini, N., De Alteriis, G., Henriot, J.P., Danobeitia, J.J. 2005. Bathymetric map of the Gulf of Cadiz, NE Atlantic Ocean: The SWIM multibeam compilation. 250th Anniversary of the 1755 Lisbon Earthquake, Lisbon (Portugal), 1-4 November, 601-602.
- Feinberg, H. 1976. Mise en place, au Pliocene, d'une nappe de glissement a l'extremite sud-occidentale de la chaine du Rif (Maroc): *C.R. somm. Geol. Soc., France*, 6, 273-276.
- Flinch, J., Bally, A. and Wu, S. 1996. Emplacement of a passive-margin evaporitic allochthon in the Betic Cordillera of Spain. *Geology*, 24, 67-70.
- Fukao, Y. 1973. Thrust faulting at a lithospheric plate boundary, the Portugal earthquake of 1969. *Earth plan. Sci. Lett.* 18, 205-216.
- Gardner, J.M. 1999. Mud volcanoes on the Moroccan Margin. *EOS Transactions*, 80(46), 483
- Gardner, J.M. 2001. Mud volcanoes revealed and sampled on the Moroccan continental margin. *Geophysical Research Letters*, 28, 339-342
- Gonzalez, A., Cordoba, D., Matias, L.M. and Torne, M. 1997. Estructura de la corteza desde la zona surportuguesa hasta la llanura abisal de la Herradura, a partir de datos de sesmica de gran angulo, reflexion vertical y gravimetria. *Abstract Volume II, Simposium on Atlantic Iberian Margin, Cadiz, Spain*, 67-68.
- Gutscher, M.-A., Malod, J., Rehault, J.-P., Contrucci, I., Klingelhoefer, F., Mendes-Victor, L. and Spakman, W. 2002. Evidence for active subduction beneath Gibraltar. *Geology*, 30, 1071-1074.

- Hornibrook, E. R. C., Longstaffe, F. J., and Fyfe, W. S. 1997. Spatial distribution of microbial methane production pathways in temperate zone wetland soils: stable carbon and hydrogen isotope evidence. *Geochimica et Cosmochimica Acta*, 61, 745-753.
- Ivanov, M.K., Kenyon, N., Nielsen, T., Wheeler, A., Monteiro, J., Gardner, J., Comas, M., Akhmanov, G., Akhmetzhanov, A. and Scientific Party of the TTR-9 cruise, 2000. Goals and principle results of the TTR-9 cruise. *Geological Processes on European Continental Margins. International Conference and Eighth Post-cruise Meeting of the Training-Through-Research Programme*, University of Granada, Spain, 31 January - 3 February 2000. IOC Workshop Reports, 168, UNESCO, 3-4.
- Kenyon, N.H., Ivanov, M. K., Akhmetzhanov, A. and Akhmanov, G. G. (eds.), 2000. Multidisciplinary study of geological processes on the North East Atlantic and Western Mediterranean margins. IOC Technical Series, 56, UNESCO.
- Kenyon, N.H., Ivanov, M. K., Akhmetzhanov, A. and Akhmanov, G. G. (eds.) 2002. Interdisciplinary studies of geological processes in the Mediterranean and Black Seas and North East Atlantic. IOC Technical Series, 62, UNESCO, 134 pp.
- Klaucke, I., Sahling, H., Burk, D., Weinrebe, W. and Bohrmann, G. 2005. Mapping deep-water emissions with sidescan sonar. *EOS Transactions*, 86, 341-346.
- Klaucke, I., Sahling, H., Weinrebe, W., Blinova, V., Burk, D., Lursmanashvili, N. and Bohrmann, G. 2006. Acoustic investigation of cold seeps offshore Georgia, eastern Black Sea. *Marine Geology*, 231, 51-67.
- Kruglyakova, R., Gubanov, Y., Kruglyakov, V., Prokoptseva, G. 2002. Assessment of technogenic and natural hydrocarbon supply into the Black Sea and seabed sediments. *Continental Shelf Research*, 22, 2395-2407.
- Lajat, D., Biju-Duval, B., Gonnard, R., Letouzey, J. and Winnock, E. 1975. Prolongement dans l'Atlantique de la partie externe de l'Arc betico rifian. *Bulletin of the Geol. Soc., France* 17, 481-485.
- Lonergan, L. and White, N. 1997. Origin of the Betic-Rif mountain belt. *Tectonics*, 16, 504-522.
- Lowrie, A., Hamiter, R., Moffett, S., Somoza, L., Maestro, A. and Lerche, I. 1999. Potential pressure compartments sub-salt in the Gulf of Mexico and beneath massive debris flows in the Gulf of Cadiz. GCS-SEPM Foundation 19th Annual Research Conference, Advanced Reservoir Characterization, 271-280.
- Lowrie, A., Lerche, I., Moffett, S., Kozlova, E. and Somoza, L. 2000. Fanfold-belt Created by a gravity-driven sliding continental margin in Gulf of Mexico, Gulf of Cadiz, and West Africa. *Gulf Coast Association of Geological Societies Abstract*.
- Maldonado, A. and Comas, M. C. 1992. Geology and geophysics of the Alboran Sea: an introduction. *Geo-Marine Letters*, 12, 61-65.
- Maldonado, A., Somoza, L. and Pallares, L. 1999. The Betic orogen and the Iberian-African boundary in the Gulf of Cadiz: geological evolution (Central North Atlantic). *Marine Geology*, 155, 9-43.
- Malod, J.A. 1982. Comparaison de l'évolution des marges continentales au nord et au sud de la Peninsule Iberique. These de doctorat d'Etat, Universite P. et M. Curie, Paris 6, 235 pp.
- Martinez del Olmo, W., Garcia-Mallo, J., Leret, G., Serrano, A. and Suarez, J. 1984. Modelo tectosedimentario del Bajo Guadalquivir. I Congreso Espanol de Geologia I, 199-213.
- Mazurenko, L. L., Soloviev, V. A., Belenkaya, I., Ivanov, M. K. and Pinheiro, L. M. 2002. Mud volcano gas hydrates in the Gulf of Cadiz, *Terra Nova*, 14, 321-329.
- Mazzini, A., Ivanov, M.K., Parnell, J., Stadnitskaia, A., Cronin, B.T., Poludetkina, E., Mazurenko, L. and van Weering, T.C.E. 2004. Methane-related authigenic carbonates from the Black Sea: geochemical characterisation and relation to seeping fluids. *Marine Geology*, 212, 153-181.
- McAuliffe, C. 1971. GC determination of solutes by multiple phase equilibration. *Chem. Tech.* 1, 46-51.
- Medialdea T., Vegas, R., Somoza L., Vazquez, J. T., Maldonado, A., Diaz-del-Rio V., Maestro, A., Cordoba, D. and Fernandez-Puga M. C. 2004. Structure and evolution of the "Olistostrome" complex of the Gibraltar Arc in the Gulf of Cadiz (eastern Central

Atlantic): evidence from two long seismic cross-sections. *Marine Geology*, 209, 173-198.

Mulder, T. 2004. Mission CADISAR 2 (27 Aout - 24 Septembre 2004), Golfe de Cadix. *Rapport Scientifique*, 39 pp.

Mulder, T., Lecroart, P., Hanquiez, V., Marches, E., Gonthier, E., Guedes, J.-C., Thiebot, E., Jaaidi, B., Kenyon, N., Voisset, M., Perez, C., Sayago, M., Fuchey, Y. and Bujan, S., 2006. The western part of the Gulf of Cadiz: contour currents and turbidity currents interactions. *Geo-Mar Lett*, 26, 31-41.

Perch-Nielsen, K. 1985. Cenozoic calcareous nannofossils. In: Bolli, H. M., Saunders, J. B. and Perch-Nielsen, K. (eds.), *Plankton Stratigraphy*. Cambridge University Press, 1032 pp.

Pinheiro, L.M., Ivanov, M.K., Sautkin, A., Akhmanov, G., Magalhaes, V.H., Volkonskaya, A., Monteiro, J.H., Somoza, L., Gardner, J., Hamouni, N. and Cunha, M.R. 2003. Mud volcanism in the Gulf of Cadiz: results from the TTR-10 cruise. *Marine Geology*, 195, 131-151.

Riaza, C. and Martinez del Olmo, W. 1996. Depositional model of the Guadalquivir-Gulf of Cadiz Tertiary basin, In: Friend, P.F. and Dabrio, C.J., (eds.). *Tertiary basin of Spain: the stratigraphic record of crustal kinematics*. Cambridge University Press, 330-338.

Roberts, D.G., 1970. The Rif-Betic orogen in the Gulf of Cadiz. *Marine Geology*, 9, 31-37.

Robinson, A. G., Rudat, J. H., Banks, C. J. and Wiles R. L. F. 1996. Petroleum geology of the Black Sea. *Marine and Petroleum Geology*, 13, 195-223.

Rosenbaum G., Lister G.S. and Duboz, C. 2002. Reconstruction of the tectonic evolution of the western Mediterranean since the Oligocene. In: Rosenbaum G. and Lister G.S. (eds.) *Reconstruction of the evolution of the Alpine-Himalayan Orogen*. *J. of Virtual Explorer*, 8, 107-126.

Ross, D.A. and Degens, E.T. 1974. Recent sediments of Black Sea. In: E.T. Degens and D.A. Ross (eds), *The Black Sea-Geology, Chemistry and Biology*. American Association of Petroleum Geologists Memoir, 20, 183-199.

Royden, L.H. 1993. The tectonic expression of slab pull at continental convergent boundaries. *Tectonics*, 12, 303-325.

Sartori R., Torelli, L., Zitellini, N., Peis, D. and Lodolo E. 1994. Eastern segment of the Azores-Gibraltar line (central-eastern Atlantic): an oceanic plate boundary with diffuse compressional deformation. *Geology*, 22, 555-558.

Somoza, L., Maestro, A. and Lowrie, A. 1999. Allochthonous blocks as hydrocarbon traps in the Gulf of Cadiz. *Offshore Technology Conference OTC 10889*, 571-577.

Somoza, L., Hernandez-Molina, FJ., Vazquez, J.T., Garcia-Garcia, A. and Diaz del Rio, V. 2000. El nivel de "BSR" en el talud superior del Golfo de Cadiz: implicaciones tecto-sedimentarias y paleoceanograficas. V Congreso Geologico de Espana, July, 2000, Alicante, Spain.

Stadnitskaia, A., Ivanov, M. and Gardner, J. 2000. Hydrocarbon gas distribution in mud volcanic deposits of the Gulf of Cadiz. Preliminary results. *Geological Processes on European Continental Margins. International Conference and Eighth Post-cruise Meeting of the Training-Through-Research Programme*, University of Granada, Spain, 31 January - 3 February 2000. IOC Workshop Report, 168, UNESCO, 17.

Terrinha, P. 1998. Structural geology and tectonic evolution of the Algarve Basin, South Portugal. Ph.D. Thesis, Imperial College, London.

Tobias, H. J. and Brenna, J. T. 1997. On-line pyrolysis as a limitless reduction source for high-precision isotopic analysis of organic-derived hydrogen. *Analytical Chemistry*, 69, 3148-3152.

Torrelli, L., Sartori, R., and Zitellini, N. 1997. The giant chaotic body in the Atlantic Ocean of Gibraltar: new results from a deep seismic reflection survey. *Marine and Petroleum Geology*, 14, 125-138

Van Rensbergen, P., Depreiter, D., Ivanov, M. and Shipboard Scientific Party of the TTR-12 Cruise, 2003. El Araiche mud volcano field. In: Kenyon, N.H., Ivanov, M. K., Akhmetzhanov, A. and Akhmanov, G. G. (eds.), *Interdisciplinary geoscience research*

on the North East Atlantic margin, Mediterranean Sea and Mid-Atlantic Ridge. IOC Technical Series, 67, UNESCO, 43-50.

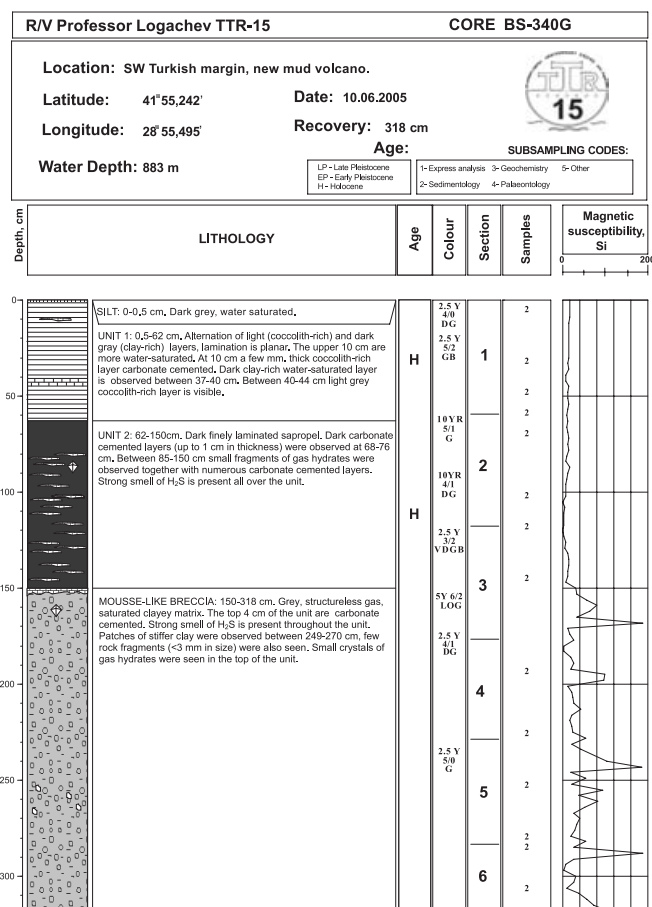
Whiticar, M. J., Faber, E. and Schoell, M. 1986. Biogenic methane formation in marine and freshwater environments: CO₂ reduction versus acetate fermentation- Isotope evidence. *Geochimica et Cosmochimica Acta*, 50, 693-709.

Wilson, R.C.L., Hiscott, M.G. and Gradstein, F.M. 1989. The Lusitanian Basin of West Central Portugal. Mesozoic and Tertiary tectonic, stratigraphy and subsidence history. In: Tankard, A.J. and Balkwill, H.R. (eds.), *Extensional Tectonics and Stratigraphy of the North Atlantic Margins*. AAPG Mem., 46, 341-361.

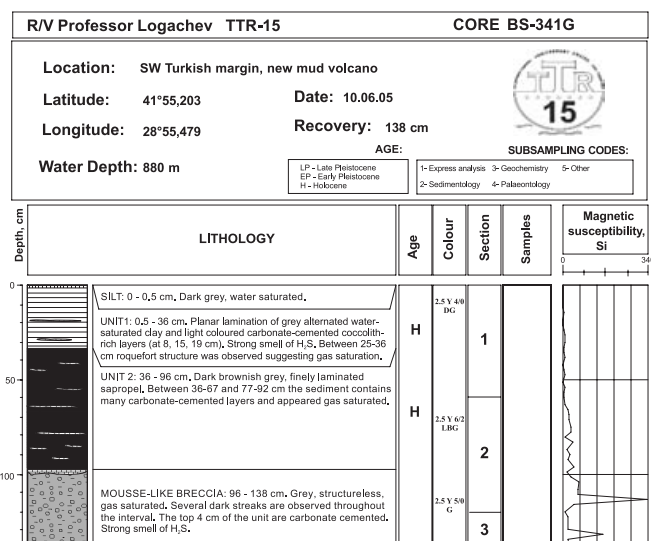
ANNEX I. CORE LOGS

LEGEND			
	Foraminifera rich sediment		corals
	marl		echinoderms
	mud/clay		gastropods
	sand		plant debris
	silt		shell fragments
	turbidite		gas hydrate
	debris flow		drop stones
			others
			lithoclasts
	slump		oxidized layer
	planar lamination		dark layer
	cross lamination		flow in
	gradational boundary		bioturbation
	irregular boundary		burrows
	fault		soupy sediment
	firm ground		
	hard ground		

ANNEX I. CORE LOGS (LEGS 1 and 2, the Black Sea)



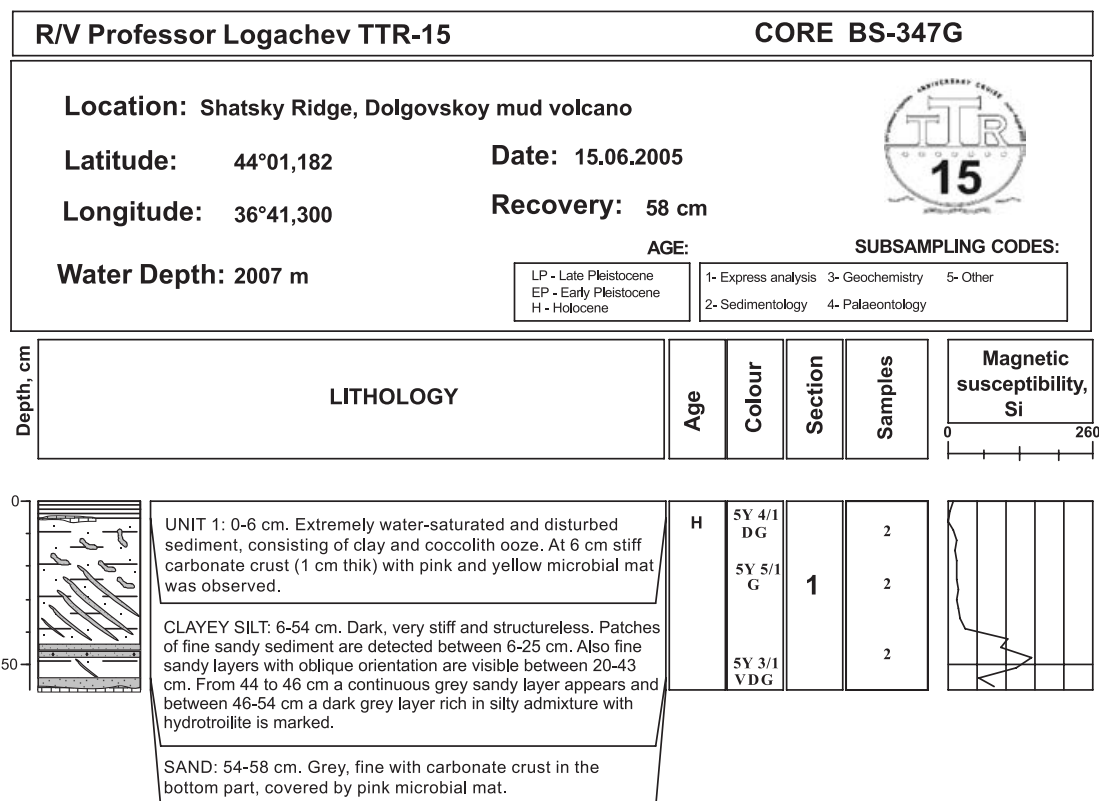
Core log TTR15-BS340G



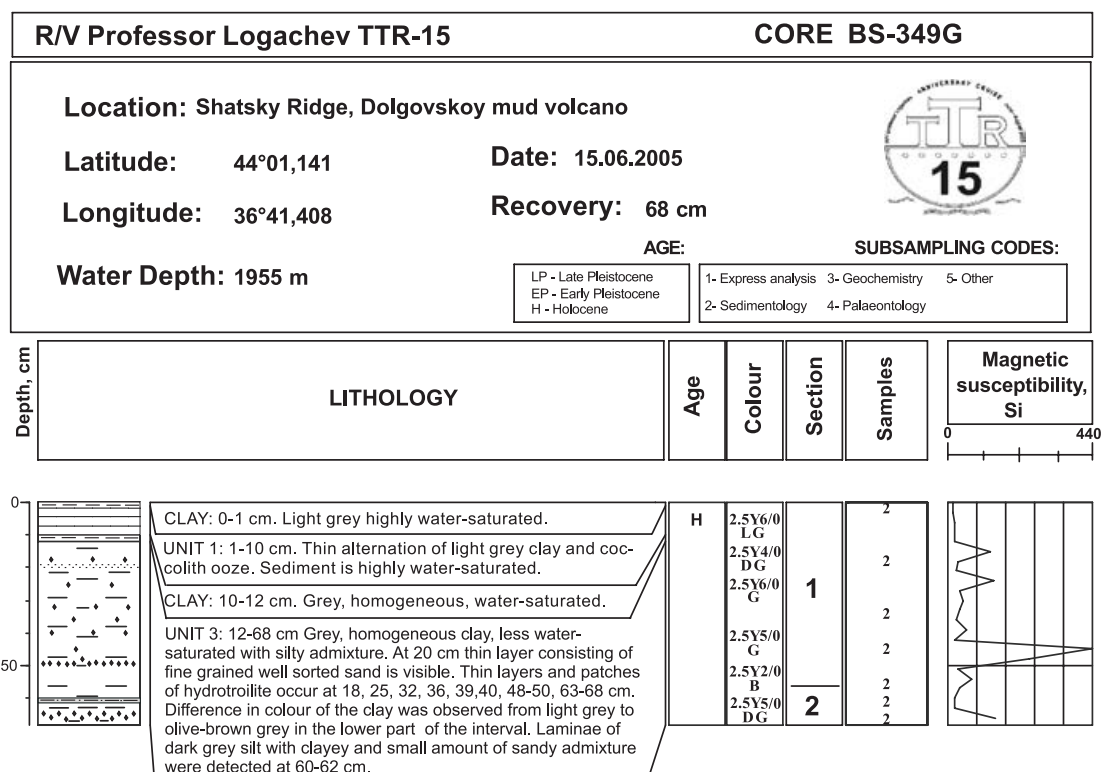
Core log TTR15-BS341G

R/V Professor Logachev TTR-15						CORE BS344G
Location:	NE Black sea, Neftyanoy mud volcano					
Latitude:	44°14,45S		Date:	13.06.2005		
Longitude:	37°27,28E		Recovery:	366 cm		
Water Depth:	1980 m		AGE:			
			LP - Late Pleistocene EP - Early Pleistocene H - Holocene		SUBSAMPLING CODES: 1- Express analysis 3- Geochemistry 5- Other 2- Sedimentology 4- Palaeontology	
Depth, cm	LITHOLOGY	Age	Colour	Section	Samples	Magnetic susceptibility, Si
0-17	UNIT 1: 0-17 cm. Planar lamination of light coccolith-rich layers and grey clay-rich layers. Very small spots of oil are visible in top part of interval.	H	2.5Y 5/0 G	1	2	
17-22	CLAY: 17-22 cm. Grey, very soft, water-saturated, homogeneous, with semilithified clasts (up to 5 mm in size) at the top.		2.5Y 3/3 DOB 2.5Y 5/0 G		2	
22-97	UNIT 2: 22-97 cm. Fine laminated grayish brown sapropel becoming darker towards the bottom. Dark grey, water-saturated, disturbed silty clay layer with clasts of poorly lithified mud stone (up to 8 cm in size) was observed between 27-30 cm. Between 30-40, 59-64 and 89-93 cm layers of grey homogeneous, structureless clay were observed cross cutting the sapropelic unit. They show sharp boundaries. Traces of oil at 37 and 59 cm.	H	2.5Y 3/3 DOB 2.5Y 5/0 G		2	
97-101	CLAY: 97-101 cm. Grey, homogeneous, structureless, with very small amount of silty admixture, same as 30-40, 59-64, 89-93 cm.		2.5Y 3/2 DO 2.5Y 5/0 G	2	2	
101-111	CLASTS-CLAY: 101-111 cm. Dark, water-saturated with clasts of mudstone (up to 7 cm in size) and visible spots of oil.	H	5Y 2.5/2 B 5Y 4/1 DG		2	
111-357	UNIT 3: 111-357 cm. Grey silty clay, darker in colour between 146-161 cm, and lighter in colour between 313-330 cm, vaguely laminated hydrotroillite-rich patches, layers and units are observed at: 132, 159, 202-250, 293, 296, 300, 301, 319, 331, 335, 336, 340, 342, 348, 352 cm. Intervals and patches containing clayey and silty matrix with poorly lithified mudstone clasts (Maicopian?) occur between 102-112, 126, 139, 142, 161, 171, 189-194, 273-281, 302-314, 321-325 cm. These layers shows irregular boundaries and are water saturated. Oil traces are observed between 98-102, 189-194, 273-281. Large clast of siderite (~12 cm in size) was observed at 173-189 cm. Some thin silty layers at 338, 342 and 343 cm.		5Y 5/1 G 10Y R 3/I VDG (clasts-rich clay)	3	2	
			5Y 2.5/1 B		2	
			2.5Y 4/0 DG	5	2	
			2.5Y 5/0 VDG		2	
			2.5Y 4/0 DG		2	
			2.5Y 5/0 VDG	6	2	
			2.5Y 4/0 DG		2	
			2.5Y 5/1 VDG	7	2	
			2.5Y 5/1 VDG		2	
357-366	CLASTS-CLAY: 357-366 cm. Mudstone clasts (varying in size from mm up to 7 cm) in a clayey silty matrix.					

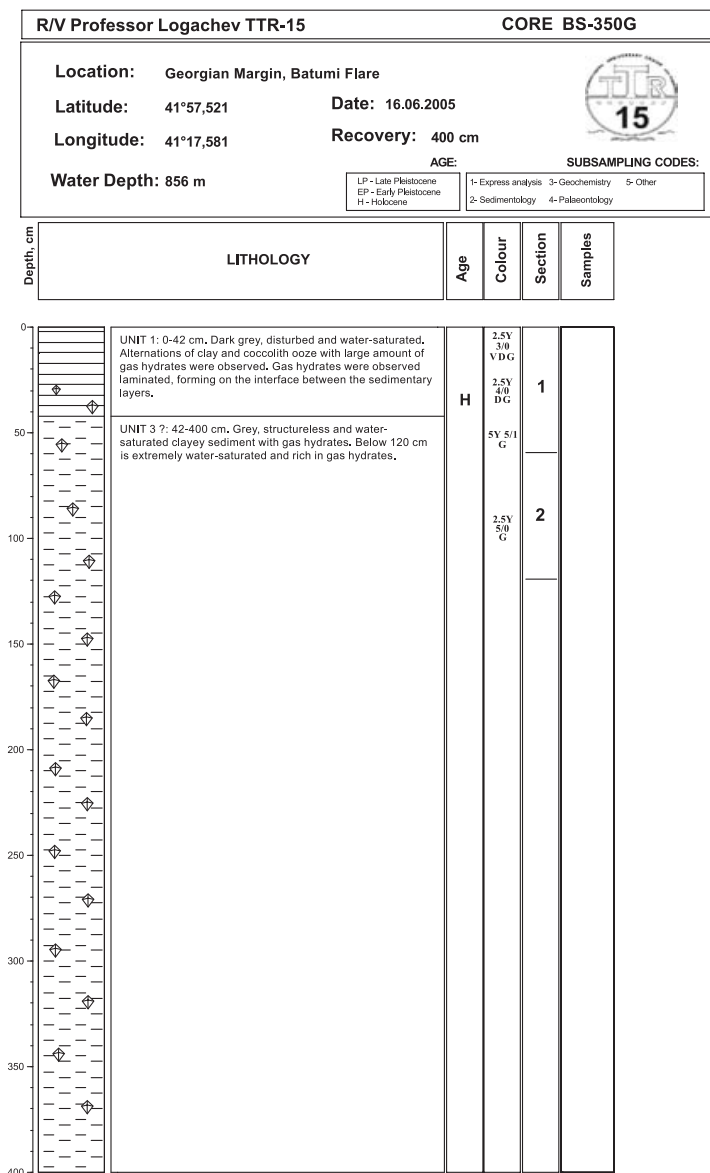
ANNEX I. CORE LOGS (LEGS 1 and 2, the Black Sea)



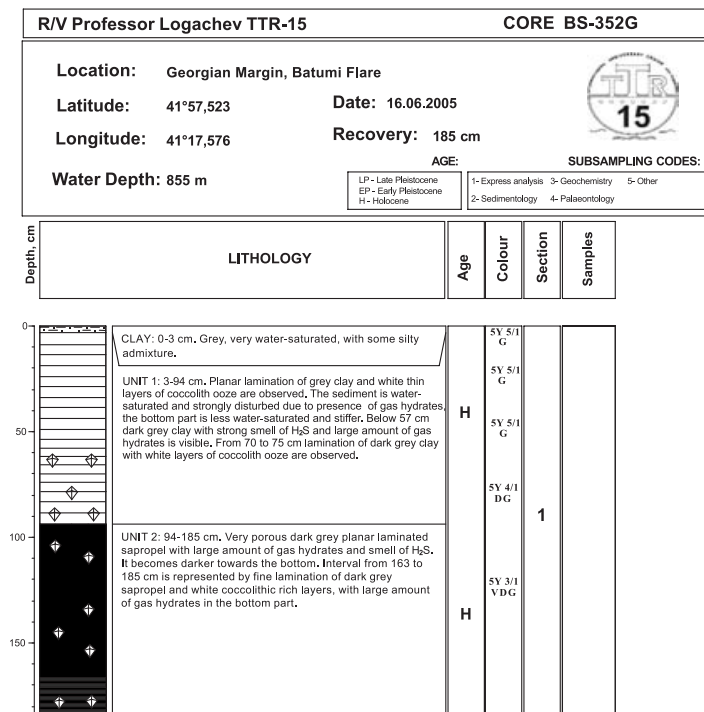
Core log TTR15-BS347G



Core log TTR15-BS349G




Core log TTR15-BS350G



Core log TTR15-BS352G

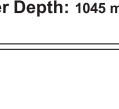
ANNEX I. CORE LOGS (LEGS 1 and 2, the Black Sea)

ANNEX I. CORE LOGS (LEGS 1 and 2, the Black Sea)

R/V Professor Logachev TTR-15				CORE BS-353G			
Location: Georgian Margin, Batumi Flare		Latitude: 41°57,52		Date: 16.06.2005			
Longitude: 41°17,5		Recovery: 310 cm		AGE:			
Water Depth: 855 m		LP - Late Pleistocene EP - Early Pleistocene H - Holocene		SUBSAMPLING CODES:		1- Express analysis 3- Geochemistry 5- Other 2- Sedimentology 4- Palaeontology	
Depth, cm	LITHOLOGY	Age	Colour	Section	Samples		
0-50	UNIT 1: 0-120 cm, Soupy and water-saturated (very disturbed) laminated with coccolith ooze layers mostly between 0-56 cm and 68-70 cm. Wood fragments were detected at 36, 58 cm. No gas hydrates were observed in this unit but evidence of vesicles throughout suggests that they quickly dissociated and could not be observed.	H	5Y 5/1 G				
0-50	UNIT 2: 120-160 cm, Dark grey laminated sapropel, less water-saturated than previous layers. Between 153-160 cm thin lamination of light coccolith ooze is visible.	H	5Y 4/1 DG	1			
0-100	UNIT 3: 160-310 cm, Light grey clay, extremely gas saturated. Large amount of gas hydrates especially in the bottom part. Gas hydrates in this unit were observed as laminae. Moussy texture was observed in this unit.	H	5Y 6/1 LG				


Core log TTR15-BS353G

R/V Professor Logachev TTR-15		CORE BS355G	
Location:	Georgia margin, Pochori oil mound		
Latitude:	41°58,772	Date:	18.06.2005
Longitude:	41°07,588	Recovery:	110 cm
Water Depth:	1045 m	AGE:	SUBSAMPLING CODES:
		LP - Late Pleistocene EP - Early Pleistocene H - Holocene	1- Express analysis 3- Geochemistry 5- Other 2- Sedimentology 4- Paleontology



Depth, cm	LITHOLOGY	Colour	Section	Samples
0		5Y4/1 DG	1	2
2				
50		5Y3/1 VDG	2	2
2				
100				2

Core log TTR15-BS355G

ANNEX I. CORE LOGS (LEGS 1 and 2, the Black Sea)

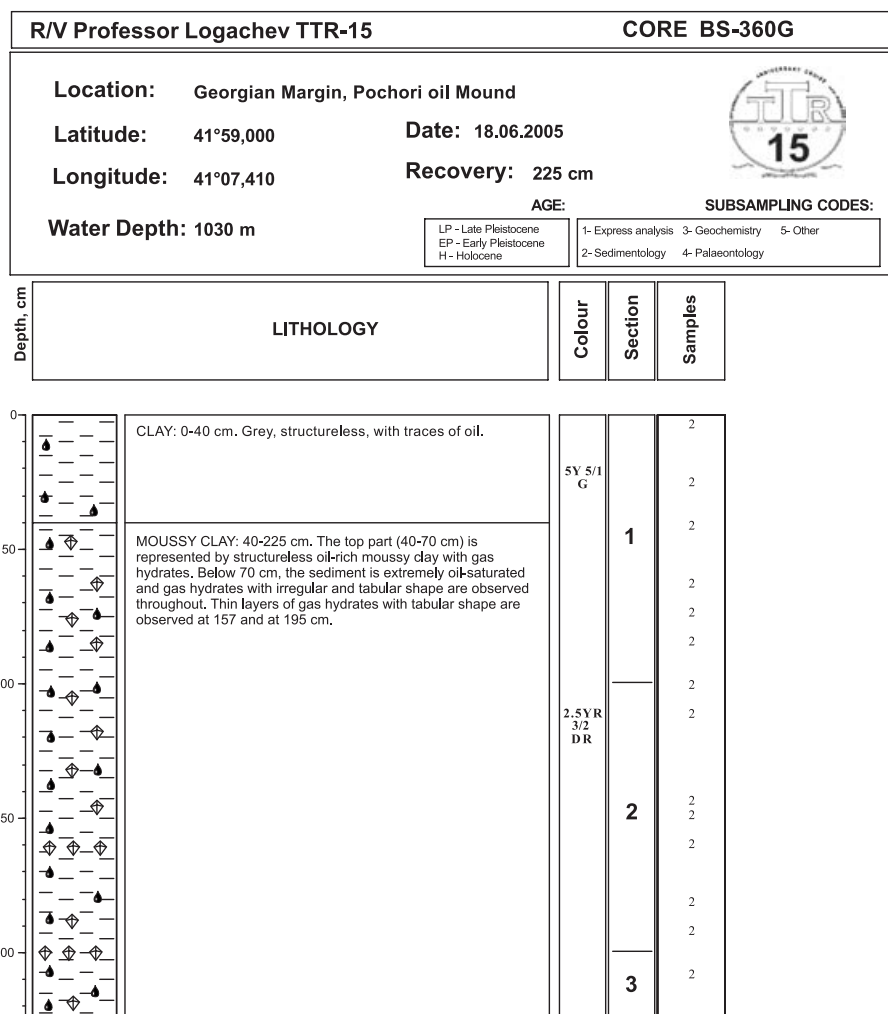
R/V Professor Logachev TTR-15		CORE BS-356G			
Location: Georgian Margin, Pochori oil Mound					
Latitude: 41°59,004	Date: 18.06.2005				
Longitude: 41°07,405	Recovery: 154 cm				
Water Depth: 1033 m	AGE: LP - Late Pleistocene EP - Early Pleistocene H - Holocene	SUBSAMPLING CODES: 1- Express analysis 3- Geochemistry 5- Other 2- Sedimentology 4- Palaeontology			
Depth, cm	LITHOLOGY	Age	Colour	Section	Samples
		H	5Y 5/1 G	1	2
			5Y 5/1 G / 5Y 7/1 LG		2
			5Y 4/2 OG		2
0	UNIT 1: 0-35 cm. Grey clay with traces of oil in the top part. The top 13 cm are soupy and water saturated, in the rest of the unit thin lighter coloured layers of coccolith ooze are observed. In the bottom part planar lamination of grey clay and white coccolith ooze is more prominent.	H	5Y 3/2 DOG	2	2
	UNIT 2 (?): 35-69 cm. Soupy dark clay extremely water and oil-saturated throughout the interval. Large amount of gas hydrates were detected.				2
					2
					UNIT 2: 69-154 cm. Dark laminated sapropel with oil between 69-94 cm. Below 94 cm the texture is mousse and more soupy in the areas where gas hydrates dissociated. Gas hydrates show tabular shape. Towards the bottom faint lamination is visible within the mousse texture.
50					
100					
150					

Core log TTR15-BS356G

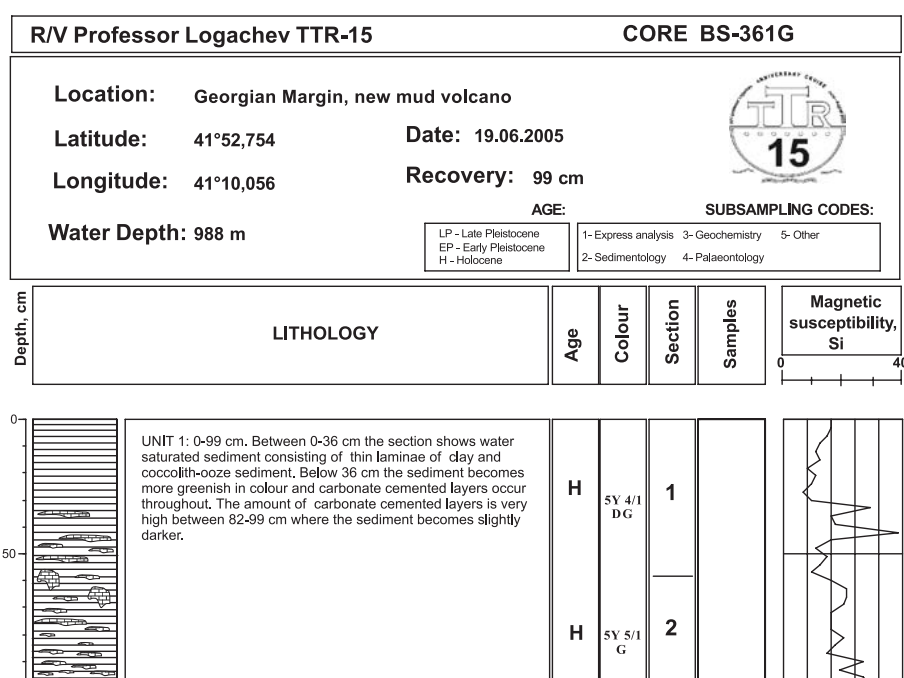
R/V Professor Logachev TTR-15			CORE BS357G			
Location: Georgian margin, Pochori oil Mound, Eastern Black Sea						
Latitude: 41°58,929		Date: 18.06.2005				
Longitude: 41°07,482		Recovery: 20 cm				
Water Depth: 1040 m		AGE:		SUBSAMPLING CODES:		
		LP - Late Pleistocene EP - Early Pleistocene H - Holocene		1- Express analysis 3- Geochemistry 5- Other 2- Sedimentology 4- Palaeontology		
Depth, cm	LITHOLOGY		Age	Colour	Section	Samples
0	 CLAY: 0-15 cm. Soupy, extremely water-, oil- and pore filling gas saturated. UNIT 1: 15-20 CM.Greenish coloured, also gas saturated and very disturbed. Moussy texture with faint layering and gas hydrates		H	5Y4/2 OG 5Y3/1G	1	
20						

Core log TTR15-BS357G

ANNEX I. CORE LOGS (LEGS 1 and 2, the Black Sea)

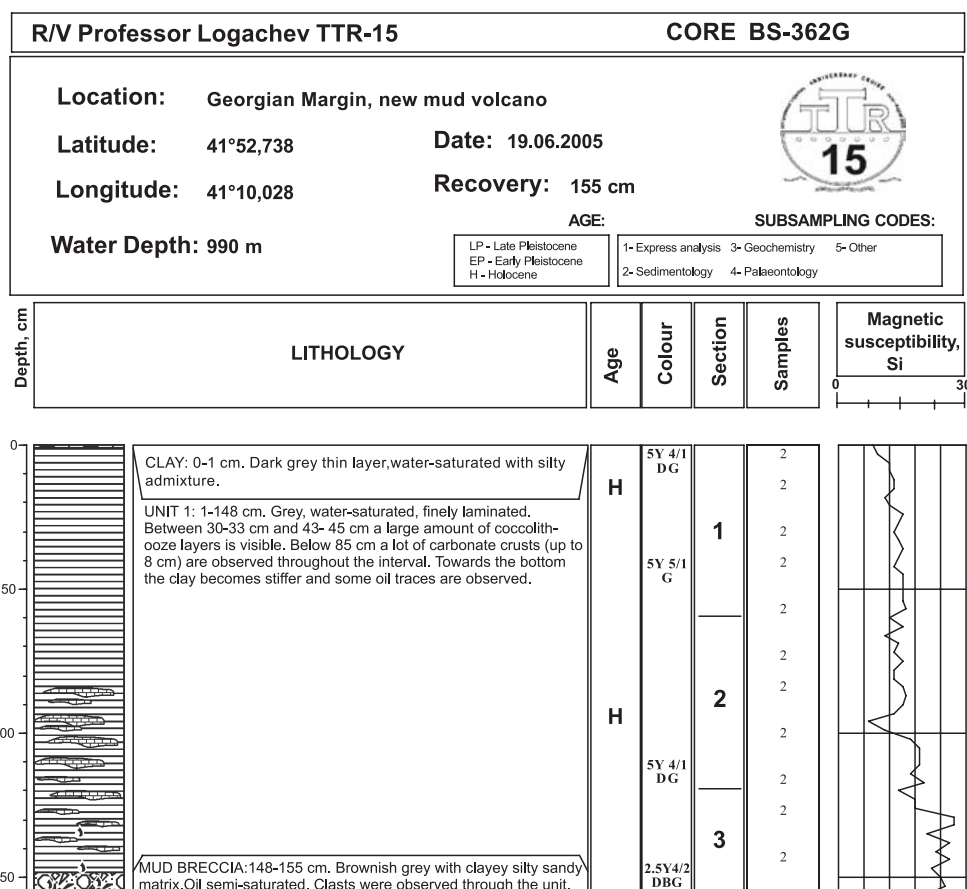


Core log TTR15-BS360G

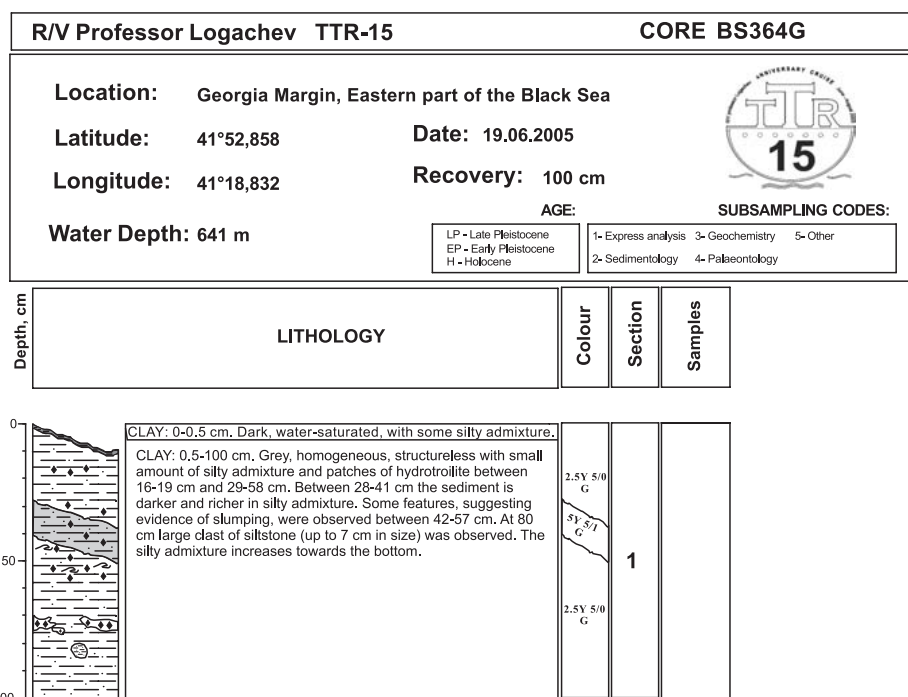


Core log TTR15-BS361G

ANNEX I. CORE LOGS (LEGS 1 and 2, the Black Sea)




Core log TTR15-BS362G



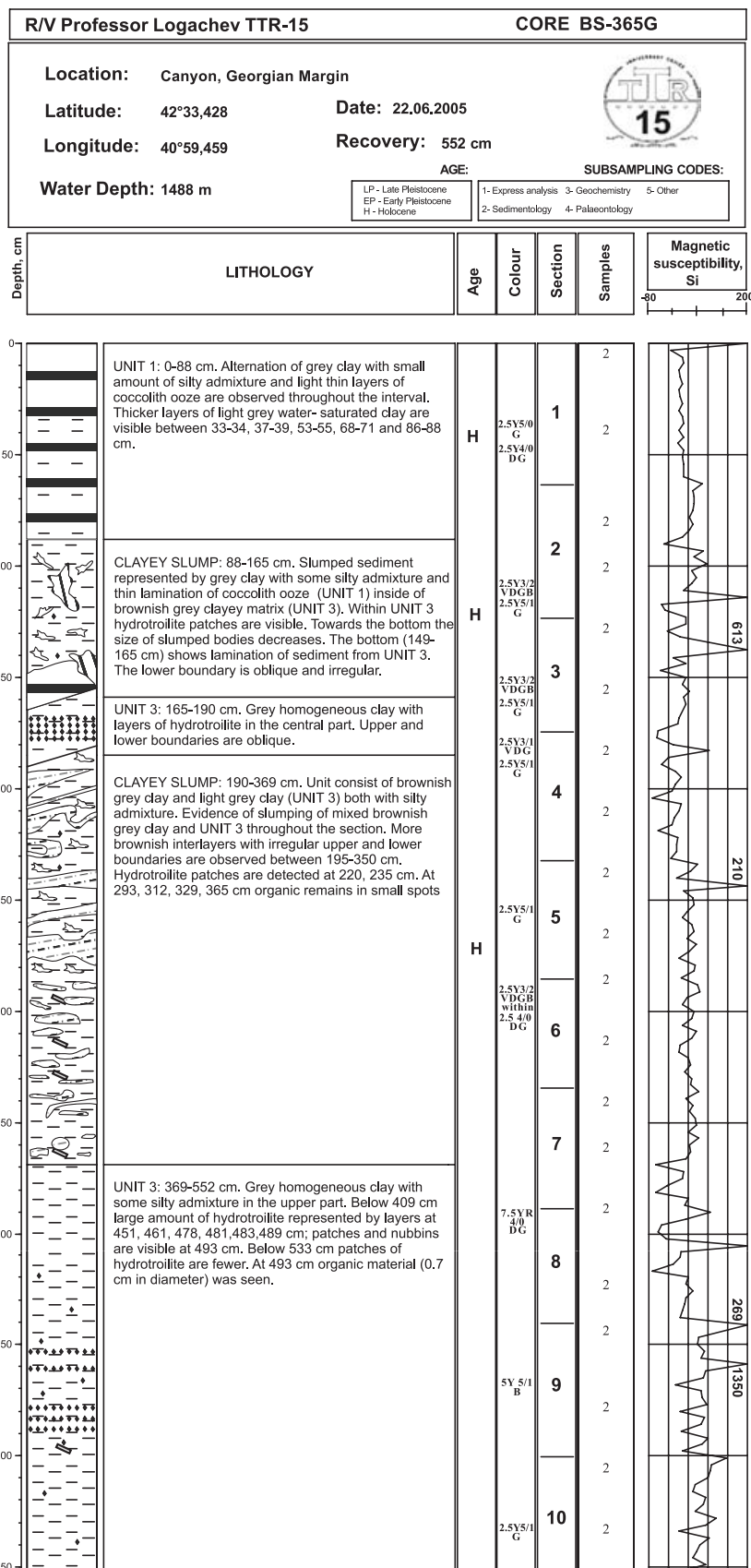
Core log TTR15-BS364G

ANNEX I. CORE LOGS (LEGS 1 and 2, the Black Sea)

R/V Professor Logachev TTR-15			CORE BS363G			
Location: Georgia Margin, Eastern part of the Black Sea						
Latitude: 41°57,256		Date: 19.06.2005				
Longitude: 41°16,734		Recovery: 435 cm				
Water Depth: 888 m		AGE: <div>LP - Late Pleistocene EP - Early Pleistocene H - Holocene</div>		SUBSAMPLING CODES: <div>1- Express analysis 3- Geochemistry 5- Other 2- Sedimentology 4- Palaeontology</div>		
Depth, cm	LITHOLOGY		Age	Colour	Section	Samples
0	<p>Unit 1: 0-107 cm. Planar lamination of grey clay with some silty admixture with white layers of coccolithic ooze. The sediments becomes stiffer towards the bottom.</p>		H	5Y 5/1 grey	1	2
2						
50					2	2
2						
100	<p>Unit 2: 107-163 cm. Dark grey sapropel, planar laminated with some coccolithic rich layers in the lower part, where the colour becomes lighter</p>	H	5Y 4/1 dark grey	2	2	
2						
50				2	2	
2						
100	<p>Unit 3: 163-265 cm. Grey planar laminated clay with silty admixture, with dark patches of hydrotroilite throughout the unit. Some hydrotroilite rich intervals are detected between 181-189, 193-195, 230-235 cm.</p>		2.5Y 4/1 light grey	3	2	
2						
50				2	2	
2						
100	<p>Unit 3: 265-377 cm. Dark stiff silty clay extremely enriched in hydrotroilite with small amount of grey clayey layers. Dark circular shaped feature hydrotroilite-rich (up to 3 cm in size) is visible at 329 cm.</p>		2.5Y 2.5/1 black	4	2	
2						
50				2	2	
2						
100	<p>Unit 3: 377-435 cm. Grey clay with small amount of silty admixture. Dark thin layers and patches of hydrotroilite are visible throughout the interval.</p>		2.5Y 5/1 grey	5	2	
2						
50				2	2	
2						
100					2	
2						

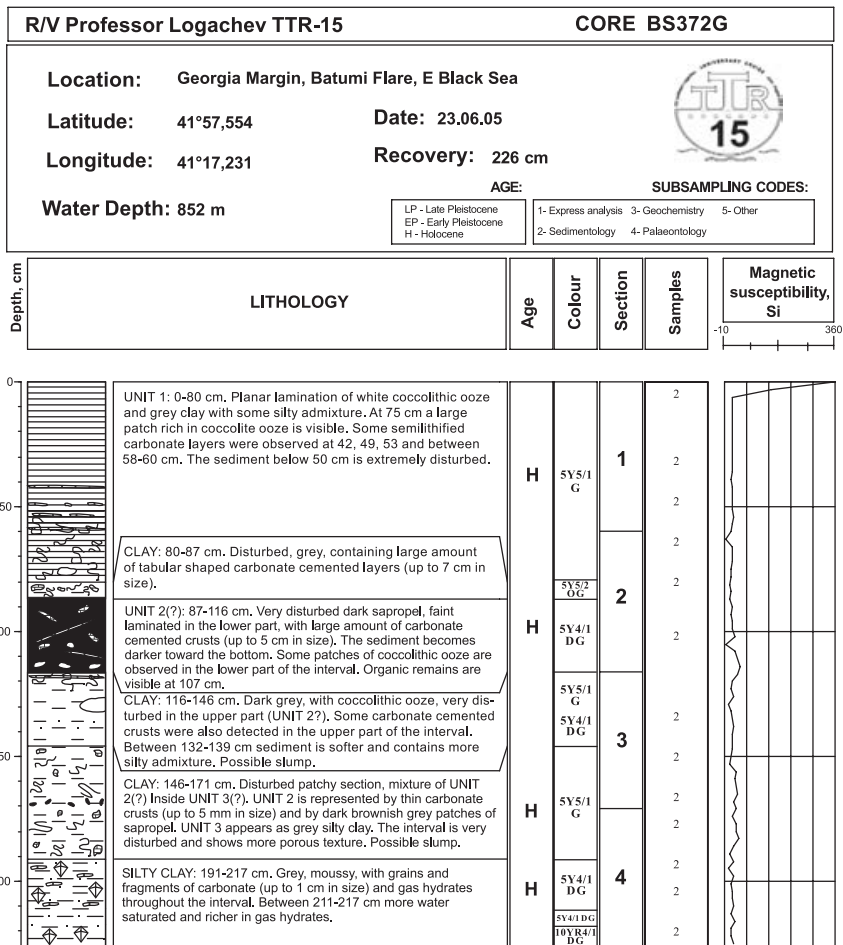
Core log TTR15-BS363G

ANNEX I. CORE LOGS (LEGS 1 and 2, the Black Sea)

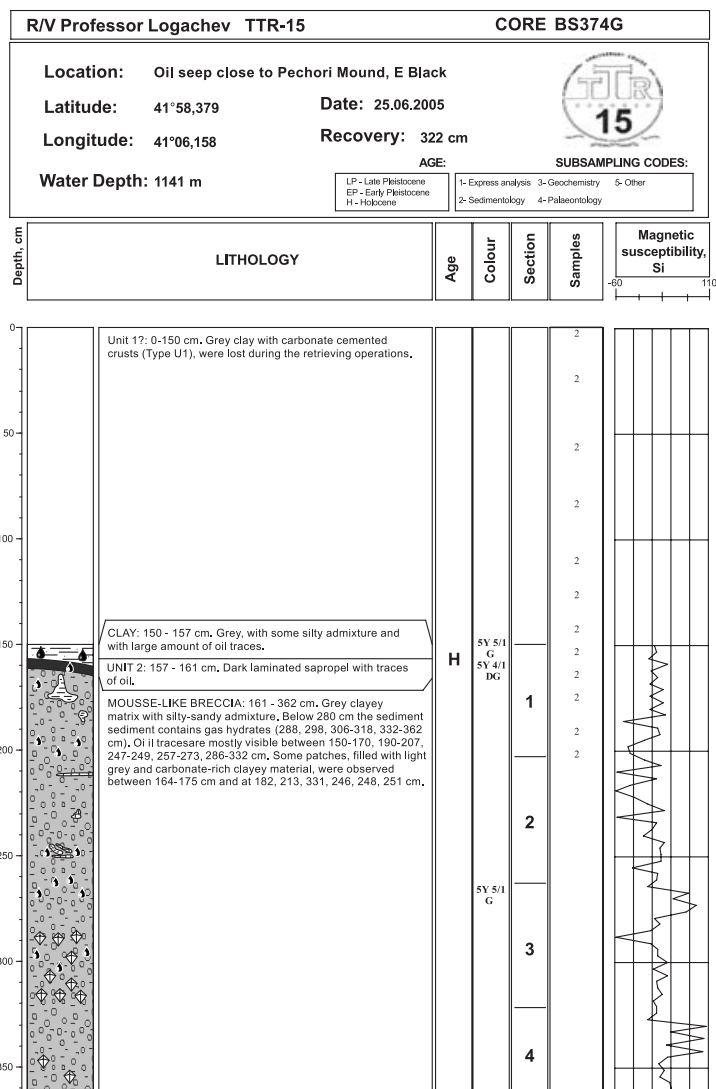


Core log TTR15-BS365G

ANNEX I. CORE LOGS (LEGS 1 and 2, the Black Sea)



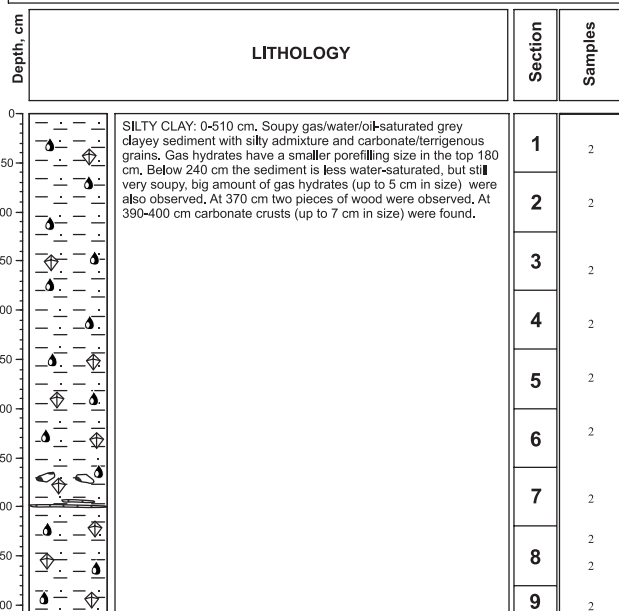
Core log TTR15-BS372G



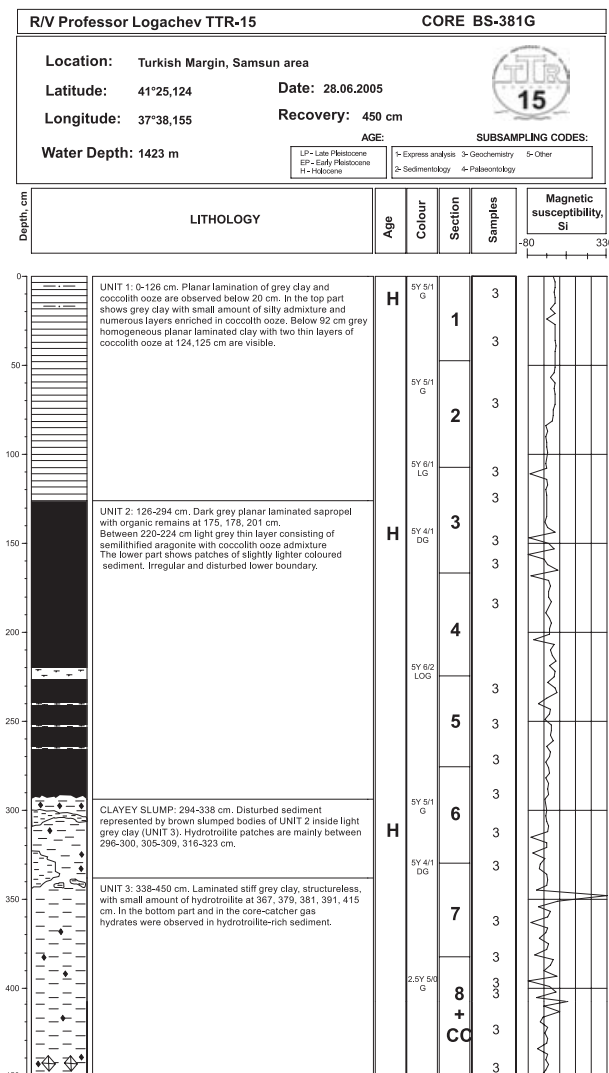
Core log TTR15-BS374G

ANNEX I. CORE LOGS (LEGS 1 and 2, the Black Sea)

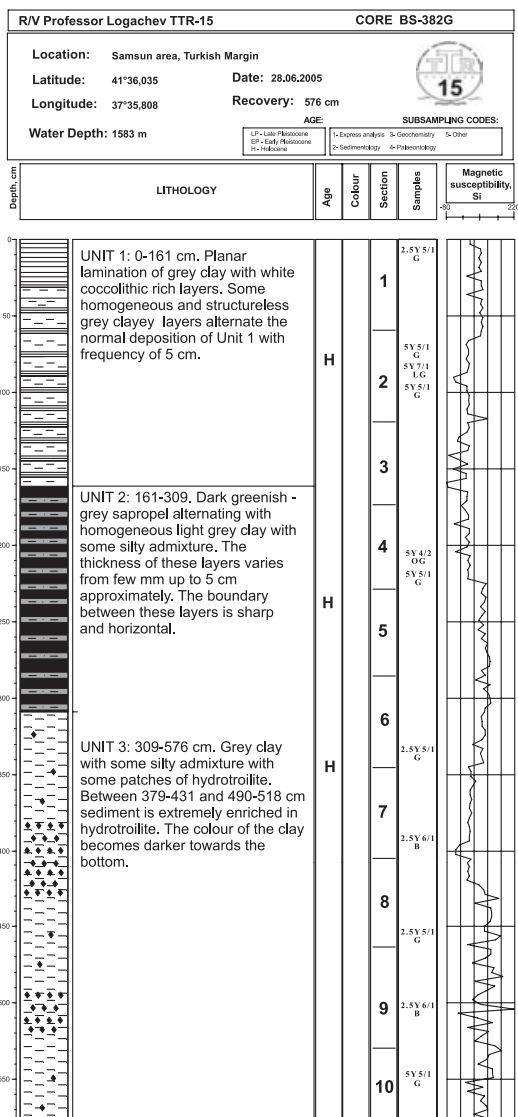
R/V Professor Logachev TTR-15		CORE BS375G	
<div> <div>Location: Oil seep close to Pechori Mound, E Black Sea</div> <div> <div>Latitude: 41°58,159</div> <div>Date: 25.06.2005</div> </div> <div> <div>Longitude: 41°06,207</div> <div>Recovery: 510 cm</div> </div> <div>Water Depth: 1132 m</div> </div> <div> <div>AGE:</div> <div> <div>LP - Late Pleistocene</div> <div>EP - Early Pleistocene</div> <div>H - Holocene</div> </div> </div> <div> <div>SUBSAMPLING CODES:</div> <div> <div>1- Express analysis</div> <div>3- Geochemistry</div> <div>5- Other</div> <div>2- Sedimentology</div> <div>4- Palaeontology</div> </div> </div>			



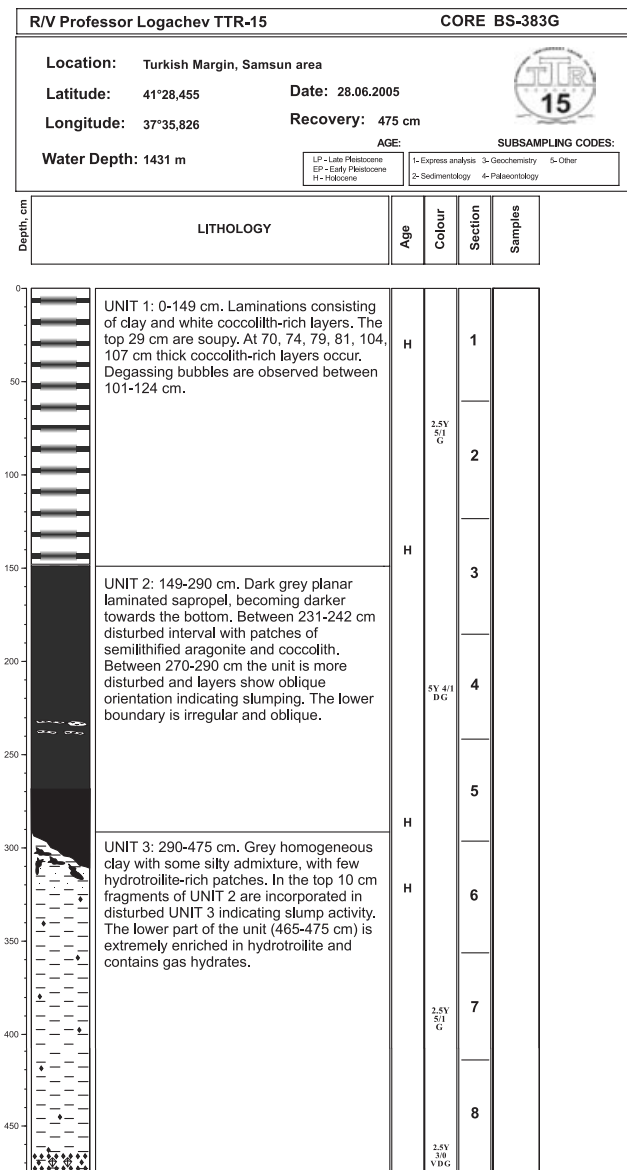
Core log TTR15-BS375G



ANNEX I. CORE LOGS (LEGS 1 and 2, the Black Sea)




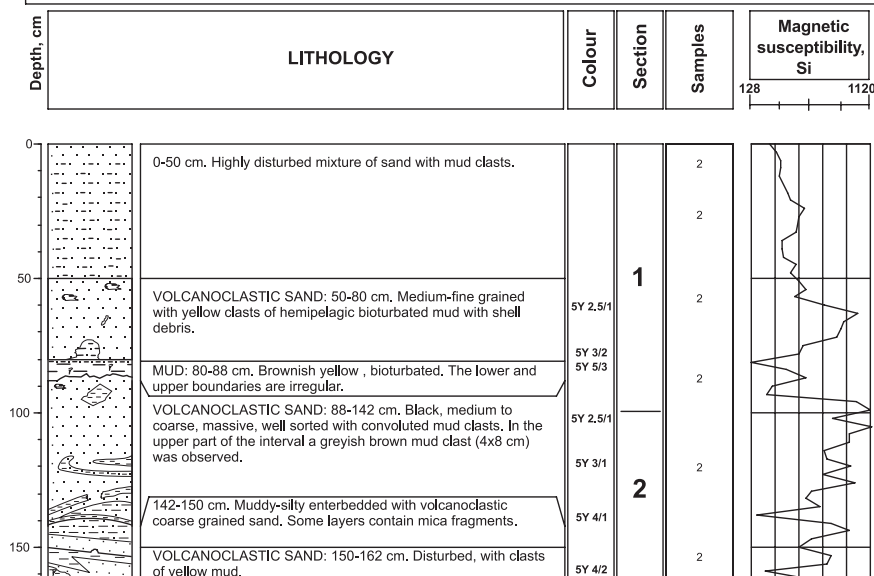
Core log TTR15-BS382G




Core log TTR15-BS383G

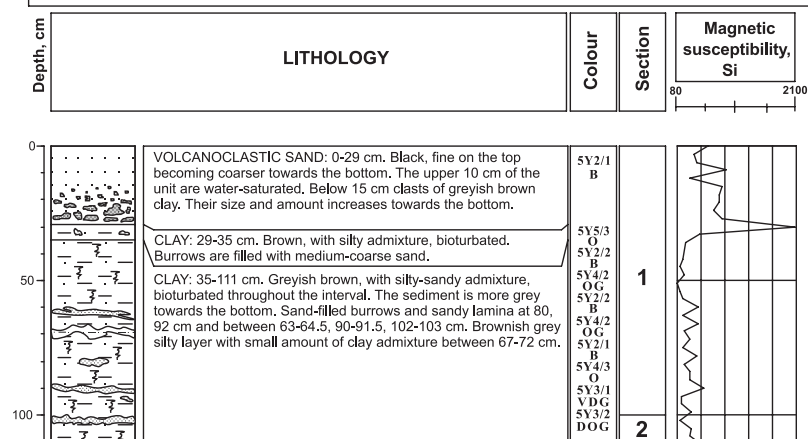
ANNEX I. CORE LOGS (LEG 3, the Tyrrhenian Sea)

R/V Professor Logachev TTR-15	CORE MS349V
Location: NW submarine slope of Stromboli volcano Latitude: 39°02,008 Date: 7.07.2005 Longitude: 15°10,880 Recovery: 162 cm Water Depth: 2508 m	
 SUBSAMPLING CODES: 1- Express analysis 3- Geochemistry 5- Other 2- Sedimentology 4- Palaeontology	





Core log TTR15-MS349V

R/V Professor Logachev TTR-15	CORE MS351V
Location: NW submarine slope of Stromboli volcano Latitude: 39°02,009 Date: 8.07.2005 Longitude: 15°10,881 Recovery: 111 cm Water Depth: 2508 m	
	


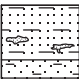



Core log TTR15-MS351V


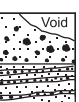
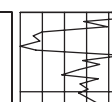
ANNEX I. CORE LOGS (LEG 3, the Tyrrhenian Sea)

R/V Professor Logachev TTR-15		CORE MS350V	
<div style="display: flex; justify-content: space-between;"> <div> Location: NW submarine slope of Stromboli volcano Latitude: 39°01,021 Longitude: 15°09,306 Water Depth: 2505 m </div> <div> Date: 7.07.2005 Recovery: 10 cm </div> <div style="text-align: center;">  </div> </div>			
Depth, cm	LITHOLOGY	Colour	Section
0 10	 <p>CLAY: 0-10 cm. Grey, with sandy-silty admixture. Small amount of black fine volcanoclastic sand was observed at the top of the unit. Sediment becomes darker towards the bottom.</p>	10YR 4/2 10YR 4/1	1

Core log TTR15-MS350V


R/V Professor Logachev TTR-15		CORE MS355K	
<div style="display: flex; justify-content: space-between;"> <div> Location: NW submarine slope of Stromboli volcano Latitude: 39°02,374 Longitude: 15°10,831 Water Depth: 2512 m </div> <div> Date: 9.07.2005 Recovery: 33 cm </div> <div style="text-align: center;">  </div> </div>			
Depth, cm	LITHOLOGY	Colour	Section
0 30	 <p>SILTY SANDY CLAY: 0-22 cm. Grey, water-saturated at the top. Burrows filled with fine dark grey water-saturated sand at 14, 17 cm.</p> <p>SAND: 22-29 cm. Dark grey, fine-medium, with admixture of clay.</p> <p>SAND: 29-33 cm. Dark greyish brown, medium-coarse with small amount of silty-clay admixture.</p>	2.5Y5/2 GB 5Y5/2 (DGC (grey) 5Y5/2 5Y4/2 5Y4/1 5Y4/1	1
			<div style="border: 1px solid black; padding: 2px;">Magnetic susceptibility, Si</div> <div style="text-align: center;">100 — 800</div> 

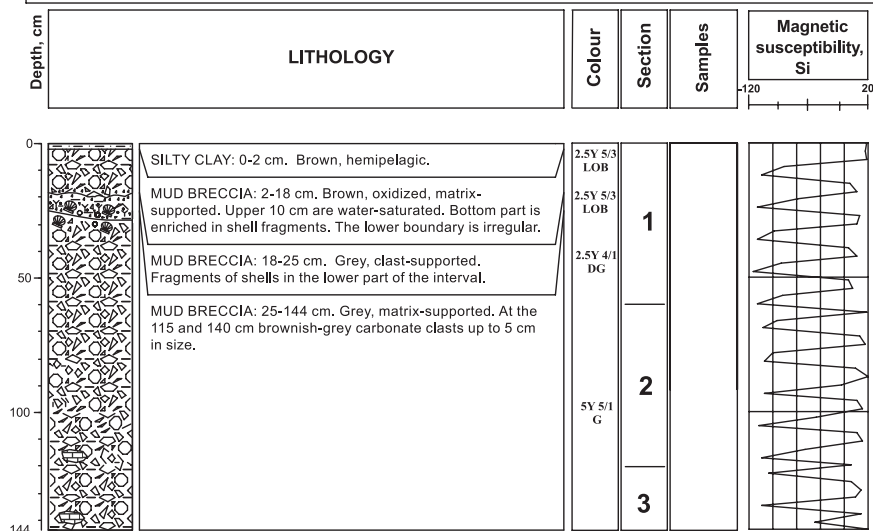
Core log TTR15-MS355K


R/V Professor Logachev TTR-15		CORE MS361GR	
<div style="display: flex; justify-content: space-between;"> <div> Location: NW submarine slope of Stromboli volcano Latitude: 38°51,451 Longitude: 15°10,796 Water Depth: 1741 m </div> <div> Date: 10.07.2005 Recovery: 59 cm </div> <div style="text-align: center;">  </div> </div>			
SUBSAMPLING CODES: 1- Express analysis 3- Geochemistry 5- Other 2- Sedimentology 4- Palaeontology			
Depth, cm	LITHOLOGY	Section	Samples
0 50	 <p>VOLCANOCLASTIC SAND: 0-32 cm. Black, fine to coarse, with fragments of volcanic rocks up to 3 cm in size. Upper part of the interval is highly disturbed.</p> <p>VOLCANOCLASTIC SAND: 32-59 cm. Black, fine to coarse, with vague parallel bedding. Sandy layers coarser in grain-size are observed throughout the unit. Fragments of scoria and lava were found in the lower part of the interval.</p>	1 3 3 3 3 3	1
			<div style="border: 1px solid black; padding: 2px;">Magnetic susceptibility, Si</div> <div style="text-align: center;">240 — 850</div> 

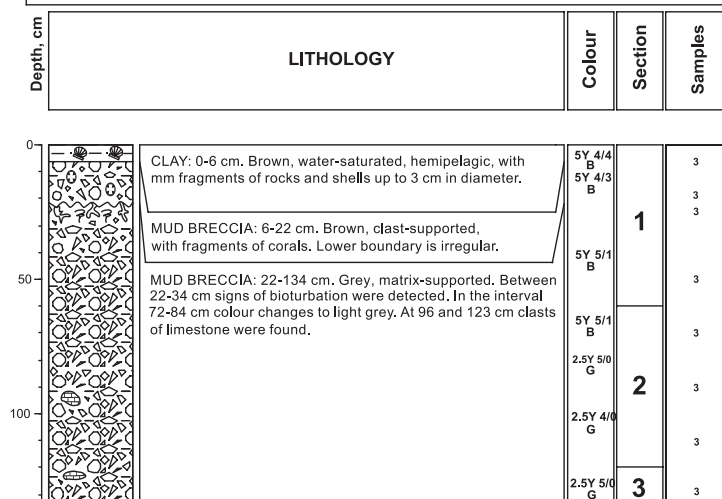
Core log TTR15-MS361Gr

ANNEX I. CORE LOGS (LEG 4, the Gulf of Cadiz)


R/V Professor Logachev TTR-15	CORE AT567G
Location: Moroccan margin, Mercator mud volcano Latitude: 35°17,920 Date: 24.07.2000 Longitude: 06°38,716 Recovery: 144 cm Water Depth: 358 m	
	
SUBSAMPLING CODES: 1- Express analysis 3- Geochemistry 5- Other 2- Sedimentology 4- Palaeontology	

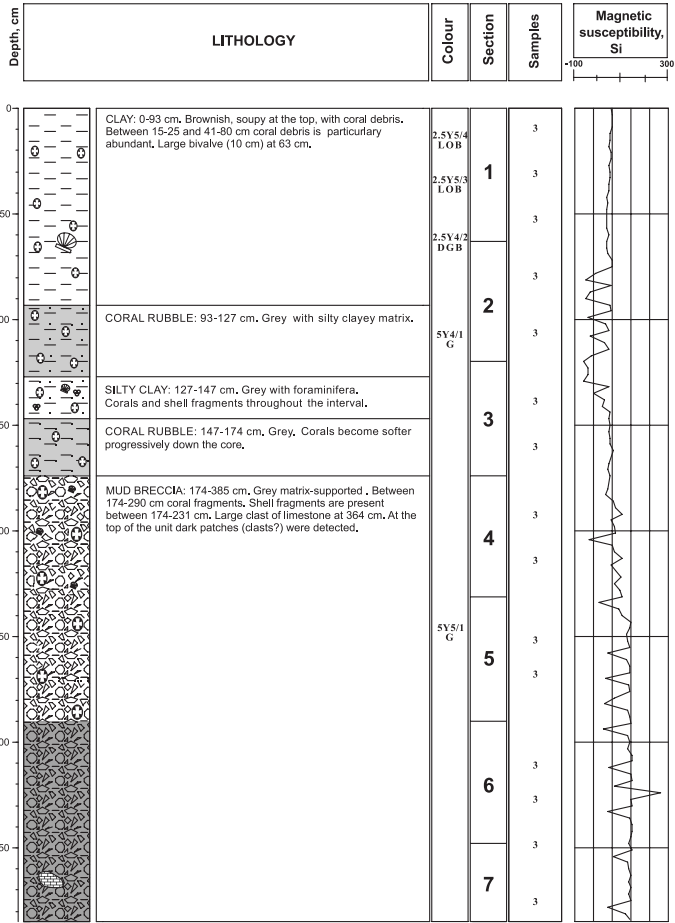
*Core log TTR15-AT567G*

R/V Professor Logachev TTR-15	CORE AT568G
Location: Moroccan margin, SW slope of Mercator mud volcano Latitude: 35°17,684 Date: 25.07.05 Longitude: 6°39,131 Recovery: 134 cm Water Depth: 418 m	
	
SUBSAMPLING CODES: 1- Express analysis 3- Geochemistry 5- Other 2- Sedimentology 4- Palaeontology	


*Core log TTR15-AT568G*

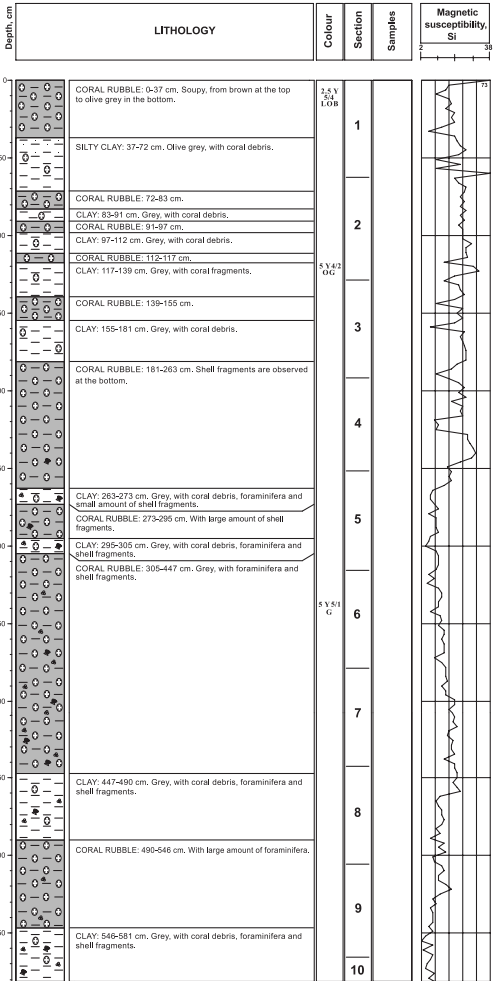
ANNEX I. CORE LOGS (LEG 4, the Gulf of Cadiz)

R/V Professor Logachev TTR-15		CORE AT570G	
<div>Location: Moroccan margin, Pen Duick escarpment</div> <div>Latitude: 35°17,406 Date: 25.07.2005</div> <div>Longitude: 06°46,996 Recovery: 385 cm</div> <div>Water Depth: 580 m</div>			
<div><div></div><div>SUBSAMPLING CODES: 1-Express analysis 3-Geochemistry 5-Other 2-Sedimentology 4-Paleontology</div></div>			




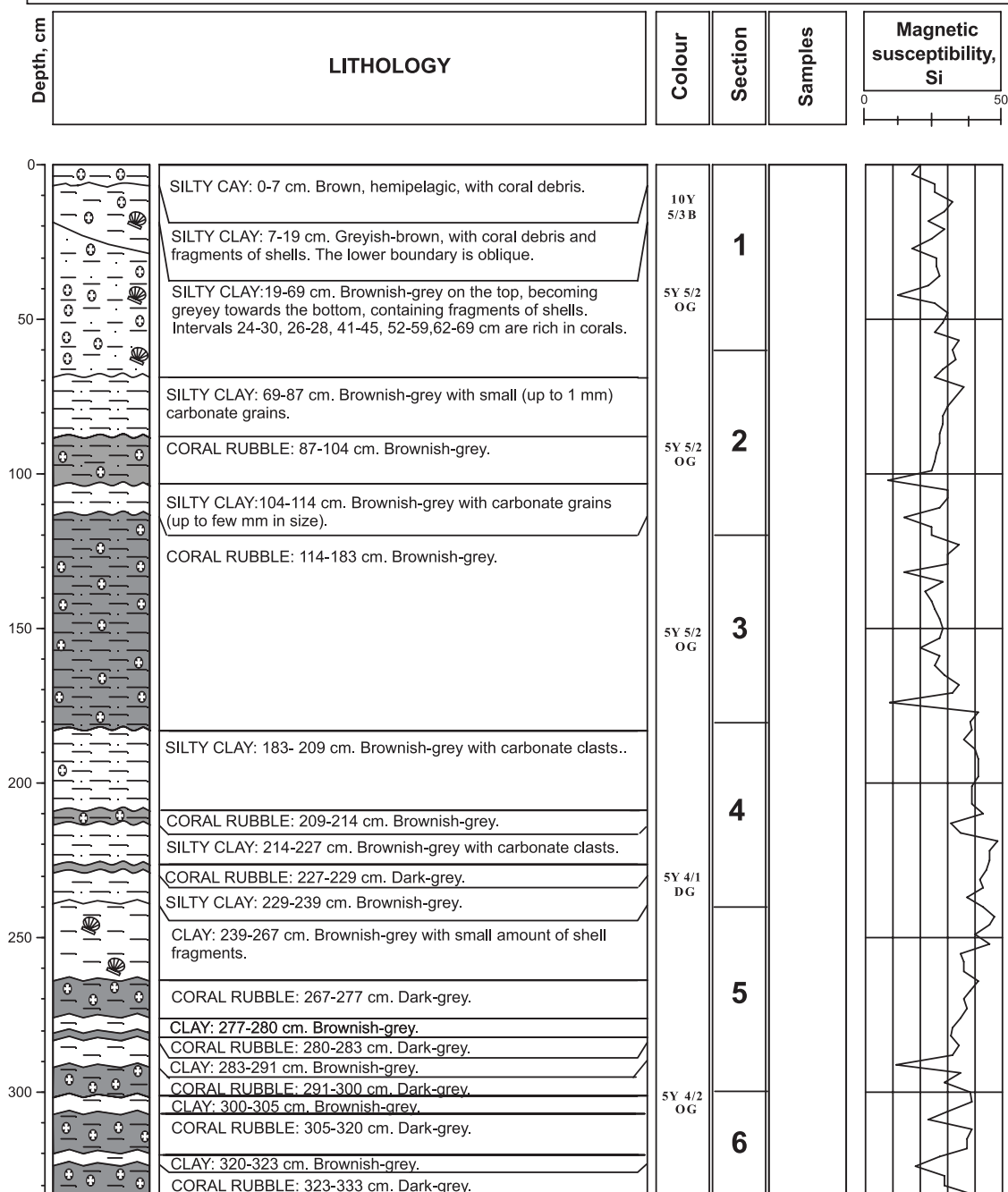
Core log TTR15-AT570G

R/V Professor Logachev TTR-15		CORE AT571G	
<div>Location: Moroccan margin, Renard ridge</div> <div>Latitude: 35°21,968 Date: 25.07.2005</div> <div>Longitude: 06°51,920 Recovery: 581 cm</div> <div>Water Depth: 580 m</div>			
<div><div></div><div>SUBSAMPLING CODES: 1-Express analysis 3-Geochemistry 5-Other 2-Sedimentology 4-Paleontology</div></div>			




ANNEX I. CORE LOGS (LEG 4, the Gulf of Cadiz)

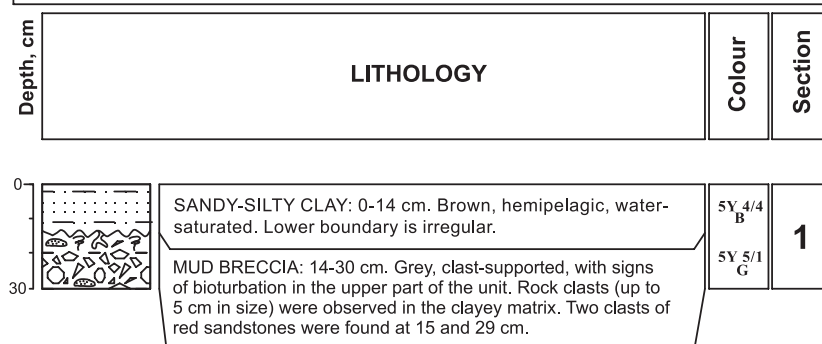
R/V Professor Logachev TTR-15		CORE AT572G							
<div style="display: flex; justify-content: space-between;"> <div> <p>Location: Moroccan margin, Renard ridge</p> <p>Latitude: 35°22,040 Date: 25.07.2005</p> <p>Longitude: 06°53,985 Recovery: 333 cm</p> <p>Water Depth: 712 m</p> </div> <div style="text-align: right;">  </div> </div> <div style="text-align: right; margin-top: 10px;"> SUBSAMPLING CODES: <table border="1" style="display: inline-table; border-collapse: collapse;"> <tr> <td>1- Express analysis</td> <td>3- Geochemistry</td> <td>5- Other</td> </tr> <tr> <td>2- Sedimentology</td> <td>4- Palaeontology</td> <td></td> </tr> </table> </div>				1- Express analysis	3- Geochemistry	5- Other	2- Sedimentology	4- Palaeontology	
1- Express analysis	3- Geochemistry	5- Other							
2- Sedimentology	4- Palaeontology								




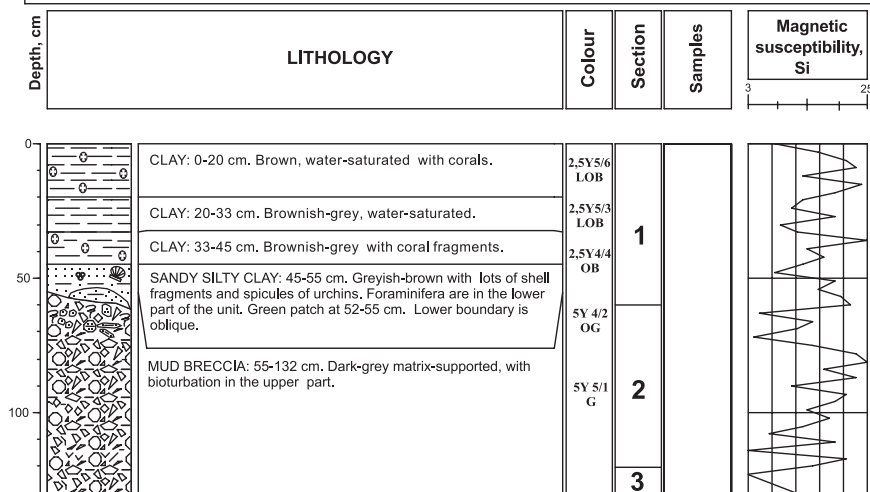
Core log TTR15-AT572G

ANNEX I. CORE LOGS (LEG 4, the Gulf of Cadiz)

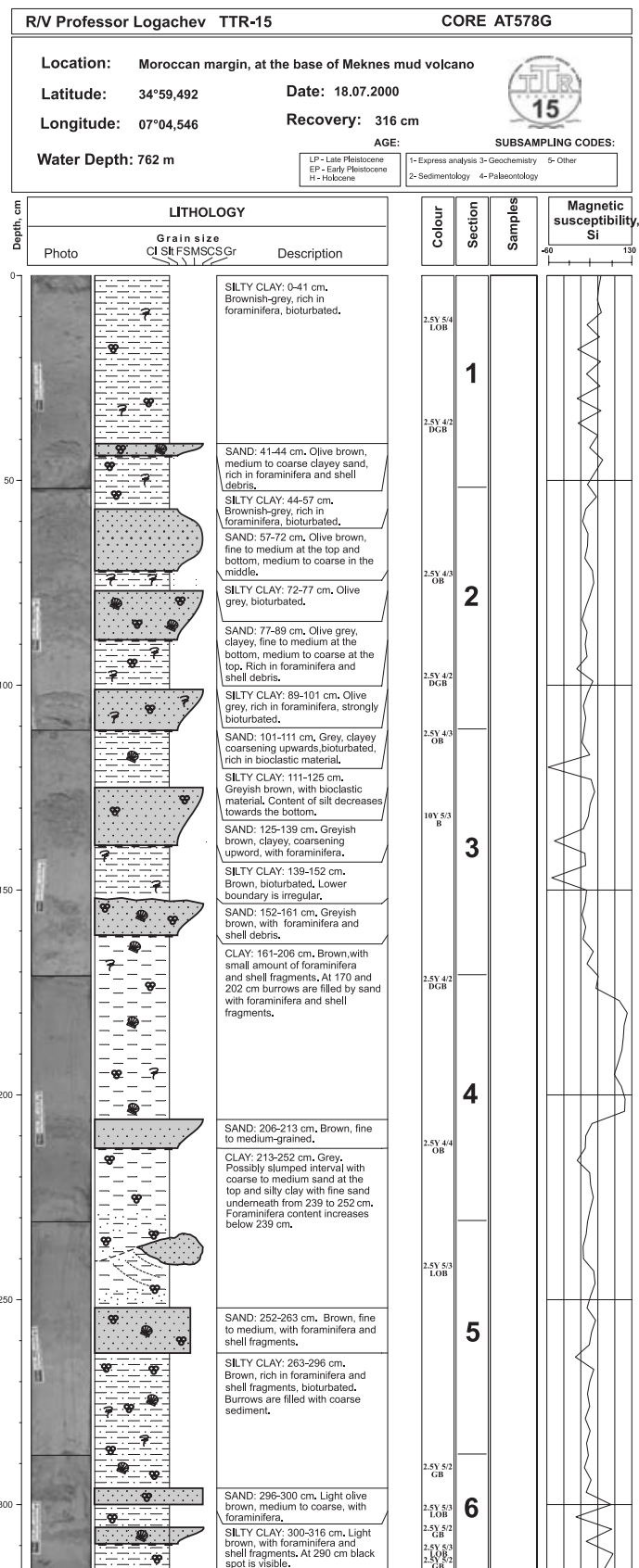
R/V Professor Logachev TTR-15	CORE AT573G
<div style="display: flex; justify-content: space-between;"> <div> <p>Location: Moroccan margin, top of Adamastor mud volcano</p> <p>Latitude: 35°21,768</p> <p>Longitude: 06°45,543</p> <p>Water Depth: 499 cm</p> </div> <div> <p>Date: 25.07.2005</p> <p>Recovery: 30 cm</p> </div> <div style="text-align: center;">  </div> </div>	

*Core log TTR15-AT573G*

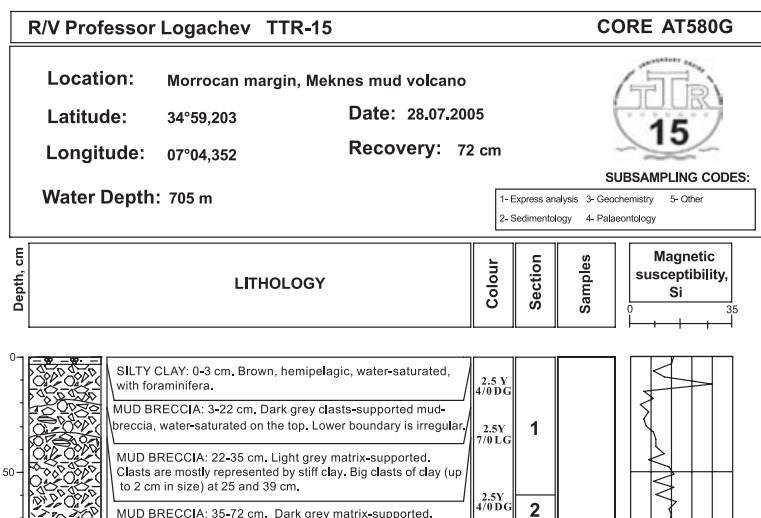
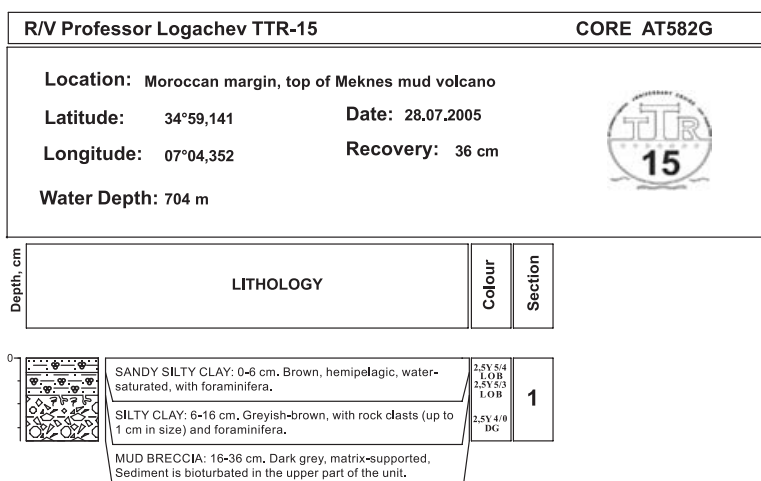
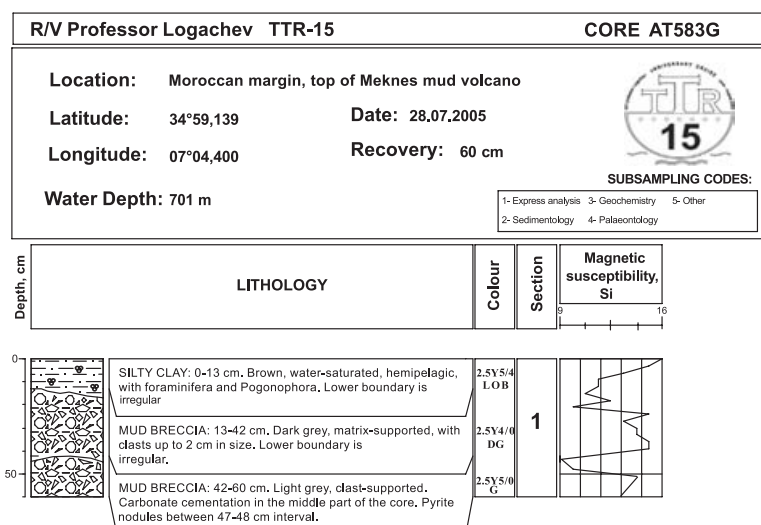
R/V Professor Logachev TTR-15	CORE AT579G						
<div style="display: flex; justify-content: space-between;"> <div> <p>Location: Moroccan margin, slope of Meknes mud volcano.</p> <p>Latitude: 34°59,301</p> <p>Longitude: 07°04,464</p> <p>Water Depth: 747 m</p> </div> <div> <p>Date: 28.07.2005</p> <p>Recovery: 132 cm</p> </div> <div style="text-align: center;">  </div> </div>							
<p style="text-align: right; margin: 0;">SUBSAMPLING CODES:</p> <table style="width: 100%; font-size: 0.8em;"> <tr> <td>1- Express analysis</td> <td>3- Geochemistry</td> <td>5- Other</td> </tr> <tr> <td>2- Sedimentology</td> <td>4- Palaeontology</td> <td></td> </tr> </table>		1- Express analysis	3- Geochemistry	5- Other	2- Sedimentology	4- Palaeontology	
1- Express analysis	3- Geochemistry	5- Other					
2- Sedimentology	4- Palaeontology						

*Core log TTR15-AT579G*

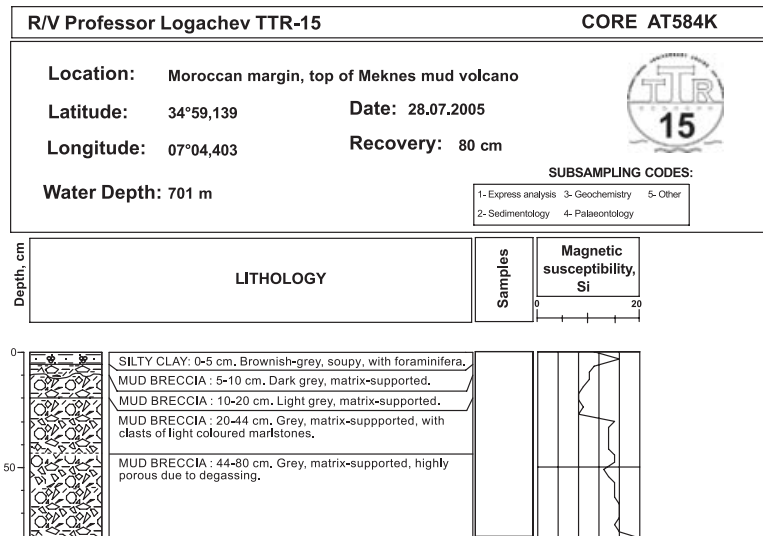
ANNEX I. CORE LOGS (LEG 4, the Gulf of Cadiz)



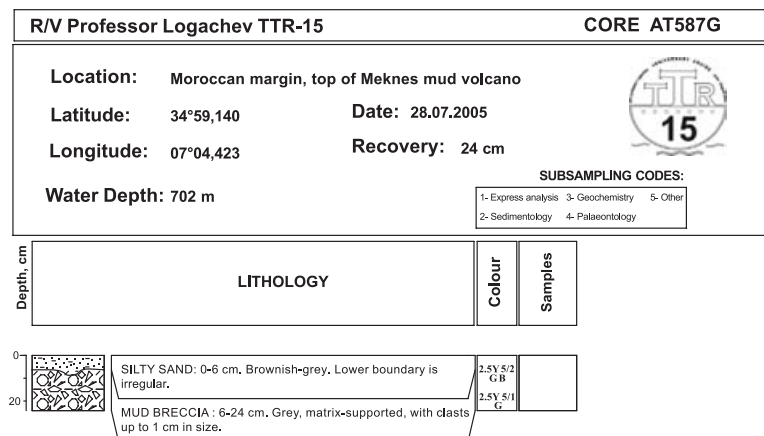
Core log TTR15-AT578G

ANNEX I. CORE LOGS (LEG 4, the Gulf of Cadiz)*Core log TTR15-AT580G**Core log TTR15-AT582G**Core log TTR15-AT583G*

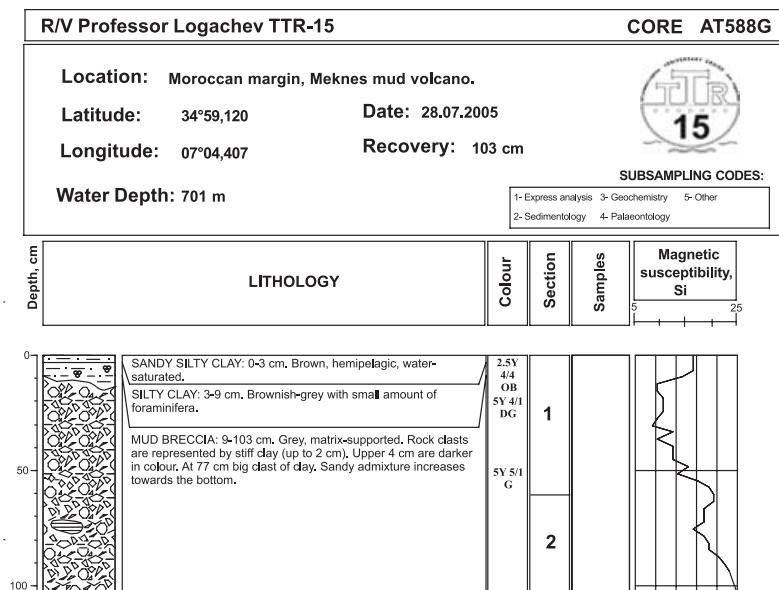
ANNEX I. CORE LOGS (LEG 4, the Gulf of Cadiz)



Core log TTR15-AT584K.



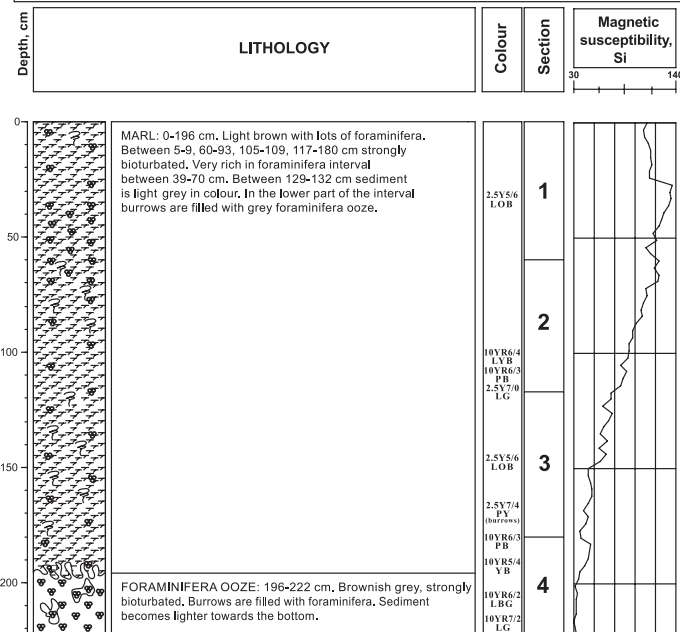
Core log TTR15-AT587G



Core log TTR15-AT588G

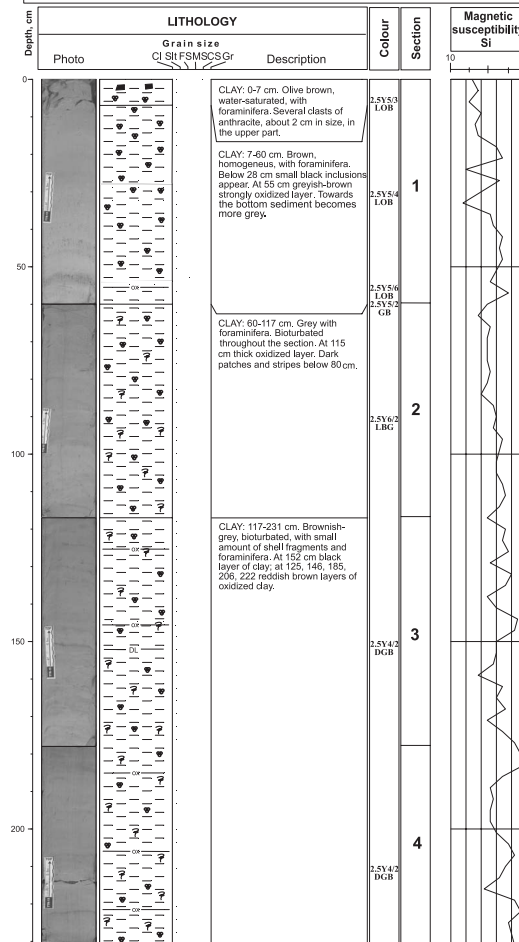
ANNEX I. CORE LOGS (LEG 4, the Gulf of Cadiz)

R/V Professor Logachev TTR-15		CORE AT589G
<p>Location: Moroccan margin, top of a seabed hill</p> <p>Latitude: 35°26,352 Date: 30.07.2005</p> <p>Longitude: 07°28,663 Recovery: 222 cm</p> <p>Water Depth: 1270 m</p>		

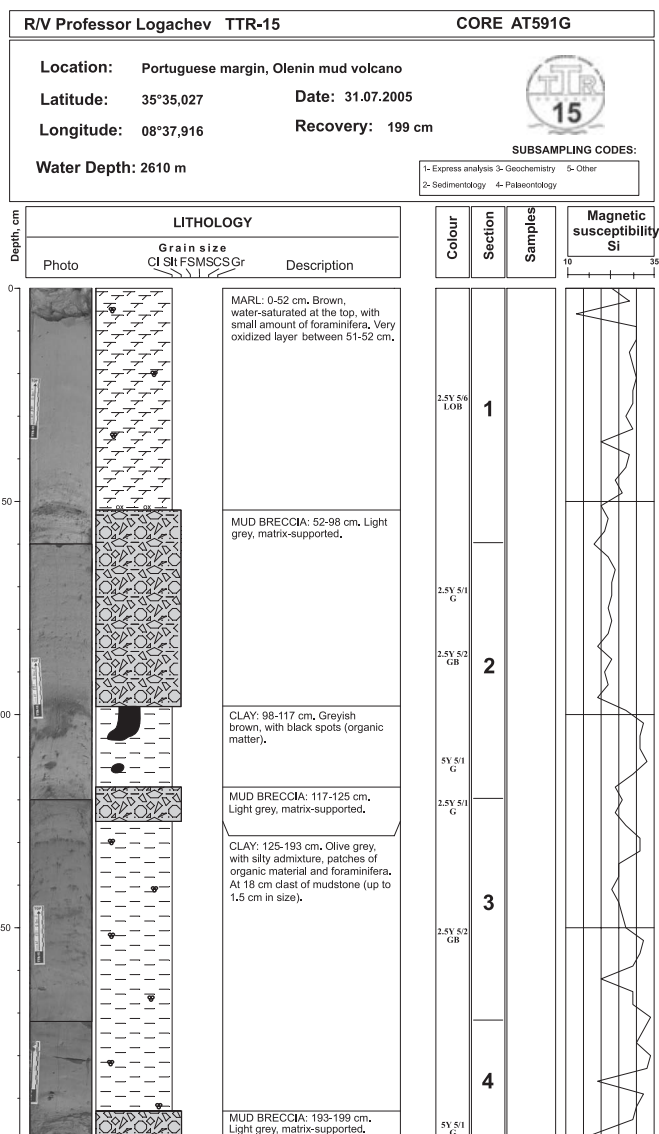


Core log TTR15-AT589G

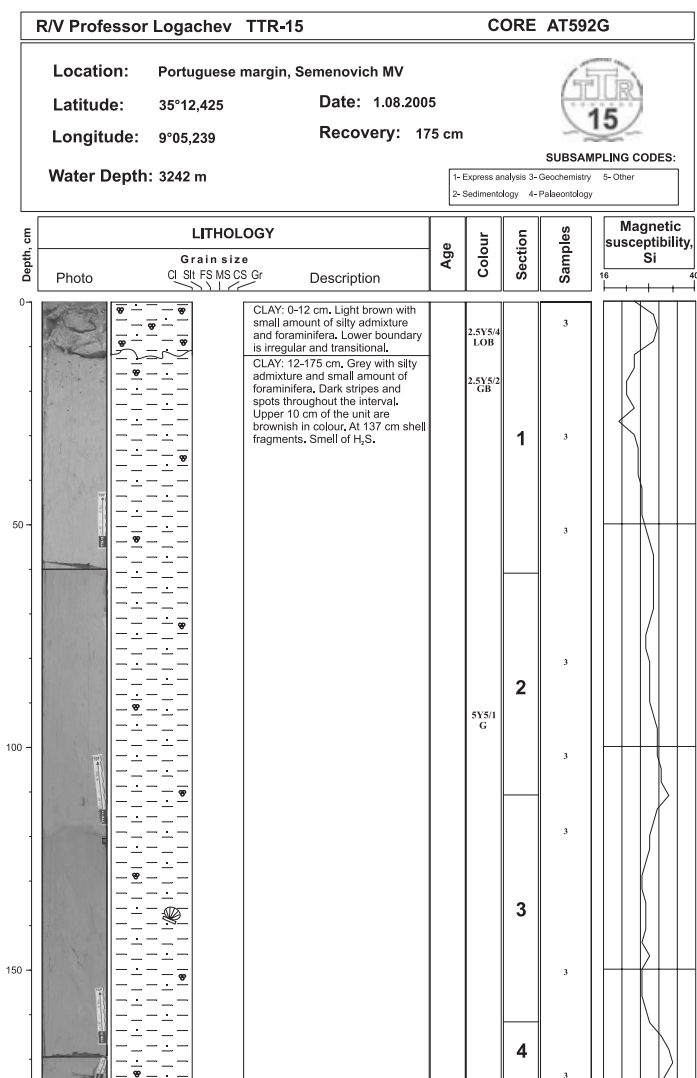
R/V Professor Logachev TTR-15		CORE AT590G
<p>Location: Portuguese margin</p> <p>Latitude: 35°34,021 Date: 31.07.2005</p> <p>Longitude: 08°34,333 Recovery: 231 cm</p> <p>Water Depth: 2586 m</p>		



Core log TTR15-AT590G



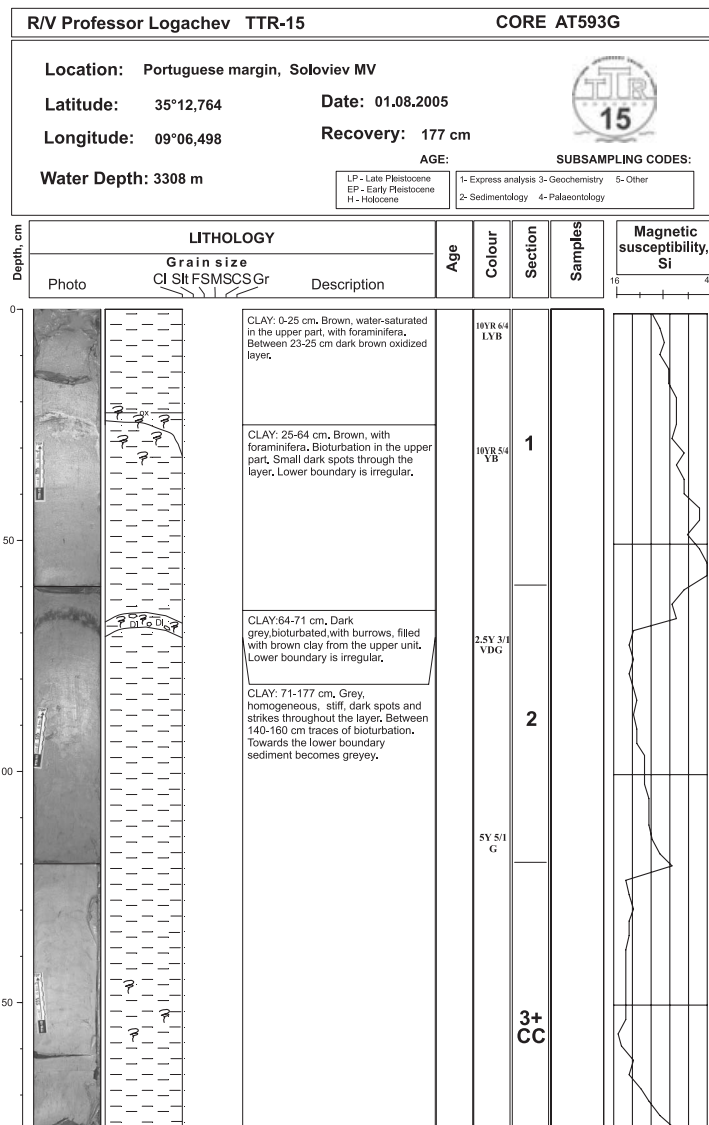
Core log TTR15-AT591G



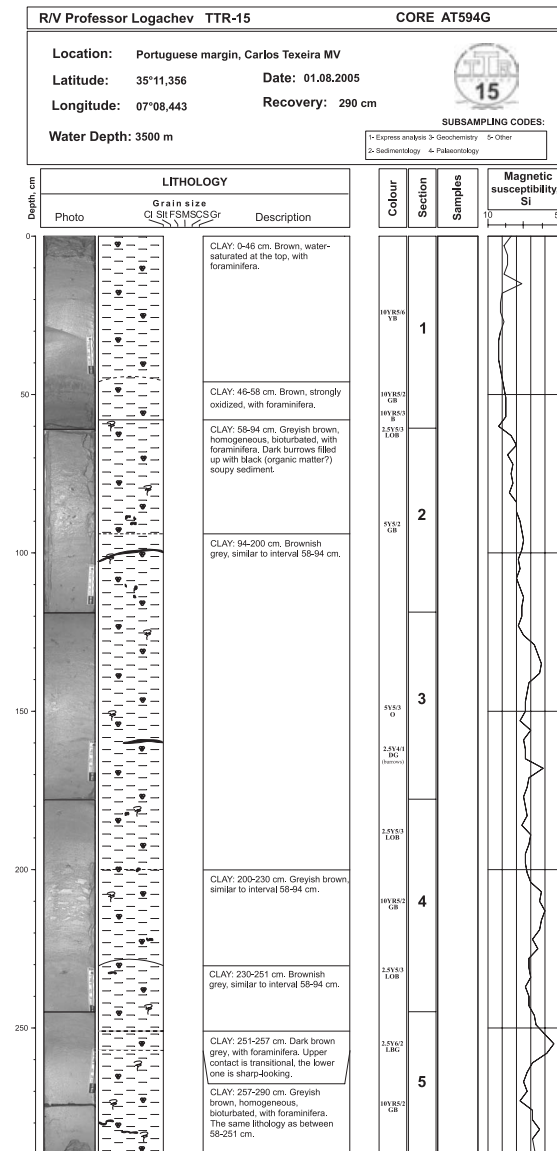
Core log TTR15-AT592G

ANNEX I. CORE LOGS (LEG 4, the Gulf of Cadiz)

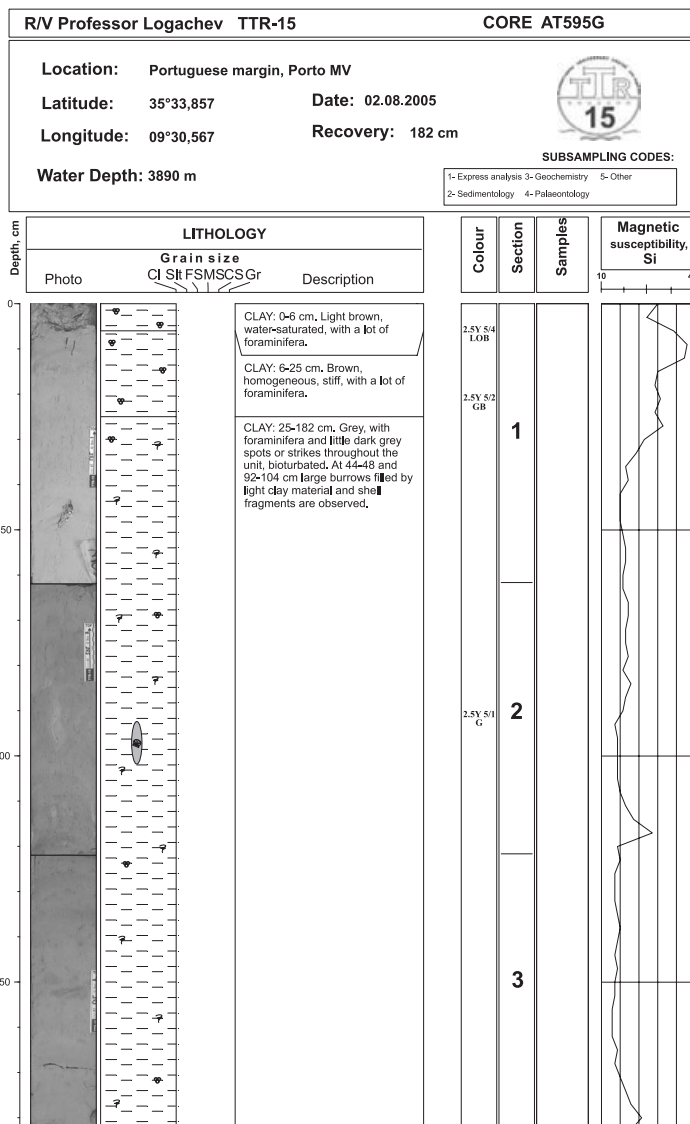
ANNEX I. CORE LOGS (LEG 4, the Gulf of Cadiz)



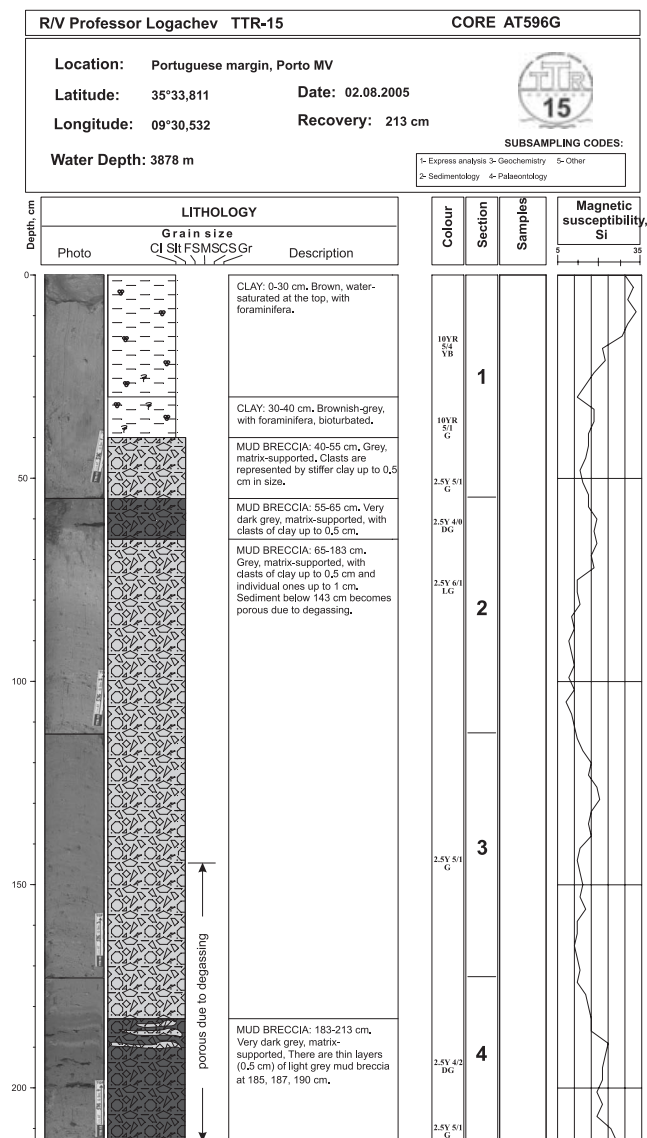
Core log TTR15-AT593G



Core log TTR15-AT594G




Core log TTR15-AT595G

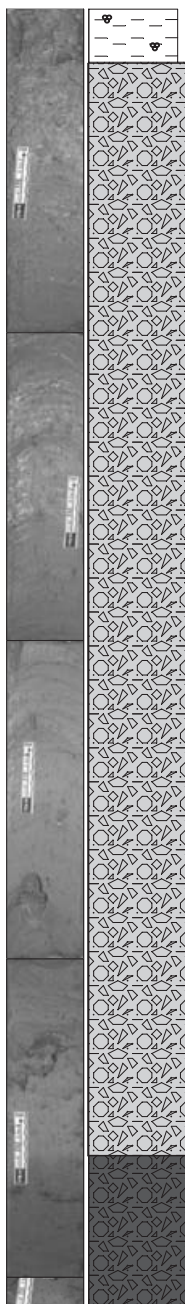

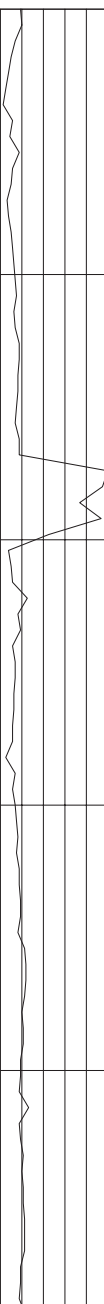


Core log TTR15-AT596G

ANNEX I. CORE LOGS (LEG 4, the Gulf of Cadiz)

ANNEX I. CORE LOGS (LEG 4, the Gulf of Cadiz)

R/V Professor Logachev TTR-15		CORE AT598G	
Location: Portuguese margin, Bonjardim mud volcano Latitude: 35°27,657 Date: 02.08.2005 Longitude: 08°59,994 Recovery: 245 cm Water Depth: 3064 m			
		SUBSAMPLING CODES: 1- Express analysis 3- Geochemistry 5- Other 2- Sedimentology 4- Palaeontology	

Depth, cm	LITHOLOGY				Colour	Section	Samples	Magnetic susceptibility, Si
	Photo	Grain size Cl Slt FSMSCSGr	Description					
0			CLAY: 0-10 cm. Brownish grey, water-saturated, with small amount of foraminifera. Clasts up to 0.8 mm in size.	2.5Y 5/4 LOB	1			
50					2			
100					3			
150					4			
200			MUD BRECCIA: 10-216 cm. Grey, light brownish grey at the top, matrix-supported, with clasts up to 5 mm represented by light grey clay. Large clasts (5 cm in size) of mudstone between 164-169 and 194-200 cm. MUD BRECCIA: 216-245 cm. Very dark grey, matrix-supported, with clast 5 cm in size at the bottom.	2.5Y 5/1 G				
				5				

Core log TTR15-AT598G

ANNEX II. LIST OF TTR-RELATED REPORTS

- Limonov, A.F., Woodside, J.M. and Ivanov, M.K. (eds.), 1992. Geological and geophysical investigations in the Mediterranean and Black Seas. Initial results of the "Training through Research" Cruise of R/V *Gelendzhik* in the Eastern Mediterranean and the Black Sea (June-July 1991). UNESCO Reports in Marine Science, 56, 208 pp.
- Limonov, A.F., Woodside, J.M. and Ivanov, M.K. (eds.), 1993. Geological and geophysical investigations of the deep-sea fans of the Western Mediterranean Sea. Preliminary report of the 2nd cruise of the R/V *Gelendzhik* in the Western Mediterranean Sea, June-July, 1992. UNESCO Reports in Marine Science, 62, 148 pp.
- "Training-Through-Research" Opportunities Through the UNESCO/TREDMAR Programme. Report of the first post-cruise meeting of TREDMAR students. Moscow State University, 22-30 January, 1993. MARINF, 91, UNESCO, 1993.
- Limonov, A.F., Woodside, J.M. and Ivanov, M.K. (eds.), 1994. Mud volcanism in the Mediterranean and Black Seas and Shallow Structure of the Eratosthenes Seamount. Initial results of the geological and geophysical investigations during the Third UNESCO-ESF "Training-through-Research" Cruise of R/V *Gelendzhik* (June-July 1993). UNESCO Reports in Marine Science, 64, 173 pp.
- Recent Marine Geological Research in the Mediterranean and Black Seas through the UNESCO/TREDMAR programme and its "Floating University" project, Free University, Amsterdam, 31 January-4 February 1994. Abstracts. MARINF, 94, UNESCO, 1994.
- Limonov, A.F., Kenyon, N.H., Ivanov, M.K. and Woodside J.M. (eds.), 1995. Deep sea depositional systems of the Western Mediterranean and mud volcanism on the Mediterranean Ridge. Initial results of geological and geophysical investigations during the Fourth UNESCO-ESF "Training through Research" Cruise of R/V *Gelendzhik* (June-July 1994). UNESCO Reports in Marine Science, 67, 171 pp.
- Deep-sea depositional systems and mud volcanism in the Mediterranean and Black Seas. 3rd post-cruise meeting, Cardiff, 30 January - 3 February 1995. Abstracts. MARINF, 99, UNESCO, 1995.
- Ivanov, M.K., Limonov, A.F. and Cronin, B.T. (eds.), 1996. Mud volcanism and fluid venting in the eastern part of the Mediterranean Ridge. Initial results of geological, geophysical and geochemical investigations during the 5th Training-through-Research Cruise of R/V *Professor Logachev* (July-September 1995). UNESCO Reports in Marine Science, 68, 127pp.
- Sedimentary basins of the Mediterranean and Black Seas. 4th Post-Cruise Meeting, Training-through-research Programme. Moscow and Zvenigorod, Russia, 29 January-3 February. Abstracts. MARINF, 100, UNESCO, 1996.
- Woodside, J.M., Ivanov, M.K. and Limonov, A.F. (eds.), 1997. Neotectonics and Fluid Flow through Seafloor Sediments in the Eastern Mediterranean and Black Seas. Preliminary results of geological and geophysical investigations during the ANAXIPROBE/TTR-6 cruise of R/V *Gelendzhik*, July-August 1996. Vols. 1, 2. IOC Technical Series, 48, UNESCO, 226 pp.
- Gas and Fluids in Marine Sediments: Gas Hydrates, Mud Volcanoes, Tectonics, Sedimentology and Geochemistry in Mediterranean and Black Seas. Fifth Post-cruise Meeting of the Training-through-research Programme and International Congress, Amsterdam, The Netherlands, 27-29 January 1997. IOC Workshop Reports, 129, UNESCO, 1997.
- Geosphere-biosphere coupling: Carbonate Mud Mounds and Cold Water Reefs. International Conference and Sixth Post-Cruise Meeting of the Training-through-Research Programme, Gent, Belgium, 7-11 February 1998. IOC Workshop Reports, 143, UNESCO, 1998.
- Kenyon, N.H., Ivanov, M.K. and Akhmetzhanov, A.M. (eds.), 1998. Cold water carbonate mounds and sediment transport on the Northeast Atlantic Margin. IOC Technical Series, 52, UNESCO, 178 pp.
- Kenyon, N.H., Ivanov, M.K. and Akhmetzhanov, A.M. (eds.), 1999. Geological Processes on the Northeast Atlantic Margin. IOC Technical Series, 54, UNESCO, 141 pp.
- Geological Processes on European Continental Margins. International Conference and Eighth Post-cruise Meeting of the Training-Through-Research Programme, University of Granada, Spain, 31 January - 3 February 2000. IOC Workshop Reports, 168, UNESCO, 2000.

Kenyon, N.H., Ivanov, M.K., Akhmetzhanov, A.M. and Akhmanov, G.G., (eds), 2000. Multidisciplinary study of geological processes on the Northeast Atlantic and Western Mediterranean margins. IOC Technical Series, 56, UNESCO, 119 pp.

Geological processes on deep-sea European margins. International Conference and Ninth Post-Cruise Meeting of the Training-through-Research Programme. Moscow/Mozhenka, Russia, 28 January - 3 February 2001. IOC Workshop Reports, 175. UNESCO, 2001, 76 pp.

Kenyon, N.H., Ivanov, M. K., Akhmetzhanov, A. and Akhmanov, G. G. (eds), 2001. Interdisciplinary Approaches to Geoscience on the North East Atlantic Margin and Mid-Atlantic Ridge. IOC Technical Series, 60, UNESCO, 134 pp.

Geosphere/Biosphere/Hydrosphere Coupling Processes, Fluid Escape Structures and Tectonics at Continental Margins and Ocean Ridges. International Conference and Tenth Post-Cruise Meeting of the Training-through-Research Programme. Aveiro, Portugal, 30 January - 2 February 2002. IOC Workshop Reports, 183. UNESCO, 2002, 50 pp.

Kenyon, N.H., Ivanov, M. K., Akhmetzhanov, A. and Akhmanov, G. G. (eds), 2002. Interdisciplinary studies of geological processes in the Mediterranean and Black Seas and North East Atlantic. IOC Technical Series, 62, UNESCO, 134 pp.

Geological and biological processes at deep-sea European margins and oceanic basins. International Conference and Eleventh Post-Cruise Meeting of the Training-through-Research Programme. Bologna, Italy, February 2-6, 2003. IOC Workshop Reports, 187. UNESCO, 2003, 32 pp.

Kenyon, N.H., Ivanov, M. K., Akhmetzhanov, A. and Akhmanov, G. G. (eds.), 2003. Interdisciplinary geoscience research on the North East Atlantic margin, Mediterranean Sea and Mid-Atlantic Ridge. IOC Technical Series, 67, UNESCO, 152 pp.

North Atlantic and Labrador Sea Margin architecture and sedimentary processes. International Conference and Twelfth Post-Cruise Meeting of the Training-through-Research Programme. Copenhagen, Denmark, January 29-31, 2004. IOC Workshop Reports, 191. UNESCO, 2004, 47 pp.

Kenyon, N.H., Ivanov, M.K., Akhmetzhanov, A.M., Kozlova, E.V. and Mazzini, A. (eds.), 2004. Interdisciplinary studies of North Atlantic and Labrador Sea Margin Architecture and Sedimentary Processes. Preliminary results of investigations during the TTR-13 cruise of RV Professor Logachev, July-September, 2003, Intergovernmental Oceanographic Commission technical series, 68 , 92 pp & annexes.

Geosphere-Biosphere coupling processes: the TTR interdisciplinary approach towards studies of the European and North African margins. International Conference and Post-Cruise Meeting of the Training-Through-Research Programme, Marrakech, Morocco, 2 - 5 February 2005. IOC Workshop Report, 197, UNESCO 2005, 71 pp.

Kenyon, N.H., Ivanov, M.K., Akhmetzhanov, A.M. and Kozlova, E.V., (eds), 2006. Interdisciplinary geoscience studies of the Gulf of Cadiz and Western Mediterranean basins. IOC Technical Series No. 70, UNESCO, 115 pp & annexes.

Geological processes on deep-water European margins. International Conference and 15th Anniversary Post-Cruise Meeting of the Training-Through-Research Programme, Moscow/Zvenigorod, Russia, 29 January-4 February 2006. IOC Workshop Report, 201, UNESCO 2007, 73 pp.

IOC Technical Series

No.	Title	Languages
1	Manual on International Oceanographic Data Exchange. 1965	(out of stock)
2	Intergovernmental Oceanographic Commission (Five years of work). 1966	(out of stock)
3	Radio Communication Requirements of Oceanography. 1967	(out of stock)
4	Manual on International Oceanographic Data Exchange - Second revised edition. 1967	(out of stock)
5	Legal Problems Associated with Ocean Data Acquisition Systems (ODAS). 1969	(out of stock)
6	Perspectives in Oceanography, 1968	(out of stock)
7	Comprehensive Outline of the Scope of the Long-term and Expanded Programme of Oceanic Exploration and Research. 1970	(out of stock)
8	IGOSS (Integrated Global Ocean Station System) - General Plan Implementation Programme for Phase I. 1971	(out of stock)
9	Manual on International Oceanographic Data Exchange - Third Revised Edition. 1973	(out of stock)
10	Bruun Memorial Lectures, 1971	E, F, S, R
11	Bruun Memorial Lectures, 1973	(out of stock)
12	Oceanographic Products and Methods of Analysis and Prediction. 1977	E only
13	International Decade of Ocean Exploration (IDOE), 1971-1980. 1974	(out of stock)
14	A Comprehensive Plan for the Global Investigation of Pollution in the Marine Environment and Baseline Study Guidelines. 1976	E, F, S, R
15	Bruun Memorial Lectures, 1975 - Co-operative Study of the Kuroshio and Adjacent Regions. 1976	(out of stock)
16	Integrated Ocean Global Station System (IGOSS) General Plan and Implementation Programme 1977-1982. 1977	E, F, S, R
17	Oceanographic Components of the Global Atmospheric Research Programme (GARP) . 1977	(out of stock)
18	Global Ocean Pollution: An Overview. 1977	(out of stock)
19	Bruun Memorial Lectures - The Importance and Application of Satellite and Remotely Sensed Data to Oceanography. 1977	(out of stock)
20	A Focus for Ocean Research: The Intergovernmental Oceanographic Commission - History, Functions, Achievements. 1979	(out of stock)
21	Bruun Memorial Lectures, 1979: Marine Environment and Ocean Resources. 1986	E, F, S, R
22	Scientific Report of the Interecalibration Exercise of the IOC-WMO-UNEP Pilot Project on Monitoring Background Levels of Selected Pollutants in Open Ocean Waters. 1982	(out of stock)
23	Operational Sea-Level Stations. 1983	E, F, S, R
24	Time-Series of Ocean Measurements. Vol.1. 1983	E, F, S, R
25	A Framework for the Implementation of the Comprehensive Plan for the Global Investigation of Pollution in the Marine Environment. 1984	(out of stock)
26	The Determination of Polychlorinated Biphenyls in Open-ocean Waters. 1984	E only
27	Ocean Observing System Development Programme. 1984	E, F, S, R
28	Bruun Memorial Lectures, 1982: Ocean Science for the Year 2000. 1984	E, F, S, R
29	Catalogue of Tide Gauges in the Pacific. 1985	E only
30	Time-Series of Ocean Measurements. Vol. 2. 1984	E only
31	Time-Series of Ocean Measurements. Vol. 3. 1986	E only
32	Summary of Radiometric Ages from the Pacific. 1987	E only
33	Time-Series of Ocean Measurements. Vol. 4. 1988	E only
34	Bruun Memorial Lectures, 1987: Recent Advances in Selected Areas of Ocean Sciences in the Regions of the Caribbean, Indian Ocean and the Western Pacific. 1988	Composite E, F, S

(continued)

No.	Title	Languages
35	Global Sea-Level Observing System (GLOSS) Implementation Plan. 1990	E only
36	Bruun Memorial Lectures 1989: Impact of New Technology on Marine Scientific Research. 1991	Composite E, F, S
37	Tsunami Glossary - A Glossary of Terms and Acronyms Used in the Tsunami Literature. 1991	E only
38	The Oceans and Climate: A Guide to Present Needs. 1991	E only
39	Bruun Memorial Lectures, 1991: Modelling and Prediction in Marine Science. 1992	E only
40	Oceanic Interdecadal Climate Variability. 1992	E only
41	Marine Debris: Solid Waste Management Action for the Wider Caribbean. 1994	E only
42	Calculation of New Depth Equations for Expendable Bathymetographs Using a Temperature-Error-Free Method (Application to Sippican/TSK T-7, T-6 and T-4 XBTs. 1994	E only
43	IGOSS Plan and Implementation Programme 1996-2003. 1996	E, F, S, R
44	Design and Implementation of some Harmful Algal Monitoring Systems. 1996	E only
45	Use of Standards and Reference Materials in the Measurement of Chlorinated Hydrocarbon Residues. 1996	E only
46	Equatorial Segment of the Mid-Atlantic Ridge. 1996	E only
47	Peace in the Oceans: Ocean Governance and the Agenda for Peace; the Proceedings of <i>Pacem in Maribus XXIII</i> , Costa Rica, 1995. 1997	E only
48	Neotectonics and fluid flow through seafloor sediments in the Eastern Mediterranean and Black Seas - Parts I and II. 1997	E only
49	Global Temperature Salinity Profile Programme: Overview and Future. 1998	E only
50	Global Sea-Level Observing System (GLOSS) Implementation Plan-1997. 1997	E only
51	L'état actuel de l'exploitation des pêcheries maritimes au Cameroun et leur gestion intégrée dans la sous-région du Golfe de Guinée (<i>cancelled</i>)	F only
52	Cold water carbonate mounds and sediment transport on the Northeast Atlantic Margin. 1998	E only
53	The Baltic Floating University: Training Through Research in the Baltic, Barents and White Seas - 1997. 1998	E only
54	Geological Processes on the Northeast Atlantic Margin (8 th training-through-research cruise, June-August 1998). 1999	E only
55	Bruun Memorial Lectures, 1999: Ocean Predictability. 2000	E only
56	Multidisciplinary Study of Geological Processes on the North East Atlantic and Western Mediterranean Margins (9 th training-through-research cruise, June-July 1999). 2000	E only
57	Ad hoc Benthic Indicator Group - Results of Initial Planning Meeting, Paris, France, 6-9 December 1999. 2000	E only
58	Bruun Memorial Lectures, 2001: Operational Oceanography – a perspective from the private sector. 2001	E only
59	Monitoring and Management Strategies for Harmful Algal Blooms in Coastal Waters. 2001	E only
60	Interdisciplinary Approaches to Geoscience on the North East Atlantic Margin and Mid-Atlantic Ridge (10 th training-through-research cruise, July-August 2000). 2001	E only
61	Forecasting Ocean Science? Pros and Cons, Potsdam Lecture, 1999. 2002	E only
62	Geological Processes in the Mediterranean and Black Seas and North East Atlantic (11 th training-through-research cruise, July- September 2001). 2002	E only
63	Improved Global Bathymetry – Final Report of SCOR Working Group 107. 2002	E only
64	<i>In preparation</i>	
65	Bruun Memorial Lectures, 2003: Gas Hydrates – a potential source of energy from the oceans. 2003	E only

(continued)

No.	Title	Languages
66	Bruun Memorial Lectures, 2003: Energy from the Sea: the potential and realities of Ocean Thermal Energy Conversion (OTEC). 2003	E only
67	Interdisciplinary Geoscience Research on the North East Atlantic Margin, Mediterranean Sea and Mid-Atlantic Ridge (12 th training-through-research cruise, June-August 2002). 2003	E only
68	Interdisciplinary Studies of North Atlantic and Labrador Sea Margin Architecture and Sedimentary Processes (13 th training-through-research cruise, July-September 2003). 2004	E only
69	Biodiversity and Distribution of the Megafauna / Biodiversité et distribution de la mégafaune. 2006 Vol.1 The polymetallic nodule ecosystem of the Eastern Equatorial Pacific Ocean / Ecosystème de nodules polymétalliques de l'océan Pacifique Est équatorial Vol.2 Annotated photographic Atlas of the echinoderms of the Clarion-Clipperton fracture zone / Atlas photographique annoté des échinodermes de la zone de fractures de Clarion et de Clipperton	E F
70	Interdisciplinary geoscience studies of the Gulf of Cadiz and Western Mediterranean Basin (14 th training-through-research cruise, July-September 2004). 2006	E only
71	Indian Ocean Tsunami Warning and Mitigation System, IOTWS. Implementation Plan, July-August 2006. 2006	E only
72	Deep-water Cold Seeps, Sedimentary Environments and Ecosystems of the Black and Tyrrhenian Seas and the Gulf of Cadiz (15 th training-through-research cruise, June–August 2005). 2007	E only

